Disruption of NFκB Driven Breast Cancer – Bone Cell Crosstalk by TRAF Inhibition

A thesis submitted in fulfilment of the requirements

for the degree of Doctor of Philosophy by

Feier Zeng

August 2023

Department of Oncology and Metabolism

Faculty of Medicine, Dentistry and Health

The University of Sheffield

致家人

Declaration

I confirm that I shall abide by the University of Sheffield's regulations on plagiarism and that all written work shall be my own and will not have been plagiarised from other paper-based or electronic sources. Where used, material gathered from other sources will be clearly cited in the text.

Acknowledgements

I want to extend my first and foremost gratitude to my supervisor, Dr. Aymen Idris, for welcoming me into your research team as a PhD candidate, and for the chance to delve into numbers of research endeavors within the field of bone and translational oncology research. I am wholeheartedly thankful for the doors you have opened for me, enabling me to travel with my research, collaborating with excellent researchers (include but not limited to Dr. Antonia Sophocleous, Dr. Shelly Lawson's group, Professor A. Sparatore, Dr Ivan Bassanini) as well as contributing to papers, books, and websites. The insight I have gained from these experiences has been invaluable. I would also like to thank our group members Dr. Boya Li, Dr. Giovana Carrascco and Dr. Ryan Bishop for their supervision, patience, motivation, teaching and disposition.

Furthermore, I extend my sincere thanks to my co-supervisors, Dr. Shelly Lawson and Dr. Ning Wang, for their willingness and invaluable guidance, providing key insights and advice concerning my PhD project and career growth. I am deeply grateful for your patience, support, and for the privilege of participating in activities within your lab group. A special thanks to Dr Karan Shah and soon-to-be Dr. Yidan Sun for carrying out *in vivo* work carefully, rigorously and efficiently in our collaborations, I learned a lot from you.

I would also like to acknowledge the following for their contribution to parts of the work presented in this thesis: I would like to thank Professor Anna. Sparatore and Dr Ivan Bassanini (University of Milan, Italy) for providing me with the TRAF6 inhibitors, giving us exclusive license to test these compounds and providing the docking data for the compound. I would like to thank our collaborator Dr. Antonia Sophocleous (European University Cyprus, Cyprus) for her patient disposition and guidance on suggesting and interpreting on my meta-analysis, I can't get this part of work in my thesis and other related work published without your unreserved guidance.

Also thank you to soon-to-be Dr. Yuhan Zhou and Dr. Jiabao Zhou their constant support and for being the best of friends in the lab over the past three years. I would also like to extend my heartfelt thanks to

my amazing friend, Miss Yufei Nie, and my genius boyfriend, Mr. Junyi Han, for all the surprises and daily joy you bring into my life.

Most importantly, I want to express my deepest gratitude to my parents and grandparents for their guidance, education, unwavering support, and understanding. Everything I am today is because of you. My love for you is constant and unending.

In the end, I want to give thanks to myself. For every night I've stayed up, every decision I've made, and for all the effort and thought I've invested. Always remember – shoot for the moon, even if you miss, and you will land among the stars.

Publications

Accepted publications

- **Zeng, F**., Carrasco, G., Li, B., Sophocleous, A. and Idris, A. I. (2023) TRAF6 as a potential target in advanced breast cancer: a systematic review, meta-analysis, and bioinformatics validation. *Scientific Reports.* DOI: 10.1038/s41598-023-31557-0

- **Zeng, F**., Liu, H., Xia, X., Shu, Y., Cheng, W., Xu, H., Yin, G. and Xie, Q. (2022) Case s Report: Brachydactyly Type A1 Induced by a Novel Variant of in-Frame Insertion in the *IHH* Gene. *Frontiers in Genetics,* DOI: 10.3389/fgene.2022.814786

- Marino, S., Hannemann, N., Bishop, R.T., **Zeng, F**., Carrasco, G., Meurisse, S., Li, B., Sophocleous, A., Sparatore, A., Baeuerle, T., Vukicevic, S., Auberval, M., Mollat, P., Bozec, A. and Idris, A. I. (2022) Anti-inflammatory, but not osteoprotective, effect of the TRAF6/CD40 inhibitor 6877002 in rodent models of local and systemic osteolysis. *Biochemical Pharmacology,* DOI: 10.1016/j.bcp.2021.114869

- Sophocleous, A., Yiallourides, M., **Zeng, F**., Pantelas, P., Stylianou, E., Li, B., Carrasco, G. and Idris, A.I. (2022) Association of cannabinoid receptor modulation with normal and abnormal skeletal remodelling: A systematic review and meta-analysis of *in vitro*, *in vivo* and human studies. *Pharmacological Research,* DOI: 10.1016/j.phrs.2021.105928

Manuscript under review

- **Zeng, F**., Harbert, K., Patel, S., Wade, A., Holley, J., Dehghanpuor, K. C. K., Hopwood, T., Sophocleous, A., and Idris, A. I. (2023) Classical Cannabinoid Receptors as Target in Cancer-induced Bone Pain: A Systematic Review, Meta-Analysis and Bioinformatics Validation. Submitted to JBMR.

Manuscripts in preparation

- **Zeng, F**., Carrasco, G., Marino, S., Bassanini, I., Conrad, S., Li, B., Mollat, P., Meli, M., Ferrandi, E., Morra, G., Rauner, M., Sparatore, A., and Idris. A. I. Pharmacological Targeting of TRAF6/NFκB Axis Suppresses Osteolysis in Female Animal Models of Inflammation and Cancer. In preparation.

- Jeffery, A., Marino, S., **Zeng, F**., Ponzettic, M., Fowles, A., Mackay, S., Rucci, N. and Idris. A. I. Differential effects of a first-in-class IKKα inhibitor on trabecular and cortical bone in a human prostate cancer xenograft model. In preparation.

- Marino, S., **Zeng, F**. and Idris. A. I. Analysis of signalling pathways by western blotting and immunoprecipitation. (Springer Bone Research Protocols.4th ed. In preparation.)

Abstracts for presentations

- Poster presentation at the "Annual Congress of the European Association for Cancer Research", 12-15 June 2023, Torino, Italy. Title: "Validation of a novel inhibitor of TRAF6/NFκB axis in models of BCa metastasis". Authors: **Zeng, F.,** Marino, S., Bassanini, I., Conrad, S., Carrasco, G., Li, B., Mollat, P., Sophocleous, A., Meli, M., Ferrandi, E., Morra, G., Rauner, M., Sparatore, A., and Idris. A. I.

- Oral presentation at the "17th Annual Mellanby Centre Research Day" (2023), University of Sheffield, United Kingdom. Title: "Inhibition of breast cancer metastasis by a novel inhibitor of TRAF6/NFκB axis". Authors: **Zeng, F**., Marino, S., Bassanini, I., Carrasco, G., Li, B., Mollat, P., Sophocleous, A., Sparatore, A. and Idris, A. I.

- Oral presentation at the "17th Annual University of Sheffield Medical School Research Meeting" (2022), University of Sheffield, United Kingdom. Title: "Inhibition of breast cancer metastasis by a novel inhibitor of TRAF6/NFκB axis". Authors: **Zeng, F**., Marino, S., Bassanini, I., Carrasco, G., Li, B., Mollat, P., Sophocleous, A., Sparatore, A. and Idris, A. I.

- Poster presentation at the "European Calcified Tissue Society PhD Training Course." (2022). Valbonne, Nice, France. Title: "Association of TRAF modulation with breast cancer: A systematic review and meta-analysis of *in vitro, in viv*o and human studies". Authors: **Zeng, F**., Carrasco, G., Li, B., Sophocleous, A. and Idris, A. I.

Other publications

- HubLE Doodle. Title: "To test if inhibition of NFκB at the level of TRAF6 reduces the aggressive behaviour of breast cancer cell *in vitro, ex vivo,* and *in vivo*". Author: **Zeng, F.**

Awards

- Travel award from the Department of Oncology and Metabolism, University of Sheffield, UK. (2023).

- Publication Scholarship from the University of Sheffield, UK. (2023)

- Institutional Open Access Fund from the University of Sheffield, UK. (2023)

List of Contents

List of Figures

List of Supplementary Figures

List of Tables

List of Supplementary Tables

List of Abbreviations

5-FU	5-Fluorouracil
ACC	Adenoid Cystic Carcinoma
ADC	Antibody-Drug Conjugates
ALP	Alkaline Phosphatase
AMPK	AMP-activated Protein Kinase
ANOVA	Analysis of Variance
ARS	Alizarin Red S
ASK1	Apoptosis Signal-Regulating Kinase 1
BAFFR	B-Cell Activating Factor Belonging to TNF Family Receptor
BCa	Breast Cancer
BCA	Bicinchoninic Acid
BMI	Body Mass Index
BMP	Bone Morphogenetic Protein
BSA	Bovine Serum Albumin
Car-T	Chimeric Antigen Receptor-Engineered T Cells
CCK8	Cell Counting Kit 8
CD40	Cluster of Differentiation 40
CHIP	Carboxyl terminus of Hsc70-interacting Protein
CNV	Copy Number Variation
CXCR4	C-X-C Chemokine Receptor Type 4
DARTS	Drug Affinity Responsive Target Stability
DMEM	Dulbecco'S Modified Eagle Medium
DMSO	Dimethyl Sulfoxide
DNA	Deoxyribonucleic Acid
EDTA	Ethylenediaminetetraacetic Acid

Ei24	Etoposide Induced 2.4
EMT	Epithelial-To-Mesenchymal Transition
EMT-TFs	EMT-Inducing Transcription Factors
ER	Estrogen Receptor
FBS	Fetal Bovine Serum
FDR	False Discovery Rate
FOXP3	Forkhead Box Protein 3
GAPDH	Glyceraldehyde 3-Phosphate Dehydrogenase
GCO	Global Cancer Observatory
GEO	Gene Expression Omnibus
GO	Gene Ontology
gp130	Glycoprotein 130
GRADE	Grading Of Recommendations Assessment, Development, And Evaluation
HER2	Human Epidermal Growth Factor Receptor 2
HR	Hazard Ratio
HRP	Horseradish Peroxidase
IARC	International Agency for Research on Cancer
IBC	Inflammatory Breast Cancer
IC50	Half-maximal Inhibitory Concentration
ICIs	Immune Checkpoint Inhibitors
IKKα	Inhibitor of κB Alpha
IKKβ	Inhibitor of κB Beta
IL-17R	Interleukin 17 Receptor
IL-1R	Interleukin 1 Receptor
IL1β	Interleukin-1 Beta
IRAK	Interleukin-1 Receptor-Associated Kinase 1
IRFs	Interferon Regulatory Factors

KEGG	Kyoto Encyclopedia Of Genes and Genomes
LPS	Lipopolysaccharides
LTβR	Lymphotoxin-B Receptor
M-PER	Mammalian Protein Extraction Reagent
MAPK	Mitogen-Activated Protein Kinase
MBC	Metaplastic Breast Cancer
MEKK	Mitogen-Activated Protein Kinase Kinase Kinase
METABRIC	Molecular Taxonomy of BCa International Consortium
miRNA	Micro Ribonucleic Acid
MRI	Magnetic Resonance Imaging
mRNA	Messenger Ribonucleic Acid
mTOR	Mammalian Target of Rapamycin
MTS	3-(4,5-Dimethylthiazol-2-Yl)-5-(3-Carboxymethoxyphenyl)-2-(4-Sulfophenyl)-2H-Tetrazolium
MTT	3-(4,5-Dimethylthiazol-2-Yl)-2,5-Diphenyltetrazolium Bromide
MUC1	Mucin1
MYD88	Myeloid Differentiation Primary Response 88
NACT	Traditional Chemotherapy and Neoadjuvant Chemotherapy
NEBC	Neuroendocrine Breast Cancer
NEMO	NF-kappa-B Essential Modulator
NFATc1	Nuclear Factor of Activated T-Cells, Cytoplasmic 1
NFκB	Nuclear Factor Kappa B
NIK	NFκB -Inducing Kinase
NLR	Nucleotide-Binding Domain and Leucine-Rich Repeat
OHAT	Office Of Health Assessment and Translation
OPG	Osteoprotegerin
OS	Overall Survival

PAM50	Prosigna Breast Cancer Prognostic Gene Signature Assay
PATH	Pathology Report Data
PBS-T	Phosphate-buffered Saline solution – Tween 20
PD-1	Programmed Death-1
PEI	Polyethylenimine
PPI	Protein-protein Interaction
PR	Progesterone Receptor
PRISMA	Systematic Reviews and Meta-Analyses
PVDF	Polyvinylidene Fluoride
RANK	Receptor Activator of NFκB
RANKL	Receptor Activator for NFκB Ligand
RAS	Resistance to Audiogenic Seizures
RIG-1	Retinoic Acid-Inducible Gene I
RING	Really Interesting New Gene
RIPA	Radioimmunoprecipitation Assay Buffer
RNA	Ribonucleic Acid
SEER	The Surveillance, Epidemiology, And End Results Program
SERD	Selective Estrogen-Receptor Degrader
SERM	Selective Estrogen-Receptor Modulator
shRNA	Short Hairpin RNA
SDS	Sodium Lauryl Sulfate
SMURF2	Specific E3 Ubiquitin Protein Ligase 2
SRE	Skeletal-Related Event
STAT1	Signal Transducer and Activator of Transcription 1
STAT3	Signal Transducer and Activator of Transcription 3
STRING	Search Tool for Retrieval Interacting Genes/Proteins
TAB2	TGF-Beta Activated Kinase 1 (Map3K7) Binding Protein 2

TANK	TRAF Family Member Associated NFκB Activator
TBK1	TANK-Binding Kinase 1
TCGA	The Cancer Genome Atlas
TGFβ	Transforming Growth Factor Beta
TGS	Tris/Glycine/SDS
TIR	Toll/interleukin-1 Receptor
TLR	Toll-like Receptor
TLR5	Toll-like Receptor 5
TNBC	Triple-negative Breast Cancer
TNF	Tumour Necrosis Factor
TNFα	Tumour Necrosis Factor Alpha
TNFR	Tumour Necrosis Factor Receptor
TNM	Primary Tumour [T], Regional Lymph Nodes [N], Distant Metastases [M]
TRAcP	Tartrate-Resistant Acid Phosphatase
TRADD	TNFR1-associated Death Domain
TRAF	TNF Receptor Associated Factor
TRIF	TIR Domain-containing Adapter Protein Inducing Interferon-beta
UCSC	University Of California Santa Cruz

Abstract

Breast Cancer (BCa) is one of the most commonly diagnosed cancers in the UK, and the fifth cause of cancer mortality worldwide. While primary tumours are treatable with surgery or chemotherapy, recurrence and metastasis remain major causes of death. Existing treatments like immunotherapy show limited success against advanced types like triple-negative BCa (TNBC), highlighting the need for additional therapies that can be used alone or in combination with existing therapy. TNF receptor associated factors (TRAFs), are essential components of the canonical NFκB signalling transduction pathway, and the TRAF/NFκB axis has been implicated in TNBC and cancer-induced bone disease. The aim of the present project is to investigate the role of the pro-inflammatory TRAF6/NFκB axis in the regulation of growth, metastatic and osteolytic behaviour of BCa cells, particularly TNBC cells, and test the hypothesis that pharmacological inhibition of the pro-inflammatory canonical NFκB signalling by a novel, selective TRAF6 inhibitor disrupts TNBC cell activity and osteolysis in mouse and human preclinical models of TNBC.

Firstly, I performed a systematic review, meta-analysis, and bioinformatics validation to identify a druggable TRAF target for TNBC metastasis. The literature-based analysis revealed that *in vitro* inhibition of TRAF2/4 is associated with reduced BCa cell migration and adhesion, TRAF2/4/6 inhibition is associated with cell invasion. Interestingly, only TRAF6 inhibition is associated with reduced cell growth. In animal models, administration of pharmacological inhibitors of TRAF2/4/6 in mice reduced BCa tumour burden but only TRAF6 inhibitors reduced metastasis. In BCa patients, high expression of TRAF6 is associated with poor survival rate. Bioinformatic analysis identified significant enrichment of TRAF6 and TRAF2 (not TRAF4) in various pro-inflammatory and immuno-modulatory pathways and processes, including osteoclast formation. Additionally, TRAF6 gain/amplification was associated with secondary BCa in bone and decreased survival rate.

Guided by these findings, I then performed a number of *in vitro* and *ex vivo* studies to test the hypothesis that TRAF2/6-mediated NFκB activation enhances BCa – bone cell crosstalk, and pharmacological

inhibition and knockdown of TRAF6 suppresses the growth, metastatic and osteolytic behaviours of human and mouse TNBC cells.

I first confirmed that the expression of TRAF2,4 and 6 in TNBC and highly metastatic cells mouse 4T1 and human MDA-MB-231, and hormone-sensitive human MCF7 and murine E0771 cells. Pharmacological studies showed that the verified CD40-TRAF6 inhibitor 6877002 and its novel congener FSAS3 and its structurally-related analogues suppressed the *in vitro* viability of all cell lines tested in a concentration- and time-dependent manner, with FSAS3 being the most potent.

Next, I showed that TRAF6 knockdown and pharmacological inhibition using 6877002 and FSAS3 inhibited the growth of osteotropic MDA-MB-231 cells more potently than their parental clones. Further functional and mechanistic studies in these cells confirmed that both TRAF6 knockdown and treatment with 6877002 and FSAS3 significantly reduced the ability of TNBC cells to grow, invade and migrate *in vitro*, and the growth inhibition by FSAS3 was significantly blunted in TRAF6-deficient TNBC cells.

Finally, I demonstrated that FSAS3 is a potent inhibitor of both TRAF6- as well as TRAF2- driven canonical NFκB activation in TNBC cells than the verified CD40-TRAF6 inhibitor 6877002. *In silico* docking analysis confirmed TRAF6 is a key target of FSAS3. Consistently, I found that FSAS3 inhibited TRAF6-IKK binding, IκB activation and p65NFκB-DNA binding, indicative of canonical NFκB inhibition which is significantly blunted in TRAF6 deficient MDA-MB-231 cells. Furthermore, FSAS3 reduced the ability of MDA-MB-231-BT to enhance osteoclast formation *in vitro*, and to cause osteolytic bone damage in mouse calvarial bone *ex vivo*, demonstrating the anti-osteoclast and anti-osteolytic properties of this novel TRAF6 inhibitor.

In summary, the present findings from the meta-analysis imply that inhibition of NFκB activation at the level of TRAF2/4/6 reduces BCa cell motility *in vitro*, suppresses metastasis *in vivo* and improves survival in patients. Follow up *in vitro* and *ex vivo* findings demonstrate that the novel TRAF6 inhibitor FSAS3 shows a promise as an anti-inflammatory, anti-tumour, anti-migratory, anti-invasive, anti-osteoclastic and anti-osteolytic agent. However, further *in vivo* studies are needed before the translation of the present *in vitro* and *ex vivo* findings into clinical practise.

Graphical Abstract

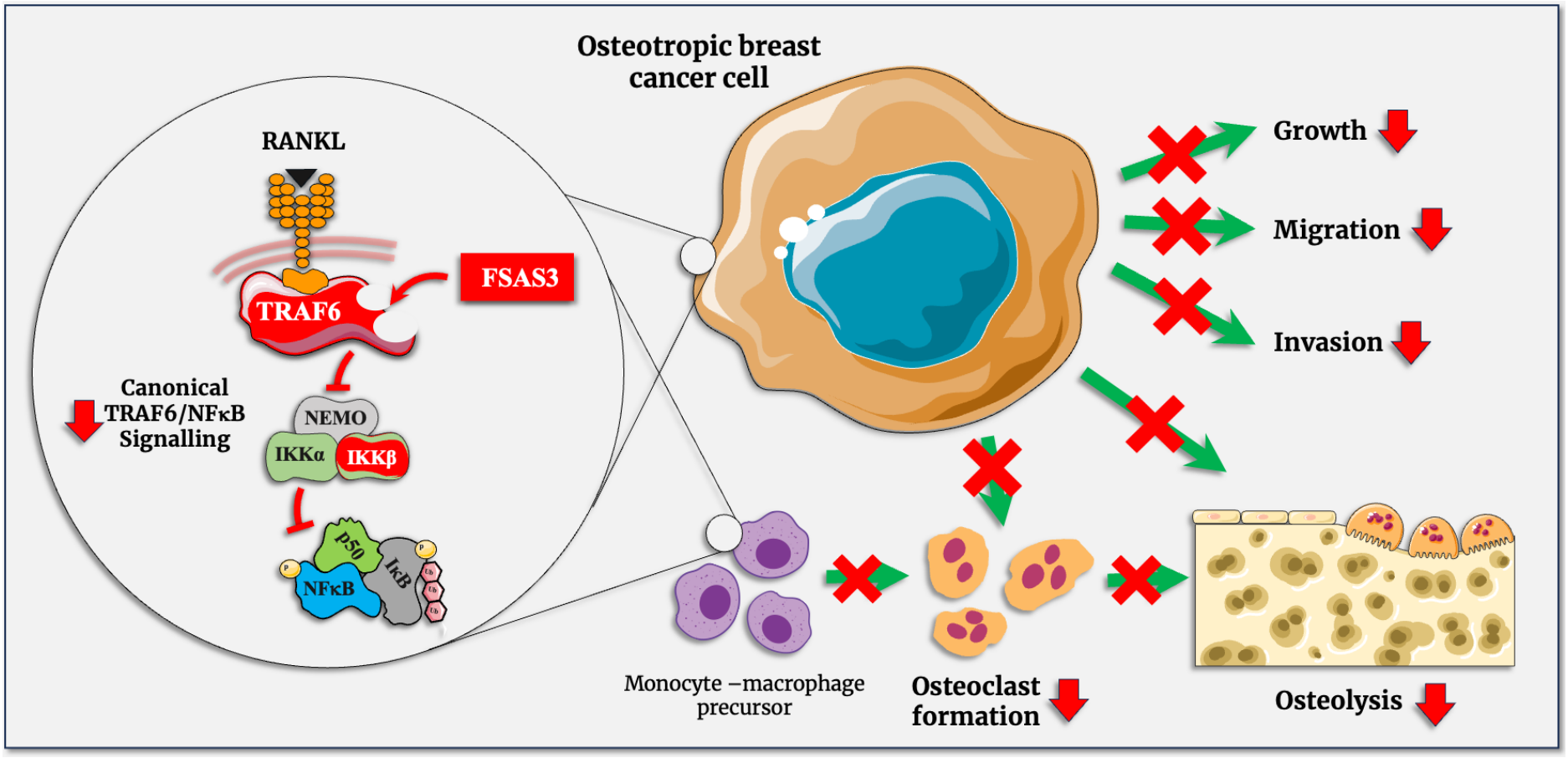

Disruption of TRAF6/NFκB signalling by the novel FSAS3 reduces breast cancer metastatic and osteolytic behaviour. Refer to 'Abstract' for more detail and to 'Introduction' for abbreviations.

CHAPTER 1. General Introduction

1.1. Breast Cancer

1.1.1. Epidemiology and genetic

Breast cancer (BCa) is one of the most diagnosed and leading cause of cancer death worldwide and it represents 11.7% of the total new cases reported worldwide, according to data released by the International Agency for Research on Cancer (IARC, https://gco.iarc.fr/today/home) and analyzed by Global Cancer Observatory (GCO, https://gco.iarc.fr/). Unlike most cancers, the incidence of BCa has continued to rise at a rate of 0.5% per year between 2008 and 2017 [1]. In 2020, BCa surpasses lung cancer as the most commonly diagnosed cancer worldwide (**Figure 1.1**), and it is now the fifth leading cause of cancer mortality (**Figure 1.2**).

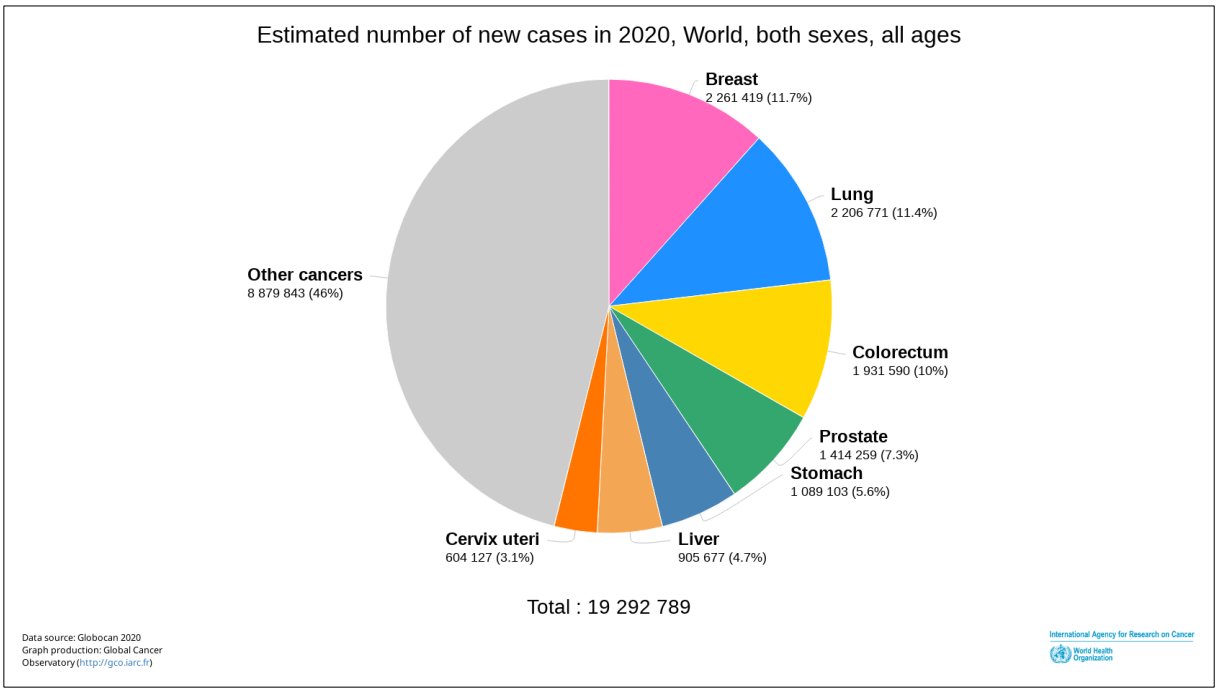

Figure 1.1. The top eight cancers in 2020 ranked according to incidence rate. Refer to text for more details. Adapted from https://gco.iarc.fr/today/fact-sheets-cancers.

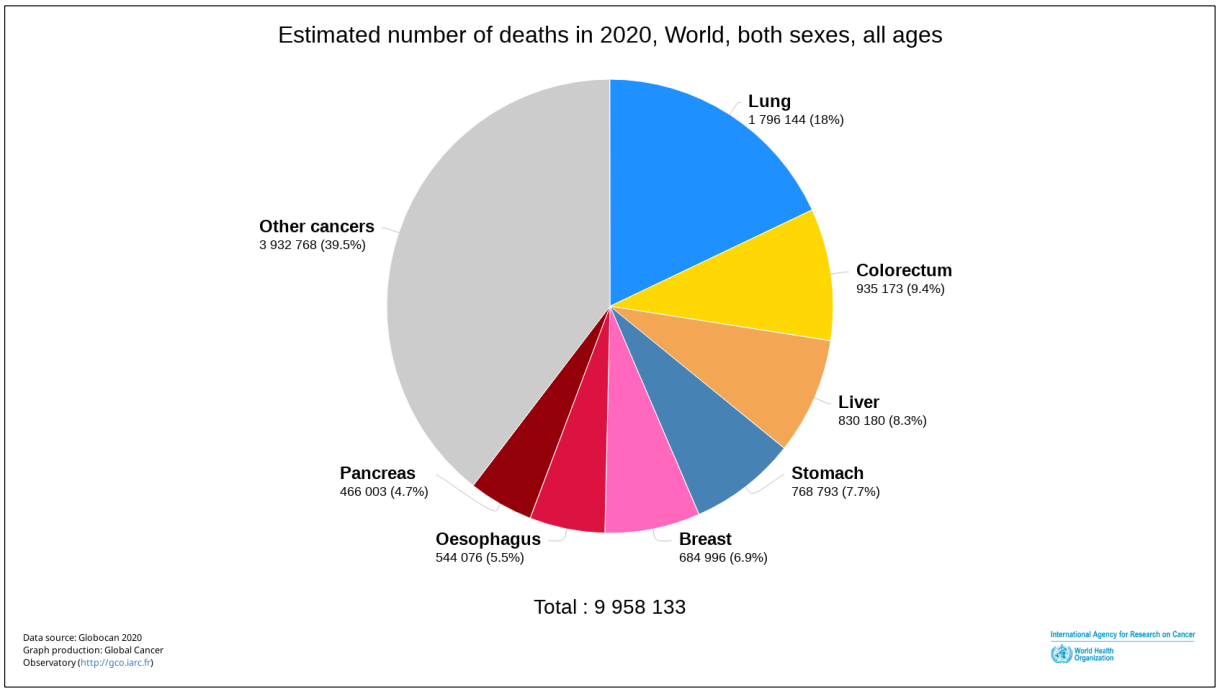

Figure 1.2. The top eight cancers in 2020 ranked according to mortality rate. Refer to text for more details. Adapted from https://gco.iarc.fr/today/fact-sheets-cancers.

1.1.2. Pathophysiology

BCa progression is classified according to the TNM Classification of Malignant Tumours. TNM staging system is the most commonly used classification that used for to describe the different stages of the disease by doctors and health care professionals. T refers to the size and extent of primary tumour, N indicates the number of the lymph nodes that exhibit cancer and M refers to whether the tumour has metastasized [2]. According to the TNM staging system, BCa is divided into five stages: Stage 0, non-invasive BCa; stage I, the tumour measures up to 2 cm but present at nearby lymph nodes; stage II, the tumour size is approximately 2 to 5 cm or the tumour has spread to the lymph nodes under the arm on the same side of the body as the primary tumour; stage III, the tumour measures more than 5 cm and it spreads to lymph nodes or other tissues and organs close to the original location of the primary tumour; stage IV, BCa has metastasised to distant parts of the body, such as the lung, bone, liver and/or brain [3].

Heterogeneity is one of the main characteristics of BCa [4]. Numerous studies have confirmed that genetic and genotype diversity among BCa cells plays a vital role in the regulation of tumour cell behaviour, namely cell proliferation, migration, invasion and death (apoptosis and necrosis). Thus,

additional four factors have been included in the BCa staging system. These factors are estrogen receptor (ER), progesterone receptor (PR), human epidermal growth factor receptor 2 (HER2), and the Nottingham histologic score (or histologic grade) [5]. Together with the traditional TNM system, the modified system provides a more comprehensive and accurate picture of the disease progression and thus aid with the design and development of better targeted treatment plans [3].

ER and PR are expressed in healthy breast epithelial cells. However, genetic and epigenetic modifications in the genes of these factors lead to the development of a hormone-dependent BCa, in which tumour growth and proliferation are predominately regulated by the two hormones [6]. ER or PR negative BCa, hormone-independent BCa, is a second type of BCa that is relatively more aggressive and metastatic than hormone-dependent BCa [7]. HER2 is another protein that promotes the growth of healthy breast cells. Enhanced expression of HER2 induces tumour cell transformation and enhances tumour growth, thus it is used as another biomarker to predict the prognosis and progression of BCa [8].

1.1.3. Diagnosis and risk factors

BCa is a disease in which malignant tumour cells in the breast grow out of control. It can occur in both men and women, but it's far more common in latter. Survival rates among BCa patients have increased, and the number of deaths associated with primary BCa is steadily declining, primarily due to factors such as early detection, a new personalized approach to treatment, and a better understanding of the disease.

Typically, BCa is diagnosed through a combination of physical examination that involves breast examination and breast self-exam, imaging of tumour site using mammograms, breast ultrasound or magnetic resonance imaging (MRI), and tumour biopsy [9].

Risk factors associated with BCa development and progression are divided into two groups: intrinsic and extrinsic factors. The list of intrinsic factors includes age, sex, race, familial susceptibility and natural hormonal changes. Extrinsic factors include dietary habits, body mass index (BMI), age at first birth, alcohol consumption and exogenous sex hormones intake [10-13]. Furthermore, a number of

studies have shown that declining fertility rate and rise in obesity among women in the United States, contributed to the increase in BCa incidence from 1980 to 2008 [1, 14].

1.1.4. Subtypes of breast cancer

1.1.4.1. Typical molecular subtypes of breast cancer

BCa is a complex and diverse disease, both genetically and clinically. It is categorized into various subtypes that have undergone significant evolution over time. The most prevalent and universally acknowledged categorization of BCa is from the standpoint of immunohistochemistry, which relies on the expression of specific hormone receptors: estrogen (ER), progesterone (PR), and human epidermal growth factor (HER2) [15]. Additionally, Ki-67 staining is also used to distinguish between low- and high-proliferative BCa subtypes [16]. Consequently, four main subtypes of BCa are predominantly recognized based on the surrogate intrinsic subtypes [15]: Luminal A, Luminal B, HER2-positive, Triple-negative/ basal-like [17-19]. Each of these subtypes is characterized by distinct molecular and clinical features which impact both the disease's prognosis and its progression, thereby informing the selection of treatment [15, 20] **(Table 1.1**).

Table 1.1 Molecular subtypes of breast cancer.

Molecular subtype	Molecular characteristics				Prognosis
	ER	PR	HER2	Ki-67	
Luminal A	+	+/-	-	Low	Good
Luminal B	+	+/-	+/-	High	Intermediate
HER2-positive	-	-	+	High/low	Poor
Triple-negative	-	-	-	High/low	Poor

HER2 = human epidermal growth factor receptor 2; ER =estrogen receptor; PR = progesterone receptor; - = negative expression; + = positive expression.

Luminal A: Luminal A BCa is the most common subtype characterized by ER and/or PR positive, and HER2 negative status. Compared to other subtypes, Luminal A tumours tend to exhibit low levels of

Ki-67, indicating a lower proliferation rate and slower growth. These characteristics contribute to a generally less aggressive nature of the disease and better prognosis for patients. Treatment for Luminal A tumours often involves endocrine therapy, such as tamoxifen or aromatase inhibitors, which target hormone receptors. Chemotherapy may also be considered based on specific factors, but it is typically not the primary treatment approach [21].

Luminal B: Luminal B BCa is positive for ER and/or PR, but it differs in that it can be either HER2 positive or negative. Additionally, Luminal B tumours typically express high levels of Ki-67, indicating a higher proliferation ability. Thus it is generally considered more aggressive than Luminal A. The treatment of Luminal B, unlike that for Luminal A, typically involves a combination of different approaches, including endocrine therapy, chemotherapy, and target therapy if the cancer is HER2-positive [21].

HER2-positive: HER2-positive/HER2 enriched subtype is negative for ER and PR, but positive for HER2, thus it exhibits rapid tumour growth. Treatments for this subtype such as trastuzumab (Herceptin) are specifically designed to target HER2 [21].

Triple-negative: Triple-negative breast cancer (TNBC) is negative for ER, PR, and HER2. As a result, TNBC does not respond to hormonal therapies such as tamoxifen or aromatase inhibitors, nor the anti-HER2 trastuzumab (Herceptin). Due to the absence of specific receptor targets, treatment options for TNBC are often limited to chemotherapy, radiation therapy and surgery. However, it's worth noting that ongoing research and clinical trials show great promise for immunotherapy such as anti-PD-1 (programmed death-1) antibody [21] and novel agents such as the novel NFκB inhibitors studied in this project among many others.

As the development of genomics and next-generation sequencing technologies advances, intrinsic subtypes of BCa are further defined by Perou and colleagues in 2000[17] to include the following subtypes: Luminal A, Luminal B, HER2-enriched, Basal-like (mostly TNBCs), and Normal-like. These subtypes with distinct gene expression patterns that reflect differences in tumour biology, have been associated with significant differences in incidence, survival, and response to therapy[22, 23]. Today,

they can be diagnosed using comprehensive genomic methods, such as the Prosigna Breast Cancer Prognostic Gene Signature Assay (PAM50), thereby leading to better understanding, improved prognosis and personalized treatment [22].

1.1.4.2. Typical subtypes of breast cancer

While the majority of BCa cases fall into a handful of well-studied categories, it's important to recognize that rarer types exist. These include, but not limited to, Inflammatory Breast Cancer (IBC), Neuroendocrine BCa (NEBC), Metaplastic BCa (MBC), Paget's Disease of the Nipple, Phyllodes Tumors, Angiosarcoma, and Adenoid cystic carcinoma (ACC). IBC, for example, is a rare and highly aggressive type of BCa which is likely to belong to the TNBC or HER2+ subtypes. It comprised approximately 2.0% of all malignancies of the breast and is responsible for approximately 7% of BCa-related mortality in a SEER based study [24]. Neuroendocrine BCa (NEBC) is another uncommon subtype of breast carcinoma that accounts for approximately 2–5% of all cases [25]. The histological similarities between NEBCs and other breast tumours led to the development of the theory that NEBCs may originate from an epithelial progenitor cell. NEBC, defined as a cancer exhibiting morphological features similar to neuroendocrine tumours in other organs, typically express oestrogen receptors, have lower Ki67 levels, and are HER2-negative. Thus, it can be diagnosed through a combination of morphological evaluation and immunohistochemistry. Due to its unclear definition and rarity, current treatments adopt the same methods used to treat invasive BCa [26]. Metaplastic BCa (MBC) is a typically triple negative type of BCa that starts from cells lining the breast ducts and then morphs into a different type of tumour that resembles a non-breast tissue [27]. Phyllodes tumour is another rare and usually benign subtype of BCa that can be very aggressive and has high risk of recurrence if becomes malignant [28]. Therefore, studies that investigate these a typical, triple-negative and rare types of BCa will help us to develop better understanding of the mechanisms that drive their malignancy, and to develop specific treatment approaches that address the disparities in survival rate among patients suffering from advanced, metastatic BCa.

1.1.5. Breast cancer metastasis

Metastasis is the hallmark of all cancers, including BCa. It is the major cause of multiple organ function failure that often leads to death in BCa patients with advanced disease [29-31] [31, 32]. Improvement in detection of metastatic BCa over recent years has led to significant advancements in the management of the disease, reduced the risk of recurrence and improved treatment regimens [33, 34]. Notwithstanding this, approximately three-quarters of women diagnosed late with stage I-III BCa develop metastatic BCa [35]. Many BCa patients with advanced disease are also receiving chemotherapy, unnecessarily [32]. Thus, there is an urgent need to identify mechanism(s) that drive BCa metastasis and to develop and test novel therapies that can be used alone or in combination with existing treatment regimens to manage the disease progression and improves patient survival rate.

BCa metastasis comprises of a series of sequential steps. Initially, metastasis begins with primary tumour cells invading surrounding tissue followed by these cells intravasating into blood vessels and lymphatic tissues [36, 37]. Invasive BCa cells are then disseminated to nearby and distant organs via the bloodstream and/or lymphatic vessels. As they continue to adapt, avoid and evade the host immune response during these stages and after they extravasate, metastatic BCa cells colonize, grow and influence the behaviour of healthy cells in distant organs.

The concept of metastasis involving both a compatible "seed" and "soil" dates back to 1889, when it was proposed by Stephen Paget. According to his theory, the development of secondary tumours, or metastases, only occurs when the cancer cells ("seeds") and the organ or tissue microenvironment ("soil") are compatible. This means that for metastases to form, the circulating cancer cells must find a suitable environment in the host tissue that supports their growth and survival [38].

BCa preferentially metastasises to the “soils” such as bones, lungs, liver and brain with an estimate ratios at around 70% [39], 60-70%, 40-50% and 10-15% of patients with advanced BCa [3]. In addition, it has been shown that BCa subgroups have different patterns of spread [40] (**Figure 1.3**): ER positive subtypes (Luminal A/B) have the highest skeletal involvement (A – 59.17%, B- 47.14%) with brain being the lowest (A - 4.13%; B - 5.86%). HER2-enriched tumours metastasise more frequently to the skeleton and the liver (34.63% and 31.69%) followed by lung and brain (26.02% and 7.65%). TNBCs

commonly metastasise to bone followed by lung and liver (35.94%, 33.02% and 21.98%). Among all subtypes, they have the highest proportion of BCa patients developing brain metastases at 9.04%. Thus, preventing BCa metastasis to distant organs with skeletal compartment such as bone and brain is likely to benefit a large number of late-stage TNBC patients.

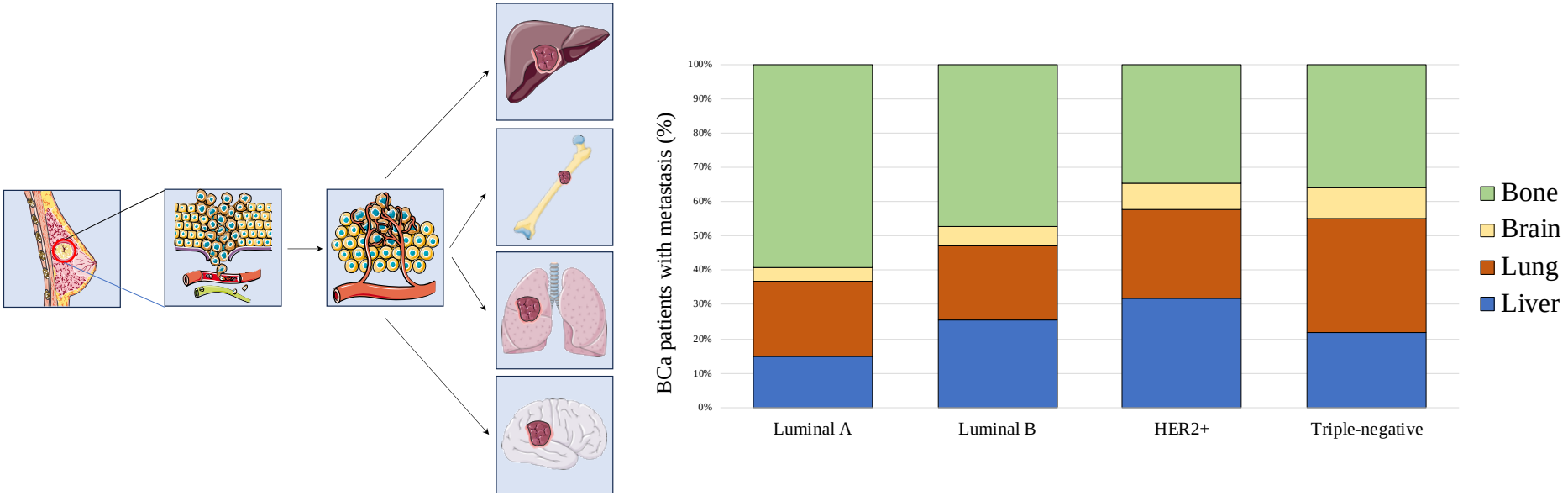

Figure 1.3. Patterns of breast cancer metastatic dissemination. Localised primary breast cancer has a favourable prognosis if caught at an early stage. However, breast cancer cells can enter the circulatory or the lymphatic systems and metastasise to the lymph nodes. Breast cancers have the potential to metastasize to remote locations, predominantly the bone, liver, lung, and brain. Once at this stage, the condition is deemed incurable. Breast cancers often spread to the bone, a phenomenon more typically linked with ER+ (Estrogen Receptor Positive) diseases. On the other hand, Triple-Negative Breast Cancer (TNBC) tends to metastasize to the lungs initially, followed by the bone. Data taken from a obtained 295,213 patients SEER database during 2010-2014 [40].

1.1.5.1. Epithelial-to-mesenchymal transition

The process of Epithelial-Mesenchymal Transition (EMT) is considered part of the "seed" preparation process and thus it plays a crucial role in the initiation of BCa metastasis (**Figure 1.4**) [36, 41]. EMT is characterized by the loss of key properties and features of healthy breast epithelial cells such as polarity and adhesion. At the same time, these cells gain new mesenchymal-like features such as machinery needed for invasion and migration capacities as well as resistance to apoptotic cell death [41]. During EMT, factors such as E-Cadherin, a key regulator of cell-cell interaction, is downregulated thereby leading to loss of ability of these cells to adhere – thus enhancing their ability to move and metastasize. Numbers of studies have reported that downregulation of E-Cadherin in BCa cells is associated with poor prognoses, increased risk of mortality [42] and metastasis [42-44]. Furthermore, a number of nonsense and frameshift mutations of E-cadherin gene that cause its downregulation have been detected in infiltrative lobular BCa [45]. On the other hand, preclinical studies such as that by Fischer *et al.* reported that BCa cells metastasize to the lungs without undergoing EMT, in some cases [46]. In addition, the work of Neelakantan *et al.* suggested that undergoing EMT is not sufficient to convey all invasion characteristics of epithelial cells, but secreted EMT-inducing transcription factors (EMT-TFs) such as Snail1, Twist1 and Six1 play an important role [47]. Nevertheless, the evidence from these limited number of studies is not sufficient to challenge the traditional view that EMT plays a key role in the regulation of BCa initiation and early progression.

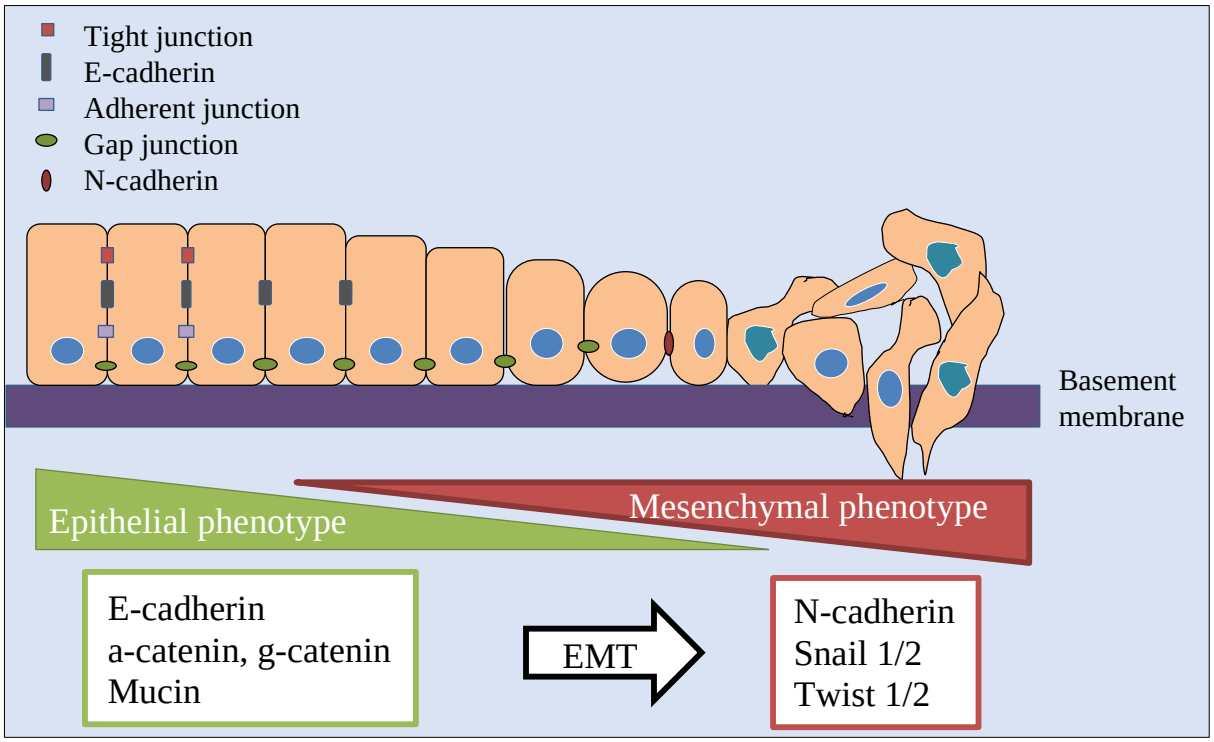

Figure 1.4. General features of EMT. During EMT, the epithelial cells prone to transit into mesenchymal phenotype have the characteristics: loss of differentiation, junctions dissociation, loss of epithelial markers (E-cadherin, catenin, Mucin). The mesenchymal phenotype acquires the mesenchymal markers (N-cadherin, vimentin) and increases expression of EMT-TFs (Snail 1/2 and Twist 1/2). Schematic was created in Microsoft PowerPoint for Office (version 11).

1.1.5.2. Breast cancer bone metastasis

As one of the most common distant metastases of BCa, bone metastases are classified into three categories based on their radiological appearance: osteolytic – leading to bone destruction, osteosclerotic (or osteoblastic) – leading to new bone formation, or mixed - both osteolytic and osteoblastic [37]. BCa cells predominantly cause osteolytic lesions [48]. These lesions are predominately characterized by significant destruction of bone matrix and replacement by tumour mass. The process involves the disruption of normal bone remodelling, which is a balance between bone formation by osteoblasts and bone resorption by osteoclasts. In osteolytic bone metastasis, cancer cells release osteolytic factors such as RANK, receptor activator of NF-κB (RANKL), numerous pro-inflammatory cytokines such as Interleukin-1β (IL1β), tumour necrosis factor α (TNFα), Cluster of differentiation 40 (CD40) that activate NF-κB and downstream components such as c-Fos and nuclear factor of activated T-cells cytoplasmic 1 (NFATc1) that positively regulate osteoclast formation and functions, leading to enhanced bone resorption. This process results in the release of stored growth factors such as

transforming growth factor β (TGFβ) within the bone matrix, which further stimulate cancer growth and bone destruction, leading to a "vicious cycle" [49]. On radiological images, osteolytic lesions appear as areas of decreased bone density, often described as "punched-out" areas. The affected bone becomes weaker and is prone to fractures and other complications: the major causes of cancer-induced bone pain and disability in BCa patients.

1.1.6. Current treatments of breast cancer

The treatment of BCa often involves a combination of several therapies depending on the stage, grade, subtype of the cancer, and the patient's overall health. Surgical removal of breast tumours is one of the most common procedures used in the treatment of primary BCa. Such approach includes conserving surgery (lumpectomy or wide local excision), surgery to remove whole breast (mastectomy) and surgery to the lymph nodes. Radical mastectomy involves complete removal of the breast and axillary lymph nodes [50-52]. Whilst effective, such procedure often cause tissue damage, upper limb edema, paresthesia and upper limb dysfunction. Over recent years, breast-conserving surgery has been combined with breast reconstruction [53, 54]. For most BCa patients, a follow-up post-surgery adjuvant treatment such as radiotherapy or hormone therapy is needed [55]. Some of the commonly used or studied drugs are summarized in **Table 1.2**.

Table 1.2. Table of commonly used and preclinical investigated drugs for breast cancer treatment.

	Drug Description	Examples of Drugs	Mechanism/Target
Chemotherapy[55, 56]	Alkylating Agents	Cyclophosphamide (Cytoxan)	DNA damage
	Antimetabolites	Capecitabine (Xeloda)	Preventing DNA/RNA production
	Anthracyclines	Doxorubicin (Adriamycin), Epirubicin (Ellence)	Interfering DNA replication
	Taxanes	Paclitaxel (Taxol), Docetaxel (Taxotere)	Interfering cell division
	Platinum Agents	Carboplatin (Paraplatin)	DNA damage
	Antitumor Antibiotics	Mitomycin	Interfering DNA replication
	Vinca Alkaloids	Vinorelbine (Navelbine)	Cell structure damage
	Topoisomerase Inhibitors	Irinotecan and Topotecan	Interfering DNA replication
Hormone Therapy[57]	SERMs[58]	Tamoxifen	ER agonists and antagonists
	SERDs[58]	Fulvestrant	Degrade ER
	Aromatase inhibitors	Letrozole, Anastrozole, Exemestane	ER synthesis
HER2 Targeted Therapy	Monoclonal antibodies[59, 60]	Trastuzumab (Herceptin), Pertuzumab (Perjeta)	Preventing dimerization of HER2, blocking HER2 receptor, activating immune system
	Antibody-drug conjugates[61, 62]	Ado-Trastuzumab Emtansine (Kadcyla), Fam-Trastuzumab Deruxtecan-nxki (Enhertu)	HER2
	Tyrosine kinase inhibitors[63-67]	Lapatinib (Tykerb), Neratinib (Nerlynx), Tucatinib (Tukysa)	HER2
Targeted Therapy	CDK4/6 inhibitors[68-71]	Palbociclib, Abemaciclib, Ribociclib	Cell division (PR)
	PARP inhibitors[72-75]	Olaparib, Talazoparib, Veliparib	DNA repair
	PI3K/AKT/mTOR inhibitors[63, 76-80]	Alpelisib Capivasertib, Ipatasertib, MK-2206 Everolimus	DNA repair, Cell survival, growth, proliferation, and intracellular trafficking
	VEGF inhibitor[81, 82]	Bevacizumab, Ramucirumab	Anti-angiogenesis
	Bone-Directed treatment[83-85]	Bisphosphonates, Denosumab	Prevention and management of SREs
Immunotherapy	Immune Checkpoint Inhibitors[86] [87, 88] [89]	Tecentriq (atezolizumab), Atezolizumab, Pembrolizumab, Nivolumab	PD-1
	Cancer Vaccines[90, 91]	NeuVax vaccine (nelipepimut-S)	
	Adoptive T cell transfer[92]	CAR-T cell therapy	
	Oncolytic Virus Therapy[93, 94]	Talimogene laherparepvec (Imlygic), also known as T-VEC	

SERMs: Selective estrogen-receptor modulators, SERDs: Selective estrogen-receptor degraders, SREs: Skeletal-related events.

As seen in **Table 1.2,** Chemotherapy is often subscribed to BCa patients, including patients with operable BCa [56]. To date, there are a variety of types of chemotherapeutic agents that exhibit different mechanisms of tumour inhibition, reducing the risk of disease recurrence and as a result prolonging survival rate among patients. BCa patients are prescribed one of two chemotherapy regimes: traditional chemotherapy and neoadjuvant chemotherapy (NACT) [55]. Research has shown that NACT reduces the need for radical mastectomy, alleviates the disease and surgery associated trauma to patients and improves the patients' life quality. The list of the most used chemotherapeutic agents in clinical practice includes Anthracyclines (such as doxorubicin and epirubicin), Taxanes (such as paclitaxel and docetaxel), 5-fluorouracil (5-FU), Cyclophosphamide and Carboplatin. These agents are prescribed in adjuvant and neoadjuvant chemotherapies, alone or in combination. Chemotherapy and hormone therapy are the most common treatments for women with primary BCa [56].

Hormone therapy (also known as endocrine therapy) is a systemic treatment approach used for BCa patients with hormone receptor-positive breast neoplasms [57]. As previously described, activation of ER or PR is associated with enhanced growth and division of BCa cells. Thus, hormone therapy aimed at blocking the effects of these hormones or reduce their production is effective in limiting the growth of hormone-sensitive breast tumours. They can be divided into two categories: agents that block the production of estrogen, such as aromatase inhibitors (Letrozole, Anastrozole and Exemestane etc.), and others that block estrogen's action that include selective estrogen receptor modulator (SERM) and selective estrogen receptor degrader (SERD) such as Tamoxifen and Fulvestrant [58].

Targeted BCa therapy involves agents that specifically normalise the changes that drive BCa development. The main advantage of this strategy is that these agents exhibit enhanced tumour selectivity than other treatment regimes. Common targeted therapy used in clinical practise include HER2 targeted therapy such as Trastuzumab and Pertuzumab, antibody-drug conjugates (ADC) such as Ado-trastuzumab emtansine, kinase inhibitors such as Lapatinib and Neratinib [63]. HR Targeted therapy include CDK4/6 inhibitors such as Palbociclib, mTOR inhibitors such as Everolimus, and PIK3 inhibitors such as Alprlisib [63, 76]. Common agents prescribed for women with BRCA gene mutations include the PARP inhibitors Olaparib and Talazoparib [72]. BCa patients with TNBC are often

prescribed agents such as sacituzumab govitecan, a trop-2-directed antibody and topoisomerase inhibitor drug conjugate [95].

In recent years, significant advances in cancer immunotherapy have led to the development of a number of agents that suppress tumour growth and spread by reducing the ability of cancer cells to evade the immune response [96]. Today, extensive research has been conducted in the development of various immunotherapeutic agents for the treatment of various cancers, including BCa. The list includes vaccine, chimeric antigen receptor-engineered T cells (Car-T) and immune checkpoint inhibitors (ICIs). The common targets for BCa vaccines under research and development include mucin1 (MUC1), HER2 and telomerase [97], dendritic cell vaccine, whole-cell vaccine and gene vaccine. Car-T therapy has achieved great success in treating haematological malignancy, however, it has been relatively ineffective in treating solid tumours such as BCa. The common targets for Car-T include MUC, HER2 and others. A number of BCa subtypes express high level of PD-L1, thereby indicating that ICIs may be effective in the treatment of these subtypes. A number of studies have also shown that the ICIs Atezolizumab [86], Pembrolizumab [87, 88] and Nivolumab [89] showed positive effects on the management of TNBC when used alone or in combination with other anti-tumour drugs.

Although a number of therapeutic strategies have been used in the clinic for the treatment of BCa, however, disease recurrence still remains a clinical problem and new treatments such as BCa immunotherapy has limited or no effect against aggressive, metastatic BCa subtypes such as TNBC. Management of osteolytic BCa metastases and associated skeletal related symptoms such as bone pain often involves the aforementioned systemic therapies that predominately treat the underlying cancer, along with bone-targeted agents such as bisphosphonates or denosumab, which are effective in halting osteoclast activity and slowing the progression of bone destruction [98, 99]. Thus, there is a need to identify new therapeutic targets for the treatment of difficult to treat BCa subtypes, such as osteolytic BCa metastases.

1.2. The TRAF/NFκB signalling pathway

The nuclear factor kappa B (NFκB) is a family of signal transduction proteins and transcription factors that regulate a variety of physiological processes such as immune response, inflammation, cell death [100]. In mammalian cells, there are five NFκB/Rel members: NFκB1 (p50 and its precursor p105), NFκB2 (p52 and its precursor p100) in the NFκB subfamily and RelA (p65), RelB and c-Rel in the Rel family. Under normal conditions, NFκB complexes exist in an inactive state in the cell cytoplasm [101]. When activated, these complexes undergo changes that allow certain component(s) to translocate to the nucleus where bind to DNA and regulate the transcription of a variety of targeted genes. NFκB signalling consists of two pathways, the canonical and non-canonical pathways (**Figures 1.5** and **1.6)**.

1.2.1. Canonical NFκB signalling

The canonical NFκB pathway is activated by receptors for a variety of pro-inflammatory, osteolytic and pro-tumour factors. The list includes, but are not limited to, tumour necrosis factor receptor (TNFR), interleukin 1 receptor (IL-1R), cluster of differentiation 40 (CD40), receptor activator for NFκB ligand (RANKL), and toll-like receptor (TLR) [102]. Activation of these receptors by their respective agents triggers a series of intracellular cytoplasmic cascades that eventually lead to the nuclear translocation of NFκB dimers (**Figure 1.4**). The ligand-bound receptor complex recruits a variety of adaptor proteins, receptor recruitment factors and cytoplasim proteins. As **Figure 1.4** shows, activation of receptors for IL1β, TNFα and Lipopolysaccharides (LPS) initiate the recruitment of adaptor proteins such as tumour necrosis factor (TNF)-receptor-associated factors (TRAFs), IRAK, MYD88 and TRADD to the receptor-ligand complex [103-105].

TRAFs are one of the main family of adaptor proteins that are recruited to receptors upon activation of canonical NFκB signalling [106, 107]. The seven known TRAFs are involved in the regulation of various cellular responses such as inflammation, immune response and cell death [108]. A number of studies have shown that TRAF2 and TRAF6 are the key signal intermediate adaptor proteins that are responsible for the regulation of canonical NFκB signalling. The recruitment of TRAF2 and/or TRAF6

to the ligand and receptor complex initiates a series of events that involves the phosphorylation and activation of members of IκB kinase (IKK) family of cytoplasmic signalling proteins [109]. The active form of IKK complex consists of phosphorylated IKKα and IKKβ and the adaptor protein IKKγ (NEMO) subunit [102]. Once phosphorylated by IKKα/β/γ, IκB undergoes proteasomal degradation, thereby freeing p50/RELA NFκB dimer to translocate to the nucleus where it functions as a transcription factor responsible for the activation of target genes implicated in inflammation, immunity and cell death.

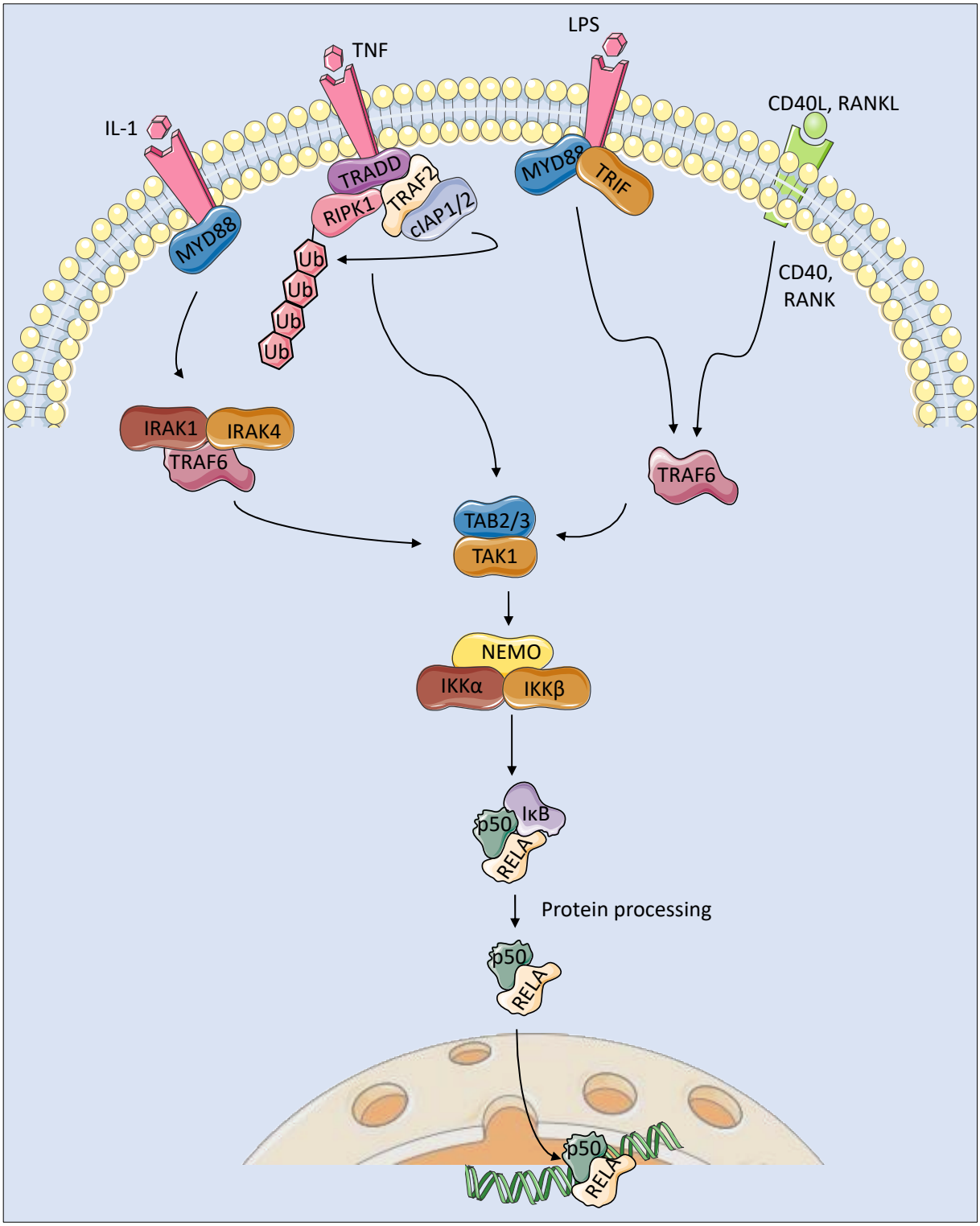

Figure 1.5. The canonical NFκB signalling transduction pathways. *Schematic was created* in Microsoft PowerPoint for Office (version 11) and selected schematic modules were obtained from https://smart.servier.com/. Refer to the text for more details.

1.2.2. Non-canonical NFκB signalling

The non-canonical NFκB pathway is activated by relatively fewer pro-inflammatory mediators that include B-cell activating factor belonging to TNF family receptor (BAFFR), CD40 and lymphotoxin-β receptor (LTβR). Unlike canonical NFκB signalling, this pathway relies on the phosphorylation and processing of p100, two processes that are initiated by the catalytic activities of the IKKα/IKKα dimer by NFκB -inducing kinase (NIK) (**Figure 1.5**). Under resting condition, the activity of NIK is kept low by the binding to TRAF-cIAP complex such as TRAF3-TRAF2-cIAP [106, 110]. Once activated, the TRAF2-TRAF3-cIAP complex is recruited to the receptor and as a result NIK is free to phosphorylate the IKKα/IKKα complex which in turn phosphorylates p100 leading to its processing into and nuclear translocation of P52/RELB dimer [111] (**Figure 1.5**).

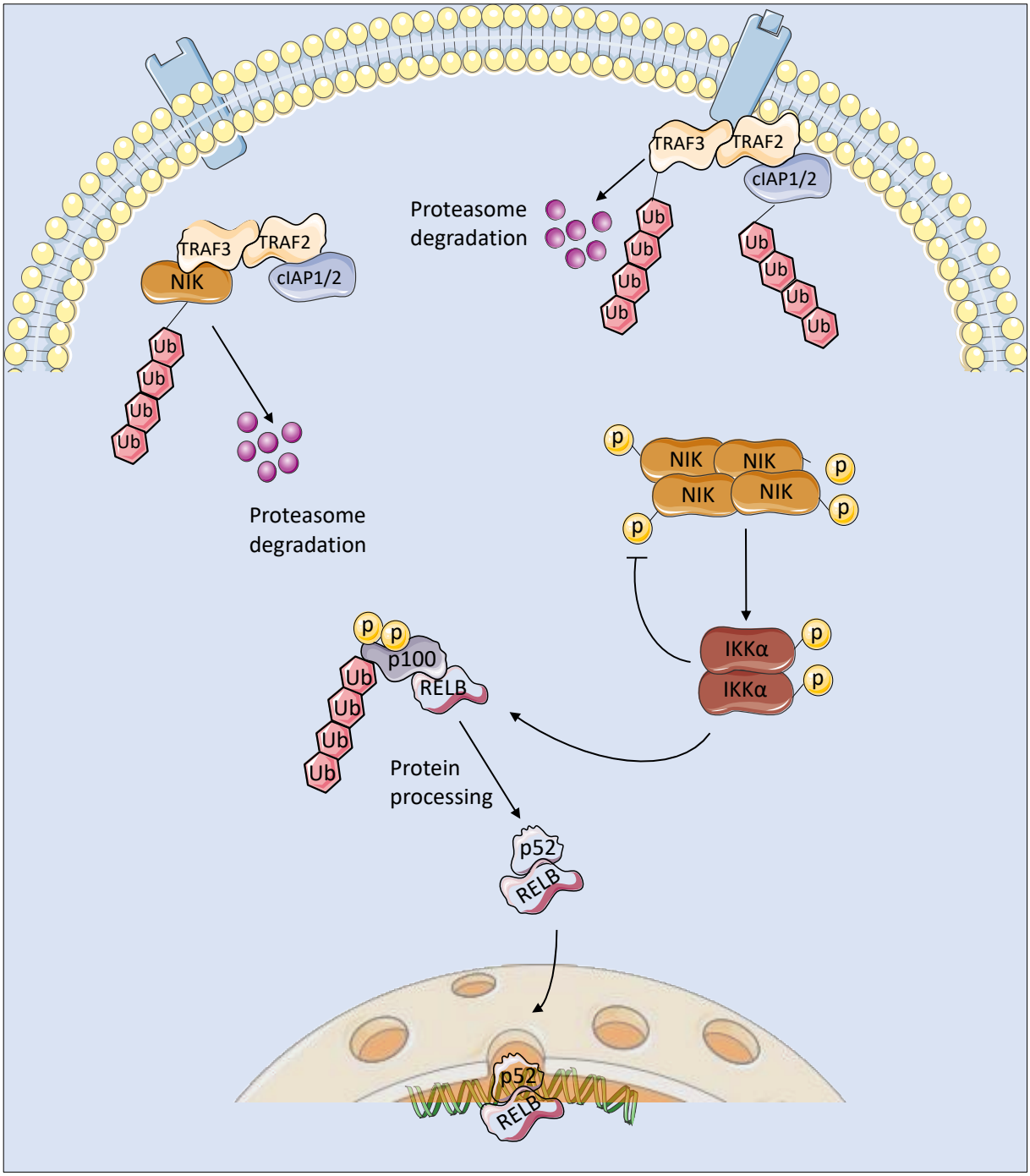

Figure 1.6. The non-canonical NFκB signalling pathway. Schematic was created in Microsoft PowerPoint for Office (version 11) and selected schematic modules were obtained from https://smart.servier.com/. Refer to the text for more details.

1.2.3. TRAF signalling in inflammation and immunity

The TRAF family of adaptor proteins and recruitment factors play a vital role in inflammation, immunity, tumorigenesis, normal and cancer induced bone remodelling. All seven TRAF1-7 are known to regulate signal transduction pathways such as - but not limited to - canonical and non-canonical NFκB, interferon

regulatory factors (IRFs) or mitogen-activated protein kinase (MAPK) signalling pathways [112]. TRAF6 is the most studied member of the TRAF family of adaptor protein and the most commonly associated with E3 ubiquitin ligase activity and inflammation among all TRAF members. TRAF6 interacts directly with a wide range of proteins implicated in the regulation of the aforementioned functions. The list includes receptors (RANK, TLR, NLR and IL1-R), adaptor proteins (MyD88, TRIF, TAB2, NEMO), enzymes (TAK1, TBK1, ASK1) and transcription factors (STAT1, STAT3) [113]. In response to signals form receptor such as RANKL, IL-1R and TLRs, TRAF6 is recruited and predominately mediates the activation of canonical NFκB as well as MAPKs signalling that lead to the transcription of various tumour-, bone- and immune-cell related. TRAF5 is another member of the TRAF family that is known to mediate TNFR/MAPs signalling [114, 115]. TRAF2 is a key component of the pro-inflammatory TNF receptor signalling as well as several other receptors [116]. In addition to NFκB activation, TRAF2-mediated signalling leads to the activation of MAPKs such as JNK and p38 that play crucial roles in inflammation and cell death [116-120]. TRAF2 and 3, as adaptor proteins and E3 ubiquitin ligases, are involved in inflammation in various organs including skin [121, 122], cardiovascular [123, 124] and bowel diseases [125]. TRAF4 is involved in various developmental, morphogenic and oncogenic processes [126] and pulmonary and bowel inflammation [127, 128]. TRAF1 has been identified to play a role in rheumatoid arthritis (RA) [129], atherosclerosis [130] and inflammation related to lung, liver, brain and bowel diseases [125, 131-133]. TRAF5 share structural similarity to TRAF2 and TRAF3 and it has been implicated in inflammation related to lung, cardiovascular and liver diseases. Similar to TRAF2, TRAF3 and TRAF6, the RING domain of TRAF7 also possesses E3 ubiquitin ligase activity [134, 135].

Current studies show that all members of the TRAF family do not only function as adaptor proteins and E3 ubiquitin ligases, but some members such as TRAF2 and TRAF3 also act as regulatory factors in immunity by regulating processes such as macrophage recruitment [136] and exocytosis [137], respectively. TRAF3 is also involved in antiviral immunity and it regulates the production of the pro-inflammatory and immune regulator β-interferon [138]. Compared to other TRAFs, TRAF6 has a specific binding site to interact directly with CD40 and RANKL[139, 140].

Table 1.3 Role of TRAFs and their activating factors and receptors in inflammatory diseases.

TRAFs	Functions	Factor/Receptor	Inflammatory diseases
TRAF1	Signalling adaptor[141]	TNFα, TLRs, TRAF2, IKKβ, NIK, ASK1, TRIF[113, 141, 142]	Rheumatoid arthritis [129], atherosclerosis [143], lung, liver [144], brain inflammation [133], inflammation related to bowel diseases.
TRAF2	Signalling adaptor and E3 ubiquitin ligase[141, 145, 146]	TNF-R, TLRs, NLRs, RIG-1 and respective receptors [116-118, 147]	Skin, cardiovascular and bowel diseases related inflammation [124, 125, 148].
TRAF3	Signalling adaptor and E3 ubiquitin ligase[141, 145, 146]	TNF-R, TLRs, NLRs, RIG-1 and respective receptors[141, 145, 146, 149]	Brains, cardiovascular, bone, liver inflammation [124, 125, 148].
TRAF4	Signalling adaptor[141, 145, 146]	GITR, NOD2, IL-17R, IL-25R, TRIF, TRAF6, IKKα, MEKK3, MEKK4, SMURF2, and $p47^{phox}$	Various developmental, morphogenic and oncogenic processes, pulmonary and bowel inflammation [148].
TRAF5	Signalling adaptor and E3 ubiquitin ligase[115]	TNF-R superfamily, TLRs, RIG-I, IL-17R, and gp130 [114, 115, 147]	Inflammation related to lung, cardiovascular and liver diseases [124, 148]
TRAF6	Signalling adaptor and E3 ubiquitin ligase[150-152]	Receptors (RANK, TLR, NLR and IL1-R), adaptor proteins (MyD88, TRIF, TAB2, NEMO), enzymes (TAK1, TBK1, ASK1) and transcription factors (STAT1, STAT3)[153-158]	Cardiovascular, liver, brain, airway inflammation and bowel inflammation diseases [124]
TRAF7	Signalling adaptor and E3 ubiquitin ligase[159]	MEKK1-3, NIK, ASK1 and TAK1[113]	No evidence from human and animal studies.

1.2.4. TRAF signalling in breast cancer

Several members of the TRAF family are implicated in the initiation and progression of various cancers [160]. Among the seven known TRAF proteins, TRAF2, TRAF3, TRAF4, and TRAF6 have been linked to BCa initiation, progression, metastasis and survival in preclinical models and patients. For in depth investigation of the association of TRAFs, particularly TRAF2,4 and 6, with all aspects of BCa in vitro, in vivo and in human, refer to **Chapter 3**.

1.2.4.1. Role of TRAF2 in breast cancer

Low expression of TRAF2 in BCa patients is associated with increased survival rate[161]. Conversely, down-regulation or inhibition of TRAF2 suppress BCa cell adhesion, migration and invasion *in vitro* and reduces the growth of tumours in animal models of BCa [162].

1.2.4.2. Role of TRAF3 in breast cancer

Several studies have shown that micro ribonucleic acids (miRNAs) that targets TRAF3 affect the growth and metastasis of BCa tumours. More specifically, miR-214 is found to be highly regulated in BCa patients and preclinical studies in rodents have shown that miR-214 targets TRAF3 in the bone resorbing cells, osteoclasts, to promote osteolytic bone metastasis of BCa *in vivo* [163]. Interestingly, miR-29-3p promotes the progression of TNBC cells via downregulating TRAF3 [164].

1.2.4.3. Role of TRAF4 in breast cancer

Down-regulation of TRAF4 is associated with inhibition of BCa cell proliferation and invasion *in vitro* and reduction of metastasis in *in vivo* models of advanced BCa [162, 165, 166]. Furthermore, low expression of TRAF4 is associated with increased cumulative and overall survival rate in BCa patients [161, 166, 167].

1.2.4.4. Role of TRAF6 in breast cancer

Numerous studies have implicated TRAF6 in all aspects of BCa (refer to **Chapter 3**). Inhibition of TRAF6 activity by genetic and pharmacological approached and its low expression are associated with reduced BCa cell adhesion, invasion and migration *in vitro* and *in vivo* [168]. It has also been demonstrated that TRAF6 regulates the activities of various oncogenic proteins particularly TGFβ, Akt and RAS, and a number of pro-inflammatory cytokines implicated in advanced metastatic BCa including RANKL, IL1β and CD40L [168-176]. Conversely, low expression of TRAF6 in BCa patients improves metastasis-free survival and cumulative survival [168, 177-179]. Collectively, these studies implicate TRAF2, 3, 4 and 6 in BCa tumour growth and metastasis.

1.2.5. TRAF signalling in bone remodelling

TRAF proteins are important mediators of various functions in the skeleton including immune responses, bone homeostasis, skeletal tumour burden and tumour induced osteolytic bone destruction. Bone remodelling is a continuous process of bone formation and bone resorption. It is a highly regulated and balanced process that is crucial for maintaining bone health and calcium homeostasis in the body. This process is primarily orchestrated by the differentiation, activity and survival of two key cell types, the bone-forming osteoblasts and bone-absorbing osteoclasts.

1.2.5.1. Role of the TRAF/NFκB axis in osteoclastogenesis and osteolysis

RANKL, as one of the master regulatory factors of osteoclast formation, activity and survival, is expressed and secreted by cells such as osteoblasts and bone marrow stromal cells. The binding of RANKL to its receptor RANK (or its decoy receptor osteoprotegerin (OPG)) triggers the lineage commitment and fusion osteoclast precursors (pre-osteoclast) as well as the activation of mature multi-nucleated osteoclasts [180-183]. TRAF proteins, especially TRAF6, are critical components of the RANKL/RANK/OPG signalling pathway. Upon the binding of RANKL to RANK, TRAF6 is recruited to the intracellular domain of RANK, thereby triggering a signalling cascade that leads to the activation

of several downstream pathways, including the IKK/IκB/NF-κB (described in **section 1.2**) and MAPKs, which ultimately promotes osteoclastogenesis and osteolysis [157, 182]. Moreover, RANKL-RANK signalling activates NFATc1 and c-Fos, which are considered to be master regulators of osteoclastogenesis [180]..

1.2.5.1. Role of the TRAF/NFκB axis in osteoblastogenesis (bone formation)

While much less is understood about the role of TRAFs in osteoblastogenesis, compared to osteoclastogenesis, some studies also implicated TRAFs in bone formation. TRAF6, for instance, is involved in Bone Morphogenetic Proteins (BMPs) signalling, crucial regulators of osteoblast differentiation and function [181].

Moreover, there is evidence to suggest that TRAF6 activation by osteolytic factors such as IL1β and CD40 acting on osteoblasts, stromal cells and their percussors [184, 185], suggest an integrative role for TRAF6 signalling in coordinating both bone resorption and formation in the bone remodelling process.

Thus, it is not surprising that dysregulation in TRAF signalling, particularly TRAF6, result in various bone disorders. For example, overactivation of TRAF6 promotes osteoclastogenesis, leading to excessive bone resorption as seen in conditions like osteoporosis and rheumatoid arthritis [129]. Conversely, impairment of TRAF6 signalling lead to impaired bone resorption that results in excessive bone volume observed in osteopetrosis [186-190].

While the roles of TRAFs, especially TRAF6, in bone remodelling are yet to be fully understood, TRAF6 inhibition shows promise in the treatment of excessive osteoclastic bone destruction associated with a variety of bone diseases.

1.2.6. Role of the TRAF/NFκB axis in breast cancer bone metastasis

Bone metastasis and pain are common complication associated with various advanced cancers, particularly BCa. Bone metastasis involves the migration, spread, homing and colonisation of tumours cells from the primary site to skeletal sites, particularly long bones, spine and cranium, where they invade adjacent bone tissues and disrupt normal bone remodelling. TRAFs, particularly TRAF6, have been implicated in multiple steps of this metastatic process:

BCa osteotropic cell behaviour: TRAF6, as well as other TRAFs, regulate the behaviour of metastatic and osteotropic (cancer cell in bone) via activation of signal transductions downstream of TNF receptor family members and the interleukin-1 receptor/Toll-like receptor superfamily that predominately responsible for activation of NFκB and MAPK signalling pathways, among others. The regulation of the behaviour of BCa, bone and immune cells in the tumour microenvironment in bone by the TRAF6/NFκB axis facilitate skeletal tumour burden, osteolysis and pain.

Bone remodelling in the metastatic niche: Metastatic BCa cells, particularly osteotropic clones, disrupt the balance of bone remodelling by interacting and altering the differentiation, activity and survival of osteoclasts, osteoblasts and their precursors [36, 191]. In BCa bone metastasis, osteoclast differentiation, activity and survival are enhanced, osteoblast-induced RANKL production is increases, whereas the bone-forming ability of osteoblasts is suppressed - thereby leading to excessive bone loss and weakened bone structure. The TRAF6/NFκB and TRAF6/MAPKs axes play key roles in these processes (**Figure 1.7**).

Tumour-induced osteolysis: The enhanced BCa cell - osteoclast – osteoblast interactions and most importantly excessive bone resorption releases a variety of pro-tumour, pro-osteolytic and pro-growth factors stored in the bone matrix, such as TGF-β, IGFs, and calcium. These factors further stimulate skeletal tumour expansion and bone destruction in the tumour microenvironment, creating a ‘vicious cycle’ (**Figure 1.7**).

Evasion of immune response: TRAF6 also plays roles in immune regulation [145, 192], and dysregulation of TRAF6 signalling contribute to the ability of metastatic BCa cells to evade immune surveillance in the bone microenvironment [146, 193].

Collectively, TRAF signalling, particularly via the TRAF6/NFκB/MAPK axis, orchestrates BCa bone metastasis through its ability to regulate the interaction and crosstalk between osteotropic BCa cells, osteoclasts, osteoblasts and immune cells. However, much remains to be discovered about the specific roles of different TRAFs and their interactions in the 'vicious cycle'. Future research in this area will provide further insights and lead to the development of novel therapeutic targets for the prevention and treatment of BCa osteolytic metastases and related bone pain.

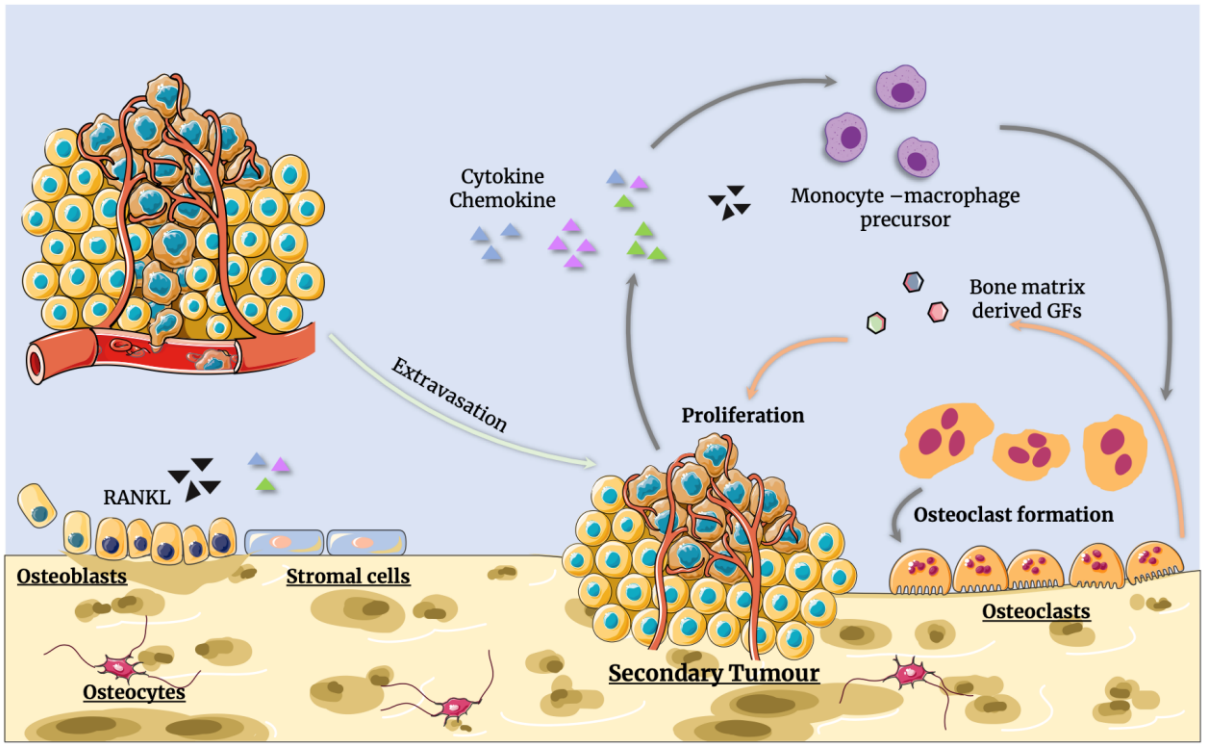

Figure 1.7. Bone Metastasis Cascade and Vicious Cycle. This diagram depicts the multi-stage process of bone metastasis and the ensuing vicious cycle. Post a dormancy phase, disseminated cancer cells colonize the bone tissue. Upon activation, these cells release substances that prompt osteoblasts to generate frail ectopic bone and secrete RANKL, thereby encouraging osteoclast formation and osteolysis. The growth factors residing in the bone further fuel tumour cell proliferation. Refer to section 1.2.6 for a detailed discussion.

1.3. TRAF6 as a potential therapeutic target in breast cancer

Advanced metastatic BCa is the fifth cause of cancer mortality worldwide. Evidence to date suggests that disease recurrence and metastasis of certain types of BCa, particularly TNBC, remains a major clinical problem. The pro-inflammatory TRAF/NFκB axis plays an essential role in most aspects of secondary BCa in bone particularly the ability of BCa cells to move and to influence healthy bone and immune cells in the tumour microenvironment in the skeleton. TRAF2/6-activating pro-inflammatory mediators such as RANKL, CD40, TNFα, and IL1β are key regulators of BCa cell – osteoblast – osteoclast crosstalk, a hallmark of metastatic BCa in bone. A number of aforementioned *in vitro* and *in vivo* studies suggest that NFκB inhibition by targeting TRAF2, 3, 4 and 6 represent a potential therapeutic strategy for the treatment of BCa bone metastasis. Of these four TRAF proteins, TRAF6 has emerged as the main regulator of the difficult-to-treat TNBC. Researchers such as Yang *et al* suggested that TRAF6 may even be an uncharacterized oncogene [171]. Furthermore, numerous studies have shown that indirect inhibition of TRAF6-mediated signalling, particularly NFκB, reduces the *in vitro* motility and *in vivo* growth and metastasis of BCa tumours that are known to metastasise to bone [173, 194].

Collectively, findings to date indicate that TRAF6 represents a potential therapeutic target in the treatment of advanced, metastatic BCa subtypes, particularly osteotropic TNBC cells. A recent study by our group has shown that inhibition of TRAF6 by targeting the CD40/RANK domain of using an agent called 6877002 reduced tumour growth and bone metastasis in mouse models of TNBC [184]. In this study, I plan to further investigate the role of the pro-inflammatory TRAF6/NFκB axis in the interactions of metastatic BCa and bone cells, and validate if pharmacological inhibition of canonical NFκB signalling by a novel, highly selective class of TRAF6 inhibitors from the FSAS3 family can reduce the growth, metastatic and osteolytic behaviour of highly aggressive mouse and human TNBC cells in preclinical models.

1.4. Hypothesis and Aims

The aim of this project was to investigate the role of the pro-inflammatory TRAF6/NFκB axis in the regulation of growth, metastatic and osteolytic behaviour of BCa cells, particularly TNBC cells, and test the hypothesis that pharmacological inhibition of the pro-inflammatory canonical NFκB signalling by a novel, selective TRAF6 inhibitor called FSAS3 reduces the ability of BCa to growth, migrate, invade and to support bone cell activity and osteolysis in mouse and human preclinical models of TNBC.

This hypothesis was investigated by:

1. Conducting a systematic review and meta-analysis to investigate current evidence to support the involvement of the seven members of the TRAF family of adaptor proteins in metastatic BCa cell behaviour *in vitro* and *in vivo*, tumour burden and metastasis in animal models and survival rate in patients.
2. Conducting a follow-up bioinformatics validation to further explore the mechanisms, functions, processes and pathological disorders by which TRAF, particularly TRAF2/6, manipulation and expression influence BCa progression and metastasis *in vitro, in vivo*, in patients.
3. Assessing the protein expression and signal transduction activity of TRAF2/6 in a panel of mouse and human BCa cells with different growth and metastatic abilities.
4. Evaluating the effects of knockdown and pharmacological inhibition of TRAF6, using a verified CD40-TRAF6 inhibitor 6877002 and its novel congener FSAS3 and other structurally-related analogues, on the ability of TRAF-activating pro-inflammatory factors, specifically RANKL (TRAF6) and TNFα (TRAF2) to
    a. activate of NFκB signalling in mouse and human parental and osteotropic TNBC cells.
    b. influence the viability, migration, and invasion of highly metastatic syngeneic mouse and human BCa cells *in vitro*.
5. Examine the mechanism(s) by which FSAS3 exert its anti-TRAF6, anti-NFκB, and anti-tumour effects *in vitro*.

6. Finally, I tested the effects of FSAS3 – alone and in combination with a panel of FDA-approved chemotherapeutic agents - on the ability to inhibit BCa cell growth *in vitro* and to exert anti-osteolytic effects in BCa cell – mouse calvarial model *ex vivo*.

CHAPTER 2. Materials and Methods

2.1. Preparation of Compounds Tested

The confirmed small-molecule CD40-TRAF6 inhibitor, 6877002, was acquired from Abcam (Item No. ab146829). Novel congeners of 6877002, designated as FSAS1-5, were synthesized by Professor Anna Sparatore's team at the University of Milan, Italy. These compounds were dissolved in dimethyl sulfoxide (DMSO; Honeywell, No. D5879) to a concentration of 100 mM, following the guidelines provided by the manufacturer, and were stored at 4 ºC.

2.2. General Tissue Culture

Cell culture procedures were executed within a Class II laminar flow cabinet. Prior to use, both the cabinet and all materials were sterilized using 70% (v/v) Industrial Methylated Spirits. Any solutions intended for cell handling were pre-warmed to 37ºC.

The cells were maintained in an environment composed of 5% CO2 and 95% humidity at 37ºC. The degree of cell confluency was evaluated through phase-contrast microscopy.

2.2.1. Cancer cell lines

Human MDA-MB-231, MCF-7, mouse E0771, 4T1 BCa cell lines were purchased from ATCC (Manassas, VA, USA). Cancer cells were cultured in 25 cm^2 or 75 cm^2 flasks and passaged every 48-72 hours at a ratio of 1:5 MDA-MB-231, 1:5 MCF7, 1:10 E0771, 1:10 4T1. The bone-seeking MDA-MB-231 and 4T1 sub-clones were previously generated through *in vivo* passaging and donated by Dr. Nadia Rucci (University of L'Aquila) and sub-cultured at a ratio of 1:10. To subculture cells, the monolayer was washed in pre-warmed PBS 1× (Thermo Fisher Scientific, No. 10010023) and detached by treatment with Trypsin-ethylenediaminetetraacetic acid (EDTA) (Sigma-Aldrich, No. T4174) for 5-10 minutes. Standard medium was added at a 3:1 ratio to trypsin in order to inactivate its proteolytic activity. The cells were transferred to a fresh sterile 15 ml tube that was then centrifuged at 300G for 5 minutes. The supernatant was removed and cells resuspended in a 1 ml standard medium. A percentage of the suspension was placed into a new 25 cm^2 or 75 cm^2 flask containing up to 15 ml standard medium. The remaining cells were counted and used for experiments.

2.2.2. Macrophage/monocyte cells

Murine macrophage-like cell line RAW264.7 were kindly provided by Professor Dominique Heymann (University of Sheffield, UK). RAW264.7 cells (passage number <15) were cultured in 15-20 ml standard medium using Dulbecco's Modified Eagle Medium (DMEM) with GlutaMAX™ (Thermo Fisher Scientific, No. 61965026) supplemented with 10% Fetal Bovine Serum (FBS; Thermo Fisher

Scientifc, No. 10270106) and 100 U/ml penicillin with 100 μg/ml streptomycin (Thermo Fisher Scientific, No. 15140-122) in 75 cm^2 flasks (Thermo Fisher Scientific, No. 156499) and passaged every 2-3 days at a ratio of 1:10 by removing 15 ml of medium, scrapping cells from the flask and adding the cell suspension to a new 75 cm^2 flask with fresh standard DMEM medium.

2.2.3. Generation of osteoclast-like cells from RAW264.7 cells

RAW264.7 macrophage-like cells are plated in a 96-well plate at a density of 2000 cells/100 μl of standard DMEM (Collin-Osdoby and Osdoby, 2012). The following day, RAW264.7 cells are given FSAS3 (0.03, 0.1, 0.3, 1, 3 mM) 1 hour prior than 100 ng/ml of RANKL alone or plus 10 ng/ml of TNFα or 20% v/v conditioned medium. Cultures were stopped on day 5. Osteoclast-like cells are fixed and stained as seen in **section 2.2.6**.

2.2.4. Preparation of conditioned medium

Human BCa cells MDA-MB-231 and murine 4T1 cells were grown in a 6-well plate (Corning, No.3516) in a 2 ml of standard medium. After reaching ~70% confluency, the medium was replaced with serum free medium. After 16 hours, conditioned medium was collected and filtered with Acrodisc® Syringe filter pore size of 0.45 mm (Pall, No. 4614) and stored in -20 ºC.

2.2.5. Cell Behaviour Assessments

2.2.5.1. Cell Viability Assay

2.2.5.1.1. AlamarBlue™ Assay

Cell viability was assessed by the Alamar Blue ™ assay. Briefly, the active ingredient of Alarm Blue ™ (Thermo Fisher Scientific, No. DAL1100) reagent, resazurin (7-Hydroxy-3*H*-phenoxazin-3-one 10-oxide), is a non-toxic and cell-permeable compound that is blue in color and virtually non-fluorescent, it can be irreversibly reduced to the pink-colored and highly fluorescent resorufin (7-Hydroxy-3*H*-phenoxazin-3-one) when entering living cells (**Figure 2.1**) [195-198]. Changes in viability can easily detected using either an absorbance- or fluorescence-based plate reader.

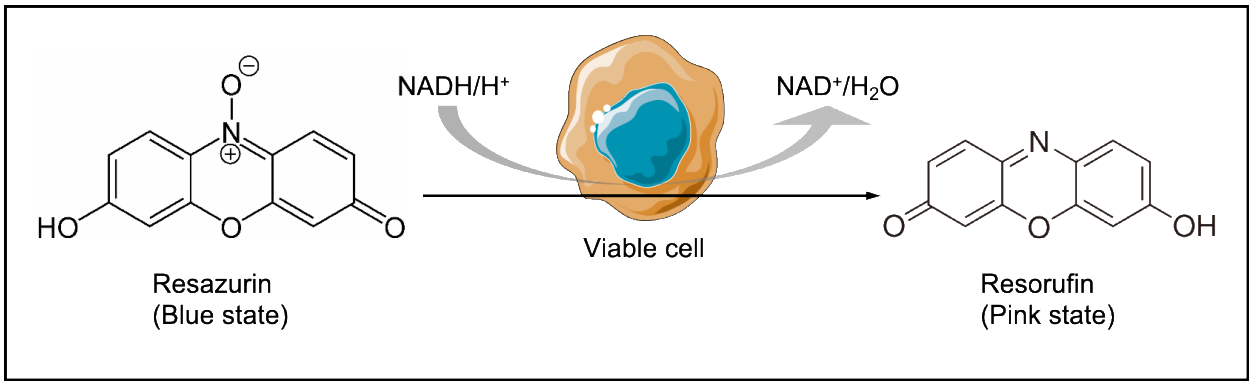

Figure 2.1. Alamar Blue™ reaction equation. Dehydrogenase enzyme of viable cells reduced resazurin in the form of fluorescent metabolic product resorufin. Refer to text for details.

Alamar Blue ™ was used to determine the effect of verified and novel TRAF6 inhibitors (6877002 and FSAS1-5) on BCa cell viability. BCa cells were seeded in a 96-well plate in standard medium at a density of parental MDA-MB-231: 3000, osteotropic MDA-231-BT: 3000, MDA-TRAF6^{KD}: 3000, MCF7: 3000, 4T1: 1500, 4T1-BT: 1500, 4T1-TRAF6^{KD}: 1500 and E0771: 3000 cells per well. After 24 hours, medium was replaced with 1% FCS DMEM and treated with 6877002, FSAS1-5 or vehicle (DMSO), as control.

Cell viability was assessed at 48- and 72-hours post-seeding, following a 3-hour incubation with Alamar Blue™ (10% v/v). Measurements were conducted at an excitation wavelength of 530 nm and emission wavelength of 590 nm using a SpectraMax M5® microplate reader (Molecular Devices), as depicted in **Figure 2.2**. To eliminate background fluorescence, a blank absorbance value (from wells containing

only medium and Alamar Blue™) was subtracted from all readings. The viability percentage was calculated by dividing each reading by the initial absorbance value of the cells. To fix the cells, the medium was replaced with 100 µl of 10% neutral buffered formalin. Images of each cell group were captured using an EVOS Cell Imaging System (Thermo Fisher Scientific) at 10X magnification.

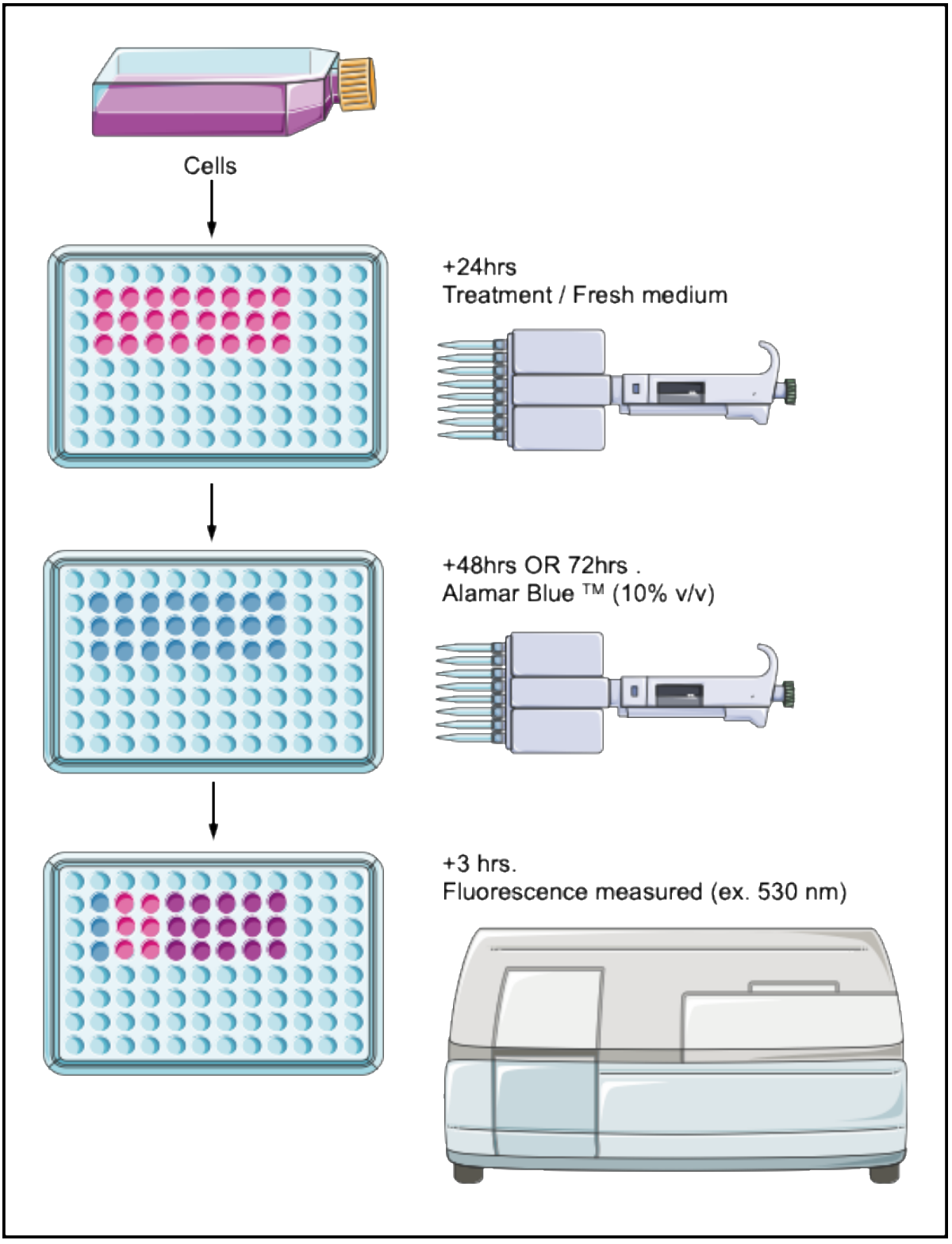

Figure 2.2. Cell viability assessed by AlamarBlue™ assay. BCa cells are plated in 96-well plates. After overnight of adherence, cells are treated with compounds or vehicle with fresh medium. After the incubation period, cells are exposed to AlamarBlue™ (10% *v/v*) for 3 hours. Fluorescence is measured using SpectraMax M5® microplate reader. Refer to text for details.

2.2.5.1.2. Drug combination assay

The assess the effect of FSAS3 when combined with different chemotherapeutic agents. A combined AlamarBlue ™ was applied and further Chou-Talalay Method[199] was used to calculate the combination index using CompuSyn software (available at: https://www.combosyn.com/). The list of anti-BCa therapies/inhibitors and the doses used in viability assay are listed in **Table 2.1**.

Table 2.1. Concentration used to in viability assay.

	Drug	**Target**	**Concentrations used to generate response curve**	**Company (Catalogue number)**
Single	FSAS1-5	TRAFs	0.00, 0.01, 0.03, 0.10, 0.30, 1.00, 3.00, 10.0, 30.0, 100μM	NA
	6877002	TRAF6 (CD40 pocket)	0.00, 0.01, 0.03, 0.10, 0.30, 1.00, 3.00, 10.0, 30.0, 100μM	Abcam, No. ab146829
Combine (+1.00, 10.0 μM FSAS3)	Docetaxel	Microtubule	0.00, 0.01, 0.03, 0.10, 0.30, 1.00, 3.00, 10.0, 30.0, 100nM	Selleckchem, No. S1148
	Doxorubicin	Topoisomerase I, II	0.00, 0.001, 0.003, 0.01, 0.03, 0.10, 0.30, 1.00, 3.00, 10.0, 30.0 μM	Sigma-Aldrich, No. T5648
	5-Fluorouracil	Thymidylate synthase	0.00, 0.03, 0.10, 0.30, 1.00, 3.00, 10.0, 30.0, 100, 300μM	Sigma-Aldrich, No. F6627
	Tamoxifen	Estrogen receptor	0.00, 0.001, 0.003, 0.01, 0.03, 0.10, 0.30, 1.00, 3.00, 10.0, 30.0 μM	Sigma-Aldrich
	Paclitaxel	Microtubule	0.00, 0.01, 0.03, 0.10, 0.30, 1.00, 3.00, 10.0, 30.0, 100nM	Selleckchem, No. S1150
	Rapamycin	mTOR	0.00, 0.001, 0.003, 0.01, 0.03, 0.10, 0.30, 1.00, 3.00, 10.0, 30.0 μM	Sigma-Aldrich
	Cyclophosphamide	DNA replication	0.00, 0.001, 0.003, 0.01, 0.03, 0.10, 0.30, 1.00, 3.00, 10.0, 30.0, 100mM	Sigma-Aldrich, No. BP1094

NA refers to not applicable.

2.2.5.2. Cell Migration Assay (wound-healing)

The wound healing assay was utilized to evaluate 2D migration capacity of human parental MDA-MB-231 and osteotropic MDA-231-BT BCa cells with a density of 40 × 10^4 plated in 24-well plate in standard DMEM. After 24 hours, the confluent monolayer was exposed to a concentration of 5 µg/ml of mitomycin-C (Sigma, No. M0440) for a span of 2 hours, aiming to inhibit proliferation. Utilizing a 10 µl pipette tip, a vertical scratch was made on the monolayer, the cells were then washed eight times with serum free medium to remove any loose cells and debris. Subsequently, the cells were treated with small molecules, dissolved in DMEM supplemented with 1% FCS. The plate was then returned to a humidity-controlled microscope chamber set at 37°C and 5% CO2. For a 16-hour duration, cell migration was monitored utilizing Olympus scanR time-lapse imaging system. Sequential images were captured at 30-minute intervals. Cell viability was measured using Alamar Blue ™ assay at the end of the migration assays. Percentage of wound closure was determined and calculated using T scratch software [200].

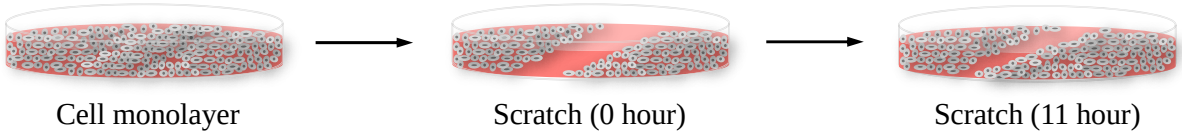

Figure 2.3. Cell migration assessed by the wound-healing assay. Cells were plated overnight to generate a monolayer. A wound was produced by scratching the middle part of the well after 2 hours treatment of mitomycin-C. The treatments were then added, sequential images were captured, and closure area were calculated.

2.2.5.3. Cell Invasion Assay (Transwell®)

Cancer cell invasion was detected via the Boyden chamber transwell invasion assay. In brief, a Corning® Costar® Transwell® cell culture insert (6.5 mm with 8 µm pore polycarbonate filter; Corning, No. 3422) was prepped with a coating of 20 µl of Phenol Red-Free Corning® Matrigel® Basement Membrane Matrix (1.5 mg/ml; Corning, No. 356237). Following the application of the coating, the insert was placed in an incubator set at 37°C and 5% CO2, and left to incubate for a duration of 3 hours.

BCa cells were trypsinised and suspensions were prepared in serum free medium at a density of 3.2 × 10^4 cells/ml. Once the gel was hardened, 200 µl cell suspension was added on to the transwell insert. Fetal bovin serum was used as a chemoattractant, thus 500 µl of standard medium was added into the 24-well plate and the transwell was then added. The insert containing plates were incubated at 37 °C and 5% CO_2 for 72 hours.

After 72 hours of incubation, medium and non-invasive cells were removed from the interior part of the insert using a damp cotton bud. Then the cells on the insert were fixed in 100% ethanol for 5 minutes followed by staining in hematoxylin solution modified according to Gill II (Sigma-Aldrich, No. 105175) and eosin Y solution (Sigma-Aldrich, No. HT110280) (H&E). Briefly, inserts were placed in 1% eosin (w/v) for 1 minute, rinsed in tap water, stained with hematoxylin for 5 minutes and rinsed in tap water again. Insert were excised and mounted on slide plus rectangular glasses (VWR, No. 631-0137) slides using Faramount queous mouting medium (Agilent, No. S3025) to avoid the generation of air bubbles. Images of the insert were taken and cells number were counted using a bright field microscope 10× magnification.

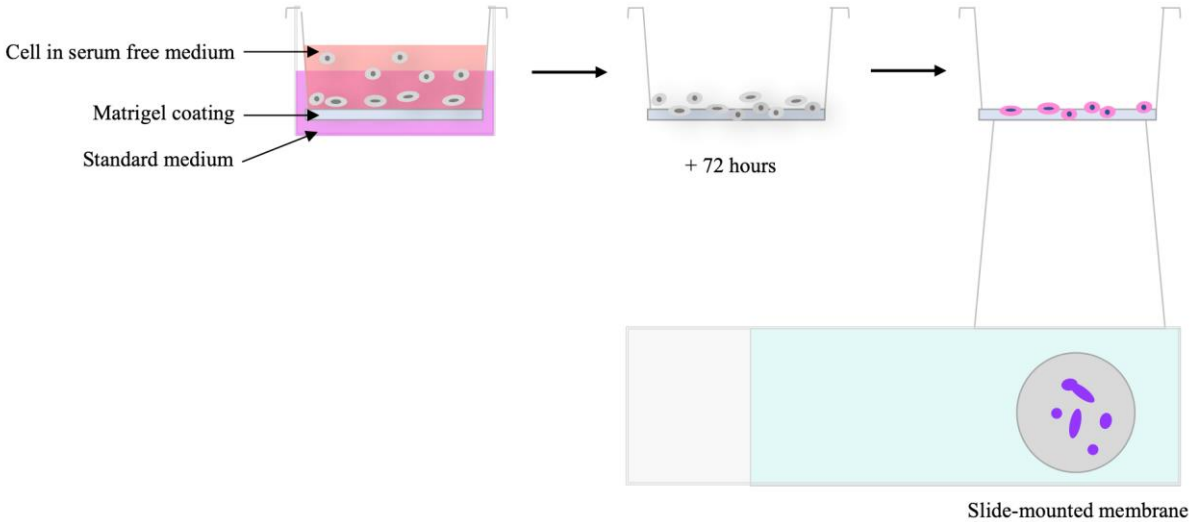

Figure 2.4. Cell invasion assessed by the Transwell® invasion assay. Cells were seeded in serum-free medium and placed in a Transwell® insert with a Matrigel® coating, situated within a well filled with standard medium, to establish a chemo-attractive gradient. After a duration of 72 hours, the Transwell® membrane was subjected to Hematoxylin/Eosin staining and subsequently mounted on a slide for further analysis.

2.2.6. Characterization and Identification of Osteoclasts

Tartrate-resistant acid phosphatase (TRAcP) staining is commonly used for the identification of osteoclasts because TRAcP is a marker enzyme that is highly expressed in osteoclasts. The color rendering principle of Tartrate-resistant acid phosphatase (TRAcP) staining is based on the enzymatic activity of TRAcP on its specific substrate (naphthol AS-BI phosphate). This reaction occurs in the presence of a diazonium salt, which leads to the formation of a colored precipitate.

2.2.6.1. Culture fixation

For osteoclast culture assessment, the existing medium was discarded, followed by rinsing the adherent cells twice using sterile PBS. Subsequently, cells were treated with a designated volume of 4% (v/v) paraformaldehyde in PBS (150 µl for 96-well) and allowed to incubate for 10 minutes at room temperature. Post-fixation, cells were rinsed again twice with PBS and store at 4°C in a solution of 70% ethanol (v/v).

2.2.6.2. Tartrate-resistant acid phosphatase (TRAcP) staining

Identification of multinucleated osteoclasts was carried out employing TRAcP staining, as delineated previously in Marino et al., 2014. Briefly, 100 µl of TRAcP staining solution (**Scientific Appendix**) was added to each well and plates, followed by a 37°C incubation period extending from 30 to 60 minutes. Subsequently, the TRAcP staining solution was then removed, and cells were rinsed twice using sterile PBSthen, stored at 4 ºC in 70% (v/v) ethanol solution. TRAcP positive cells (TRAcP+) with three or more nuclei were considered to be osteoclasts. Manually enumeration of these cells was executed under a Zeiss Axiovert light microscope using a 10× and 20× objective lens.

2.2.7. Assessment of breast cancer-induced osteoblast growth, differentiation and bone nodule formation

The influence of BCa cells and the soluble factors they produce on osteoblast differentiation and bone nodule development was evaluated using alkaline phosphatase (ALP) and Alizarin Red S (ARS) staining methods. Human osteoblast-like Saos-2 cells, generously provided by Dr. Ning Wang (University of Sheffield, UK), were seeded (3×10^4 cells/well) in 24-well plates filled with standard medium. For promoting bone nodule development, cells were administered osteogenic medium every other day for a span of 10 days. This medium comprised DMEM supplemented with 1% FBS, L-ascorbic acid (50 μM, Sigma-Aldrich, No. A4544), and following confluence, β-glycerophosphate (2 mM, Sigma-Aldrich, No. G9422) was added. Cells were also introduced to conditioned medium derived from human and mouse BCa cancer cell lines, namely MDA-MB-231 and 4T1 (20% v/v), and were treated with FSAS3 or a vehicle (DMSO) (0.1%). Cells that were not exposed to conditioned medium served as a negative control. On the 5th, 7th, and 10th days, assessments were made on Saos-2 cell viability, differentiation, and bone nodule formation using AlamarBlue® assay, alkaline phosphatase (ALP) and Alizarin Red S (ARS) staining techniques.

2.2.7.1. Osteoblast viability

Saos-2 were plated in 96-well plates (7×10^3 cells/well in 100 μl of standard medium). After 24 hours, the desired treatments were added and left for 24, 48 and 72 hours. Cell viability was analysed using AlamarBlue® assay (**section 2.3.1**)

2.2.7.2. Characterization and Identification of Osteoblast differentiation - Alkaline Phosphatase (ALP) assay

Human osteoblast-like Saos-2 cells seeded (3×10^4 cells/well) in standard medium in 24-well plates. After 5-, 7-, and 10-days treatment, to assess osteoblast maturation and differentiation. At the experiment endpoint, cells were washed three times with iced PBS and then lysed with 50 μl ALP lysis buffer (**Scientific Appendix**) overnight at -80 °C. Before assessing the ALP activity, plate with cells was

agitated on a shaker at room temperature for 20 minutes to make sure ice crystal are fully deforested. pNPP + PicoGreen solution (**Scientific Appendix**) were prepared and wrapped with aluminium foil to avoid light. Cell lysate was added into 96-well plate in duplicates. The DNA standard samples were prepared using TE buffer (1x) and DNA stock (2 µg/mL) from the Quanti-IT PicoGreen dsDNA reagent and kits (Invitrogen, No. P11496). Standard samples were added into 96-well plate in duplicates as follow:

Standard	**DNA standard (2µg/mL) (µl)**	**1x TE buffer (µl)**	**Final DNA conc. (µg/ml)**
1	0	50	0
2	1.25	48.75	0.05
3	2.5	47.5	0.10
4	5	45	0.20
5	10	40	0.40
6	15	35	0.60
7	20	30	0.80
8	25	25	1.00

Add 150 ul of **pNPP + PicoGreen solution** at the plate reader bench and measuring ALP activity at absorbance (405 nm) with a SpectraMax M5® microplate reader (Molecular Devices) at 37 °C every 15 minutes for 30 minutes. Once finished, measure the PicoGreen intensity at standard fluorescein wavelengths (excitation ~480 nm, emission ~520 nm).

The ALP activity was calculated using the following equation:

$$ALP\ activity(\mathrm{U/ml}) = \frac{(At - A0) \times v \times d}{t \times \boldsymbol{\varepsilon} \times l}$$

In this equation,

At = absorbance at endpoint 't'

A0 = absorbance at initial time

V = total volume in the well (150 µl assay solution + 50 µl sample = 200 ml in this experiment)

d = dilution factor of the sample in the total volume (200:50 = 4 for this experiment)

t = time between initial and final reading in minutes (30 min)

ε = molar extinction coefficient for pNPP (18.75mM^{-1} cm^{-1})

l = path length in cm (0.639cm for this experiment)

The dsDNA content for each well was calculated by interpolating the fluorescence readings based on a standard curve. The ALP activity was calculated using the equation above and normalized by the dsDNA content of the samples and expressed as percentage response relative to control.

2.2.7.3. Characterization and identification of bone nodule formation – Alizarin Red Staining (ARS)

The ability for osteoblasts to form bone nodules was evaluated by fixing the cells with 70% ethanol. After a 24-hour period, the plates were rinsed with PBS three times, treated with 500µl of ARS solution (**Scientific Appendix**) to stain calcium deposits, and rinsed with deionized H_2O. The plates were then allowed to air dry and were scanned to obtain representative images. For quantifying bone nodule formation, the cell monolayer was destained through the application of 1 ml destaining solution (10% v/v, cetylpyridinium chloride monohydrate, Sigma-Aldrich, No. C0732) in 10 mM sodium phosphate (pH 7.0, Sigma-Aldrich, No. 342483) for a 15-minute duration at room temperature on a rocker. ARS was evaluated by measuring the absorbance at 564 nm using a Bio-Tec Synergy HT microplate reader (BioTec® Instruments), and the percentage of ARS was ascertained using ImageJ software.

2.3. Molecular Biology Techniques

2.3.1. TRAF6 knockdown

2.3.1.1. Lentiviral gene delivery – short hairpin RNA (shRNA)

To generate knockdown of TRAF6 expression in human parental MDA-MB-231 and osteotropic MDA-231-BT BCa cells, a vector-based short hairpin RNA (shRNA) approach was used, adhering to the manufacturer's guidelines. The utilization of lentiviral vectors received approval from the University of Sheffield Biosafety Committee, sanctioned under project license GMO2014_11. The described protocol was optimised by Silvia Marino, PhD and Ryan Bishop, PhD at our laboratory (University of Sheffield, UK). Briefly, HEK293ET cells (at a density of 10×10^4 cells/ml) were seeded in a 25 cm^2 flask, and upon reaching confluency, the existing medium was substituted with a transfection blend (5 μg shRNA of PLKO.1, $TRAF6^{KD1}$, $TRAF6^{KD2}$, $TRAF6^{KD3}$ plasmids, 5 μg PPAX2 packaging plasmid, 5 μg pMD2.G envelope plasmid, 40 μl Polyethylenimine (PEI) transfection reagent and 450 μl of serum free DMEM in 4.5 ml of standard DMEM medium). After 24 hours, the medium was refreshed, and on the subsequent day, the medium now enriched with viral particles, was transitioned into Falcon™ 15 ml conical centrifuge tubes (Thermo Fisher Scientific, No. 352097), centrifuged and filtered through a 0.45 μm (low protein binding) filter, prior to storage at -80 ºC.

Table 2.2. Human TRAF6 shRNA construct and target sequences.

Name	Construct	Targeting Sequence
$TRAF6^{KD1}$	TRCN0000007348	GCCACGGGAAATATGTAATAT
$TRAF6^{KD2}$	TRCN0000007349	CGGAATTTCCAGGAAACTATT
$TRAF6^{KD3}$	TRCN0000007352	CCTGGATTCTACACTGGCAAA

2.3.1.2. Lentiviral transfection

The recipient parental MDA-MB-231 and osteotropic MDA-231-BT BCa cells (1×10^4 cells/cm^2) were seeded into 25 cm^2 flask. The virial supernatant (1ml) was added to 9 ml of standard DMEM with polybrene (Sigma-Alderich, No. 32160801) at a final concentration of 5 μg/ml. After 24 hours, the medium was replaced with selection medium containing standard DMEM and a concentration of puromycin, which would kill all non-transfected cells after 48 hours (1 μg/ml). The chosen selection

concentration was determined by dose-response curves on non-transfected parental MDA-MB-231 and osteotropic MDA-231-BT BCa cells (data not shown). The transfected cells were maintained in selection for at least two passages until knockdown was confirmed. The efficacy of TRAF6 knockdown was determined by Western blot analysis (**section 2.3.2).**

2.3.2. Western blot

2.3.2.1. Preparation of cell lysates

Cells were seeded in standard DMEM to 80% confluency in 6- or 24- well plates at 200 $\times 10^3$ and 20 $\times 10^3$ cells/well, respectively. Following the desired treatments, the medium was discarded, and cells were rinsed with iced-cold PBS, followed by a 5-minute incubation with 100 µl (6-well plate) or 50 µl (24-well plate) of RIPA lysis buffer (**Scientific Appendix**) containing 2% (v/v) protease inhibitor and 0.4% (v/v) phosphatase inhibitor on ice. Cells were gently scraped and transferred to an Eppendorf tube and centrifuged at 13.3g for 10 minutes at 4 °C. The supernatant fraction was transferred to Eppendorf tubes and stored at -20 °C for subsequent use (**Figure 2.5A**).

2.3.2.2. Measuring protein concentration

Pierce™ Bicinchoninic acid (BCA) protein assay was utilized to quantify protein amount in cell lysates, following the guidelines provided by the manufacturer. Protein concentrations were assessed using the Pierce™ bovine serum albumin (BSA) standard prediluted set as reference (Thermo Scientific, No. 23208). A total of 10 µl from each serial dilution (ranging from 0-2000 µg/ml) was placed in duplicate in a 96-well plate alongside the cell lysate sample, diluted 1:5 with distilled water. Following this, 200 µl of BCA solution, comprised of 1 in 50 copper sulphate (Sigma-Aldrich, No. C2284) diluted in BCA (Sigma-Aldrich, No. B9643), was dispensed into all wells. After 30 minutes of incubation at 37 °C, the absorbance was measured at 562 nm on a SpectraMax M5® microplate reader (Molecular Devices) (depicted in **Figure 2.5B**). Utilizing the known BSA concentrations, a standard curve was plotted to

estimate the total protein content of each lysate and ascertain the volume of protein extract required to obtain 70 µg.

2.3.2.3. Gel electrophoresis and electrophoretic transfer

Before the gel loading process, quantified samples were combined with a 4× loading buffer (refer to **Scientific Appendix**) and heated at 95 °C for a duration of 5 minutes for denaturation purposes (as depicted in **Figure 2.5C**). The denatured proteins were then segregated via electrophoresis on 12% CriterionTM TGXTM Precast Midi protein gels (Bio-Rad Laboratories, No. 5671043), placed within a vertical electrophoresis chamber filled with 1X Tris/Glycine/SDS (TGS) running buffer (prepared from a 1 to 10 dilution of 10X TGS; Bio-Rad Laboratories, No. 161-0772, mixed with distilled water). 2 µl of Magic Marker XP Western Protein Standard (Thermo Fisher Scientific, No. LC5602) was utilized as a molecular weight reference. Following an hour of operation at 180 V, the proteins residing on the gel were transitioned onto a polyvinylidene membrane (PVDF; Bio-Rad Laboratories, No. 1704273), compiled between filter papers (Bio-Rad Laboratories, No. 1704273) (shown in **Figure 2.5D**) that were pre-soaked in transfer buffer, and then positioned within the Transblot Turbo® transfer system (Bio-Rad Laboratories) for 7 minutes, maintaining a constant current of 2.5 A and 21 V.

2.3.2.4. Membrane blocking and antibody incubation

The PVDF membrane was blocked to ensure blocking of the remaining binding surface and non-specific binding sites by 5% (w/v) milk blocking solution (non-fat milk powder in Tris buffer saline solution (TBS) (**Scientific Appendix**) with 0.1% TWEEN® 20 (Sigma-Aldrich, No. P9416), known as TBST) for 1 hour with gentle rocking in room temperature. The membrane was washed three times with TBST for 10 minutes on a rocker with medium speed and incubated overnight at 4 °C with gentle rocking in each primary antibody. The primary antibodies used were TRAF2(C192) Rabbit mAb (Cell signalling Technology, No. 4724), TRAF4(D1N3A) Rabbit mAb (Cell signalling Technology, No.18527), TRAF6(D21G3) Rabbit mAb (Cell signalling Technology, No. 8028), GAPDH(14C10) Rabbit mAb

(Cell signalling Technology, No 2118), β-Actin(D6A8) Rabbit mAb (Cell signalling Technology, No. 8457), Phospho-IκBα (Ser32) (14D4) Rabbit mAb (Cell signalling Technology, No 2859), IκBα (44D4) Rabbit mAb (Cell signalling Technology, No 4812). Subsequently, the membrane was washed three times with TBST on a rocker with medium speed for 15 minutes and incubated with the secondary antibody peroxidase AffiniPure donkey Anti-Rabbit IgG (H+L) (Jackson ImmunoResearch, No. 711-035-152) at a concentration of 1:10000 in 5% w/v dried non-fat milk in TBST for 1 hour at room temperature with gentle rocking.

2.3.2.5. Immunostaining and antibody detection

The membranes were washed three times with TBST for 10 minutes and it was visualized using chemiluminescent substrate (Clarity™ western ECL substrate, Bio-Rad Laboratories, No. 170-5061) with the chemiluminescent detection system on ChemiDoc™ Imaging System (Bio-Rad Laboratories) (**Figure 2.5E**). Band quantification was performed with the use of Image Lab 6.0 software (Bio-Rad Laboratories).

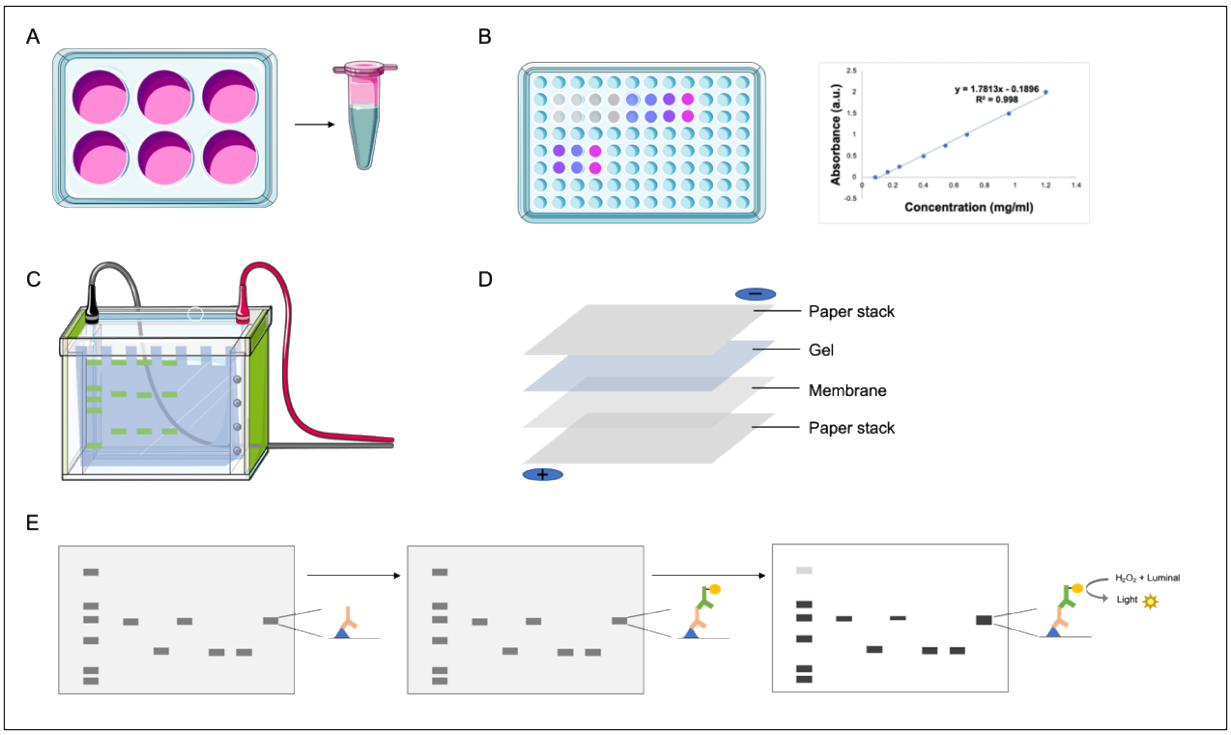

Figure 2.5. Flow diagram of Western Blot Analysis. (A) Proteins are extracted from whole cell lysates using RIPA buffer. (B) The concentration of proteins is assessed through BCA, based on the standard curve derived from the Pierce™ bovine serum albumin (BSA) standard prediluted kit. (C) Cell samples are prepared, heated and separated by electrophoresis for 1 hour with 180 V. (D) The gel is placed over the PVDF membrane, assembled together between filter papers (pre-soaked in transfer buffer). The PVDF membrane is blocked in 5% (w/v) milk blocking solution, washed with TBST and (E) incubated with each primary antibody. The membrane is washed with TBST and incubated with the secondary antibody peroxidase AffiniPure donkey Anti-Rabbit IgG (H+L) and washed before visualization using Clarity™ western ECL substrate with the chemiluminescent detection system on ChemiDoc™ Imaging System. BSA=Bovine Serum Albumin. R^2=Square of the correlation.

2.3.3. Immunoprecipitation

2.3.3.1. Preparation of cell lysates

Cultures were plated in standard DMEM to 80% confluency in 25 cm^2 flask. Cultures were then treated as desired; medium was removed, cells were washed with iced-cold PBS for 5-minutes incubation in 500 μl of M-PER lysis buffer (Pierce, No. 78501) containing 2% (v/v) protease inhibitor and 0.4% (v/v) phosphatase inhibitor on ice. Cells were gently scraped and transferred to an Eppendorf tube and centrifuged at 13.3g for 10 minutes at 4 °C. The supernatant fraction was transferred to fresh Eppendorf tubes and stored at -20 °C until future use (**Figure 2.5A**). Protein concentrations were detected using a standard commercially available protein assay such as bicinchoninic acid (BCA) Pierce® protein assay (Pierce, UK).

2.3.3.2. Binding and elution

The SureBeads (Bio-Rad Laboratories, No. 161-4023) were resuspend fully and 100 μl (1 mg at 10 mg/ml) of the solution were transferred into 1.5 ml tubes. The beads were magnetized using the SureBeads Magnetic Rack (Bio-Rad Laboratories, No. 161-4916) and supernatant were discarded. After washed with 1 ml PBS-T (PBS + 0.1% Tween 20) three times, 5 μg of polyclonal or monoclonal antibody specific for protein of interest were added in a final volume of 200 μl SureBeads and resuspended and rotated for 10 minutes at room temperature (RT). After incubation, beads were washed with 1 ml PBS-T using Magnetic Rack three times and 500 μl of cell lysate containing 250 to 500 μg total protein were added and rotated for 1 hour at room temperature. After washed with 1 ml PBS-T three times, 40 μl of 1×Laemmli buffer were added and incubated for 10 minutes at 70 °C. Finally, beads were magnetized, and eluent were transfer to a new vial for lateral immunoblotting.

2.3.3.3. Western blot

Refer to **section 2.4.2.3 – 2.4.2.5**.

2.3.4. NFκB activation assay

BCa cancer cell nuclear proteins were extracted with Nuclear Extract Kit (Active Motif, No. 40010). Then, NFκB p65 Transcription Factor Assay Kits (Active Motif, No. 40096) was used to detected nuclear p65 content, according to the manufacturer's instructions. Briefly, sample preparation involved the dilution of 20 µl of the specimen in complete lysis buffer, while the positive control consisted of 5 µl of the provided Raji nuclear extract diluted in 15 µl complete lysis buffer. The blank was 20 µl of complete lysis buffer. These were incubated for an hour at room temperature with gentle agitation at 100 rpm. Following this, the wells were washed three times with 200 µl of 1X wash buffer. After the wash, 100 µl of anti-NF-κB p65 antibodies, diluted 1:1000, were added to each well and left to incubate for another hour. Subsequently, 100 µl of horseradish peroxidase (HRP)-conjugated secondary antibody, diluted 1:1000, was added and the incubation continued for an additional hour. After the incubation period, the wells were washed four more times. Each well was then treated with 100 µl of developing solution and incubated for 2 minutes away from light. Lastly, 100 µl of stop solution was added to each well and the absorbance was read within 5 minutes at a wavelength of 450 nm.

2.3.5. Drug Affinity Responsive Target Stability (DARTS) assay

To identify and study the protein-ligand interaction between TRAF6 and FSAS3, DARTS assay [201] was used on FSAS3 treated RAW264.6 cell lysate and the digested by pronase. As shown in **Figure 2.6**, when a small molecular compound binds to a protein, the interaction stabilizes the target protein's structure so that it turns into more resistant to proteases than non-treated proteins.

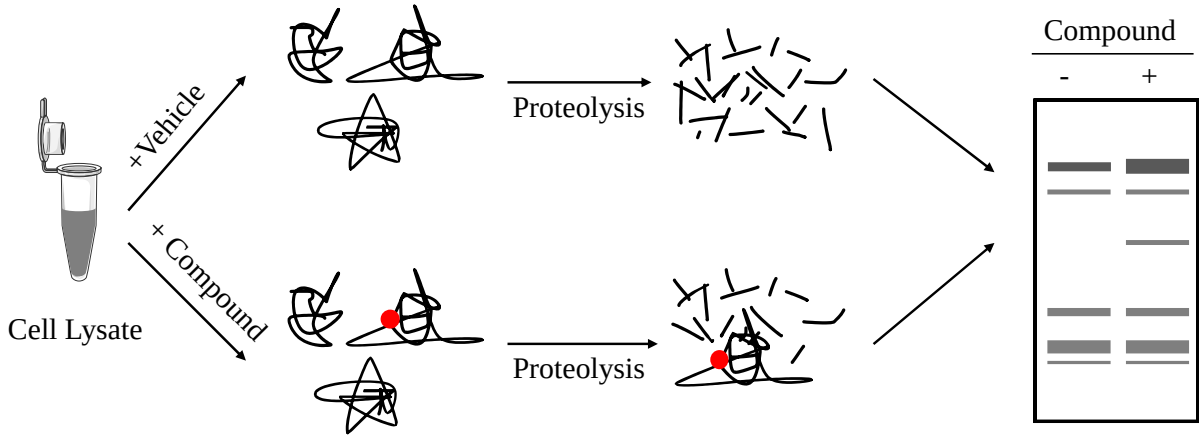

Figure 2.6. Workflow of DARTS assay. Cell lysate was incubated in the presence or absence of small molecule compound, followed by proteolysis and electrophoresis.

2.3.5.1. Preparation of cell lysates

RAW264.7 cells were plated in T75 flask and incubate at 37 °C and 5% CO_2 to reach 70% confluence. Then, cultures were then treated as desired; medium was removed, cells were washed with iced-cold PBS three times and then added 600 µl of M-PER lysis buffer (Pierce, No. 78501) containing 2% (v/v) protease inhibitor and 0.4% (v/v) phosphatase inhibitor on ice. Cells lysate was collected with a cell scraper by holding the flask at an angle and gently scraping from the top to bottom. Lysate was then transferred into a 1.5 ml prechilled tube, mixed by pipetting gently several times and incubated for 10 minutes.

2.3.5.2. Prepare cell lysates for DARTS assay

After incubation, centrifuged the cell lysate at 18,000 × g, 4 °C, 600 µl of the supernatant fraction was transferred to fresh Eppendorf tube and added with 66.7 µl 10× TNC buffer (**Scientific Appendix**) and mixed well. BCA assay was performed to ensure the concentration of protein lysate was between 4 to 6 µg/µl. Then lysate was spited into two samples with 294 µl in each. Then, 6 µl DMSO or FSAS3 was added to one tube respectively and mixed immediately by gently flicking several times and incubate at room temperature for 2 hours.

2.3.5.3. Protein proteolysis (Pronase assay)

A stock of pronase (**Scientific Appendix**) was thawn on ice and added 140 μl of 1× TNC buffer and served as the 1:100 pronase solution. Dilute the 1:100 pronase serially by mixing with 1× TNC to create 1:300, 1:1000, 1:2000, 1:3000, 1:4000, 1:5000, 1:6000, 1:10,000 pronase stock solutions.

As shown in **Figure 2.7**, lysates were split into 6 tubes with 50 μl in each. 2 μl pronase of different dilution ratio was added at a 30-second interval to begin digestions and terminated after 30 minutes by adding 10 μl sample buffer and heated at 95 °C for 5 minutes. Sample were for western blot electrophoresis immediately or stored at -20 °C for later use. Refer to **section 2.3.2.3 – 2.3.2.5**.

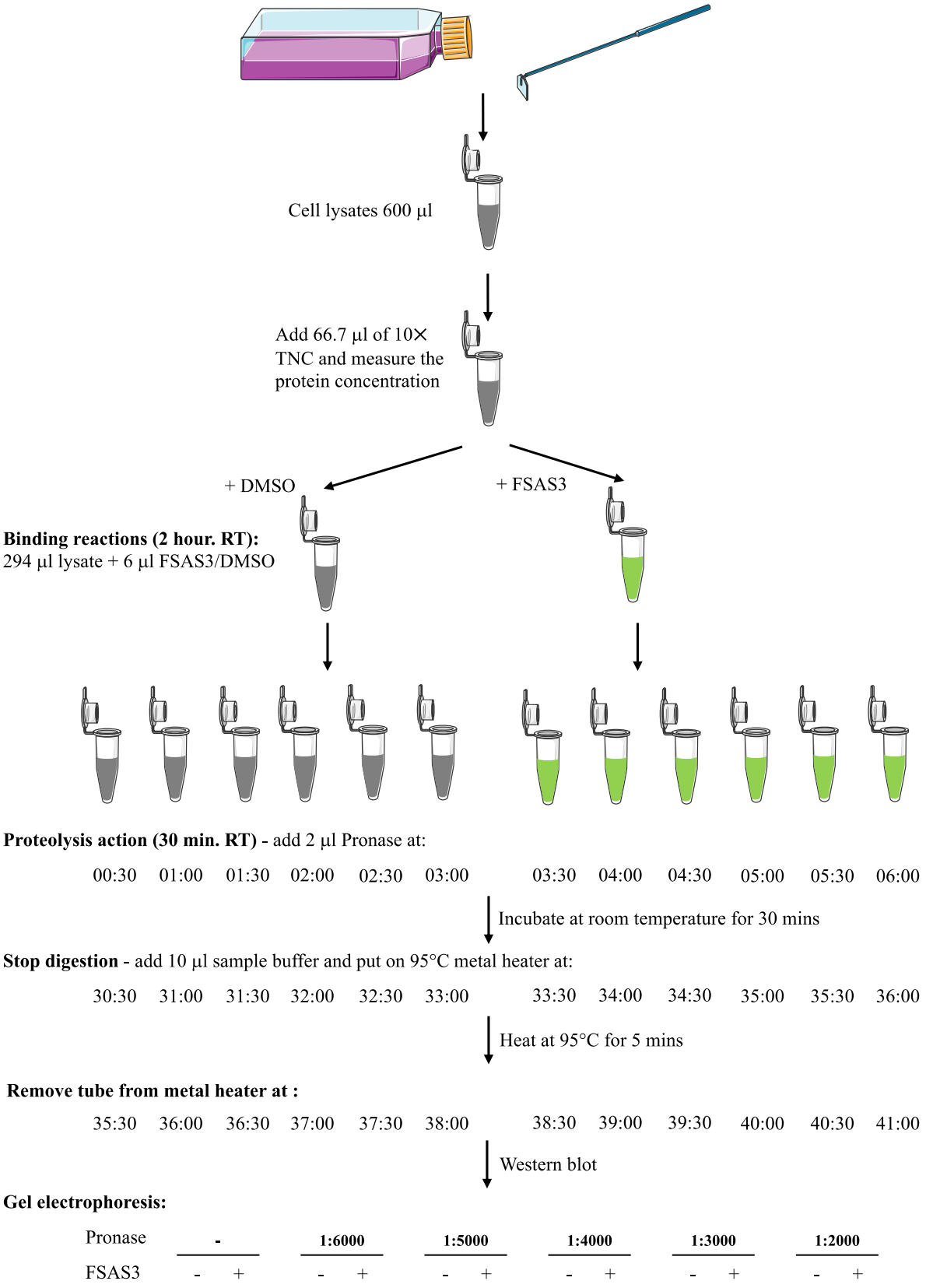

Figure 2.7. Experimental scheme of DARTS using RAW264.7 cell lysates. Cell lysate was incubated in the presence or absence of small molecule compound, followed by proteolysis and western blot.

2.4. Mouse calvaria – BCa cell co-culture system

The effect of FSAS3 on osteolysis induced by human BCa cells was investigated *ex vivo* via a modified version of the mouse calvarial organ culture method as outlined in reference [202]. Briefly, BCa cells (1×10^2 cells/ well) were seeded in 48-well plates containing standard medium. Mouse calvarias were isolated from 2-day-old mice, divided into equal halves along the medium sagittal suture and each half was placed into culture on stainless steel rafts in 48-well plates containing BCa cells. Tissue culture medium containing test small molecules was changed every 48 hours and the cultures were terminated after 7 days. Assessment of bone volume was conducted utilizing μCT (Skyscan 1172 instrument, Bruker, Belgium) at a resolution of 5 μM. Image reconstruction and analysis were carried out using Sky NRecon and CTAn software (also from Bruker, Belgium) in accordance with the manufacturer's guidelines and as described [203].

2.5. Ethics

All procedures involving mice and their care were approved by and performed in compliance with the guidelines of Institutional Animal Care and Use Committee of University of Edinburgh (Scotland, UK).

2.6. Retrospective and Bioinformatic Studies

2.6.1. Systematic Review and Meta-analysis

2.6.1.1. Literature search strategy

The present meta-analysis was conducted in accordance with the Preferred Reporting Items for Systematic Reviews and Meta-analyses (PRISMA) statement [204]. Briefly, we performed a comprehensive search for relevant articles in Medline, Web of Science and Scopus databases from inception to June 27, 2021. Keywords related to TRAF1-7 and BCa metastasis (**Supplementary Table 1**), their combination and alternatives were used to identify articles that reported relevant studies. Articles were curated, and duplicates identified and removed using EndNote X9 (Clarivate, London, UK).

2.6.1.2. Study selection

Studies that utilized animal intervention (*in vivo*) and *in vitro* models to examine the effects of pharmacological and/or genetic manipulation of TRAF1-7 on BCa cell behaviour were included. Human studies that reported overall and disease-specific (including metastasis-free) survival for BCa were included. Reviews, editorials, commentaries, case reports and abstracts were excluded. We also excluded articles that were published in a language other than English, and those that reported unspecified outcomes (**Supplementary Table 2**).

2.6.1.3. Types of interventions

Included pharmacological inhibitors of TRAF1-7 must be synthetic chemicals (e.g. TJ-M2010-2 and 6877002) or bioactive extracts (e.g. Wogonoside and plumbagin) that have been verified to exert significant reduction in the expression and activity of at least one member of the TRAF family. Genetic manipulation of TRAF1-7 must be performed using standard techniques such as shRNA, microRNA (e.g. miR146a, miR146b, miR146a/b, miRZip-892b) and others (e.g. Ei24, TLR5, CHIP) that have been verified to have significant modification in the specified gene.

2.6.1.4. Study outcomes

Eligible studies include a selected panel of outcomes obtained from *in vitro, in vivo,* and human studies (**Supplementary Table 3-5**). Included *in vitro* studies assessed cell migration by wound healing or trans-well assays, cell invasion by trans-well assay, cell proliferation by MTT (3-(4,5-dimethylthiazol-2-yl)-2,5-diphenyltetrazolium bromide), MTS (3-(4,5-dimethylthiazol-2-yl)-5-(3-carboxymethoxyphenyl)-2-(4-sulfophenyl)-2H-tetrazolium) or CCK8 (Cell counting Kit 8) assays, colony formation by counting the numbers of 1% crystal violet stained colonies, apoptosis by using the Annexin V/PI apoptosis kit (**Supplementary Table 3**), respectively. Included *in vivo* studies assessed tumorigenesis by measuring tumour volume/weight, and metastasis by using bioluminescent imaging or immunohistochemical staining (**Supplementary Table 4**). Included human studies assessed survival rates for BCa by Kaplan Meier analysis (**Supplementary Table 5**).

2.6.1.5. Data extraction

Items obtained from relevant studies include authors' name, publication year, experimental design, sample size, outcome measures. For human studies, Hazard Ratio (HR (95%CI)) was extracted from relevant studies, or calculated according to relevant numerical values from Kaplan-Meier curve [205, 206]. WebPlotDigitizer (https://apps.automeris.io/wpd/) was used to extract mean and standard deviation (SD) or standard error measurement (SEM) from each relevant figures or tables. If mean ± SEM was reported, the SD was obtained using the following formula ($SEM = SD / \sqrt{N}$).

2.6.1.6. Data analysis

Meta-analysis was performed using Review Manager (RevMan 5). Mean difference was used as the effect measure if the same outcome/unit of measure were used, otherwise standardized (std.) mean difference was used. If heterogeneity was considered small to moderate (i.e. $I^2<50\%$), then the fixed effect analysis model was employed. The random effect analysis model was used if heterogeneity was

considered high (i.e. I^2>50%). For studies that involved human subjects, HR (95%CI) and number of patients were extracted from the Kaplan-Meier curve, unless HR was provided in manuscript. HR > 1 indicates poor survival rate. Ln (HR) was used as the effect measure if the same outcome and unit of measure were used in all studies included in a forest plot. Ln (HR) was calculated using the generic inverse variance method. Random effect analysis model was used if heterogeneity was high (i.e. I^2>50%).

2.6.1.7. Quality assessment

Quality assessment of all eligible *in vivo* and *in vitro* studies were assessed using the Syrcle risk of bias [207], and OHAT (Office of Health Assessment and Translation) risk of bias rating tool [208, 209], respectively. The following criteria were used for the Syrcle risk of bias rating: baseline characteristics, sequence generation, random housing and outcome assessment, allocation concealment, blinding of researchers and outcome assessors, incomplete outcome data, selective outcome reporting and other sources of bias. The OHAT risk of bias rating criteria that were used for *in vitro* studies are as follows: randomization, identical experimental conditions, allocation concealment, complete outcome data, blinding of researchers, outcome assessment, exposure characterization, outcome reporting and no other potential threats [208, 209]. For human studies, the quality of eligible studies was assessed by a scoring method that assesses cancer diagnosis; numbers of the cases; representativeness of collected cases; TRAFs judgement criteria; and the source of HR (95%CI) [210].

2.6.1.8. Certainty of evidence

The grading of recommendations assessment, development, and evaluation (GRADE) approach was used to assess Certainty of the evidence from eligible human studies [211]. An adapted GRADE approach for preclinical systematic reviews was used for *in vivo* and *in vitro* experimental outcomes [212].

2.6.1.9. Publication bias

No funnel plot asymmetry analysis was carried out since none of the pooled analyses included 10 or more studies, as previously described [213].

2.6.2. Bioinformatic Studies

2.6.2.1. Genetic alternation studies

Copy number variation (CNVs) and gene mutations in TRAFs in samples selected based on PATH sample in metastatic setting: primary (n=166) and metastatic (n=335) BCa patients were obtained from the Metastatic BCa Project (ongoing - published to cBioportal [214, 215]). Patients were separated into those who exhibited amplification (Amp), deletion (Del) and mutation (Mut) in TRAFs, and analysis was carried out using GraphPad (Prism, version 9).

2.6.2.2. Gene expression analysis

To compare gene expression between breast tumour and normal tissue and generate the heatmap of TRAF protein expression patterns, The Cancer Genome Atlas (TCGA) data of BCa patients sample of cancer samples (n=1104) and normal samples (n=114) were obtained via the University of California Santa Cruz (UCSC) Xena platform (https://xena.ucsc.edu/cite-us; [216]).

2.6.2.3. Protein-protein interaction (PPI) analysis

A PPI network of all seven TRAF family members with each other was reconstructed and obtained from the Search Tool for Retrieval Interacting Genes/proteins (STRING) (https://string-db.org/; [217]), I utilized the minimum required interaction score as high confidence (0.7)[218]. The PPIs with a combined score of >0.7 were considered significant in determining the significance of the association between genes and node degrees.

2.6.2.4. Kaplan-Meier survival analyses

Kaplan-Meier survival analysis was performed to assess the overall survival (OS) in a cohort of 2509 of BCa patients. Data was obtained from the Molecular Taxonomy of BCa International Consortium (METABRIC) [219, 220]. The Kaplan-Meier estimator was used to estimate the survival rate on TRAF6 expression (diploid and amplification). The log-rank test was used to compare survival rate between groups, and the hazard ratio was estimated using the Cox proportional hazards model. The statistical significance level was set at $p<0.05$.

2.6.2.5. Microarray validation of TRAFs in metastatic BCa patients

The normalized gene expression profiles of microarray datasets for BCa metastasis were obtained from Gene Expression Omnibus (GEO). Two datasets of tissue samples from metastatic BCa patient, GSE14020 [221, 222] and GSE56493 [223-226] of tissue samples from metastatic BCa patient were used. To achieve a large sample population, batch effect was corrected using BatchSever (https://lifeinfor.shinyapps.io/batchserver/; [110]). A total of 184 tissue samples were identified (bone n=23, brain n=22, liver n=32, lung n=22, lymph nodes n=44, skin n=22, and breast n=19) for analysis of TRAFs expression.

2.6.2.6. Gene Ontology (GO) and Kyoto Encyclopedia Genes and Genomes (KEGG) Pathway enrichment analysis

To identify enriched biological pathways and functions associated with TRAFs, KEGG (Kyoto Encyclopedia of Genes and Genomes) and GO (Gene Ontology) enrichment analysis were performed using the STRING (Search Tool for the Retrieval of Interacting Genes/proteins) database (version 11.5)[217]. Enrichment scores were calculated as Log10(observed/expected). The minimum required interaction score was set to high confidence (0.7), and the cut-off threshold was set to have an FDR (False Discovery Rate) value of less than 0.05 [218]. Bubble charts were generated using MATLAB 9.12.

2.7. Statistical Analysis

Results presented are mean ± standard deviation (SD) derived from three independent experiments. All calculations were performed utilizing GraphPad Prism 7. For statistical analysis, data from two groups in a single experiment were evaluated through an unpaired *T* test, while comparisons between either a single group or more than two groups on an independent variable were made through an ordinary one-way analysis of variance (ANOVA) succeeded by a Tukey *post hoc* test for multiple inter-group comparisons. The inhibitory concentration 50% (IC50) was assessed by log 10 transformation, followed by nonlinear regression analysis using variable slope fit equation for normalized dose-inhibitory response and a two-way ANOVA followed by Dunnet *post hoc* test for multiple comparisons between groups with two independent variables. A p-value of 0.05 or below was considered statistically significant, and a p-value of 0.01 or below highly statistically significant.

CHAPTER 3. A Systematic Review and Meta-analysis of Association between TRAF1-7 and BCa Metastasis

3.1. Summary

TRAF6 is a key regulator of BCa. However, the TRAF family constitutes of seven members that exhibit distinct and overlapping functions. To examine which TRAF represents a potential therapeutic target for BCa metastasis, I searched Medline, Web of Science and Scopus for relevant studies from inception to June 27, 2021. We identified 14 *in vitro*, 11 *in vivo* and 4 human articles. A meta-analysis of pharmacological studies showed that *in vitro* inhibition of TRAF2/4 (mean difference (MD):-57.49, CI-66.95,-48.02, P<0.00001) or TRAF6 (standard(Std.)MD:-4.01, CI:-5.75,-2.27, P<0.00001) is associated with reduction in BCa cell migration. Consistently, inhibition of TRAF2/4 (MD:-51.08, CI-64.23,-37.94, P<0.00001) and TRAF6 (Std.MD:-2.80, CI:-4.26,-1.34, P=0.0002) is associated with reduced BCa cell invasion, whereas TRAF2/4 inhibition (MD:-40.54, CI:-52.83,-28.26, P<0.00001) is associated with reduced BCa cell adhesion. Interestingly, only inhibition of TRAF6 (MD:-21.46, CI:-30.40,-12.51, P<0.00001) is associated with reduced cell growth. In animal models of BCa, administration of pharmacological inhibitors of TRAF2/4 (Std.MD:-3.36, CI:-4.53,-2.18, P<0.00001) or TRAF6 (Std.MD:-4.15, CI:-6.06,-2.24, P<0.0001) in mice is associated with reduction in tumour burden. In contrast, TRAF6 inhibitors (MD:-2.42, CI:-3.70,-1.14, P=0.0002) reduced BCa metastasis. In BCa patients, high expression of TRAF6 (Hazard Ratio:1.01, CI:1.01,1.01, P<0.00001) is associated with poor survival rate. Overall, TRAF6 inhibition shows promise in the treatment of advanced BCa. However, low study number and scarcity of evidence from preclinical and human studies may limit the translation of present findings into clinical practice.

3.2. Introduction

The TNF receptor associated factor (TRAF) family of adaptor proteins is implicated in various physiological functions, particularly inflammation and immunity[108, 227-230]. The seven known members of the TRAF family, namely TRAF1 to 7 - serve as common targets for a number of pro-inflammatory and immune-modulatory factors implicated in the regulation of oncogenic activity of a variety of cancer cells [160, 227-229, 231-235]. Given their ubiquitous expression in healthy and cancerous tissues[113, 119, 160, 234, 236], a number of TRAFs have emerged as potential therapeutic targets in the treatment of difficult-to-treat cancers, including advanced, metastatic BCa[160, 231]. Among TRAFs, TRAF6 is the most studied in BCa. A number of studies have shown that TRAF6 is highly expressed in BCa tumours of primary and metastatic origin[160, 231]. Furthermore, TRAF6 is commonly associated with E3 ubiquitin ligase activity, as well as other homeostatic processes implicated in various aspects of hormone-dependant and triple-negative BCa[108, 160, 227, 231, 237]. TRAF6 (and to a lesser extent TRAF2-5) is also known to act as a point of convergence for multiple BCa-driver signal transduction pathways such as PI3K/AKT/mTOR, Toll-like receptor (TLR), mitogen-activated protein kinase (MAPK), NFκB, Ras/Src Family Kinases, and members of the activator protein 1 (AP-1) family[108, 227, 231, 237, 238]. Therefore, TRAF6 is an important regulator of BCa tumorigenesis and metastasis, but evidence from studies in advanced BCa patients also suggests that the expression of TRAF2 and 4 is associated with poor survival rates. Furthermore, findings from a number of *in vitro* and *in vivo* studies have also shown that manipulation of TRAF2, 3 and/or 4 influences the behaviour of BCa cells [160, 161, 163-167, 239].

It is known that different members of the TRAF family exhibit distinct and overlapping functions. Therefore, different TRAFs exert various physiological and pathophysiological effects through different mechanisms [108, 227, 238, 240]. Selecting which TRAF to study and ultimately target for the treatment of a complex disease such as advanced, metastatic BCa is a difficult challenge. Therefore, I carried out a systematic review to examine the hypothesis that TRAF modulation is associated with BCa progression and metastasis. To investigate this hypothesis, I first evaluated the association between pharmacological and genetic manipulation of the seven members of the TRAF family and BCa cell

motility, adherence, proliferation and apoptosis *in vitro* and tumour burden and metastasis in rodent models. Next, I examined the association between TRAF1-7 expression and overall survial in BCa in patients.

3.3. Aims

The aims of this chapter were to explore which TRAF represents a potential druggable target for the treatment of BCa metastasis. Using publicly-available databases and resources, I assessed the association between genetic and pharmacological manipulation of TRAF1-7 and tumorigenesis and metastasis in BCa *in vitro, in vivo* and human studies.

The aims were achieved using qualitative and quantitative (meta-analysis) methods that examined:

- The association of TRAFs genetic and pharmacological modulation with *in vitro* growth, migration, invasion, adhesion of human and animal BCa cells.
- The association of TRAFs genetic and pharmacological modulation with *in vivo* BCa tumorigenesis and metastasis in models of animal and human BCa cells.
- The association of TRAFs with metastasis and survival rate in BCa patients.

3.4. Results

3.4.1. Articles selection

A total of 1895 articles were identified using the search strategy described in Table S1. The flow diagram that shows literature searches, selection process and study number is shown in Figure 1. Briefly, 1575 articles were deemed irrelevant after duplicates were removed, and title and abstracts were reviewed for relevant studies. A total of 44 full-text articles were assessed for eligibility, and an additional 16 articles were excluded after full text assessment (**Supplementary Table 2**). Articles excluded at the full-text stage together with reasons for exclusion are shown in Table S2. As shown in **Figure 3.1**, 28 relevant articles that reported 8 human survivals, 12 *in vitro* and 22 *in vivo* studies were included in the qualitative synthesis. Finally, 18 articles that featured 2 human, 11 *in vivo* and 14 *in vitro* studies were included in the present meta-analysis.

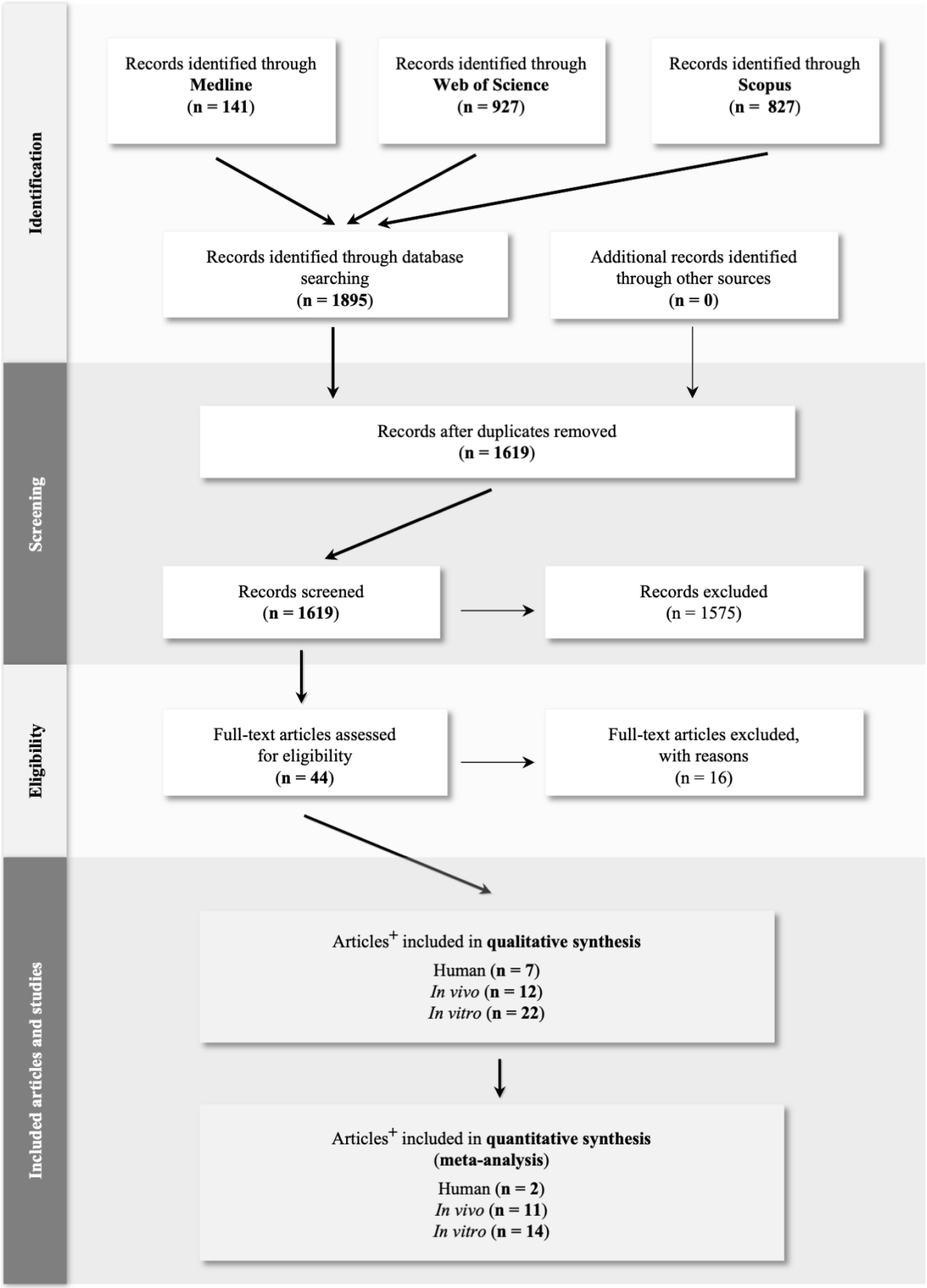

+A number of included articles featured more than one study type (i.e. *in vitro*, *in vivo* and/or human study).

Figure 3.1. Systematic Reviews and Meta-analysis (PRISMA) flow diagram of evidence search and study selection process. N denotes number of articles.

3.4.2. Study characteristics

The 18 studies included in the quantitative analysis were published from 2011 to 2021. It is important to note that a number of included articles featured more than one study type (i.e. *in vitro*, *in vivo* and/or human study). At least two researchers independently reviewed each article and identified relevant studies in each article included. The main characteristics of the included studies are summarized in **Table 3.1** and **Supplementary Tables 3 to 5**.

Table 3.1. Summary the number and characteristics of included *in vitro*, *in vivo* and human studies.

***In vitro* study characteristic (number)**	***In vivo* study characteristic (number)**	***Human* study characteristic (number)**
Intervention/modification Pharmacological manipulation (50) Genetic manipulation (55) **Target TRAFs** TRAF2 (54) TARF4 (49) TRAF6 (51) **Species** Mouse (7) Human (97) **Cell lines** MDA-MB-231 (47) MDA-MB-435 (7) BT-474 (7) BT-549 (8) MCF7 (25) B16F10 (3) ZR-75-30 (3) 4T1 (4) **Study outcomes** Proliferation (23) Migration (36) Invasion (31) Adhesion (13) Apoptosis (1)	**Intervention/modification** Pharmacological manipulation (25) Genetic manipulation (12) **Target TRAFs** TRAF2 (9) TRAF (14) TRAF6 (15) **Species (cells)** Human (28) Mouse (9) **Strains (mice)** C57BL/6 (28) BALB/c (9) **Cell lines** MDA-MB-231 (22) MCF7 (6) 4T1 (9) **Study outcomes** Tumour weight/ volume (28) Metastasis Lung metastasis (4) Bone metastasis (4) Liver metastasis (1)	**Intervention/modification** Genetic association studies (7) **Target TRAFs** TRAF2 (1) TRAF4 (3) TRAF6 (3) **Species** Human (7) **Patient number** TRAF2 (46) TRAF4 (373) TRAF6 (346) **Study types** Kaplan-Meier survival analysis (7) **Study outcomes** Hazzard ratio (HR (95%CI)) (4) Kaplan-Meier survival curve (3)

3.4.2.1. *In vitro* studies

As shown in **Table 3.1** and **Supplementary Table S3**, the included *in vitro* data were obtained from studies that used BCa cells from mouse (7 studies) and human (97 studies) to assess the effects of pharmacological (50 studies) and/or genetic (55 studies) manipulation of TRAF2 (54 studies), TRAF4 (49 studies) and TRAF6 (51 studies) on cancer cell proliferation (23 studies), migration (36 studies), invasion (31 studies), adhesion (13 studies) and apoptosis (1 study) (**Tables 3.1** and **Supplementary Table 3**). Summary of meta-analysis from these studies is shown in **Table 3.2** and **Supplementary Table 6**, respectively, and discussed under '*In vitro regulation of BCa cell behaviour by TRAF modulation*'.

3.4.2.2. *In vivo* studies

The included *in vivo* data were obtained from studies that tested the effects of pharmacological (25 studies) or genetic manipulation (12 studies) of TRAF2 (9 studies), TRAF4 (14 studies) and TRAF6 (15 studies) on tumour burden (weight/volume, 27 studies) and metastasis (lung, 4 studies; bone, 4 studies; liver, 1 study) using histology and bioluminescence imaging (**Table 3.1** and **Supplementary Table 3**). Summary of meta-analysis from these studies is shown in **Table 3.3** and **Supplementary Table 7**, and discussed under '*In vivo regulation of BCa tumorigenesis and metastasis by TRAF modulation*'.

3.4.2.3. Human studies

The included human data were obtained from studies that examined the association between survival rate and TRAF2 expression (1 studies), TRAF4 expression (2 studies) or TRAF6 expression (2 studies) (**Tables 3.1** and **Supplementary Table 5**). Sample size varied; four studies had fewer than 200 patients, three studies had more than 200 patients. All articles featured Kaplan-Meier survival curves and provided sample size: 4 studies provided HR (95%CI) and Kaplan-Merrier survival curves, and 3 studies provided Kaplan-Merrier survival curves and thus HR (95%CI) was estimated as previously described[206].

3.4.3. Quality assessment

Risk of bias for *in vitro* studies is shown in **Supplementary Figure 2**. Out of the 9 criteria only 'blinding of research personnel during the study' (criterion 4) was scored as 'Probably high risk' for *in vitro* studies. However, this was of no concern since it is rather uncommon for researchers to be blinded when performing *in vitro* experiments. Amongst the remaining criteria, 8 articles were considered 'Probably low risk' for criterion 6 (Exposure characterization [162, 184, 194, 241-246]), all studies were considered 'Probably low risk' for criterion 5 (Missing outcome data) and criterion 7 (Outcome assessment). The overall risk of bias for *in vitro* studies was 'probably low' to 'definitely low', and thus no study was excluded solely based on their quality. Risk of bias for *in vivo* studies was assessed using the Syrcle tool[207] (**Supplementary Figure 1**). Out of the 10 items, 4 scored as 'high risk' for most *in vivo* studies. These were item 1 - Sequence generation, item 3 - Allocation concealment, item 5 - Blinding of researchers, and item 7 - Blinding of outcome assessors. Although these quality items are imperative for high quality clinical studies, we believe that it is rather uncommon for *in vivo* studies to fulfil them; thus their prevalence was expected. Furthermore, 3 items scored as 'unclear' for a number of *in vivo* studies. These were item 1 – Sequence generation, 6 - Random outcome assessment, and item 8 - Incomplete outcome data. Once again, these were of no particular concern. If we exclude the 4 items that most articles scored 'high risk' (items 1, 3, 5 and 7) and the 3 items that most articles scored 'unclear' (items 1, 6 and 8), all articles indicated an overall high quality and hence were not excluded based solely on their quality. The overall quality of the included human studies is high apart from 1 study which was considered of medium quality due to a small sample size (**Supplementary Figure 9**)[210].

3.4.4. Narrative synthesis

Data in studies from 14 articles were considered too heterogeneous to pool or not reported in a format suitable for pooling. These articles were included in the narrative synthesis (**Table 3.5**). A number of these articles featured more than one *in vitro*, *in vivo* and/or human studies.

3.4.5. Certainty of evidence

The overall quality of outcomes of *in vitro* and *in vivo* studies was judged as follows: (A) very low for *in vitro* cell proliferation, migration, invasion, and adhesion; (B) very low for *in vivo* tumour volume, bone metastasis, liver metastasis; (C) low for *in vivo* tumour weight and lung metastasis. For human studies, the overall quality of outcomes was judged very low due to imprecision and small sample size.

3.4.6. Meta-analysis of outcomes

3.4.6.1. Association of TRAF modulation with *in vitro* breast cancer cell behaviour

First, we evaluated the association between pharmacological and genetic modulation of TRAF1-7 with BCa cell proliferation, migration, invasion, adherence, and apoptosis *in vitro*. Using the aforementioned search strategy, we identified 105 individual studies from 28 relevant articles that tested the effects of pharmacological (50 studies) and genetic (55 studies) manipulation of TRAF2 (54 studies), TARF4 (49 studies) or TRAF6 (51 studies) on the *in vitro* proliferation (23 studies), migration (36 studies), invasion (31 studies), adhesion (13 studies) and apoptosis (1 study) of human (97 studies - MDA-MB-231, 47 studies; MDA-MB-435, 7 studies; BT-474, 7 studies; BT-549, 8 studies; MCF-7, 25 studies; B16F10, 3 studies) and mouse (7 studies - ZR-75-30, 3 studies and 4T1, 4 studies) BCa cells (**Tables 3.1 and 3.2**).

3.4.6.1.1. *In vitro* regulation of breast cancer cell migration by TRAF2/4/6

Meta-analysis of included studies that tested the effects of TRAF1-7 modulation on migration of BCa cells *in vitro* (**Table 3.2**) showed that pharmacological inhibition of TRAF2, TRAF4 (6 studies, mean difference -57.49, 95% CI -66.95,-48.02, Z score 11.91 (P<0.00001)), or TRAF6 (12 studies, Std. mean difference -4.01, 95% CI -5.75,-2.27 Z score 4.52 (P<0.00001)) is associated with significant reduction in the ability of human hormone-dependent MCF-7 and triple-negative MDA-MB-435, BT549 and MDA-MB-231-BT BCa cells to migrate *in vitro* (**Table 3.2**). Consistent with findings from these pharmacological studies, genetic inhibition of TRAF2 in MDA-MB-231 and B16F10 (3 studies, mean

difference -46.88, 95% CI -79.80,-13.96, Z score 2.79 (P=0.005)), TRAF4 in MDA-MB-231 and MCF-7 (3 studies, mean difference -407.97, 95% CI -525.57,-290.37, Z score 6.80 (P<0.00001)), or TRAF6 in MCF-7 (3 studies, mean difference -0.32, 95% CI -0.65,0.01, Z score 1.92 (P=0.05)) is associated with significant reduction in cell migration *in vitro* (**Table 3.2**). Conversely, genetic upregulation of TRAF4 in MCF-7 (3 studies, mean difference -89.52, 95% CI -139.93, -39.12, Z score 3.48 (P=0.0005)), or TRAF6 in MCF-7 (3 studies, mean difference 0.25, 95% CI 0.23,0.27, Z score 3.14 (P=0.002)) is associated with significant increase in cell migration *in vitro* (**Table 3.2**). Based on findings from pooled studies, we conclude that inhibition of TRAF2, 4 and/or 6 is associated with reduced *in vitro* migration of the hormone-dependent and triple negative BCa cells described. A review of studies that were considered too heterogeneous to pool or not reported in a format suitable for pooling (**Table 3.1**) confirmed that TRAF6 expression is associated with *in vitro* motility of the hormone-dependent MCF-7 and triple-negative MDA-MB231 BCa cells [247].

Table 3.2. Summary of meta-analysis of included studies showing significant association of *in vitro* BCa cell behaviours and modulation of TRAF2/4/6.

Outcome		Intervention	Type of cell cultures (no. studies)	Subgroup (std.) mean difference (95% CI)	Overall (std.) mean difference (95% CI)	Statistical method	Test for heterogeneity	Test for overall effect
TRAF2	Migration	Pharmacological inhibition +	MCF7 (2) MDA-MB-231 (2) MDA-MB-435 (2)	-62.02 [-82.69, -41.35] -52.16 [-72.11, -32.20] -58.25 [-78.05, -38.44]	-57.49 [-66.95, -48.02]	Mean Difference (IV, Random, 95% CI)	$Tau^2 = 111.52$; $Chi^2 = 25.49$, df = 5 (P = 0.0001); $I^2 = 80\%$	Z = 11.91 (P < 0.00001)
		Genetic inhibition	MDA-MB-231 (2) B16F10 (1)	-59.97 [-88.86, -31.09] -24.12 [-30.99, -17.25]	-46.88 [-79.80, -13.96]	Mean Difference (IV, Random, 95% CI)	$Tau^2 = 778.00$; $Chi^2 = 30.10$, df = 2 (P < 0.00001); $I^2 = 93\%$	Z = 2.79 (P = 0.005)
	Invasion	Pharmacological inhibition *	MCF7 (2) MDA-MB-231 (2) MDA-MB-435 (2)	-61.41 [-92.43, -30.40] -44.83 [-68.12, -21.53] -47.48 [-73.02, -21.94]	-51.08 [-64.23, -37.94]	Mean Difference (IV, Random, 95% CI)	$Tau^2 = 247.97$; $Chi^2 = 63.60$, df = 5 (P < 0.00001); $I^2 = 92\%$	Z = 7.62 (P < 0.00001)
		Genetic inhibition	MDA-MB-231 (2)	NA	-45.54 [-56.46, -34.62]	Mean Difference (IV, Fixed, 95% CI)	$Chi^2 = 0.38$, df = 1 (P = 0.54); $I^2 = 0\%$	Z = 8.17 (P < 0.00001)
		Genetic upregulation	MDA-MB-231 (3) ZR-75-30 (2)	2.65 [0.41, 4.89] 5.95 [1.70, 10.19]	3.37 [1.39, 5.35]	Std. Mean Difference (IV, Fixed, 95% CI)	$Chi^2 = 6.79$, df = 4 (P = 0.15); $I^2 = 41\%$	Z = 3.33 (P = 0.0009)
	Proliferation	Genetic upregulation	MDA-MB-231 (1) ZR-75-30 (1)	2.61 [2.10, 3.12] 3.34 [2.98, 3.70]	3.00 [2.28, 3.71]	Mean Difference (IV, Random, 95% CI)	$Tau^2 = 0.22$; $Chi^2 = 5.19$, df = 1 (P = 0.02); $I^2 = 81\%$	Z = 8.23 (P < 0.00001)
	Adhesion	Pharmacological inhibition £	MCF7 (2) MDA-MB-231 (2) MDA-MB-435 (2) BT-474 (2)	-58.48 [-76.86, -40.11] -42.59 [-62.58, -22.60] -41.32 [-62.61, -20.02] -19.78 [-30.75, -8.82]	-40.54 [-52.83, -28.26]	Mean Difference (IV, Random, 95% CI)	$Tau^2 = 287.52$; $Chi^2 = 83.94$, df = 7 (P < 0.00001); $I^2 = 92\%$	Z = 6.47 (P < 0.00001)

TRAF4	**Migration**	Pharmacological inhibition +	MCF7 (2) MDA-MB-231 (2) MDA-MB-435 (2)	-62.02 [-82.69, -41.35] -52.16 [-72.11, -32.20] -58.25 [-78.05, -38.44]	-57.49 [-66.95, -48.02]	Mean Difference (IV, Random, 95% CI)	Tau² = 111.52; Chi² = 25.49, df = 5 (P = 0.0001); I² = 80%	Z = 11.91 (P < 0.00001)
		Genetic inhibition	MCF7 (1) MDA-MB-231 (2)	-309.10 [-358.84, -259.36] -459.60 [-523.02, -396.18]	-407.97 [-525.57, -290.37]	Mean Difference (IV, Random, 95% CI)	Tau² = 8896.64; Chi² = 13.71, df = 2 (P = 0.001); I² = 85%	Z = 6.80 (P < 0.00001)
		Genetic upregulation	MCF7 (3)	NA	-89.52 [-139.93, -39.12]	Mean Difference (IV, Random, 95% CI)	Tau² = 1728.25; Chi² = 16.94, df = 2 (P = 0.0002); I² = 88%	Z = 3.48 (P = 0.0005)
	Invasion	Pharmacological inhibition *	MCF7 (2) MDA-MB-231 (2) MDA-MB-435 (2)	-61.41 [-92.43, -30.40] -44.83 [-68.12, -21.53] -47.48 [-73.02, -21.94]	-51.08 [-64.23, -37.94]	Mean Difference (IV, Random, 95% CI)	Tau² = 247.97; Chi² = 63.60, df = 5 (P < 0.00001); I² = 92%	Z = 7.62 (P < 0.00001)
		Genetic inhibition	MDA-MB-231 (4)	NA	-7.00 [-10.05, -3.96]	Mean Difference (IV, Random, 95% CI)	Tau² = 6.67; Chi² = 38.27, df = 3 (P < 0.00001); I² = 92%	Z = 4.51 (P < 0.00001)
	Adhesion	Pharmacological inhibition £	MCF7 (2) MDA-MB-231 (2) MDA-MB-435 (2) BT-474 (2)	-58.48 [-76.86, -40.11] -42.59 [-62.58, -22.60] -41.32 [-62.61, -20.02] -19.78 [-30.75, -8.82]	-40.54 [-52.83, -28.26]	Mean Difference (IV, Random, 95% CI)	Tau² = 287.52; Chi² = 83.94, df = 7 (P < 0.00001); I² = 92%	Z = 6.47 (P < 0.00001)
TRAF6	**Migration**	Pharmacological inhibition	BT549 (3) MCF7 (1) MDA-MB-231 (4) MDA-MB-231-BT (4)	-5.60 [-11.76, 0.56] -9.20 [-18.23, -0.17] -6.28 [-11.63, -0.93] -3.21 [-5.33, -1.08]	-4.01 [-5.75, -2.27]	Std. Mean Difference (IV, Random, 95% CI)	Tau² = 2.56; Chi² = 16.53, df = 11 (P = 0.12); I² = 33%	Z = 4.52 (P < 0.00001)
		Genetic inhibition	MCF7 (3)	NA	-0.32 [-0.65, 0.01]	Mean Difference (IV, Random, 95% CI)	Tau² = 0.08; Chi² = 476.58, df = 2 (P < 0.00001); I² = 100%	Z = 1.92 (P = 0.05)

		Genetic upregulation	MCF7 (3)	NA	0.25 [0.23, 0.27]	Mean Difference (IV, Random, 95% CI)	Chi^2 = 1.85, df = 2 (P = 0.40); I^2 = 0%	Z = 3.14 (P = 0.002)
	Invasion	Pharmacological inhibition	BT549 (3) MCF7 (1) MDA-MB-231 (4) MDA-MB-231-BT (4)	-5.78 [-12.04, 0.47] -9.50 [-18.82, -0.19] -5.62 [-10.34, -0.90] -1.36 [-2.53, -0.19]	-2.80 [-4.26, -1.34]	Std. Mean Difference (IV, Random, 95% CI)	Tau^2 = 2.23; Chi^2 = 19.22, df = 11 (P = 0.06); I^2 = 43%	Z = 3.76 (P = 0.0002)
	Proliferation	Pharmacological inhibition	BT549 (4) MCF7 (4) MDA-MB-231 (8)	-5.78 [-12.04, 0.47] -9.50 [-18.82, -0.19] -5.62 [-10.34, -0.90]	-21.46 [-30.40, -12.51]	Mean Difference (IV, Random, 95% CI)	Tau^2 = 321.80; Chi^2 = 677.01, df = 15 (P < 0.00001); I^2 = 98%	Z = 4.70 (P < 0.00001)
		Genetic upregulation	MCF7 (1) 4T1 (3)	0.12 [0.09, 0.15] 0.38 [0.24, 0.52]	0.31 [0.12, 0.51]	Mean Difference (IV, Random, 95% CI)	Tau^2 = 0.04; Chi^2 = 158.59, df = 3 (P < 0.00001); I^2 = 98%	Z = 3.19 (P = 0.001)

The analysis shows the mean difference or standard mean difference of different studies comparing the effects of the TRAF6 pharmacological inhibition, genetic inhibition or upregulation on cell migration as assessed by trans well assay or wound healing assay, cell invasion as assessed by trans-well assay and proliferation as assessed by cell viability assay. Std., standardised; IV, inverse-variance weighting; NA, not applicable. + refers to studies using the same intervention which inhibit both TRAF2 and 4 on cell invasion, * refers to studies using the same intervention which inhibit both TRAF2 and 4 on cell invasion, $^{£}$ intervention modulated the activity of both TRAF2 and TRAF4.

3.4.6.1.2. *In vitro* regulation of breast cancer cell invasion by TRAF2/4/6

Analysis of pooled *in vitro* studies showed that pharmacological inhibition of TRAF2 and 4 (6 studies, mean difference -51.08, 95% CI -64.23,-37.94, Z score 7.62 (P<0.00001)), or TRAF6 (12 studies, Std. mean difference -2.80, 95% CI -4.26,-1.34, Z score 3.76 (P=0.0002)) is associated with significant reduction in the *in vitro* invasion of human MCF-7 and triple-negative MDA-MB-435 and BT549 BCa cells (**Table 3.2**). Consistently, genetic inhibition of TRAF2 in MDA-MB-231 (3 studies, mean difference -45.54, 95% CI -56.46, -34.62, Z score 8.17 (P<0.00001)) and TRAF4 in MDA-MB-231 (4 studies, mean difference -7.00, 95% CI -10.05,-3.96, Z score 4.51 (P<0.00001)) is associated with significant reduction in cell invasion *in vitro* (**Table 3.2**). Conversely, genetic upregulation of TRAF2 in MDA-MB-231 and ZR-75-30 (5 studies, Std. mean difference 3.37, 95% CI 1.39,5.35, Z score 3.33 (P=0.0009)) is associated with significant reduction in cell invasion *in vitro* (**Table 3.2**). Thus, TRAF2, 4 and 6 regulate the *in vitro* invasion of the hormone-dependent and triple-negative BCa cells described. Findings from non-pooled papers (**Table 3.5**) partially complement this and confirm that TRAF6, but not TRAF2 or 4, regulates the invasion of MCF-7 and MDA-MB231 BCa cells *in vitro* [247], and indirectly enhances the interaction between tumour-associated fibroblasts and BCa cells in co-culture models [248]. In contrast to the aforementioned pro-migratory and pro-invasive roles of TRAF2 in BCa, evidence from non-pooled study by Sirinian *et al.* suggest that TRAF2 directly interacts with an isoform of the RANK receptor termed RANK-c to inhibit the migration and invasion of MDA-MB-231 and SKBR3 BCa cells *in vitro*, and to reduce the metastatic abilities of a clone of SKBR3 BCa cells in mice [249].

3.4.6.1.3. *In vitro* regulation of breast cancer cell adherence by TRAF2/4

Analysis of pooled *in vitro* studies showed that pharmacological inhibition of TRAF2/4 (8 studies, mean difference -40.54, 95% CI -52.83, -28.26, Z score 6.47 (P< 0.00001)) is associated with significant reduction in the *in vitro* adherence of human hormone-dependent MCF-7 and the triple-negative MDA-MB-231, MDA-MB-435 and BT549 BCa cells (**Table 3.2**).

3.4.6.1.4. In vitro regulation of breast cancer cell proliferation by TRAF6

Meta-analysis of pooled *in vitro* studies that examined BCa cell survival and apoptosis showed that pharmacological inhibition of TRAF6 (16 studies, mean difference -21.46, 95% CI -30.40, -12.51, Z score 4.70 (P<0.00001)) is associated with significant reduction in the ability of the triple-negative human BCa cells BT549, MCF-7, MDA-MB-231 to proliferate *in vitro* (**Table 3.2**). Analysis of pooled studies that examined genetic manipulation of TRAF1-7 showed that knockdown of TRAF4 (4 studies, mean difference -7.00, 95% CI -10.05, -3.96, Z score 4.51 (P<0.00001)) is associated with significant reduction in MDA-MB-231 cell invasion *in vitro* (**Table 3.2**). Conversely, genetic upregulation of TRAF2 in MDA-MB-231 and ZR-75-30 (2 studies, mean difference 3.00, 95% CI 2.28,3.71, Z score 8.23 (P<0.00001)) and TRAF6 in human MCF-7 and mouse 4T1 (4 studies, mean difference 0.31, 95% CI 0.12,0.51, Z score 3.19 (P=0.001)) is associated with an increase in cell proliferation *in vitro* (**Table 3.2**). In broad agreement with these findings, we also found evidence from non-pooled studies to indicate that exposure of MCF-7 and MDA-MB-231 cells to TJ-M2010-2, an inhibitor of MyD88 homodimerization, reduced TRAF6 expression and caused apoptotic cell death[246]. Similarly, TRAF6 inhibition was also found to be associated with the anti-proliferative and pro-apoptotic effects of miR-146a/b in human MCF-7 cells [242, 244, 250]. Although TRAF1 has been found to promote cell survival and death[160], Wang and colleagues showed that its over-expression in MCF-7 cells failed to protect these cells against the anti-proliferative and pro-apoptotic effects of the chemotherapeutic agent paclitaxel[251]. Thus, we conclude that TRAF2/4/6 modulation is associated with altered *in vitro* behaviour of the hormone-dependent and triple-negative BCa cells described.

3.4.6.2. Association of TRAF modulation with tumourigenesis and metastasis

As shown in **Table 3.1**, we identified 37 studies that tested the effects of pharmacological (25 studies) and genetic (12 studies) manipulation of TRAF2 (9 studies), TRAF4 (14 studies) or TRAF6 (15 studies) on tumour weight/volume (28 studies) and metastasis to the lung (3 studies), skeleton (4 studies) and

liver (1 studies) in rodents bearing human (28 studies: MDA-MB-231, 22 studies and MCF-7, 6 studies) or mouse 4T1 (9 studies) BCa cells.

3.4.6.2.1. *In vivo* regulation of breast cancer tumour burden by TRAF2/4/6

Analysis of pooled *in vivo* studies showed that administration of inhibitors of TRAF2 and TRAF4 (2 studies, Std. mean difference -3.36, 95% CI -4.53,-2.18, Z score 5.61 (P<0.00001)), or TRAF6 (6 studies, Std. mean difference -4.15, 95% CI -6.06,-2.24, Z score 4.25 (P<0.0001)) is associated with significant reduction in tumour weight and volume in female rodents bearing the human triple-negative MDA-MB-231 (TRAF2, TRAF4 and TRAF6) and mouse 4T1 (TRAF6) BCa cells (**Table 3.3**). Conversely, genetic upregulation of TRAF2 in MDA-MB-231 (2 studies, mean difference 5.81, 95% CI 3.91,7.72, Z score 5.98 (P<0.00001)), and TRAF6 in MDA-MB-231 or 4T1 (3 studies, Std. mean difference 5.79, 95% CI 3.74,7.84, Z score 5.53 (P<0.00001)) are associated with significant increase in tumour weight and volume in mice (**Table 3.3**).

Table 3.3. Summary of meta-analysis of included studies showing significant association of *in vivo* tumour burden and overt metastasis with modulation of TRAF2/4/6.

Outcome		Intervention	Type of cell cultures (no. studies)	Subgroup (std.) mean difference (95% CI)	Overall (std.) mean difference (95% CI)	Statistical method	Test for heterogeneity	Test for overall effect
TRAF2	**Tumorigenesis**	Pharmacological inhibition *	MDA-MB-231 (2)	NA	-3.36 [-4.53, -2.18]	Std. Mean Difference (IV, Fixed, 95% CI)	$Chi^2 = 0.00$, df = 1 (P = 0.95); $I^2 = 0\%$	Z = 5.61 (P < 0.00001)
		Genetic upregulation	MDA-MB-231 (2)	NA	5.81 [3.91, 7.72]	Mean Difference (IV, Fixed, 95% CI)	$Chi^2 = 0.83$, df = 1 (P = 0.36); $I^2 = 0\%$	Z = 5.98 (P < 0.00001)
TRAF4	**Tumorigenesis**	Pharmacological inhibition *	MDA-MB-231 (2)	NA	-3.36 [-4.53, -2.18]	Std. Mean Difference (IV, Fixed, 95% CI)	$Chi^2 = 0.00$, df = 1 (P = 0.95); $I^2 = 0\%$	Z = 5.61 (P < 0.00001)
	Metastasis	Genetic inhibition	MDA-MB-231 (1) MDA-MB-231 (2)	-3.21 [-4.21, -2.21] -1.68 [-3.00, -0.37]	-2.65 [-3.45, -1.85]	Mean Difference (IV, Fixed, 95% CI)	$Chi^2 = 3.27$, df = 2 (P = 0.19); $I^2 = 39\%$	Z = 6.51 (P < 0.00001)
TRAF6	**Tumorigenesis**	Pharmacological inhibition	MDA-MB-231 (2) MCF7 (2) 4T1 (2)	-4.42 [-6.16, -2.68] -7.32 [-9.97, -4.67] -1.93 [-3.59, -0.27]	-4.15 [-6.06, -2.24]	Std. Mean Difference (IV, Random, 95% CI)	$Chi^2 = 23.86$, df = 5 (P = 0.0002); $I^2 = 79\%$	Z = 4.25 (P < 0.0001)
		Genetic upregulation	MDA-MB-231 (1) 4T1 (2)	4.63 [1.74, 7.51] 6.97 [4.06, 9.89]	5.79 [3.74, 7.84]	Std. Mean Difference (IV, Fixed, 95% CI)	$Chi^2 = 1.36$, df = 2 (P = 0.51); $I^2 = 0\%$	Z = 5.53 (P < 0.00001)
	Metastasis	Pharmacological inhibition	4T1 (2)	NA	-2.42 [-3.70, -1.14]	Mean Difference (IV, Random, 95% CI)	$Tau^2 = 0.70$; $Chi^2 = 5.57$, df = 1 (P = 0.02); $I^2 = 82\%$	Z = 3.69 (P = 0.0002)

The analysis shows the mean difference or standard mean difference of different studies comparing the effects of the TRAF2/4/6 pharmacological inhibition, genetic inhibition or upregulation on tumour (weight (gram)/volume, %) and overt metastasis (histology and bioluminescence imaging). Std., standardised; IV, inverse-variance weighting; NA, not applicable. * intervention modulated the activity of both TRAF2 and TRAF4.

3.4.6.2.2. In vivo regulation of breast cancer metastasis by TRAF4/6

Our meta-analysis also included studies that examined the effects of TRAF1-7 manipulation on overt metastases in female mice bearing human and mouse BCa cells. As shown in **Table 3.3**, pharmacological inhibition of TRAF6 (2 studies, mean difference -2.42, 95% CI -3.70, -1.14, Z score 3.69 (P=0.0002) is associated with significant reduction in bone metastasis in rodents bearing an osteotropic clone of 4T1 cells. Consistently, genetic inhibition of TRAF4 in human MDA-MB-231 cells (3 studies, mean difference -2.65, 95% CI -3.45, -1.85, Z score 6.51 (P < 0.00001)) is also associated with significant reduction in bone (2 studies) and lung metastases (**Table 3.2**). In contrast, a review of non-pooled studies (**Table 3.5**) revealed that TRAF3 activity is associated with an anti-metastatic effect[163]. Moreover, Liu *et al*. showed that the osteoprotective effects of osteoclastic miR-214 in mice bearing MDA-MB-231 cells was accompanied by also significant increase in intraosseous level of TRAF3 [163].

3.4.6.3. Association of TRAF with survival rate in breast cancer patients

As shown in **Table 3.1**, our research identified 7 human studies that examined the association of TRAF2 (1 study), TRAF4 (3 studies), and TRAF6 (3 studies) with survival rate in BCa patients (719 patients). As shown in **Table 3.4**, the present meta-analysis included 5 genetic association studies (TRAF4: 2 studies, 46 patients, and TRAF6: 2 studies, 212 patients).

3.4.6.3.1. TRAF6 expression is associated with survival rate in breast cancer patients

Analysis of data from 212 patients collected from 2 pooled studies showed that high expression of TRAF6, not TRAF4, is associated with poor survival rate in BCa patients over a 5-year period (Log Hazard Ratio [HR]:1.01, 95% CI:1.01,1.01, P<0.00001) (**Table 3.4**) (**Supplementary Table 8**). A review of non-pooled studies (**Table 3.5**) confirmed that high expression of TRAF6 was detected in patient biopsies from both human breast carcinoma and lymph node metastasis [252]. Based on these

findings from pooled studies it is reasonable to conclude that therapeutic targeting of TRAF6, but not TRAF2 and 4, can be of value in the treatment of BCa. However, evidence from non-pooled studies (**Table 3.5**) implicates both TRAF2 [253] and TRAF4 [166, 254-256] in advanced BCa. Briefly, TRAF4 was found to be highly expressed in breast tumours [254, 255]. and its expression is associated with disease- and relapse-free survival in BCa patients [166, 256]. Similarly, TRAF2 expression was also found to be associated with distant metastasis-free survival in BCa patients [253].

Table 3.4. Summary of meta-analysis of included studies showing significant association of overall survival in BCa patients and modulation of TRAF6.

Intervention	Outcome	Type of survival (no. studies)	Subgroup hazard ratio (95% CI)	Overall hazard ratio (95% CI)	Statistical method	Test for heterogeneity	Test for overall effect
TRAF6 expression	Cumulative survival rate	Kaplan-Meier survival analysis (2)	NA	1.01 [1.01, 1.01]	Hazard Ratio (IV, Fixed, 95% CI)	$Chi^2 = 0.06$, df = 1 (P = 0.81); $I^2 = 72\%$	Z = 5.01 (P < 0.00001)

Table 3.5. Articles included in the narrative synthesis.

Study	Author/year	Title
In vitro	Mestre-Farrera *et al.* 2021 [248]	Glutamine-directed migration of cancer-activated fibroblasts facilitates epithelial tumor invasion.
	Wang *et al.* 2005 [251]	Differential effect of anti-apoptotic genes Bcl-xL and c-FLIP on sensitivity of MCF-7 breast cancer cells to paclitaxel and docetaxel.
	Kim *et al.* 2020 [247]*	AMPK alpha 1 regulates lung and breast cancer progression by regulating TLR4-mediated TRAF6-BECN1 signaling Axis.
	Sirinian *et al.* 2018 [249]	RANK-c attenuates aggressive properties of ER-negative breast cancer by inhibiting NF-kappa B activation and EGFR signaling.
	Liu *et al.* 2015 [242] +	FOXP3 controls an miR-146/NF-kappa B negative feedback loop that inhibits apoptosis in breast cancer cells.
	Liu *et al.* 2020 [246] +	The MyD88 inhibitor TJ-M2010-2 suppresses proliferation, migration and invasion of breast cancer cells by regulating MyD88/GSK-3 beta and MyD88/NF-kappa B signalling pathways.
	Zheng *et al.* 2015 [244] +	CXCR4 3'UTR functions as a ceRNA in promoting metastasis, proliferation and survival of MCF-7 cells by regulating miR-146a activity.
In vivo	Liu *et al.* 2017 [163] #	Osteoclastic miR-214 targets TRAF3 to contribute to osteolytic bone metastasis of breast cancer.
Human	Camilleri et al. 2007 [255]*$	TRAF4 overexpression is a common characteristic of human carcinomas.
	Regnier et al. 1995 [252]	Presence of a new conserved domain in CART1, a novel member of the tumor necrosis factor receptor-associated protein family, which is expressed in breast carcinoma
	Wang et al. 2015 [254]#	Expression of tumor necrosis factor receptor-associated factor 4 correlates with expression of Girdin and promotes nuclear translocation of Girdin in breast cancer
	Choi et al. 2013 [253]+	EI24 regulates epithelial-to-mesenchymal transition and tumor progression by suppressing TRAF2-mediated NF-κB activity
	Zhou *et al*., 2014 [256]+	TRAF4 mediates activation of TGF-β signaling and is a biomarker for oncogenesis in breast cancer
	Zhang *et al*., 2013 [166]	TRAF4 promotes TGF-beta receptor signaling and drives breast cancer metastasis

+Data extracted but not pooled in meta-analysis; *Data not extracted; $ *In vivo* data analysed by narrative synthesis. # Human data analysed by narrative synthesis.

3.5. Discussion

3.5.1. Study rationale and design

Metastasis is a major cause of death in advanced BCa patients [29, 35]. Therefore, there is a need to develop drugs that target new mechanism(s) involved in the regulation of metastatic behaviour of BCa cells. Inflammation regulates all aspects of metastatic BCa [108, 227], and different approaches have been used to study the involvement of the pro-inflammatory TRAF/NFκB axis in the interactions of BCa cell with healthy cells such as bone cells [231]. To explore which TRAF(s) to target for metastatic BCa treatment, I conducted a systematic review and meta-analysis to test the hypothesis that pharmacological modulation of TRAF1-7 can be of value in the treatment of advanced BCa. I included studies that featured standard BCa related methods, parameters and outcomes in cell culture systems, animal models and clinical studies. To explore the behaviour of metastatic BCa cells, my search strategy included *in vitro* and *in vivo* studies that examined human and animal BCa cell migration, invasion, adherence, apoptosis and proliferation in culture, and growth and metastasis in animals. In BCa patients, I used meta-analysis to establish the association between TRAF1-7 expression and BCa metastasis and survival.

3.5.2. Summary of Findings

The meta-analysis yielded 5 key outcomes: **(1)** TRAF2/4/6 inhibition is associated with reduced BCa cell motility *in vitro* and tumour weight/volume *in vivo*; **(2)** TRAF2/4 inhibition is associated with reduced BCa cell adherence *in vitro*; **(3)** TRAF6 inhibition is associated with reduced BCa cell proliferation *in vitro;* **(4)** TRAF4/6 inhibition is associated with reduced BCa cell metastasis *in vivo*; **(5)** TRAF6 expression is associated with BCa survival rate. Based on these findings, I conclude that TRAF6 expression/modulation is associated with BCa cell behaviour *in vitro*, tumour burden and metastasis in mice, and survival rate in BCa patients.

3.5.3. Therapeutic Implications

A number of studies have demonstrated TRAF6 involvement in most processes implicated in BCa, most notably inflammation, metastasis and immunity [108, 160, 227, 231, 237]. The findings from pooled human studies confirm the association between TRAF6 and BCa survival rate. This finding has important implications. First, it suggests that TRAF6 may be a biomarker for the identification of BCa in patients with advanced disease, and may help to identify patients who are likely to benefit from treatments that include anti-inflammatory agents that directly or indirectly inhibit TRAF6-mediated signalling. Secondly, the evidence from clinical studies adds more credence to the interpretation of the present *in vitro* and *in vivo* data that implicates TRAF6 in growth and metastatic behaviour of BCa cells. However, it is important to note that data from the included *in vitro* and *in vivo* – but not human – studies also suggest that TRAF2 and TRAF4 also regulate BCa cell behaviour. Data from non-pooled human studies show support this and show that TRAF2 and TRAF4 are highly expressed in breast tissues [254, 255], and their high expression is associated with disease-free survival in BCa patients [253, 256]. These are important observations since underlying mechanisms by which TRAF2, 4 and 6 individually or cooperatively regulate BCa cell behaviour are poorly understood and remain unexplored. Recently, Bishop et al, from our laboratory, have reported that administration of a small-molecule that selectively inhibits TRAF6 activity by binding to the CD40 pocket in the TRAF6 protein was sufficient to reduce overt metastasis. However, this compound failed to reduce BCa-induced bone loss, a hallmark of BCa bone metastasis [184]. BCa cell growth, mobility and their interaction with bone and immune cells in the skeleton is regulated by a myriad of immune- and bone-derived factors. The list includes TNFα, IL1β and TGFβ that can act both dependently and independently of the TRAF6/CD40 axis. Therefore, I conclude that agents that target multiple TRAFs - particularly TRAF2/4/6 - may represent a more promising strategy to treat a multi-factorial and -faceted disease such as metastatic BCa. However, potential off-target side-effects associated with such multi-targeted therapy [257], in particular inhibition of the immune response, may limit their usefulness. Thus, the therapeutic relevance of the evidence from my present study is limited. Careful exploration of potential off/side effects associated with inhibition of multiple TRAFs in BCa and healthy cells in the tumour micro-environment, coupled

with utilization of immuno-competent animal models will aid with our understanding of the therapeutic potential of TRAF manipulation, and ultimately guide future clinical research in human.

3.5.4. Strengths and Limitations

The strength of our present meta-analysis is warranted by the systematic approach and comprehensive appraisal of up-to-date evidence on articles and featured studies in three major databases, namely Medline, Web of Science and Scopus, coupled by the use of the online tool WebPlotDigitizer (https://apps.automeris.io/wpd/) to obtain the mean and standard deviation or standard error measurement from relevant figures in all included *in vitro*, *in vivo* and human studies. Therefore, no study data was deemed non-retrievable. The evidence from *in vitro* and *in vivo* studies is also supported by a wide range of experimental techniques and strategies that examined TRAF modulation using pharmacological, molecular biology and genetic approaches. Using these criteria for metastatic behaviour of BCa cells *in vitro* and *in vivo* together with metastasis and survival rate in BCa patients ensured a degree of homogeneity of the study outcomes.

However, there were a number of limitations in my study: **(1)** the number of relevant articles included in the meta-analysis is low; **(2)** a number of included articles featured more than one study type (i.e. *in vitro*, *in vivo* and/or human study); **(3)** the search was restricted to English language articles; **(4)** included *in vivo* studies were restricted to mouse experiments that used xenograft models, immortalized BCa cell lines and specific mouse strains [258, 259]; **(5)** different non-selective TRAF inhibitors, concentrations/doses, administration schemes, treatment regimes, and analytical techniques used are likely to influence the reported outcomes of *in vitro* and *in vivo* studies; **(6)** the reported BCa survival rate is likely to be affected by diversity among patients studied; **(7)** the small-study effect cannot be excluded because of the insufficient number of relevant, pooled studies needed to perform subgroup analyses, meta-regression, Egger's test and/or Funnel plot analysis. Thus, the clinical relevance of current evidence is limited.

CHAPTER 4. Bioinformatics Evaluation of the Role of TRAF2/4/6 in BCa Metastasis

4.1. Summary

TRAF proteins (TRAF1-7) are key regulators of many biological activities and alternations in their expression are commonly found in various types of tumours. Evidence from previous studies [165, 168, 177, 184, 237, 239, 260, 261] and the present systematic review and meta-analysis (**Chapter 3)** confirmed the involvement of TRAF2, TRAF4 and TRAF6 in BCa progression and metastasis. However, the number of relevant studies in meta-analysis was low and the processes and signalling transduction pathways implicated in TRAF6 driven BCa cell behaviour at metastatic sites, particularly in bone, remain poorly understood. In this chapter, I conduced KEGG pathway and gene Ontology (GO) enrichment analyses to gain more understanding into the functions and processes by which TRAF6 influence the metastatic spread of BCa.

Firstly, the involvement of different members of the TRAF family in a number of cancer-related biological activities was confirmed. My analysis showed that the expression of all TRAFs, except TRAF1, is significantly altered in BCa patients when compared to normal patient samples. Additionally, high levels of expression of TRAF3, 4, and 6 are significantly associated with poor overall survival in a large set of BCa patients. Using a combined BCa patients' dataset, I confirmed that TRAF6 expression levels are significantly higher in samples from BCa bone metastasis patients than those of primary tumours. Further analysis of these datasets also revealed that a number of functions, processes and pathways are significantly enriched for TRAF6 and TRAF2 (but no TRAF4). The list includes osteoclast formation and a number of pro-inflammatory and immuno-modulatory pathways and processes implicated in BCa metastasis. Next, I carried out a number of *in vitro* mechanistic studies using Western blot analysis that further confirmed that TRAF6 expression levels is significantly higher than TRAF2 and TRAF4 in the TNBC cells human MDA-MB-231 and mouse 4T1 cells. More importantly, TRAF6 level of expression is significantly higher in the osteotropic clones of these TNBC cells than their parental clones, suggesting a major role of TRAF6 in BCa metastasis and in the behaviour of osteotropic BCa cells in the skeleton.

4.2. Introduction

Osteolytic BCa metastasis is incurable and it occurs in approximately 75 - 80% of patients with advanced disease. [262, 263]. A number of studies have shown that constitutive activation of both canonical and non-canonical NFκB signalling transduction pathways are linked to all aspects of metastatic BCa including progression, metastasis and colonisation of distant organs, particularly skeleton. TRAFs are one of the adapter proteins recruited to the majority of receptors associated with canonical and non-canonical NFκB signalling in BCa and bone remodelling [106, 107]. The seven known TRAFs are directly or indirectly involved in the regulation of key signalling pathways downstream of the majority of pro-inflammatory, pro-osteolytic, pro-tumour and pro-metastatic cancer-driver mediators such as RANKL, CD40, TNFα, IL1β and others. Previous studies in the scientific literature [165, 166, 168, 177, 184, 237, 239, 260, 261] and the present systematic review and meta-analysis described in **Chapter 3** indicate that TRAF2, TRAF4 and TRAF6 play an important role in BCa metastasis.

In this chapter, I first utilized bioinformatics analysis to (1) validate TRAFs expression in a large cohort of BCa patients, (2) identify key genetic mutations and copy number alternations (CNAs) in TRAFs and their association with BCa metastasis, (3) investigate the association of TRAFs expression and survival of BCa pateints, (4) identify TRAFs level in different metastases of BCa patients and (5) explore the enriched pathways, functions, and processes associated with TRAFs in order to gain a better understanding of the mechanism(s) by which they regulate the behaviour of BCa cells. Secondly, I performed follow-up *in vitro* mechanistic studies to validate the findings from the aforementioned studies by examining the expression of identified TRAFs in metastatic and osteotropic BCa cells and their parental clones.

4.3. Aims

The aims of this chapter were to investigate the association of expression and modulation of TRAFs with advanced BCa, and to gain more understanding of the mechanisms by which TRAF2/4/6 influence the progression and metastasis of advanced BCa.

This aim was investigated by:

1. Using publicity-available databases to explore:
    - The biological functions, processes and signalling pathways of TRAF family members.
    - The interaction of members of the TRAF family.
    - The gene expression of TRAF1-7 in normal and tumour tissue from BCa patients.
    - The CNVs in TRAFs in primary and metastatic BCa tumours in large clinical datasets.
    - The association of TRAF 1-7 and overall survival in TNBC patients.
    - The expression of TRAF 1-7 in various metastasis, including bone metastasis, in BCa patients.

2. Using Western blot analysis to quantify
    - The protein expression of TRAF2,4,6 in human and mouse osteotropic TNBC cell lines and their primary clones.

4.4. Results

4.4.1. Altered expression of TRAF proteins in breast cancer patients

4.4.1.1. Involvement of TRAF members in breast cancer

To investigate the association of TRAF proteins with BCa progression, a variety of publicly available resources including The Cancer Genome Atlas (TCGA) BCa cohort, Gene Expression Omnibus (GEO) datasets, The Molecular Taxonomy of BCa International Consortium (METABRIC [219]), Gene Ontology (GO) and Kyoto Encyclopedia Genes and Genomes (KEGG) projects were used. First, it was confirmed that all TRAFs, except TRAF7, are implicated in cancer (hsa05200: pathways related to cancer) (**Figure 4,1 and Supplementary Table 12**). The analysis also revealed that that out of all 7 TRAFs, only TRAF2 and TRAF6 are involved in osteoclast differentiation (hsa05200)[182, 264] (**Figure 4,1 and Supplementary Table 12**). As shown in **Figure 4,2 and Table Supplementary 13**, TRAF2, TRAF6 as well as TRAF3 contribute to a variety of immune activities that include regulation of immunoglobulin secretion (GO 0051023), immune effector process (GO 0002697:) and cytokine production (GO 0002726). Mechanistically, my analysis confirmed that canonical IκB/NFκB signalling is mediated by activation of TRAF1 to 6 (GO 0043122), whereas only TRAF2, TRAF4, TRAF6 and TRAF7 are directly involved in the regulation of protein kinase activity (GO:0032147). Interestingly, only TRAF2, TRAF6 and TRAF7 are also involved in the activation of MAPK (GO 0043406), whereas JNK activation is positively regulated by TRAF1 to 6 (GO 0046330).

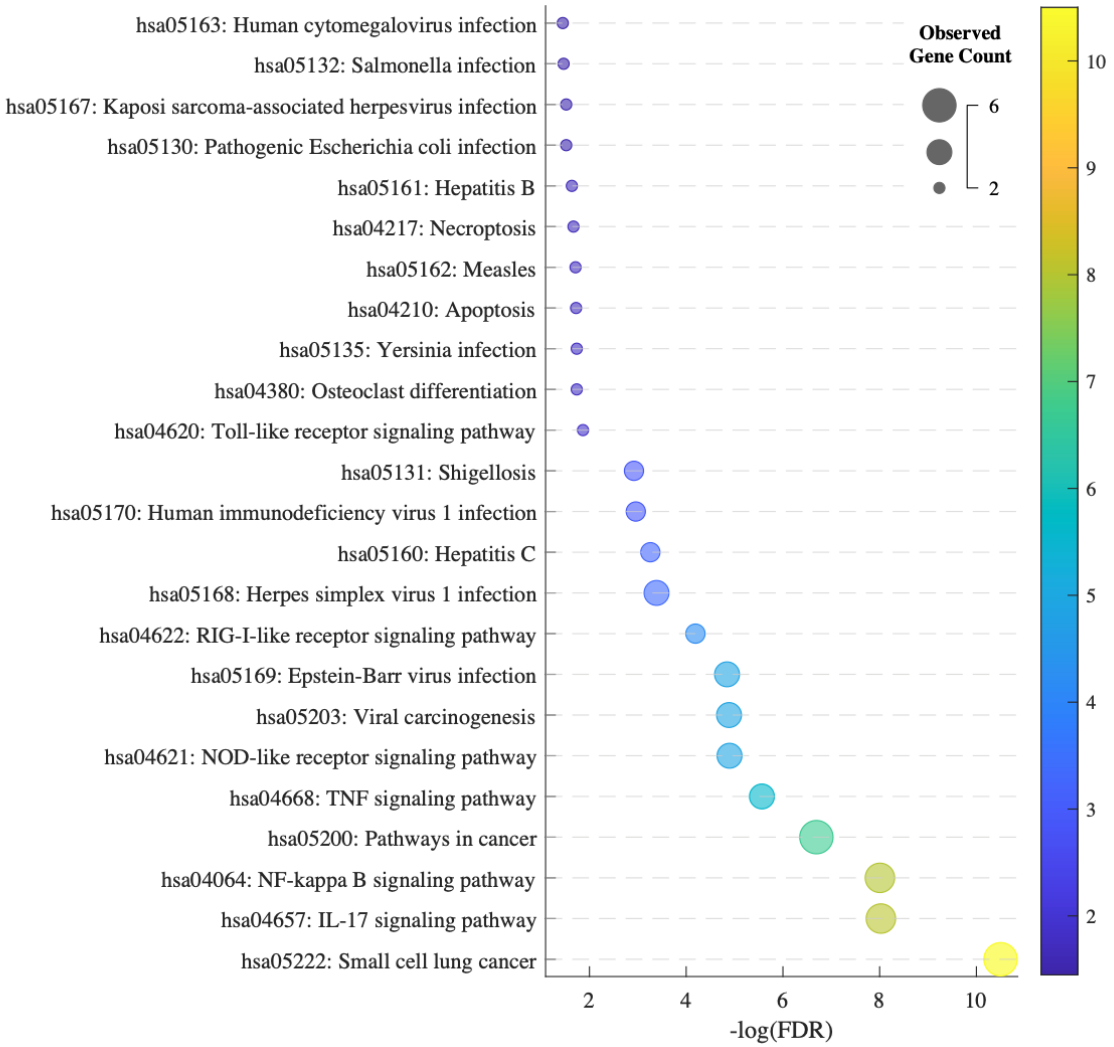

Figure 4.1. KEGG pathway enrichment of seven TRAF family members. Twenty-four significantly enriched KEGG pathways among TRAF1-7. The degree of significant enrichment is represented by (-Log10 (FDR)). The numbers of genes observed in a pathway corresponds to the size of the circle.

Figure 4.2. GO pathway enrichment of seven TRAF family members. Thirty-seven significantly enriched GO terms including Biological Process (BP), Cellular Components (CC) and Molecular Function (MF) among TRAF1-7. The degree of significant enrichment is represented by (-Log10 (FDR)). The numbers of genes observed in a pathway corresponds to the size of the circle.

The seven members of the TRAF family are known to exhibit distinct and overlapping functions. To gain a better understanding of this, I next examined the interactions between different TRAF1 to 7 using STRING. As shown in **Figure 4.3**, most interactions between TRAFs are between TRAF1,2, 3, 5, and 6. In contrast, TRAF4 and TRAF7 have no reported interaction with other members.

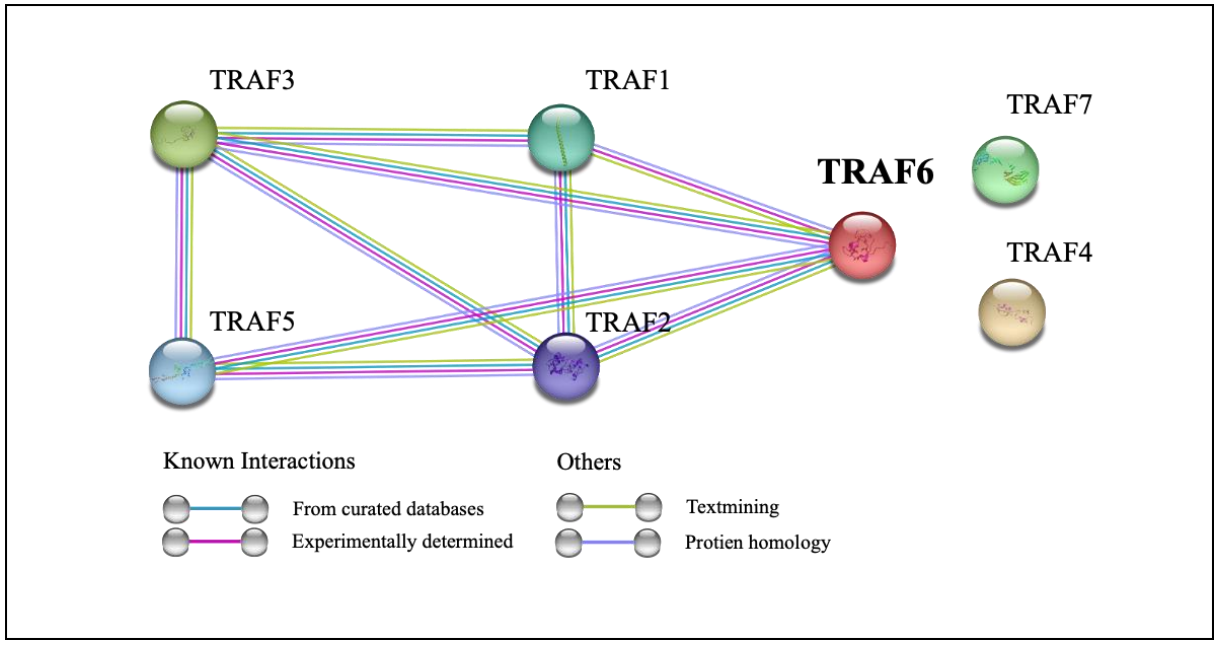

Figure 4.3. Reported interactions of TRAF proteins found in STING database. TRAF1-7 predicted and experimentally confirmed interactions between each other. Blue line indicates information from curated databases, pink line represents experimentally determined interactions, green line represents text-mining and purple line indicates protein homology.

4.4.1.2. Expression patterns of TRAFs in breast cancer patients

Next, I studied the gene expression of the seven members of the TRAF family in clinical samples obtained from healthy individuals and BCa patients in breast invasive carcinoma sequencing data (TCGA-BRCA project). **Figure 4.4** shows the heatmap expression pattern and **Figure 4.5** shows the gene expression of TRAF1 to 7. When compared to their expression in healthy individuals, there is a significant amplification in the expression of TRAF2, TRAF3, TRAF4, TRAF5 and TRAF7 proteins in

BCa patients (**Figure 4.5**). In contrast, there is a non-significant amplification of TRAF1 in BCa patients, and the expression of TRAF6 is significantly less in primary tumour samples than healthy control (**Figure 4.5**).

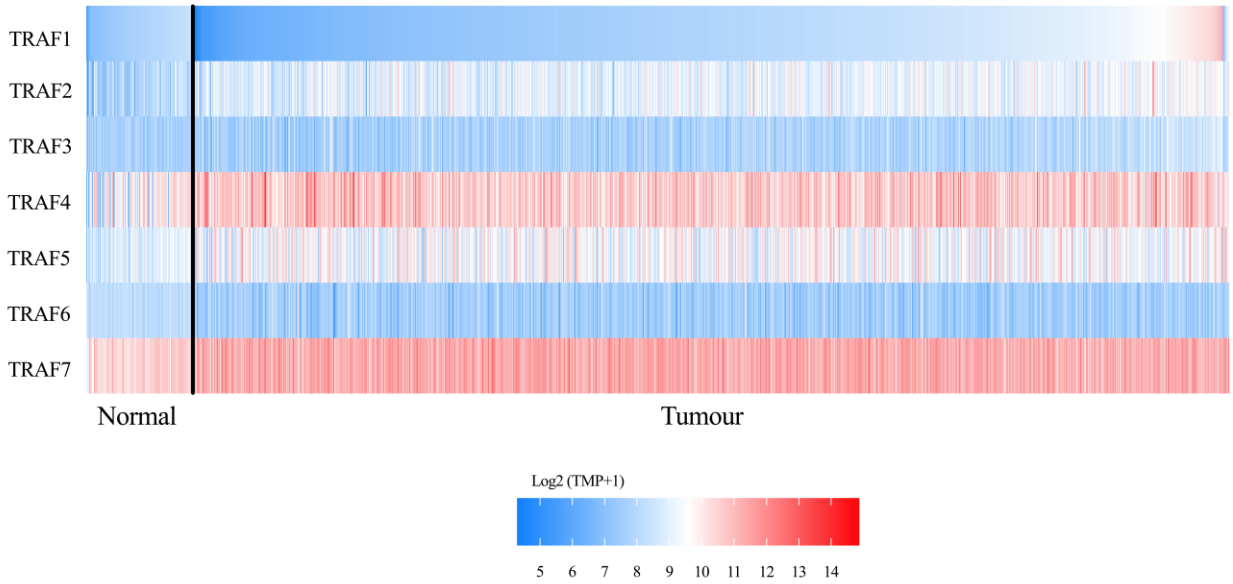

Figure 4.4. Expression patterns of TRAF proteins from healthy and BCa patients. Data obtained from TCGA databases of normal (n=115) and tumour (n=1104) samples from BCa patients. Blue colour represents least expression, pink represents moderate expression and red indicates highest expression. TPM=Transcripts Per Million.

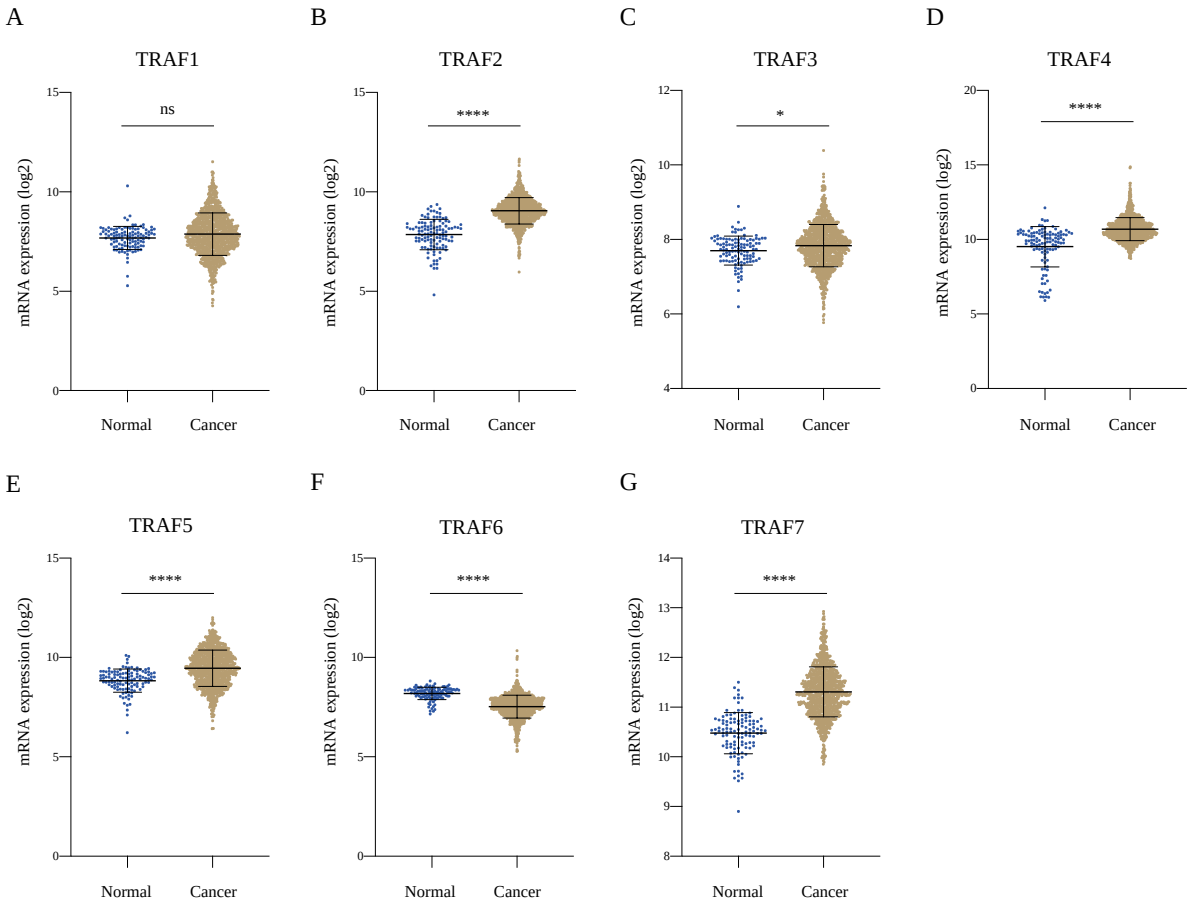

Figure 4.5. Gene expression of TRAF proteins. (A-G) Expression of TRAF1-7 in TCGA BCa samples (n=1104) compared to normal breast tissue (n=115). Each dot represents a single sample. Horizontal black lines indicate mean and standard deviation. P-values were determined using unpaired T test. ****p<0.0001, *p<0.05 compared to healthy group gene expression.

4.4.1.3. Association of TRAFs copy number alternations (CNAs) with metastatic breast cancer in patients

BCa is known to be driven by genomic copy number alternations (CNAs) [12]. Therefore, I examined CNAs in a large cohort of BCa patients to determine acquired modifications at DNA level regarding the expression of TRAF1 to 7. As shown in **Figure 4.6**, all seven members of the TRAF family present amplified CNAs in primary breast tumours. The percentage of samples with amplified TRAF7 is 43%, followed by TRAF2 (29.8%), TRAF5 (28.3%), TRAF4 (21.7%), TRAF3 (18.4%), TRAF1 (16.7%) and TRAF6 (7.2%). Percentage reduction in amplification of TRAF5, TRAF3, TRAF2 and TRAF7 in metastatic samples are 14%, 11.8%, 11% and 3.6%, respectively. In contrast, the percentages of TRAF6, TRAF4 and TRAF1 in metastatic sample increased by 2.1%, 6.1% and 8.1%, respectively. Little or no modifications in the percentage of mutations in all TRAFs (no more than 2%) were found at both

primary and metastasis stages. Additionally, little or no deletions of TRAF4 and TRAF5 were detected in primary and advanced tumour samples, whereas percentages of TRAF7, TRAF1 and TRAF6 deletion in metastasis decreased by 2.7%, 1.1%, 1% and 0.7% when compared to primary samples.

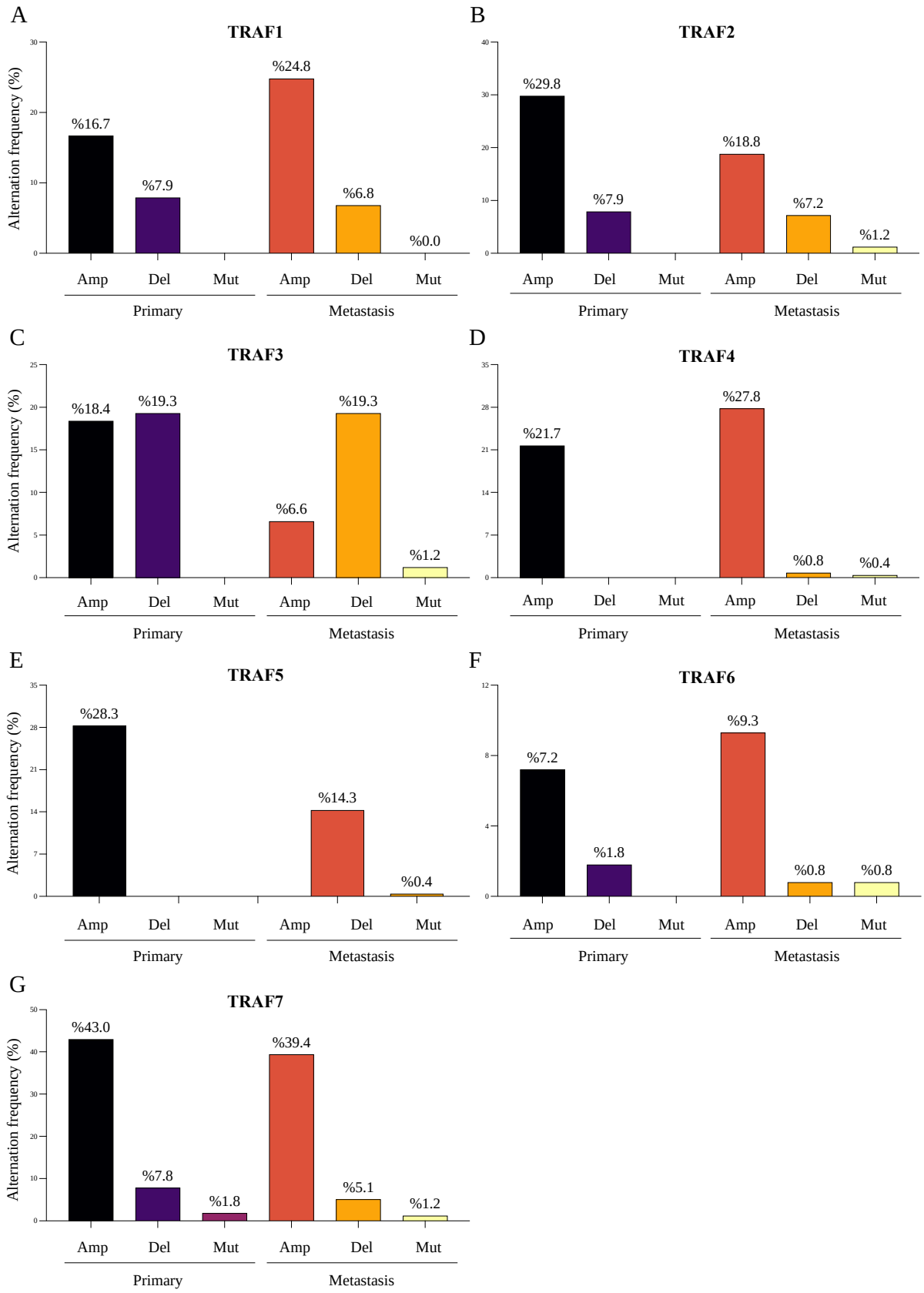

Figure 4.6.Copy-number alternation of TRAFs in primary and metastatic BCa patients. Percentage of frequency in volving amplification (Amp), deletion (Del) and mutation (Mut) found in TRAF1-7 from different stages of BCa. Combined data obtained from Metastatic BCa Project (2020 and 2021) database of primary (n=166) and metastatic (n=335).

4.4.1.4. TRAF6 expression is associated with bone and brain metastasis

TRAFs alternation differed in primary and metastatic BCa patients (**Figures 4.1 to 4.6**). Next, I carried out further validation of clinical data using a large study population with 183 metastatic BCa patients to examine the association between the expression of TRAFs and tissue-specific metastatic potential of advanced BCa (**Figure 4.7**). The expression level of TRAF1 to 7 was studied in patients with a variety of distant metastases including bone, brain, lung, liver, lymph node, skin and breast. Microarray data of BCa metastases at different organs were obtained from GSE14020 and 56493 and combined to assess TRAF expression at site of metastasis to that at primary site. As shown in **Figure 4.7**, TRAF1, TRAF4 and TRAF6 expression is significantly higher in bone metastasis than in primary breast tumours. Whereas TRAF5 was significantly lower (**Figure 4.7A, D, E, F**). In contrast, TRAF1 and TRAF4 levels were significantly higher in brain metastasis whereas TRAF5 was significantly lower than primary (**Figure 4.7A, D, E**). In samples from lung metastasis patients, there is high level of TRAF1 and low level of TRAF3 than primary site (**Figure 4.7A, C**). Tumours from lymph nodes exhibited higher level of TRAF3 than breast tumours (**Figure 4.7A**).

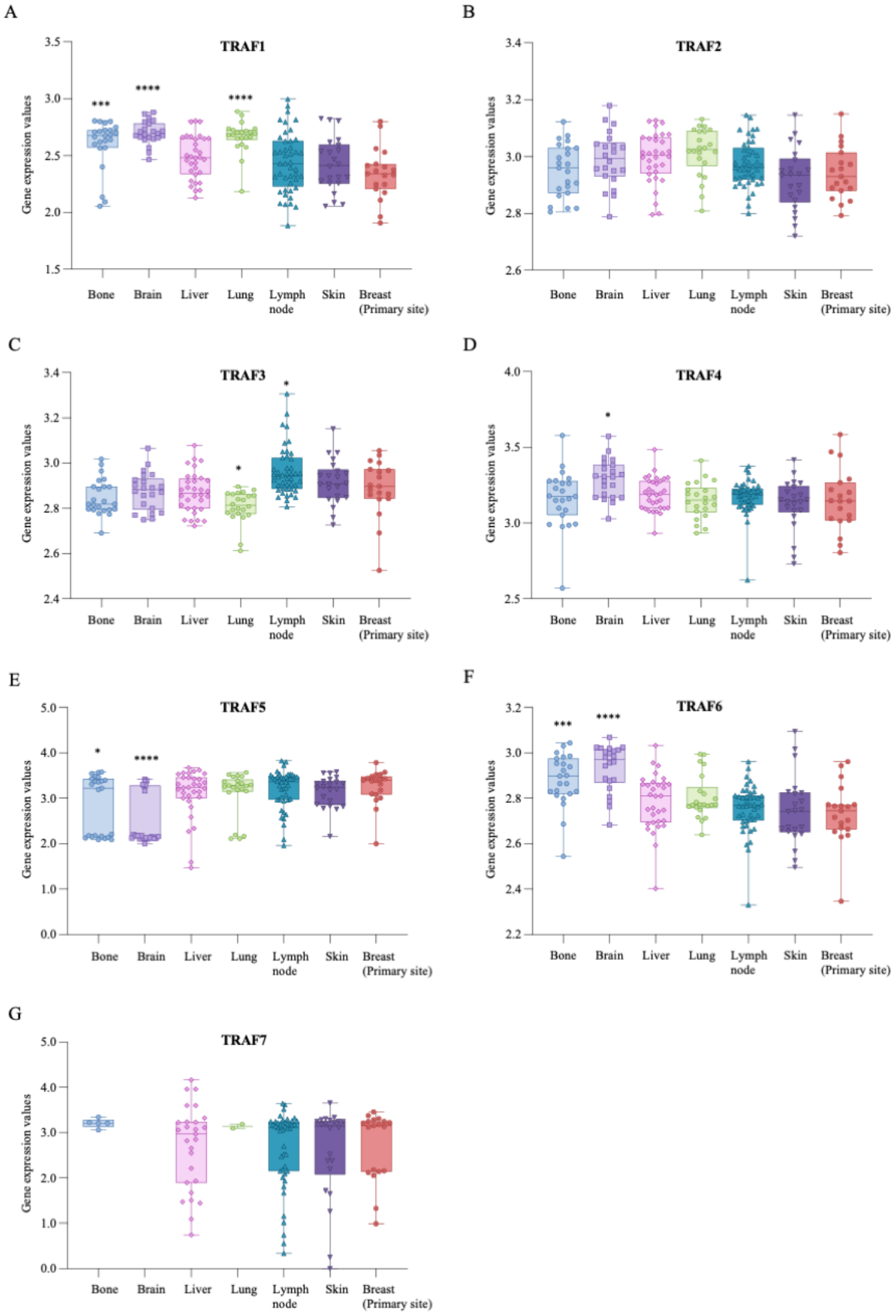

Figure 4.7. Microarray validation. TRAF6 expression in bone (n=23), brain (n=22), liver (n=32), lung (n=22), lymph node (n=44), skin (n=22) breast (n=18) in metastatic breast cancer patients (The Molecular Taxonomy of Breast Cancer International Consortium (METABRIC) dataset).

4.4.1.5. TRAF6 expression is associated with breast cancer survival

Next, I provided further evidence from bioinformatics analysis to confirm the finding from the aforementioned meta-analysis (**Chapter 3**) that first uncovered the association of TRAFs with survival rates in BCa patients. As shown in **Figure 4.8**, the evidence from the present bioinformatics analysis shows that tumours from BCa patients with TRAF3 (n=120), TRAF4 (n=298) or TRAF6 (n=181) amplification exert poorer overall survival when compared to patients with no changes in these genes (TRAF3, n=1350; TRAF4, n=1219; TRAF6, n=1454). I also compared the overall survival of patients with TRAFs deletion to a neutral group (**Supplementary Figure 3**) and this analysis showed that only TRAF5 deletion was significantly associated with poor survival in patients. Next, I focused my analysis on a cohort of triple negative BCa (TNBC) patients within this dataset, and I observed that TNBC patients with TRAF3 amplification had poorer overall survival than those in the neutral group (**Supplementary Figure 4C)**.

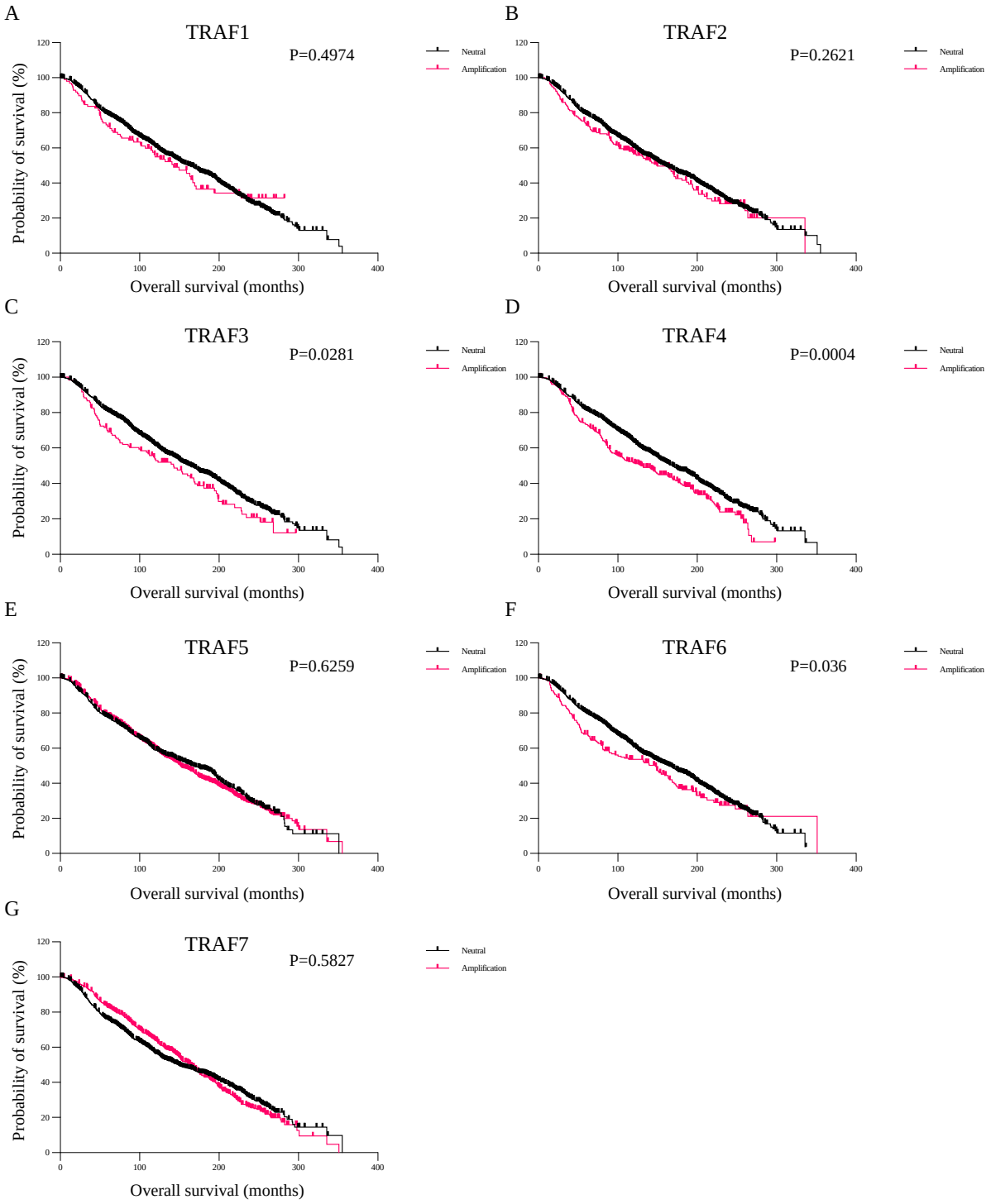

Figure 4.8. BCa patients with TRAF6 copy number variants (CNVs) have significantly shorter overall survival. Retrospective analysis of data obtained from METABRIC via cBioPortal indicated that breast cacner patients with gain or amplification of TRAF6 (n=213) have significantly reduced overall survival compared to patients that are diploid for TRAF6 (n=1738), *p<0.05.

4.4.2. TRAF2/4/6 expression in a panel of human and mouse breast cancer cell lines

4.4.2.1. The triple negative human MDA-MB-231 and mouse 4T1 express higher level of TRAF6 than TRAF2 and 4

Once confirmed the roles of TRAF2, TRAF4, and most importantly TRAF6 in metastasis in advanced BCa patients, particularly those with osteolytic metastasis such as secondary cancer in the skeleton and brain in the meta-analysis (Chapter 3), and retrospective and bioinformatics studies in this chapter (**section 4.4.1**), I used Western Blot analysis to examine TRAF2, TRAF4 and TRAF6 expression in a panel of human and mouse of BCa cell lines with different molecular subtypes and different growth and metastatic abilities.

Table 4.9 shows the molecular subtypes and hormone receptor status of the BCa cells used in the present Western Blot experiments. As shown in **Supplementary Figure 7**, the murine E0771, 4T1, human MCF7 and MDA-MB-231 BCa cell lines expressed all three TRAFs of interest, namely TRAF2, TRAF4 and TRAF6. More importantly, it is evident that TRAF6 expression level was significantly higher in both human and murine TNBC cell lines MDA-MB-231 (**Figure 4.9A**) and 4T1 (**Figure 4.9B**) than TRAF2 and TRAF4 levels.

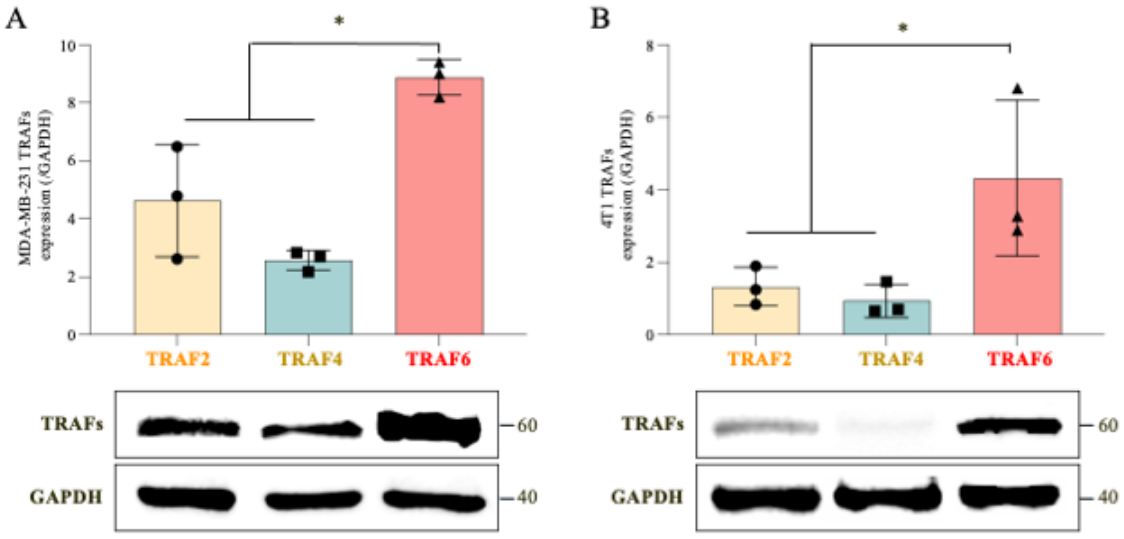

Figure 4.9. Triple negative breast cancer cells express higher level of TRAF6 than TRAF2 and TRAF4. Western blot analysis of cell lysates from (A) human (MDA-MB-231) and (B) murine (4T1) triple negative BCa showed TRAF6 expressed higher than TRAF2 and TRAF4 in both. Values are mean ± SD from 3 independent experiments. *p < 0.05 compared to TRAF6.

Table 4.1. Molecule subtype and hormone receptor status of a panel of human and murine breast cancer cell lines.

	MDA-MB-231	**MCF7**	**4T1**	**E0771**
Species	Human	Human	Mouse	Mouse
Subtype	TNBC	Luminal A	TNBC	Luminal B
ER	-	+	-	ER-α - ER-β -
PR	-	-	-	+
HER2	-	-	-	+

ER refers to oestrogen receptor, PR refers to progesterone receptor, HER2 refers to human epidermal growth factor receptor 2, TNBC refers to triple negative breast cancer.

4.4.2.2. Osteotropic, highly metastatic clones of human MDA-MB-231 and mouse 4T1 breast cancer cells express higher level of TRAF6

Once confirmed the high expression of TRAF6 in the murine and human TNBC cell lines used (**Figure 4.9**) and the association between TRAF6 and BCa bone metastasis in precious studies (**sections 3.4.6.2.2 and 4.4.1.4**), I compared the TRAF6 expression level between parental (P) and osteotropic (BT) clones of the human MDA-MB-231 (MDA-231-BT) and murine 4T1 (4T1-BT). As shown in **Figure 4.10,** the two highly aggressive, metastatic, and osteotropic clones MDA-231-BT and 4T1-BT expressed a higher level of TRAF6 than their own parental clones (**Figure 4.10**).

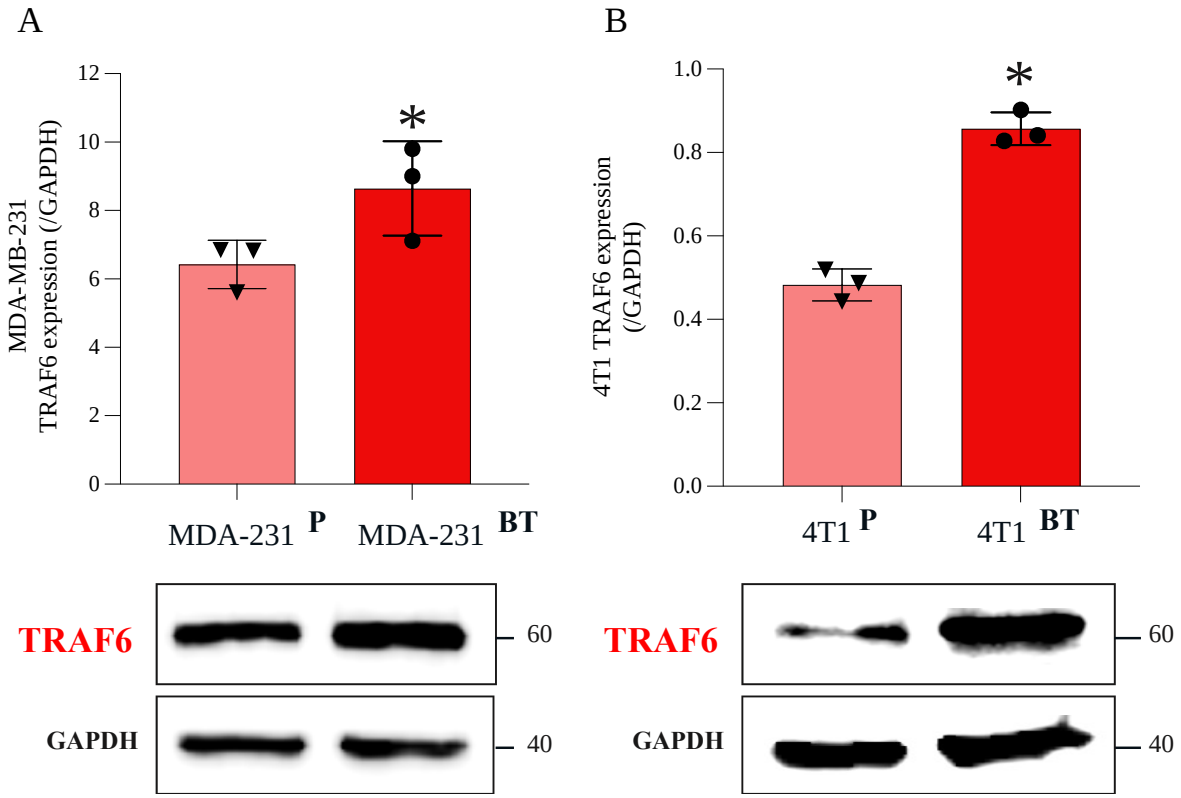

Figure 4.10. Osteotropic, highly metastatic clones of human MDA-MB-231 and mouse 4T1 breast cancer cells express higher level of TRAF6. Western blot analysis of cell lysates from (A) human (MDA-231-BT) and (B) murine (4T1-BT) triple negative BCa showed TRAF6 expressed higher than parental MDA-MB-231 and 4T1, respectively. Values are mean ± SD from 3 independent experiments. *p < 0.05 compared to parental clones.

4.5. Discussion

Members of the TRAF family are key regulators of many biological and oncogenic activities and thus alternations in their expression are commonly detected in tumours, including BCa. Encouraged by evidence from previous studies in the scientific literature [165, 166, 168, 177, 184, 237, 239, 260, 261] and my own findings from the systematic review and meta-analysis (**Chapter 3)** which confirmed the involvement of TRAF2, TRAF4 and TRAF6 in BCa progression and metastasis, I carried out a series of dry science investigations that involve retrospective and bioinformatic analysis of the association between genetic modifications of TRAF proteins and initiation, progression and metastasis of BCa. To enhance the credibility of this investigation, I combined data from several public databases, and then followed this with performing a number of wet laboratory experiments that used Western Blot analysis to confirm the expression of the identified TRAF proteins in human and mouse BCa cell lines with different degrees of malignancy and abilities to metastasise to and cause secondary BCa in distant tissues including bone and brain.

First, functional predictions from GO and KEGG enrichment analysis as well as PPI revealed the involvement of all members of the TRAF family, except TRAF7, in cancer. This finding can be explained by the fact that TRAF7 is not considered a classical member of TRAF family due to lack of the highly conserved TRAF domain needed for interactions with the TNFR superfamily members[160]. Next, TRAF2 and TRAF6 have been found to be involved in osteoclast differentiation as previously reported [156, 182, 191, 264]. I also found that TRAF2, TRAF6 as well as TRAF3 contribute to a variety of immune activities that include regulation of immunoglobulin secretion, immune effector process and cytokine production. Mechanistically, my analysis confirmed that canonical IκB/NFκB signalling is mediated by activation of TRAF1 to 6, whereas only TRAF2, TRAF4, TRAF6 and TRAF7 are directly involved in the regulation of protein kinase activity. Interestingly, only TRAF2, TRAF6 and TRAF7 are also involved in the activation of MAPK, whereas JNK activation is positively regulated by TRAF1 to 6.

Next, analysis of TRAFs expression patterns in BCa patients showed that with the exception of TRAF1, all other TRAFs exhibited a modified expression in cancer when compared to healthy tissue. While my own findings showed that TRAF6 expression is significantly higher in TNBC than in other subtypes

[265], its expression is slightly lower in samples from BCa patients when compared to samples from healthy individuals. This is in consistent with prostate cancer [266], but in contrast with cancers such as colon cancer [267], liver cancer[268], pancreatic cancer [269] and renal cell carcinoma [270]. More importantly, it implies that TRAF6 plays a relatively minor role in the initiation and early stages of the disease, but its role becomes more prominent in advanced, metastasis BCa including bone metastasis. Moreover, expression level of TRAF6 that inconsistent with cancer initiation also appears in lung cancer. In contrast with some studies that showed that TRAF6 expression level is higher in lung cancer than healthy control [192, 271], works from Liu et al [272] showed an increase level of miR-146a-5p, which is a TRAF6 suppressor, in serum of non-small cell lung cancer (NSCLC) is significantly higher than in normal control. Sample size, cancer subtypes and stage, patient background, measurement approaches could be the factors compounding the aforementioned discrepancies and thus further research that involves large, and diverse datasets is needed. Take for example the present combined microarray studies in GEO datasets that implicated TRAF6 as well as TRAF1, TRAF5 in bone metastases and TRAF3, TRAF4 and TRAF6 in TNBC and survival rate, confirming the involvement of TRAF proteins in BCa progression compared to healthy individuals. Future studies should also examine somatic TRAFs expression among different subtypes or stages of the disease among large cohorts of patients and healthy control.

Tumours from different BCa subtypes and stages contain various mutations in oncogenes and tumour suppressor genes, copy number alternation was deemed as a major characteristic of many stages of BCa, including metastasis [12]. With this in mind, I examined CNAs in a large cohort of BCa patients to reveal that TRAF6 as well as TRAF4 exhibited an increased ratio of amplification in metastasis than in primary tumours from BCa patients, confirming the role of these two TRAFs in metastatic BCa. This finding is in agreement with the hypothesis of this project and with findings from the present meta-analysis (**Chapter 3**).

Finally, western blot analysis of protein expression confirmed that TRAF2, 4, 6 are expressed in both human and mouse TNBC cell lines, but TRAF6 expression is significantly higher than TRAF2 and 4. When compared to parental BCa cells, osteotropic subclones of MDA-MB-231 and 4T1 that were generated through *in vivo* passaging in mouse long bones have been found to express significantly higher

level of TRAF6 [184, 273]. This finding is important because it complement data from the present investigations as well as previous studies that implicated TRAF6 and its related signalling pathways to key factors and receptors implicated in BCa[160, 231], inflammation [108, 227, 231, 237, 238, 274] and bone metastasis [184, 275-277].

To conclude, **Table 4.2** summarised the main findings of this chapter. Briefly, my meta-analysis of pooled *in vitro, in vivo*, and human studies, coupled together with bioinformatics validation and Western blot confirm that TRAF6 inhibition may be of value in the management of multiple aspects of advanced BCa. However, evidence from included studies indicates that other TRAFs, particularly TRAF2 and TRAF4, are also implicated in advanced BCa. Thus, we hypothesise that agents that target multiple TRAFs, particularly TRAF2/4/6, can be of greater therapeutic value in the treatment of difficult-to-treat BCa subtypes than those that inhibit the activity of individual TRAF. However, it is important to note that potential side-effects associated with the therapeutic use of multi-TRAF inhibitors are unknown. Therefore, further preclinical validation of the anti-tumour, anti-metastatic and anti-osteolytic efficacy of TRAF inhibitors in multiple models of advanced BCa are needed.

Table 4.2. Involvement of TRAFs in breast cancer initiation, progression and metastasis. ± denotes neutral, + represents moderately high, ++ high, – indicates moderately low, -- low.

	TRAF1	TRAF2	TRAF3	TRAF4	TRAF5	TRAF6	TRAF7
Cancer	++	++	++	++	++	++	-
Osteoclastgenesis	-	++	-	-	-	++	-
Expression in cancer versus normal tissue	±	++	+	++	++	--	++
Hazard ratio in overall survival	no	no	yes	yes	no	yes	no
DNA amplification in metastasis than primary	+	--	--	+	--	+	-
Expression in bone metastasis than primary	++	±	±	±	-	++	±

CHAPTER 5. Effects of Cancer-specific Knockdown and Pharmacological Inhibition of TRAF6 on Metastatic Breast Cancer Cell Behaviour *in vitro*

5.1. Summary

Previous studies have shown that TRAF6 plays an important role in BCa, particularly TNBC. In **Chapter 3 and 4,** I have shown that TRAF6 is implicated in various aspects of advanced metastatic BCa, including secondary BCa in bone and brain, and its high expression is associated with osteoclastogenesis and poor survival rate in patients. However, the effects of pharmacological and genetic manipulation of cancer-specific TRAF6 activity on the metastatic and osteolytic behaviour of BCa cells have been poorly investigated. Thus, the role of cancer-specific TRAF6 on osteotropic BCa cell growth, migration and invasion were investigated. To achieve this, I used a number of genetic as well as pharmacological approaches (using verified and novel TRAF6 inhibitors) to manipulate TRAF6 in selected human and mouse TNBC cancer cells, and then examine the effects of these changes on their ability to grow and move *in vitro*. Firstly, I successfully knocked down TRAF6 in triple negative human MDA-MB-231 and its *in vivo* passaged osteotropic clone, MDA-231-BT, by lentiviral transduction using three shRNA constructs. Secondly, I studied the anti-growth, anti-migratory, and anti-invasive ability of a verified CD40-TRAF6 inhibitor, called 6877002 and its novel family of congeners FSAS1 to FSAS5 on wild type and genetically modified clones of the aforementioned BCa cells. My *in vitro* investigation showed that FSAS3 is more potent than 6877002 (and other FSAS members) in all cultures of human and mouse BCa cells tested. Interestingly, FSAS3 inhibited the growth of osteotropic TNBC cells more potently than their parental clones. Additionally, FSAS3 enhanced the cytotoxic efficacy of a panel of chemotherapeutic agents, particularly Docetaxel and Paclitaxel. Further functional studies confirmed that both TRAF6 knockdown and pharmacological inhibition using 6877002 and FSAS3 significantly reduced the ability of TNBC cells to grow, invade and migrate *in vitro*. Finally, inhibition of cell viability and NFκB activation in cultures of human MDA-MB-231 and their osteotropic clones MDA-231-BT cells were significantly blunted in TRAF6-deficient clones of these cells when compared to mock control. Collectively, these studies confirm that cancer-specific inhibition by genetic and using the novel TRAF6 inhibitor FSAS3 exert anti-growth, anti-migratory, and anti-inflammatory in the BCa models described.

5.2. Introduction

The TRAF/NFκB signal transduction pathway plays an important role in inflammation[278-280], immunity[281] and cancer[282], especially in metastasis[283, 284]. As key components of NFκB signalling, TRAF2, TRAF3, TRAF4, and TRAF6 activation have been linked to BCa metastasis and survival rate in patients. Conversely TRAF2[162] or TRAF4[162, 165, 166] down-regulation or inhibition suppresses BCa cell adhesion, motility *in vitro* and reduces the growth of tumours in animal models of BCa. Previous work from our group has shown that TRAF2 enhances the skeletal tumour growth and promotes osteolysis in osteotropic BCa cells [239]. Several studies by other groups have also shown that micro ribonucleic acids that target various TRAFs affect the growth and metastasis of BCa cells. For example, miR-214 has been found to be highly regulated in BCa patients, and preclinical studies have shown that it targets TRAF3 in the bone resorbing cells, osteoclasts, to promote osteolytic bone metastasis of BCa *in vivo* [163]. Additionally, miR-29-3p promotes the progression of TNBC cells via downregulating TRAF3 [164].

Among all TRAFs, TRAF6 has been the most studied in cancer, particularly BCa [231, 285]. In 2014, Chatzigeorgiou et al. identified 6877002 as a small molecule inhibitor that targets the CD40-TRAF6 interaction [140]. The compound 6877002 selectively inhibited the CD40-TRAF6 pathway by binding to residues 119 and 129 rather than CD40-TRAF2/3/5, showing promising effect on improving insulin sensitivity and decreasing recruitment of inflammatory cells *in vivo*[286, 287]. In the work of Zarzycka et al., six small-molecule inhibitors, including 6877002, were used to reduce peritoneal inflammation and further studies revealed that inhibition of TRAF6 with 6877002 and one of its derivatives increased the survival rate of mice with polymicrobial sepsis-induced systemic inflammation[155]. Previous studies by our group[184, 185] demonstrated that the CD40-TRAF6 inhibitor 6877002 exerts anti-inflammatory, anti-metastasis, but not osteoprotective, effect in rodent models of rheumatoid arthritis, BCa bone metastasis and RANKL-induced osteolysis. Together, these findings highlighted the potential of CD40-TRAF6 inhibitors such as 6877002 as anti-inflammatory agents that can be used alone or in combination with existing treatments for the reduction of metastatic spread, but not osteolytic ability, of BCa cells. Encouraged by this hypothesis, we designed, synthesised and tested the effects of a new series of novel congeners of 6877002. This family of compounds called FSAS and it consists of five members,

namely FSAS1, FSAS2, FSAS3, FSAS4 and FSAS5. In her PhD project, D. Giovana Carrasco G., a previous member of our group, has examined the effects of pharmacological inhibition and knockdown of TRAF6 on prostate cancer-induced bone cell activity and osteolysis. Briefly, Carrasco and other colleagues have shown that the novel congener FSAS3 inhibited the *in vitro* viability, migration and invasion of mouse and human prostate cancer cells (White Rose ethesis, University of Sheffield, UK: https://etheses.whiterose.ac.uk/27832/).

In this chapter, I took the decision to test the effect of BCa- specific of TRAF6 inhibition using a genetic and pharmacological approach (i.e. FSAS1-5), on BCa cell behaviours *in vitro*.

5.3. Aims

The aim of this chapter was to examine the hypothesis that TRAF6 knockdown and pharmacological inhibition of TRAF6 using the verified CD40-TRAF6 inhibitor 6877002 and its novel congeners FSAS1-5 reduces the *in vitro* behaviour of TNBC cells.

This aim will be achieved by:

- Successfully knocking down the expression of TRAF6 in human parental MDA-MB-231 cells and their highly metastatic, and osteotropic clone MDA-231-BT BCa cells.
- Investigating the effect of TRAF6 knockdown and treatment with the verified CD40-TRAF6 inhibitor 6877002 and its novel congeners FSAS1to 5 on the *in vitro* viability, migration and invasion of the aforementioned TNBC cells.

5.4. Results

5.4.1. Effects of TRAF6 genetic inhibition on breast cancer cell behaviour *in vitro*

5.4.1.1. Confirmation of successful knockdown of TRAF6 in human MDA-MB-231 and osteotropic (BT) cells

In **Chapter 4**, I confirmed that the human osteotropic MDA-231-BT express higher levels of TRAF6 than their parental control, which I also found that it expresses high levels of TRAF6 when compared to the hormone-dependent MCF7 cells. Here, I stably knocked down TRAF6 in both parent MDA-MB-231 and their osteotropic clone MDA-231-BT cells using lentiviral vectors expressing three individual TRAF6 shRNA clones and one empty vector (mock) as control. Successful TRAF6 knockdown was confirmed by quantifying TRAF6 protein expression in TRAF6-deficient and mock control via Western Blot. As shown in **Figure 5.1**, TRAF6 expression was significantly reduced in all three colonies of parental MDA-MB-231 and osteotropic MDA-231-BT BCa cells when compared to their mock group. Colonies expressing between approximately 70 and 93% of reduction in TRAF6 expression, namely shT6KD^{1} and shT6KD^{3} of each cell line were chosen for subsequent experiments.

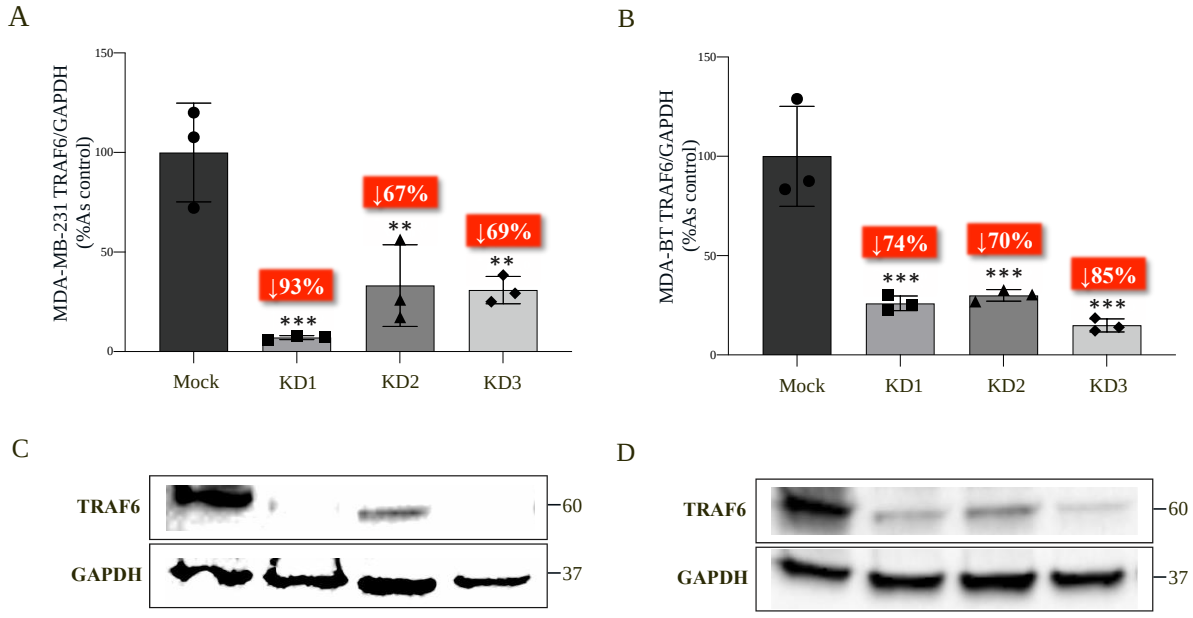

Figure 5.1. Successful TRAF6 knockdown expression in MDA-MB-231 and MDA-231-BT breast cancer cells. Percentage of relative TRAF6 from the three shRNA TRAF6 constructs using MDA-MB-231 (A) and MDA-231-BT (B) BCa cells. Representative images of MDA-MB-231 (C) and MDA-231-BT (D) cell samples by Western Blot. Data obtained from three independent experiments. P-values were obtained from ordinary ANOVA test followed by Tukey *post hoc* test. ***$p < 0.0005$, **$p < 0.01$ compared to mock transfected cells.

5.4.1.2. TRAF6 knockdown reduced breast cancer cell growth *in vitro*

Next, the viability of TRAF6-deficient parental MDA-MB-231 and osteotropic MDA-231-BT TNBC cells and their mock controls was assessed using Alamar Blue™ cell viability assay as described in **section 2.3.4.1**. As shown in **Figure 5.2**, TRAF6 knockdown significantly reduced the viability of both MDA-MB-231 and MDA-231-BT cells in a time-dependant manner after 48, 72 and 96 hours. As expected, these trends were consistent with the efficacy of TRAF6 knockdown in both parental and osteotropic TNBC cells used. After 24, 48, 72 and 96 hours, MDA-MB-231 TRAF6^{KD1} cells exhibited less growth than MDA-MB-231 TRAF6^{KD3} cells, consistent with lower TRAF6 expression in MDA-MB-231 TRAF6^{KD1} than MDA-MB-231 TRAF6^{KD3}. Similarly, MDA-231-BT TRAF6^{KD3} cells exhibited lower growth than MDA-231-BT TRAF6^{KD1} at all time points which again is consistent with TRAF6 expression (**Figure 5.1**, and **Supplementary Table 14)**.

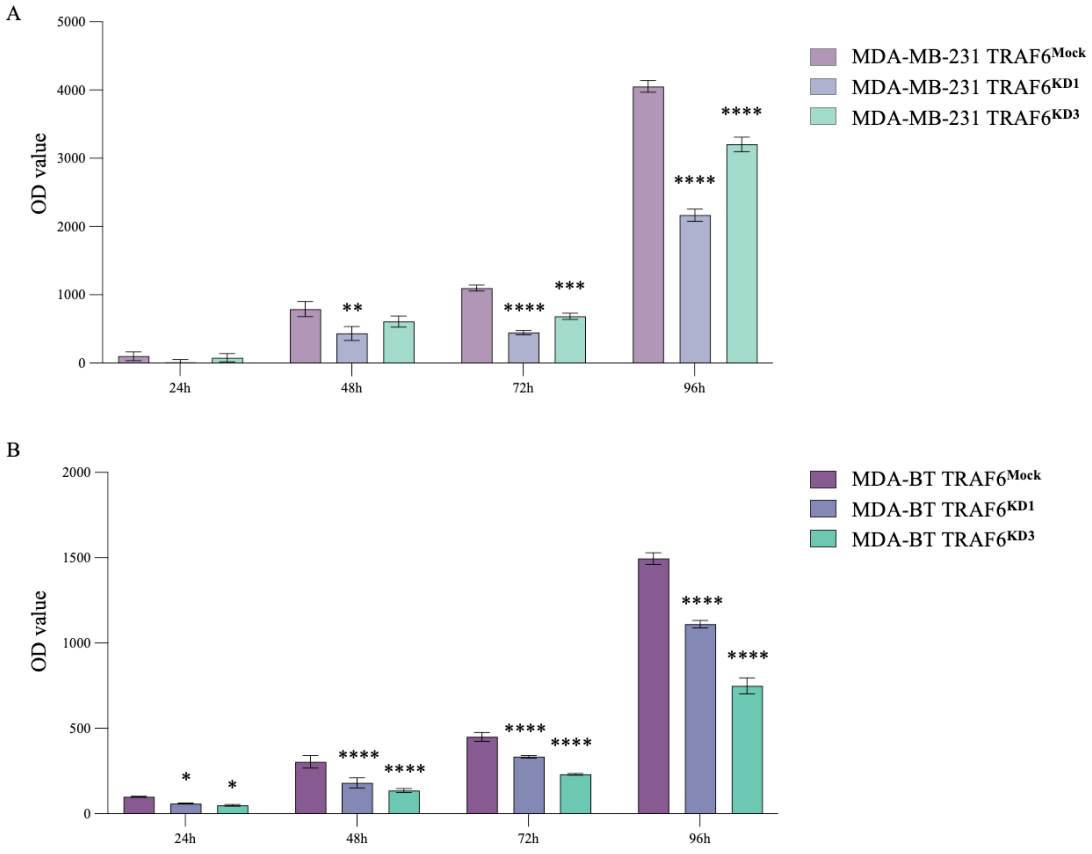

Figure 5.2. TRAF6 knockdown in triple negative breast cancer cell lines MDA-MB-231 and its osteotropic clone MDA-231-BT reduced cell growth *in vitro*. Percentage of viability of MDA-MB-231 (A) and MDA-231-BT (B) TRAF6 knockdown BCa cells compared to cells silenced with control shRNA. Data obtained from three independent experiments. P-values were obtained from ordinary ANOVA test followed by Tukey *post hoc* test. ****p < 0.0001, ***p < 0.0005, **p < 0.01, *p < 0.05 compared to mock transfected cells.

5.4.1.3. Knockdown reduced the migration of breast cancer cells *in vitro*

The TRAF6/NFκB axis plays an important role in the motility of BCa, and downregulation of TRAF6, by overexpression of miR-146a or treatment with the small molecular inhibitor TJ-M2010-2, inhibited the migration of MCF7 BCa cell *in vitro*[244, 246]. Here, the effects of TRAF6 knockdown on the *in vitro* migration of human MDA-MB-231 and their osteotropic clone MDA-231-BT BCa cells was assessed by wound healing assay as described in **section 2.2.6.1**. As shown in **Figure 5.3**, knockdown of TRAF6 reduced 2D-directed migration of human MDA-MB-231 TRAF6$^{\mathbf{KD1}}$ cells by 25.9% and that of MDA-MB-231 TRAF6$^{\mathbf{KD3}}$ by 19.5%. More importantly, knockdown of TRAF6 reduced the migration of the human osteotropic MDA-231-BT TRAF6$^{\mathbf{KD1}}$ cells by 20.4% and that of MDA-231-BT TRAF6^{KD3} by 25.7% when compared to their mock control.

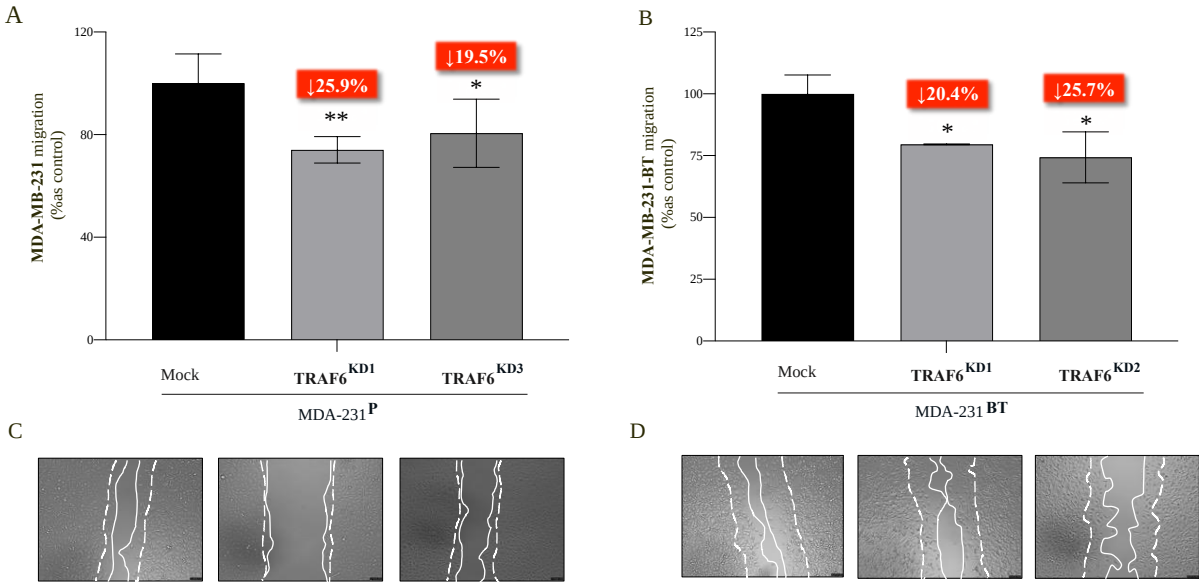

Figure 5.3. TRAF6 knockdown decreased MDA231 parental and osteotropic cell migration *in vitro*. Percentage of cell migration from BCa cells silenced with control shRNA compared to TRAF6 knockdown MDA-MB-231 (A) and MDA-231-BT (B) BCa cells. Representative images showing initial and final positions of motility in timepoints 0 (dotted lines) and 11 hours (continuous lines) from MDA-MB-231 (C) and MDA-231-BT (D) cells. Data obtained from three independent experiments. p-values were obtained from one-way ANOVA test followed by Tukey post hoc test. **p<0.01 and *p<0.05 compared to mock transfected cells. Scale bar = 100 μM.

5.4.1.4. TRAF6 knockdown reduced the invasion of breast cancer cells *in vitro*

Previous studies have shown that downregulation of TRAF6 inhibited the invasion of MCF7 and MDA-MB-231 BCa cell *in vitro*[184, 244]. Here, the effects of TRAF6 knockdown on the *in vitro* invasion human MDA-MB-231 and their osteotropic clone MDA-231-BT was assessed by the Transwell® invasion assay as described in **section 2.2.7.1**. As shown in **Figure 5.4**, knockdown of TRAF6 reduced MDA-MB-231 cell invasion by 42,8% in TRAF6^{KD1} and 61.7% in TRAF6^{KD3}. Consistently, knockdown of TRAF6 also reduced MDA-231-BT cell migration by 36.3% in TRAF6^{KD1}, and 48.5% in TRAF6^{KD3} after 72 hours when compared to their mock controls.

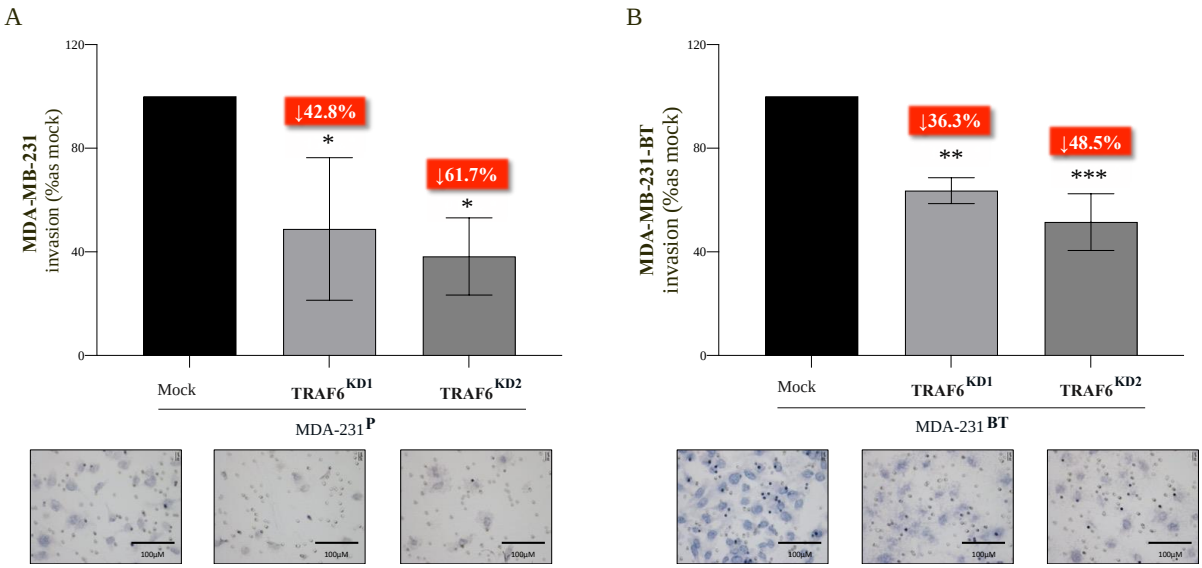

Figure 5.4. TRAF6 knockdown decreased MDA-MB-231 parental and osteotropic cell invasion *in vitro*. Percentage of cell invasion from BCa cells silenced with control shRNA compared to TRAF6 knockdown MDA231 (A) and BSI (B) BCa cells. Representative images of cells invasion after 72 hours from MDA231 (C) and BSI (D) cells. Values are expressed as mean ± SD and were obtained from three independent experiments. p-values were obtained from one-way ANOVA test followed by Tukey post hoc test. **p<0.01 and *p<0.05 compared to mock transfected cells. Scale bar = 100 µM.

5.4.2. Effects of pharmacological inhibition of TRAF6 on breast cancer cell behaviour *in vitro*

Once confirmed the role of TRAF6 on BCa cell behaviour, I used a pharmacological approach to test the anti-tumour, anti-migratory and anti-invasive properties of the verified TRAF6 inhibitor and its novel congeners FSAS1 to 5 in cultures of mock and TRAF6-deficienct BCa cells. The targeting and inhibition of CD40-TRAF6 interaction by 6877002 our collaborator Nicolaes and colleagues (University of Maastricht, Netherlands) [155, 286, 288]. Previous *in vitro*, *ex vivo* and in vivo research by our group which I took part [184, 185] have shown that 6877002 exerts an anti-metastasis, anti-inflammatory, but not an osteoprotective, effects. To develop a TRAF6 inhibitor that has a potential to exert anti-osteolytic effects, Dr A. Idris (University of Sheffield, UK) and his collaborators Professor A. Sparatore and Dr Ivan Bassanini (University of Milan, Italy) have developed a number of novel congeners of 6877002, called FSAS1 to FSAS5.

5.4.2.1. The novel FSAS3 is a potent inhibitor of human and mouse breast cancer cell viability *in vitro* than 6877002

In this section, the effects of five structurally-related novel congeners of the inhibitor of CD40-TRAF6 6877002, called FSAS1 to 5, on the viability of a panel of human and murine BCa cells was assessed using the Alamar Blue™ assay (**section 2.2.5.1**). The list of BCa cells used include human hormone-dependent MCF7, triple-negative MDA-MB-231, triple-negative osteotropic MDA-231-BT BCa cells and murine hormone-dependent E0771, triple-negative 4T1, triple-negative osteotropic 4T1-BT BCa cells as shown in **Supplementary Table 15**. As shown in **Table 5.1** and **Supplementary Table 16**, FSAS3, FSAS5 and 6877002 inhibited the viability of all BCa cells tested in a dose-dependent manner with different degree of potency, as determined by IC_{50} values. FSAS3 was significantly more potent than 6877002 and other FSAS ($p < 0.05$). Drug-respond curves and representative images for FSAS3 and 6877002 are shown in **Figure 5.5**. Altogether, these results indicate that both 6877002 and FSAS3 are potent inhibitors of BCa cell viability *in vitro*, however FSAS3 was significantly more potent that all others at the concentration of 1, 3, 10 μM in MCF7, MDA-MB-231, 1, 3, 10, 30 μM in osteotropic MDA-231-BT, 10 μM in 4T1 and 30 μM in 4T1-BT. In contrast, 6877002 was more potent at the

concentration of 30 and 100 μM in MDA-MB-231, and there was no difference at the concentration of 30 and 100 μM in all cultures. Thus, FSAS3, out of all other FSAS compounds, was selected for subsequent experiments.

Table 5.1. Effects of the verified CD40-TRAF6 inhibitor 6877002 and five congeners on the viability of a panel of murine and human breast cancer cells with different metastatic abilities *in vitro*. Cell viability was measured after 72 hours of continuous exposure to the six profiled TRAF inhibitors. Calculation of half maximal inhibitory concentration (IC_{50}) was performed as previous described. Values are expressed as mean ± SD and were obtained from three independent experiments.

			Half maximal inhibitory concentration (IC50) in µM after 72 hours					
	Cell type	**Classification**	**FSAS1**	**FSAS2**	**FSAS3**	**FSAS4**	**FSAS5**	**6877002**
Murine cell lines	E0771	Hormone dependent	5.22±2.34	4.58±2.34	0.33±0.18	29.32±7.64	22.9±13.80	14.47±3.16
	4T1	Triple negative	>100	92.68±6.40	29.54±4.82	>100	30.41±0.29	87.88±3.52
	4T1-BT	Triple negative -Osteotropic	>100	50.17±10.77	29.24±1.49	>100	36.92±4.56	92.24±3.92
Human cell lines	MCF7	Hormone dependent	>100	>100	5.99±1.18	>100	41.00±0.65	25.64±6.60
	MDA-MB-231	Triple negative	55.00±10.19	29.03±0.58	8.67±3.19	>100	70.63±11.72	23.1±3.94
	MDA-MB-231-BT	Triple negative -Osteotropic	>100	20.68±6.80	5.61±2.76	>100	13.33±2.76	44.53±7.37

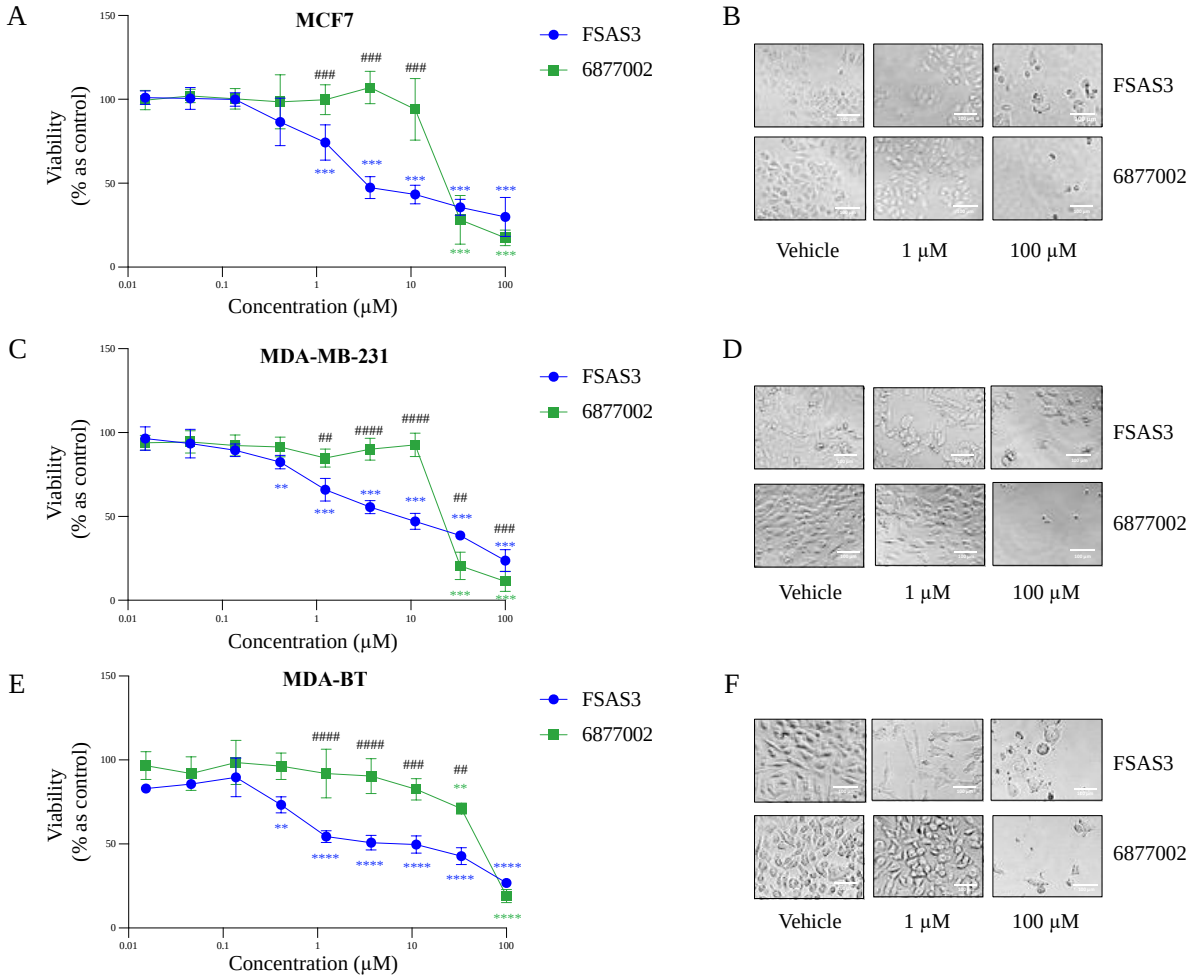

Figure 5.5. Effects on cell viability of a panel of human breast cancer cells treated with verified CD40-TRAF6 inhibitor 6877002 and the most potent novel TRAF6 inhibitor FSAS3 *in vitro*. Dose-response curves of the verified 6877002 and novel FSAS3 on the viability of hormone-dependent MCF7 (A), triple-negative MDA-MB-231 (C) and osteotropic triple-negative MDA-231-BT (E) BCa cells after 72 hours, as assessed via Alamar Blue™ assay. Representative images of cells invasion after 72 hours from MCF7 (B), MDA-MB-231 (D) and MDA-231-BT (F) cells. Values are expressed as mean ± SD and were obtained from three independent experiments. p-values were obtained from two-way ANOVA test followed by Tukey post hoc test. ****p < 0.0001, ***p < 0.0005, **p < 0.005 and *p < 0.05 compared to vehicle, ####p < 0.0001, ###p < 0.0005, ##p < 0.005 compare FSAS3 to 6877002. Scale bar = 100 μM.

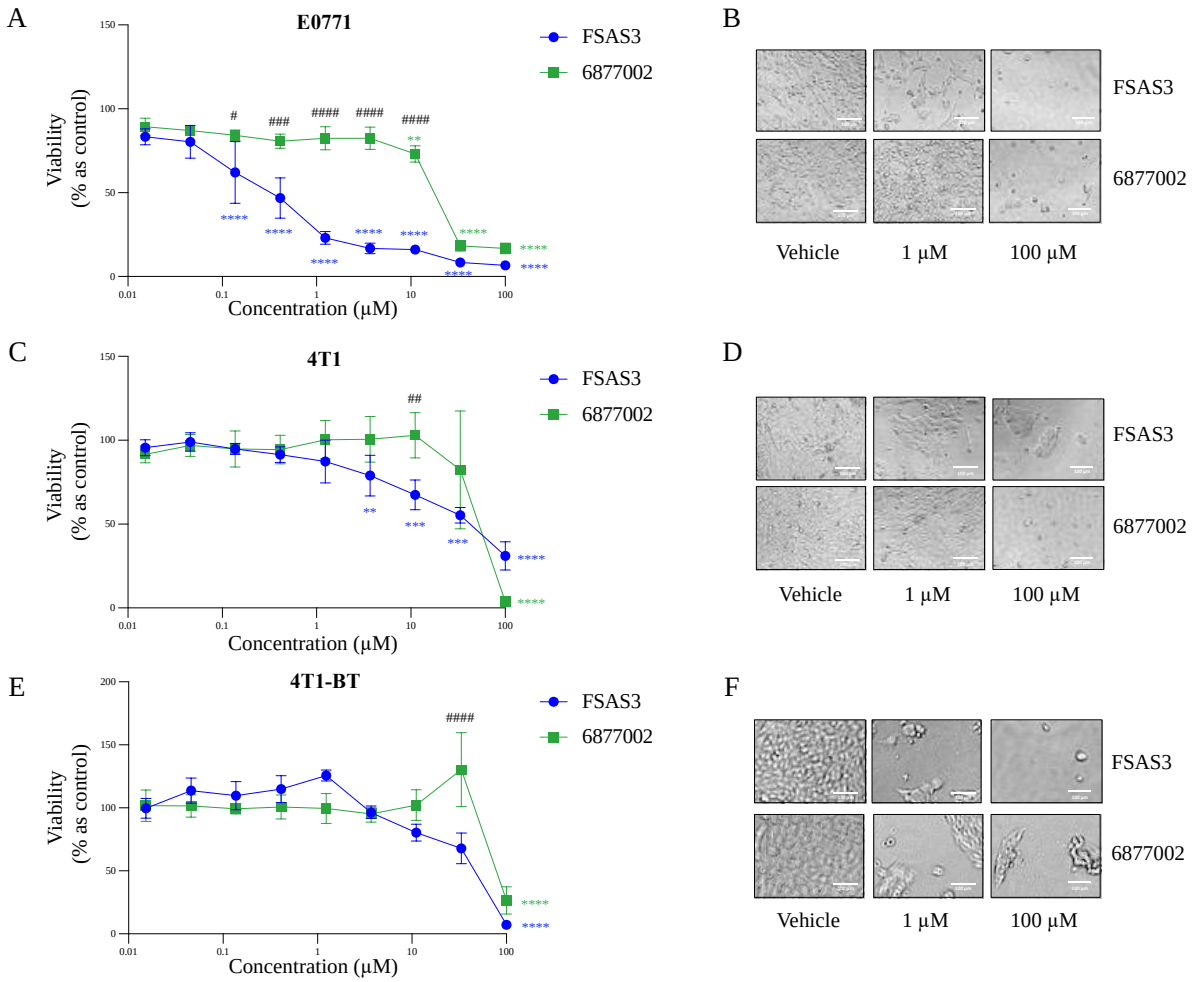

Figure 5.6. Effects on cell viability of a panel of murine breast cancer cells treated with verified CD40-TRAF6 inhibitor 6877002 and the most potent novel TRAF6 inhibitor FSAS3 *in vitro*. Dose-response curves of the verified 6877002 and novel FSAS3 on the viability of hormone-dependent E0771 (A), triple-negative 4T1 (C) and osteotropic triple-negative 4T1-BT (E) BCa cells after 72 hours, as assessed via Alamar Blue™ assay. Representative images of cells invasion after 72 hours from E0771 (B), 4T1 (D) and 4T1-BT (F) cells. Values are expressed as mean ± SD and were obtained from three independent experiments. p-values were obtained from two-way ANOVA test followed by Tukey post hoc test. ****p < 0.0001, ***p < 0.0005, **p < 0.005 and *p < 0.05 compared to vehicle, ####p < 0.0001, ###p < 0.0005, ##p < 0.005 compare FSAS3 to 6877002. Scale bar = 100 μM.

5.4.2.2. FSAS3 enhanced the cytotoxic efficacy of a panel of chemotherapeutic agents *in vitro*

Currently, unlike ER/PR and HER2 positive BCa, there are no targeted therapies available for triple-negative BCa due to the lack of hormone receptor. As a result, patients with triple-negative BCa are often treated with chemotherapy, either as a single agent or in combination with other drugs. Moreover, chemotherapy drugs are often used for neoadjuvant treatment of triple-negative BCa, with the aim of reducing the tumour to a certain volume range before surgical removal [289]. Several research has demonstrated that the activation of the NFκB pathway contributes to chemotherapy resistance in various types of cancer, including BCa [290]. Therefore, inhibiting this pathway pharmacologically could potentially improve the effectiveness of chemotherapy. Given to these reasons, I chose to test the impact of our novel drug, administered in conjunction with a range of clinically relevant compounds possessing different mechanisms of action, on the viability of TNBC cells. The chemotherapeutic agents include docetaxel, paclitaxel, cyclophosphamide, 5-fluorouracil, rapamycin, tamoxifen and doxorubicin.

Briefly, a concentration of FSAS3 (10μM) that reduced around 20% viability of 4T1 was picked in combination with the selected chemotherapies in a serial dilution concentration (refers to **section 2.2.5.1.2**). As shown in **Figures 5.7,** murine 4T1 cells response to all drugs at a dose-dependent manner. Interestingly, taxane (docetaxel, paclitaxel) were effective in the nanomolar range, cyclophosphamide was only effective in the millimolar range. The dose-response curve of FSAS3 combined chemotherapy drugs (white circles) significantly shifts downward compared to when single drug (black circles) in docetaxel, paclitaxel, cyclophosphamide, rapamycin and tamoxifen at the concentrations of 10 μM which inhibit the viability less than 80% whereas only slightly shifted in 5-fluorouracil and doxorubicin.

According to the IC50 values in **Table 5.2,** all compounds alone achieved IC50 values in the micromolar range except taxane (docetaxel, paclitaxel) and doxorubicin, which had IC50 values in the nanomolar after 72 hours. Whereas cyclophosphamide was only effective at the millimolar range. Moreover, IC50 of docetaxel, tamoxifen, rapamycin and cyclophosphamide was significantly reduced in the combination of FSAS3 at 10 μM.

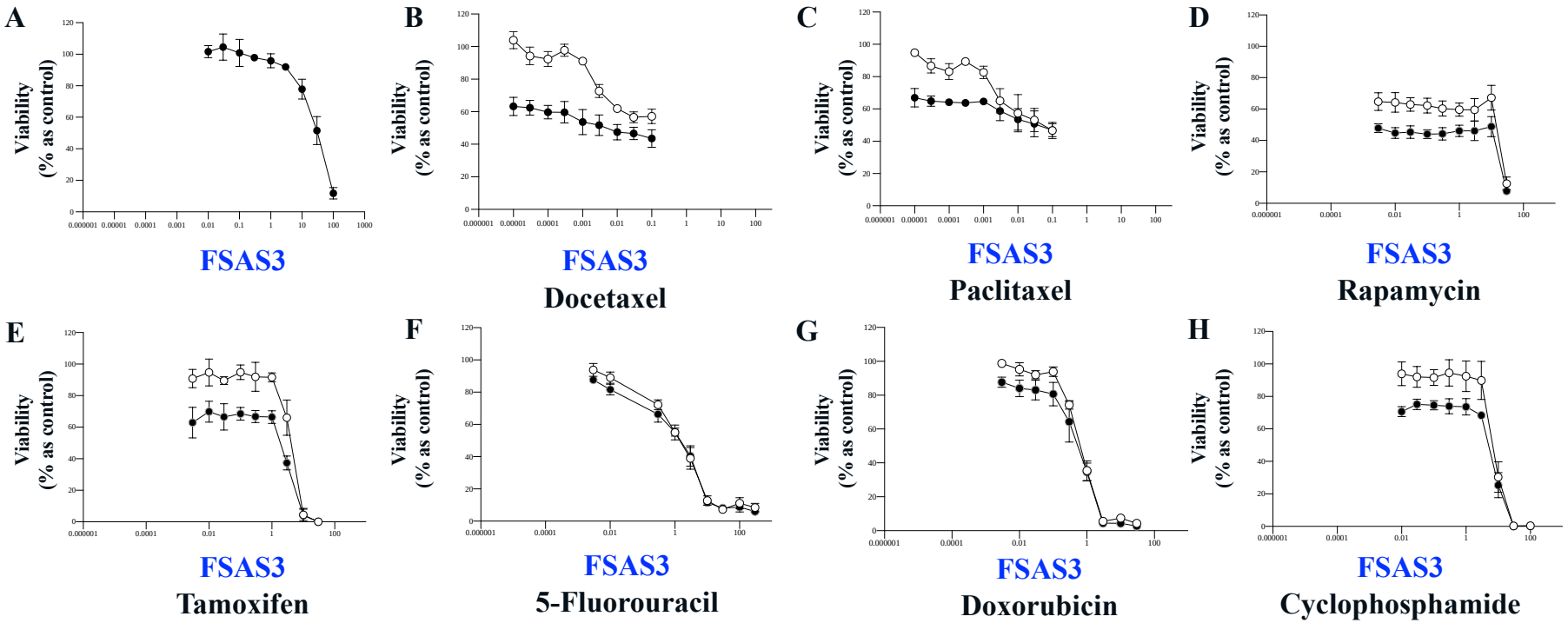

Figure 5.7. FSAS3 enhances the efficacy of a panel of chemotherapeutic agents. Murine 4T1 cells were plated in 96 well plates and treated with the indicated of FSAS3 (A) or the indicated doses of Docetaxel (B), Paclitaxel (C), Rapamycin (D), Tamoxifen I, 5-Fluorouracil (F), Doxorubicin (G), Cyclophosphamide (H) alone (white circles) or with FSAS3 (10μM; black circles). Cell viability was determined using the AlamarBlue™ assay and expressed as a percentage of the values of the vehicle treated cells. Values are means ± standard deviation from at least three independent experiments.

Table 5.2 Half maximal inhibitory concentration (IC50) values of chemotherapeutic agents alone or combined with FSAS3 (10μM) on 4T1 cell viability after 72 hours.

Compound	IC50 (μM)		
	Single Agent	+ FSAS3 (10 μM)	P-value
Docetaxel	0.08897	0.006212	0.0301
Paclitaxel	0.04595	0.06774	0.9268
Doxorubicin	0.632	0.443	0.2005
5-Fluorouracil	1.327	1.109	0.3385
Tamoxifen	3.590	0.784	0.0013
Rapamycin	8.353	0.1856	0.02
Cyclophosphamide	7.263×10^3	2.149×10^3	0.0011

Next, I did the same experiments in human MDA-MB-231 culture. As shown in **Figure 5.8**, human MDA-MB-231 cells response to all drugs at a dose-dependent manner. The dose-response curve of FSAS3 combined chemotherapy drugs (white circles) significantly shifts downward compared to when single drug (black circles) in all drugs at the concentrations inhibit the viability less than 80%. Similarly, taxane (docetaxel, paclitaxel) were most effective among all which acted in the nanomolar range, the rest of drugs were effective in the micromolar range except cyclophosphamide which was only effective in the millimolar range.

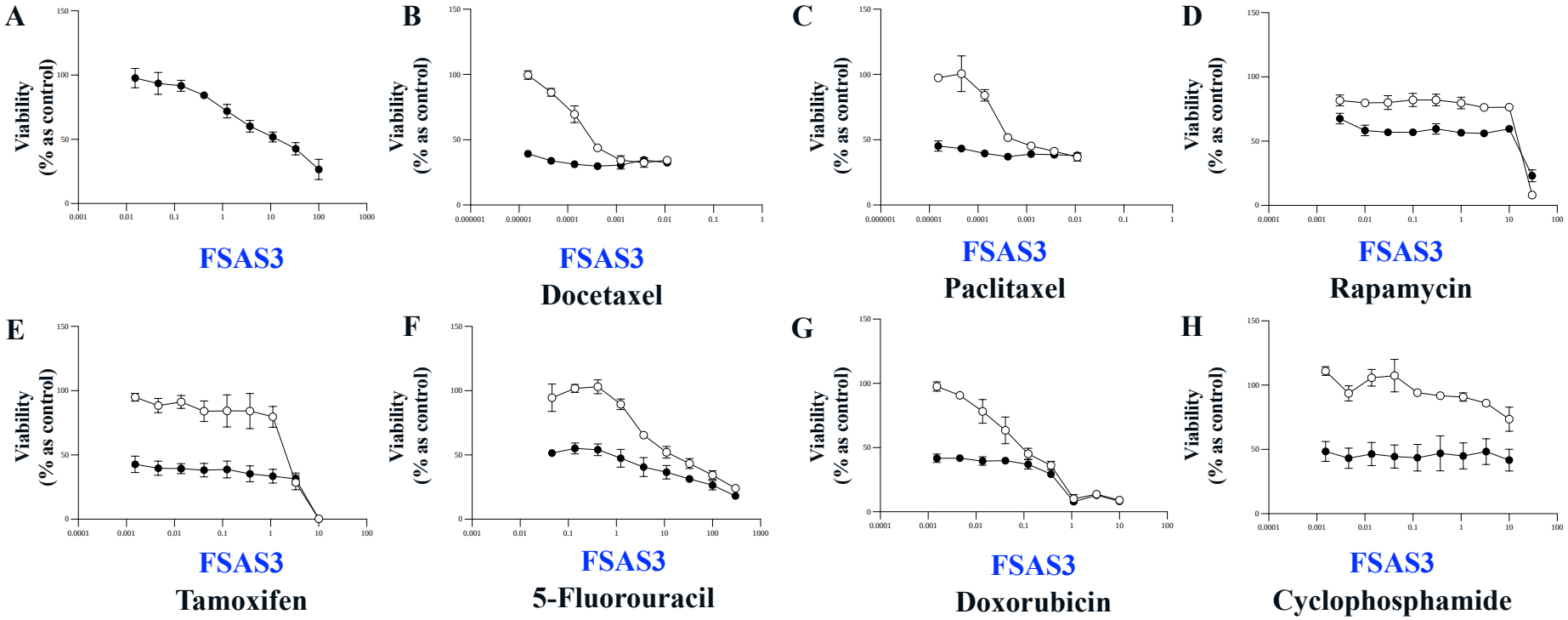

Figure 5.8. FSAS3 enhances the efficacy of a panel of chemotherapeutic agents. Human MDA-MB-231 cells were plated in 96 well plates and treated with the indicated of FSAS3 (A) or the indicated doses of Docetaxel (B), Paclitaxel (C), Rapamycin (D), Tamoxifen (E), 5-Fluorouracil (F), Doxorubicin (G), Cyclophosphamide (H), alone (white circles) or with FSAS3 (10μM; black circles). Cell viability was determined using the AlamarBlue™ assay and expressed as a percentage of the values of the vehicle treated cells. Values are means ± standard deviation from at least three independent experiments.

According to the IC50 values in **Table 5.3,** docetaxel, paclitaxel and doxorubicin achieved IC50 values in the nanomolar range, rapamycin, tamoxifen and 5-fluorouracil had IC50 values in the micromolar range after 72 hours. Whereas cyclophosphamide was only effective at the millimolar range the same as in 4T1 culture. Moreover, IC50 of all drugs was significantly reduced in the combination of FSAS3 at 1 μM.

Table 5.3 Half maximal inhibitory concentration (IC50) values of chemotherapeutic agents alone or combined with FSAS3 (1μM) on MDA-MB-231 cell viability after 72 hours.

Compound	IC50 (μM)		
	Single Agent	+ FSAS3 (1 μM)	P-value
Docetaxel	0.00055	0.000021	0.0016
Paclitaxel	0.0014	4.53×10^{-5}	<0.0001
Doxorubicin	0.106	0.041	0.0128
Rapamycin	11.3233333	3.936	0.0003
Tamoxifen	1.814	0.004	0.0055
5-Fluorouracil	19.46	1.09	0.0079
Cyclophosphamide	18.54×10^{3}	0.559×10^{3}	0.0112

A lot of cancers evolve resistance mechanisms to bolster survival, culminating in the development of resistant tumours. Therefore, it is important to find synergistic anti-cancer combinations. For this reason, I used the Chou-Talalay Method using CompuSyn Software to calculate the Combination Index (CI) values of the indicated drug combinations. To determine synergism or antagonism, the 'potency' and the 'shape' of the dose-effect curve for each drug must be known. The dose-effect parameters of each drug alone, as well as in combination are calculated, and the CI is determined. Fa – CI plot to provides a visual representation of the effect of the drug combination across a range of Fa values. Briefly, "Fa" stands for "Fraction affected," which is the fraction (or percentage) of cells that are inhibited or affected by a drug or drug combination. Fa ranges from 0 to 1, where 0 signifies no effect and 1 signifies total effect (100% inhibition). "CI" stands for "Combination Index," which is a quantitative measure of the degree of drug interaction in terms of additive effect (CI=1), synergism (CI<1), or antagonism (CI>1)[199].

As the results shown in **Figure 5.9**, in the cultures of murine 4T1 cells, the CI of docetaxel/paclitaxel + FSAS3 (10 μM) ranges from 0 – 1, indicating docetaxel and paclitaxel acted synergistically with FSAS3 (10 μM) at all doses tested (9/9) (**Figure 5.9 A-B**). Rapamycin (**Figure 5.9 C**) acted synergistically (CI ranges from 0 – 1) with FSAS3 (10 μM) at most doses (8/9) tested except one additive (CI=1.05). Doxorubicin (**Figure 5.9 F**) acted either synergistically (5/9) or additive (2/9) with FSAS3. However, the majority of the doses of tamoxifen (**Figure 5.9 D**) showed either synergistic (4/9) or antagonistic (4/9) interactions, the majority of the doses of 5-fluorouracil (**Figure 5.9 E**) showed either synergistic (3/9) or antagonistic (4/9) interactions, the combination of cyclophosphamide (**Figure 5.9 G**) and FSAS3 were shown to be antagonistic with the more than half doses (6/9) tested of CI values greater than 1.

As the results shown in **Figure 5.10**, in the cultures of human MDA-MB-231 cells, docetaxel, paclitaxel, rapamycin and cyclophosphamide acted synergistically with FSAS3 (1 μM) at all doses tested (9/9) (**Figure 5.10 A-D**). Tamoxifen (**Figure 5.10 E**) and doxorubicin (**Figure 5.10 G**) acted synergistically with FSAS3 (1 μM) at most doses tested (6/9), 5-fluorouracil (**Figure 5.10 F**) also acted synergistically with FSAS3 (1 μM) at most doses tested (7/9).

These results show a promising combination administration for TNBC treatment especially using FSAS3 in combination with docetaxel, paclitaxel and rapamycin.

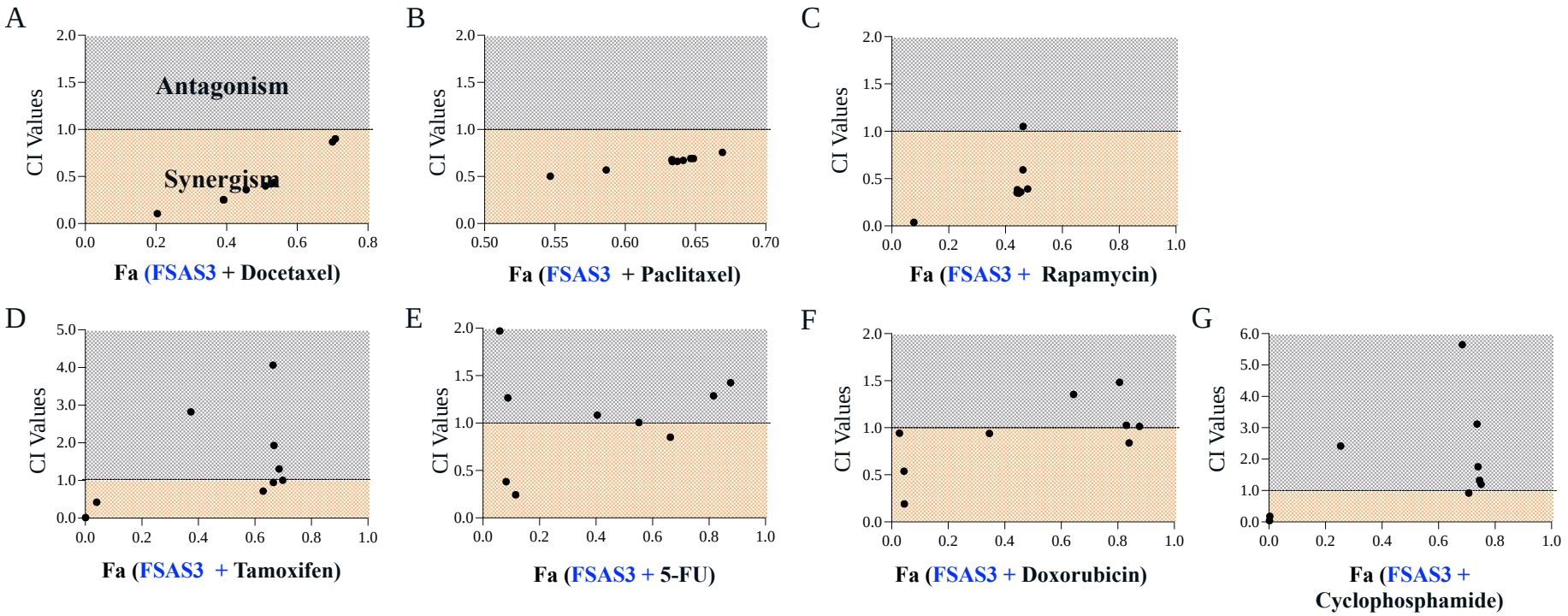

Figure 5.9. FSAS3 and Docetaxel, Paclitaxel and Rapamycin act synergistically at almost all doses whereas Tamoxifen, Cyclophosphamide, Doxorubicin and 5-Fluorouracil are antagonistic at some doses. 4T1 cells were plated in 96-well plates and treated with Docetaxel (A), Paclitaxel (B), Rapamycin (C), Tamoxifen (D), 5-Fluorouracil (E), Doxorubicin (F), Cyclophosphamide (G), alone or with FSAS3 (10μM). Cell viability was determined using the Alamar Blue assay. The Chou-Talalay Method was used to calculate CI values plotted against Fa values to assess potential drug combination synergy. Synergistic CI <1 (yellow), Additive = 1 (dotted line), Antagonistic CI>1 (grey) Values are calculated using the means from at least three independent experiments

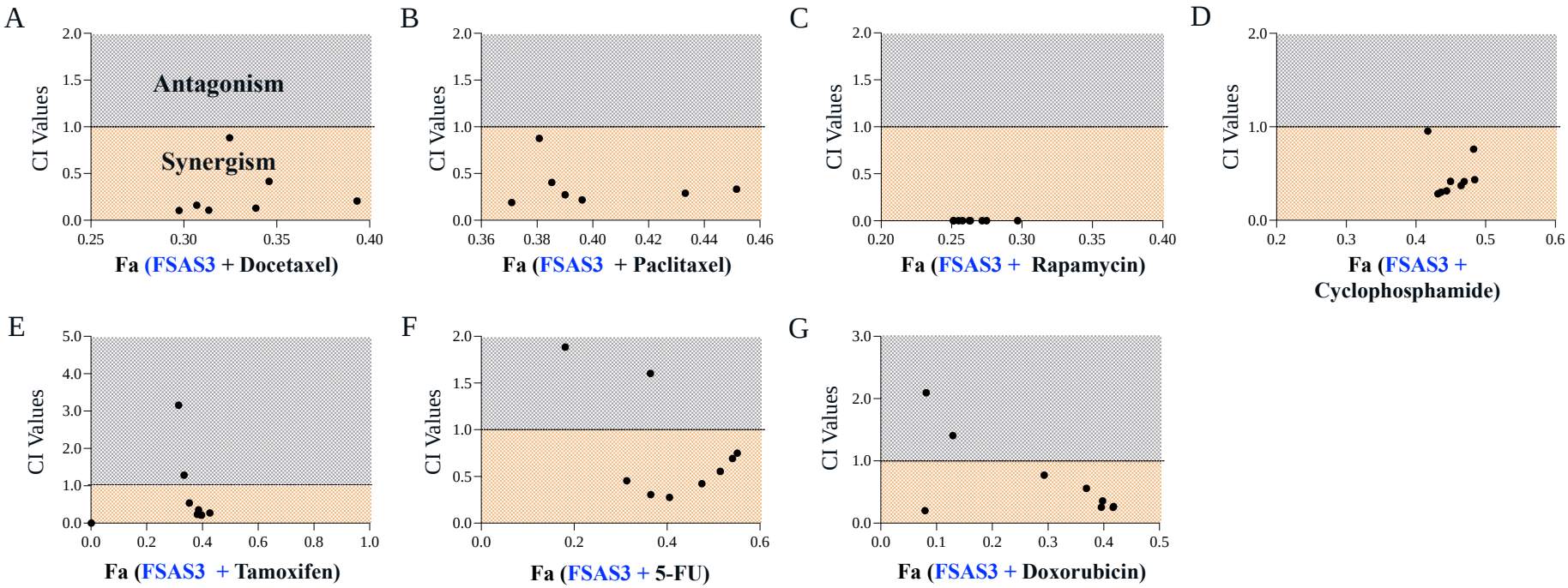

Figure 5.10. FSAS3 and Docetaxel, Paclitaxel, Rapamycin and Cyclophosphamide act synergistically at almost all doses whereas Tamoxifen, Doxorubicin and 5-Fluorouracil are antagonistic at some doses. MDA-MB-231 cells were plated in 96-well plates and treated with Docetaxel (A), Paclitaxel (B), Rapamycin (C), Cyclophosphamide (D), Tamoxifen (E), 5-Fluorouracil (F), Doxorubicin (G) alone or with FSAS3 (1μM). Cell viability was determined using the Alamar Blue assay. The Chou-Talalay Method was used to calculate CI values plotted against Fa values to assess potential drug combination synergy. Synergistic CI <1 (yellow), Additive = 1 (dotted line), Antagonistic CI>1 (grey) Values are calculated using the means from at least three independent experiments

5.4.2.3. The novel FSAS3 reduced the *in vitro* viability of parental and osteotropic human MDA-MB-231 BCa cells via TRAF6 inhibition

To explore the anti-TRAF6 effects of FSAS3, I tested the effect of FSAS3 on the viability of TRAF6 deficient clones of parental MDA-MB-231 and osteotropic MDA-231-BT BCa cells using Alamar Blue™ cell viability assay. As shown in **Figure 5.11A**, FSAS3 (0.03 μM) reduces viability of human patental MDA-MB-231 by 5.3% and of their osteotropic clone MDA-231-BT by 14.5%. As expected, FSAS3 (0.03 μM) had no significant effect on the viability of TRAF6 deficient clones of both parental and osteotropic cell lines when compared to mock controls. Similar trends were also observed at higher concentration of FSAS3 at 0.1 μM, cell viability was reduced by 9.6% in MDA-MB-231$^{\mathbf{Mock}}$ and 13.3% in MDA-231-BT$^{\mathbf{Mock}}$, while no or little decrease observed in TRAF6 deficient clones in **panel (B)**, suggesting FSAS3 decreased cell viability via a TRAF6 dependent mechanism. Interestingly, this reduction in cell viability was more evident when higher concentration of FSAS3 was used, and in cultures of the TRAF6 deficient BCa osteotropic cells MDA-231-BT TRAF6KD1 and MDA-231-BT TRAF6KD2 (**Figure 5.11C**). Drug-response curves of FSAS3 and 6877002 on MDA-MB-231 and MDA-231-BT deficient in TRAF6 and mock cells after 72 hours and 48 hours are shown in **Supplementary Figures 10** respectively.

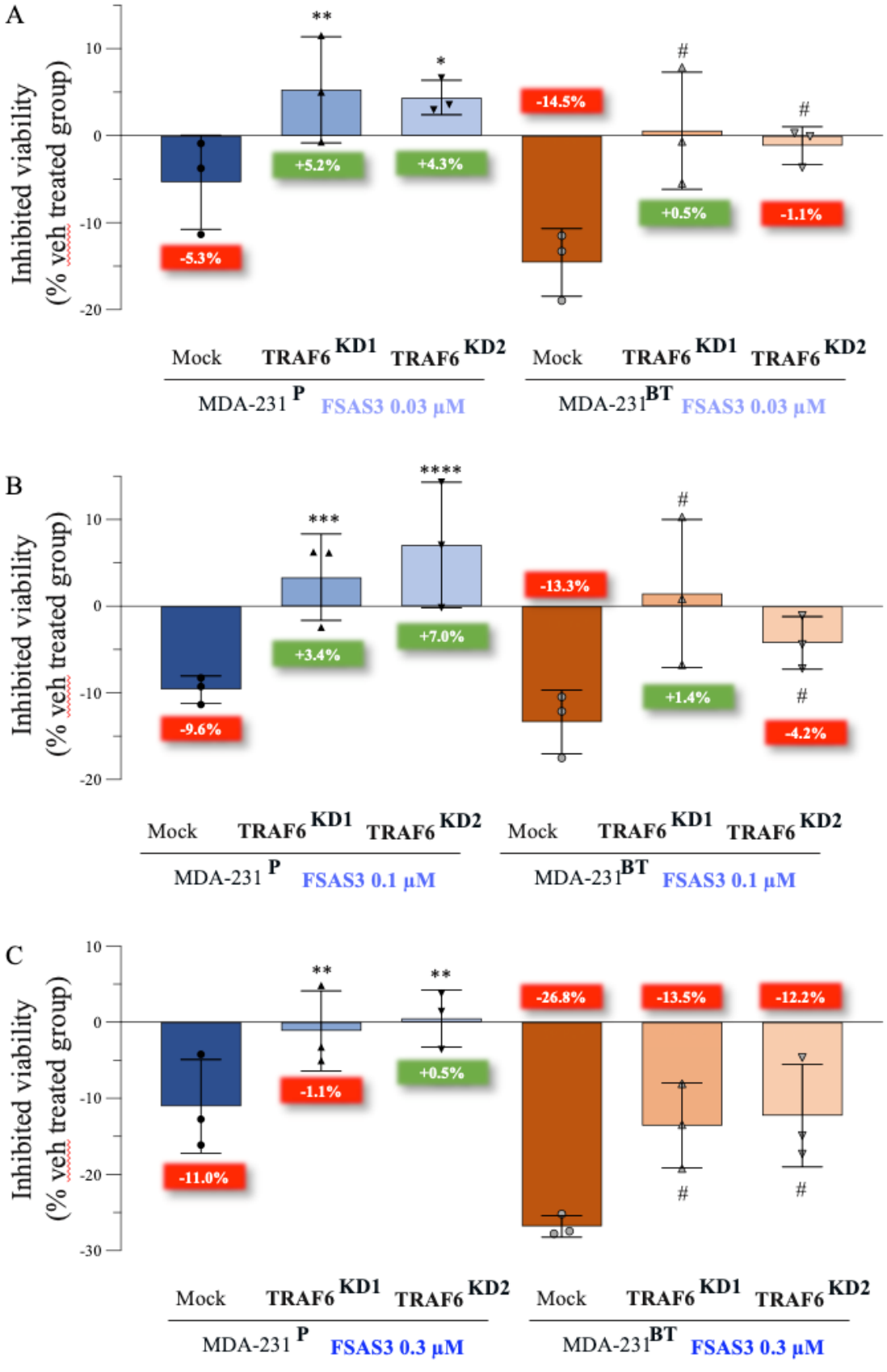
A
Inhibited viability
(% veh treated group)
10
0
-10
-20
**
*
#
#
-5.3%
+5.2%
+4.3%
-14.5%
+0.5%
-1.1%
Mock
TRAF6 KD1
TRAF6 KD2
Mock
TRAF6 KD1
TRAF6 KD2
MDA-231 P
FSAS3 0.03 µM
MDA-231 BT
FSAS3 0.03 µM
B
Inhibited viability
(% veh treated group)
10
0
-10
-20
***
****
#
#
-9.6%
+3.4%
+7.0%
-13.3%
+1.4%
-4.2%
Mock
TRAF6 KD1
TRAF6 KD2
Mock
TRAF6 KD1
TRAF6 KD2
MDA-231 P
FSAS3 0.1 µM
MDA-231 BT
FSAS3 0.1 µM
C
Inhibited viability
(% veh treated group)
10
0
-10
-20
-30
**
**
#
#
-11.0%
-1.1%
+0.5%
-26.8%
-13.5%
-12.2%
Mock
TRAF6 KD1
TRAF6 KD2
Mock
TRAF6 KD1
TRAF6 KD2
MDA-231 P
FSAS3 0.3 µM
MDA-231 BT
FSAS3 0.3 µM

Figure 5.11. FSAS3 reduced cell viability of MDA-MB-231 and MDA-231-BT TRAF6 knockdown cells and their mock control *in vitro*, and FSAS3 was less potent in TRAF6 knockdown clones. Percentage of viability of MDA-MB-231 TRAF6 knockdown clones and mock control (dark and light blue bars), MDA-231-BT TRAF6 knockdown clones and its mock control (dark and light orange bars) treated with FSAS3 at 0.03 μM (A), 0.1 μM (B) and 0.3 μM (C) for 48 hours, as assessed via Alamar Blue™ assay. Values are expressed as mean ± SD and were obtained from three independent experiments. P values obtained from unpaired t test, *p < 0.05, **p < 0.01, ***p < 0.001, ****p <0.0001 compared to MDA-MB-231 mock, #p < 0.05 compared to MDA-231-BT mock.

5.4.2.4. The novel FSAS3 reduced breast cancer cell migration *in vitro*

Once established that the anti-tumour effect of FSAS3 is dependant, at least in part, on TRAF6 inhibition, I went on to examine its effect on the motility of human parental MDA-MB-231 cells and their osteotropic clone MDA-231-BT cells. As shown in **Figure 5.12**, treatment with the novel TRAF6 inhibitor FSAS3 (1 μM) reduces the 2D-directed migration of both parental MDA-MB-231 by 27.3% and osteotropic MDA-231-BT by 37.7% after 16 hours, as assessed by the wound-healing assay decribed in **section 2.2.5.2**. Although a 9.2% reduction in cell viability was observed in MDA-MB-231 cells after 16 hours (**Figure 5.12A**), FSAS3 still inhibits migration (18.1%) in parental MDA-MD-231 cells. Furthermore, FSAS3 inhibits the migration of osteoptropic clones without affecting their growth after 16 hours (**Figure 5.12B**). Altogether, these findings demonstrate that FSAS3 is a more potent inhibitor of migration of osteotropic triple negative BCa cells.

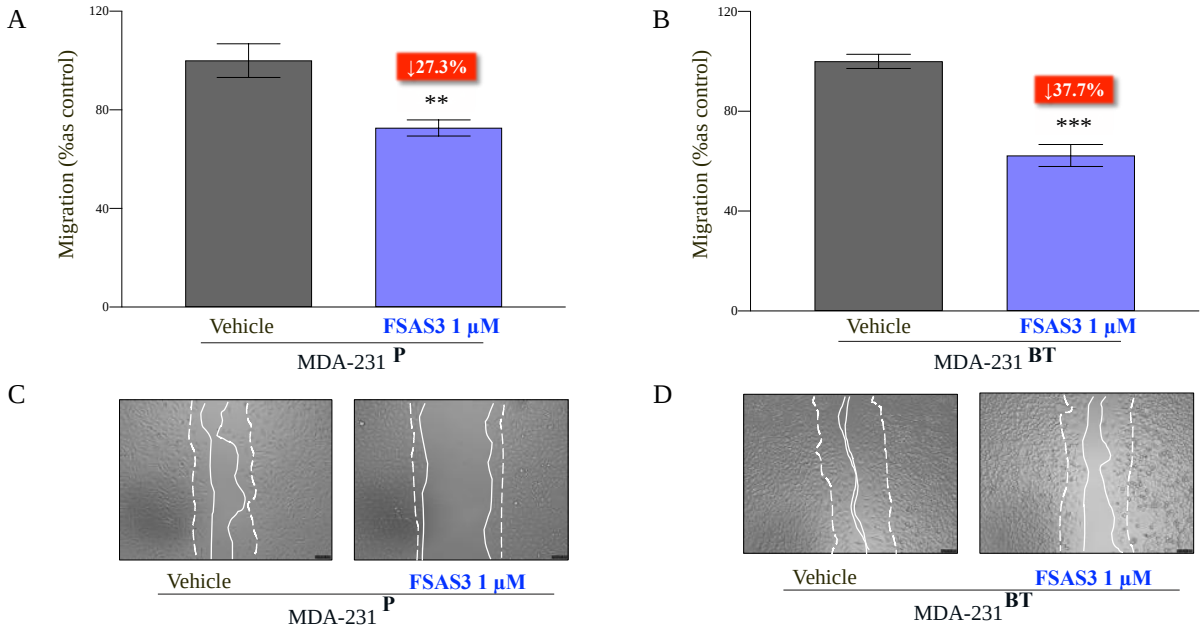

Figure 5.12. FSAS3 reduced MDA231 parental and osteotropic cell migration, and FSAS3 was more potent in osteotropic cells *in vitro*. Percentage of cell migration of BCa cells MDA-MB-231 (A) and MDA-231-BT (B)

treated with vehicle (DMSO) or 1 μM of the verified TRAF6 inhibitor FSAS3. Representative images showing initial and final positions of motility in timepoints 0 (dotted lines) and 16 hours (continuous lines) of MDA-MB-231 (C) and MDA-231-BT (D) cells. Data obtained from three independent experiments. p-values were determined using unpaired T-test. ***p<0.0005, **p<0.01 compared to cells treated with vehicle. Scale bar=100 μM.

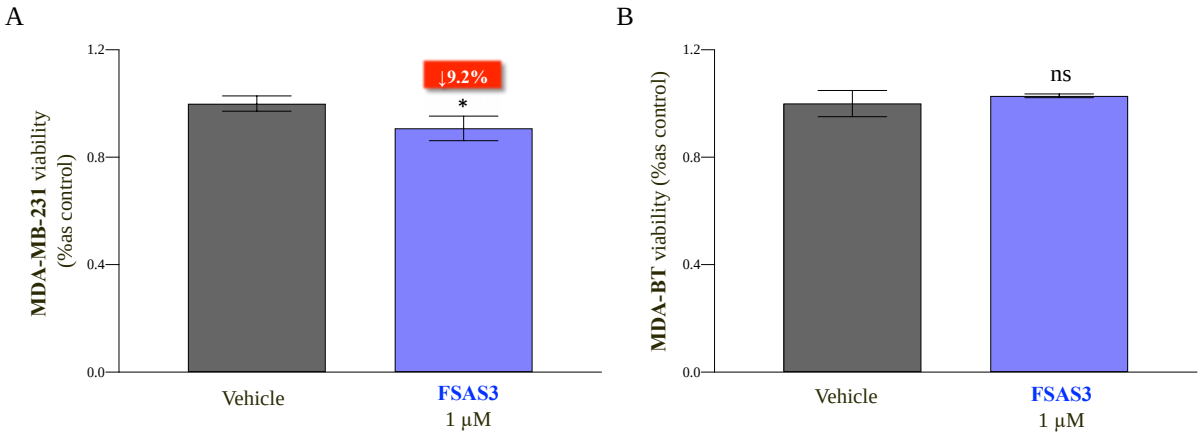

Figure 5.13. FSAS3 reduced cell viability of MDA231 parental and didn't influence the viability of osteotropic cell at the endpoint of migration *in vitro*. Percentage of cell viability from BCa cells MDA-MB-231 (A) and MDA-231-BT (B) treated with vehicle and FSAS3 1 μM. Data obtained from three independent experiments. p-values were obtained from one-way ANOVA test followed by Tukey post hoc test. **p<0.01 and *p<0.05 compared to mock transfected cells.

5.4.2.5. The novel FSAS3 reduces breast cancer cell invasion *in vitro*

Next, I assessed the effects of FSAS3 on the invasive ability of parental and osteotrpic BCa cells by the Transwell® invasion assay as described in **section 2.2.7.1**. The concentration of 0.03 μM of FSAS3 was chosen for this assay because it had no effect on cell viability after 72 hours (see **Figure 5.5C**). As shown in **Figure 5.14**, FSAS3 (0.03 μM) significantly reduces cell invasion in cultures of human osteotropic MDA-231-BT (41.2% reduction) more significantly than in parental MDA-MB-231 (31% reduction), consistent with its potent effects on osteotropic BCa cells.

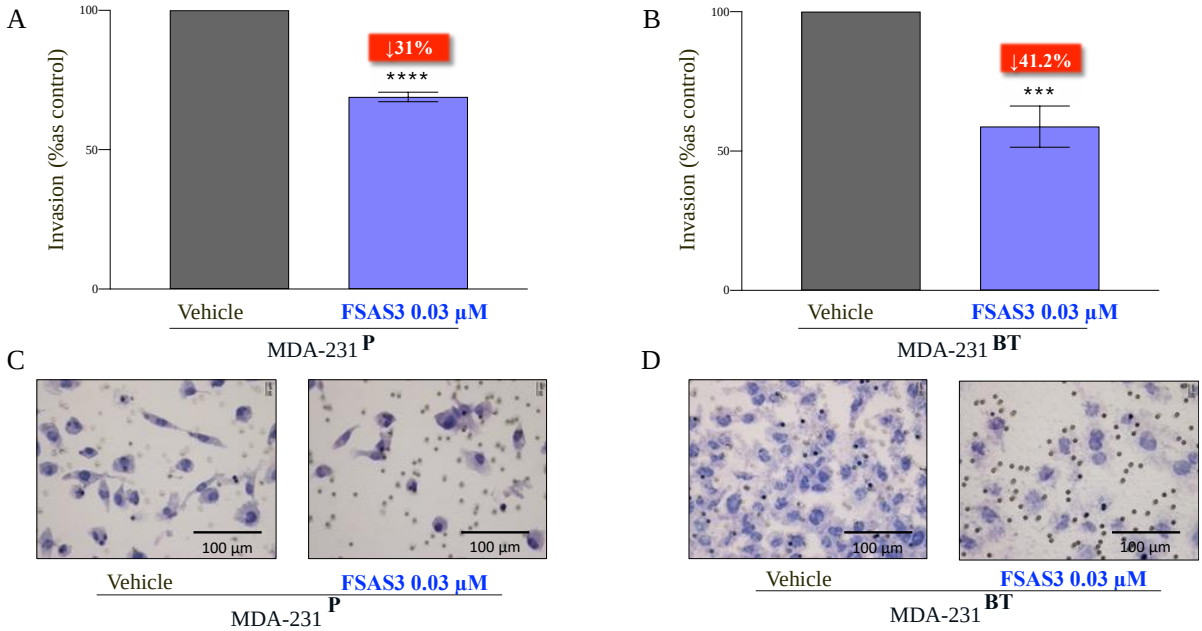

Figure 5.14. FSAS3 reduced MDA231 parental and osteotropic cell invasion, and FSAS3 was more potent in osteotropic cells *in vitro*. Percentage of cell migration of BCa cells MDA-MB-231 (A) and MDA-231-BT (B) treated with vehicle or 0.03 µM of the novel TRAF6 inhibitor FSAS3. Representative images of cells invasion after 72 hours from MDA-MB-231 (C) and MDA-231-BT (D) cells. Data obtained from three independent experiments. p-values were determined using unpaired T-test. ***p<0.0005, **p<0.01 compared to cells treated with vehicle. Scale bar=100 µM.

5.5. Discussion

In **Chapter 3**, evidence from pooled studies in the meta-analysis confirmed that TRAF2, TRAF4 and TRAF6 play important roles in the regulation of human and mouse BCa growth, adherence, migration, and invasion *in vitro*. Based on these findings, I conducted bioinformatic studies to show the expression of TRAFs in large cohort of clinical breath cancer patients and to explore the mechanisms, functions and processes involved in TRAF-driven BCa cell behaviour in **Chapter 4**. Consistently with the findings from the meta-analysis in **Chapter 3**, I have found that TRAF6 high expression is significantly associated with poor survival in BCa patients. More importantly, higher level of TRAF6 is detected in bone and brain metastases which are known to have an osteolytic component. The link of TRAF6 to osteolytic behaviour of BCa cells was also confirmed in my Western Blot analysis that showed osteotropic human and mouse TNBC cells MDA-231-BT and 4T1-BT express higher level of TRAF6 than their parental clones. These results, when combined with previous studies of our group[184, 276], indicate that inhibition of TRAF6 in BCa and/or host cells can be of value in the reduction of their metastatic and osteolytic properties. Therefore, I decided to investigate the effects of cancer specific knockdown and pharmacological inhibition of TRAF6 on the ability of highly metastatic and osteotropic clones of BCa cells to grow, invade, and migrate *in vitro*.

First, TRAF6 knockdown in the highly metastatic human MDA-MB-231 cells and their osteotropic clones MDA-231-BT was successfully obtained. Two knockdown clones and their mock controls were chosen for the subsequent studies that explored the effects of TRAF6 knockdown on the ability of BCa cells to grow, migrate and invade, and to test the hypothesis that the anti-tumour effect of the novel FSAS3 is mediated, at least in part, via TRAF6 inhibition.

Consistent with findings from **chapter 3** and my recently published work [275], I demonstrated that TRAF6 knockdown and FSAS3 treatment significantly reduced the growth, migration and invasion of both parental and osteotropic TNBC cells, proving further support to my hypothesis that TRAF6 is a potential druggable target in the treatment of metastatic BCa.

Next, I carried out a head-to-head comparison of the effects of the verified CD40-TRAF6 inhibitor 6877002[184, 185, 286, 287] and the novel family of FSAS1 to 5, which were developed as congeners

of 6877002 in collaboration with the University of Milan (Italy). Among 6 tested drugs, both FSAS3 and 6877002 reduced the viability of a panel of human and mouse, hormone-dependent TNBC cells at a time- and concentration-dependent manner. It is important to note that FSAS3 was the most potent compound among all those were tested in all cultures.

Previous studies from our laboratories have shown that 6877002 enhanced the *in vitro* anti-tumour and *in vivo* anti-metastatic effects of docetaxel [184]. Considering the lack of effective treatment for TNBC, and the ability of TNBC to resist hormonal therapies, and standard first-line chemotherapy, as well as combined chemotherapy and neoadjuvant chemotherapy strategies [289, 291], I decided to test the effects of the novel FSAS3 in combination with a panel of clinically available FDA-approved chemotherapies on triple negative BCa cell viability *in vitro*. As expected, FSAS3 significantly reduced the IC50 value of almost all of the chemotherapies tested. Further analysis of these results confirmed that FSAS3 acts synergistically with docetaxel, paclitaxel, rapamycin to exert anti-tumour effects at most concentrations tested in both the human and mouse TNBC cell lines tested. Interestingly, a randomized phase 3 trial [291] showed that the median progression-free survival time for the group treated with nab-paclitaxel/cisplatin was significantly higher than that of the control group treated with gemcitabine/cisplatin. This study demonstrates the effectiveness of Taxane when used in combination therapy in the treatment of TNBC. Thus, I speculate that FSAS3 in combination of Taxane, especially docetaxel, show a promise in the treatment of TNBC.

The role of tumour-specific TRAF6 is poorly investigated. Thus, I treated both TRAF6-deficienct and mock control BCa cells with FSAS3 to explore whether its anti-tumour effect is mediated by TRAF6. As expected, the anti-growth effect of FSAS3 was significantly blunted or totally prevented in TRAF6 deficient clones of both parental MDA-MB-231 and osteotropic MDA-231-BT BCa cells when compared to mock control, suggesting a TRAF6-mediated effect. Additionally, I showed that both TRAF6 knockdown and FSAS3 treatment significantly reduced the migration and invasion of BCa cells, consistent with findings from **chapter 3** and my recently published work [275]. More interestingly, FSAS3 action was significantly potent in osteotropic clones of human MDA-MB-231 and mouse 4T1 BCa cells than in parental clones, which can be partly explained by my results that showed that

osteotropic cells express high level of TRAF2 and TRAF6 than parental cells (**Chapter 4)**. It is important to note that this growth inhibition of FSAS3 was not completely prevented in TRAF6 deficient cells treated with high concentrations suggesting a possible "off-target" effect and/or complementary expression of other genes (or proteins) related to TRAF6. Thus, further mechanistic studies that examine knock down of other members of the TRAF family in TRAF6-defieicnt cells, for example, are needed.

Overall, the results of this chapter confirms that TRAF6 plays a role in the metastatic behaviour of the human and mouse TNBC cells tested, cancer-specific inhibition of TRAF6 by our novel small-molecule FSAS3 exert anti-tumour, anti-migratory, and anti-invasive effects *in vitro*, and this action is mediated, at least in part, by TRAF6.

Given the important role that the TRAF6/NFκB axis plays in BCa, bone remodelling and inflammation [275], and the encouraging results from this and previous chapters and published studies, further mechanistic studies were carried out in **Chapter 6** to test the hypothesis that FSAS3 inhibits NFκB activation in BCa cells predominantly via TRAF6 inhibition.

CHAPTER 6. Effects of FSAS3 on Breast cancer related TRAF6/NFκB signalling *in vitro*

6.1. Summary

In **Chapter 5** I showed that FSAS3 reduced the ability of BCa cells to grow, migrate and invade, and the anti-tumour effect of this novel agent is dependent, at least in part, on TRAF6 inhibition. In this chapter, I further explored the mechanism(s) by which FSAS3 affect TRAF6/NFκB signalling in metastatic BCa cells. Precisely, I tested the effects of FSAS3 on RANKL/TRAF6- and TNFα/TRAF2-induced NFκB activation in mock and TRAF6-deficient TNBC and their osteotropic clones using a number of mechanistic techniques, namely Western Blot, Immunoprecipitation, *in silico* Molecular Docking and Drug Affinity Responsive Target Stability (DARTS).

First, I used Western blot to demonstrate that the novel FSAS3 is a potent inhibitor of both RANKL(TRAF6)- as well as TNFα(TRAF2)-induced canonical NFκB activation in BCa cells than the verified CD40-TRAF6 inhibitor 6877002. Next, I identified TRAF6 as a target of FSAS3. I showed that FSAS3 interacts with and protects TRAF6 from proteolysis using DARTS followed by Western Blot. Mechanistically, this finding confirms the results from *in silico* predicted pose and docking analysis that suggested that FSAS3 binds to CD40 and another novel pocket called P1 at the c-terminus of TRAF6. Using a combination of Immunoprecipitation and Western Blot analysis, I went on to demonstrate that FSAS3 disrupts a number of pathways downstream of TRAF6/2. Briefly, FSAS3 inhibited TRAF6-TAK-1 and TRAF6-TAB1 binding, IKKα/-IKKβ binding, IκB phosphorylation and p65NFκB-DNA binding, indicative of canonical NFκB inhibition. More importantly, inhibition of IκB phosphorylation by FSAS3 is significantly blunted in TRAF6 deficient MDA-MB-231 cells than their mock control, confirming the TRAF6-mediated effect observed in **Chapter 5**. On the other hand, I observed that FSAS3 also exerted a relatively mild, but significant, inhibition of TNFα-induced NFκB activation in TRAF6 deficient MDA-MB-231 cells, indicating an off-target effect.

Overall, findings from these mechanistic studies suggest that FSAS3 is a selective, but not exclusive, inhibitor of inflammation- and osteolysis-induced TRAF6/NFκB activation in TNBC cells. Thus, it can be is of value in the treatment of multi-faceted and multi-factorial cancer such as metastatic BCa in the skeleton. Therefore, further *ex vivo* and *in vivo* studies to validate its anti-osteolytic as well as anti-metastatic effects, alone and in combination with chemotherapy, are needed.

6.2. Introduction

Different members of the TRAF family exhibit distinct and overlapping functions in cancer, and therefore they exert different physiological and pathophysiological effects through different mechanisms [108, 227-230, 238, 240]. Among TRAFs, TRAF6 is the most implicated member in most aspects of advanced BCa, particularly metastasis to distant organ such as the skeleton. TRAF6 is commonly associated with E3 ubiquitin ligase activity, and other processes implicated in hormone-dependant and triple-negative BCa[108, 160, 227, 231, 237]. One reason for this is that TRAF6 (and to a lesser extent TRAF2) acts as a point of convergence for multiple BCa-driver signalling pathways such as NFκB and many others including PI3K/AKT/mTOR, Toll-like receptor (TLR), mitogen-activated protein kinase (MAPK), Ras/Src Family Kinases, and members of the activator protein 1 (AP-1) family[108, 227, 231, 237, 238].

Previous studies in the scientific literature including my recently published article [275] have shown that TRAF6, together with TRAF2, are key adaptor proteins responsible for the regulation of canonical NFκB signalling in advanced, metastatic cancers, such as BCa bone metastasis. The recruitment of TRAF6 and/or TRAF2 to the ligand-receptor complex initiates a series of signalling pathways that lead to the phosphorylation and activation of members of IκB kinase (IKK) family of cytoplasmic signalling proteins [109].

In this chapter, I focused my investigation on exploring the selective as well as off-target effects of FSAS3 on RANKL(TRAF6)- and TNFα(TRAF2)- induced canonical and non-canonical NFκB activation in TNBC and their osteotropic clones. I used a novel strategy that combines data from Western blot, immunoprecipitation, *in silico* molecular docking prediction and DARTS methods to examine the mechanism(s) by which FSAS3 influence the TRAF6/NFκB axis in osteotropic BCa cells exposed to the classic osteolytic RANKL and pro-inflammatory TNFα factors.

6.3. Aims

The aim of this chapter was to validate the hypothesis that FSAS3 inhibits inflammation and osteolysis related canonical NFκB activation by interacting and disrupting TRAF6 activation in osteotropic BCa cells.

This hypothesis was investigated by examining the effects of FSAS3 on:

- RANKL(TRAF6)- and TNFα (TRAF2)-induced canonical IκB/IKK activation in TRAF6 deficient and mock BCa cells.
- RANKL(TRAF6) and TNFα (TRAF2)-induced TRAF6-TAK1/TAB2 binding in BCa cells.
- *In silico* docking of FSAS3 with TRAF6 and TRAF2.
- *In situ* interaction of FSAS3 with TRAF6 or TRAF2.

6.4. Results

6.4.1. Effects of FSAS3 on TRAF6-driven NFκB activation *in vitro*

As an adaptor protein, TRAF6 plays a major role in the activation of several signalling pathways in BCa, in particular canonical NFκB activation [109]. With the premise that NFκB is constitutively active in BCa and plays an important role in the behaviour of BCa cells at distant metastatic sites such as bone [292], I first studied the effect of the novel FSAS3 on RANKL- induced TRAF6/NFκB activation by assessing the expression of phosphorylated IκB-α and total IκB-α in human MDA-MB-231 and mouse 4T1 BCa cells using western blot (see **section 2.3.2**).

6.4.1.1. The novel FSAS3 inhibited TRAF6-mediated, RANKL-induced canonical NFκB activation in human and mouse TNBC cells *in vitro*

First, I performed a number of pilot experiments to define the optimal time point at which to study the effects of FSAS3 on IκB-α phosphorylation in human MDA-MB-231 and mouse 4T1 TNBC cells as well as murine macrophage-like RAW264.7, (osteoclast precursors) (**Supplementary Figure 18-21**). Briefly, human MDA-MB-231 and mouse 4T1 BCa cells and murine macrophage-like RAW264.7 were starved for 16 hours (overnight), exposed to FSAS3, 6877002 or vehicle for 1 hour, and then stimulated with RANKL (100 ng/ml) for a previously determined period of time. As shown in **Figure 6.1A, B**, RANKL (100 ng/ml) significantly enhanced the phosphorylation of IκB-α by 1.5-fold ($p<0.05$) in human MDA-MB-231 cells, and pre-exposure to the novel FSAS3 (50 μM) significantly inhibited this effect by 31% ($p<0.05$) when compared to RANKL treated vehicle. In contrast, pre-treatment of these cells with 6877002 (50 μM) had no significant effect. Exposure to RANKL (100 ng/ml) also increased the phosphorylation of IκB-α by 1.6-fold ($p<0.05$) in 4T1 cells, and pre-treatment with FSAS3 (50 μM) significantly reduced this effect by 75% ($p<0.01$) when compared to RANKL treated vehicle (**Figure 6.1C, D**). 6877002 (50 μM) was less potent than FSAS3 and it inhibited RANKL (100 ng/ml) induced

phosphorylation of IκB-α by 65% (p<0.01) when compared to RANKL treated vehicle (**Figure 6.1C, D**).

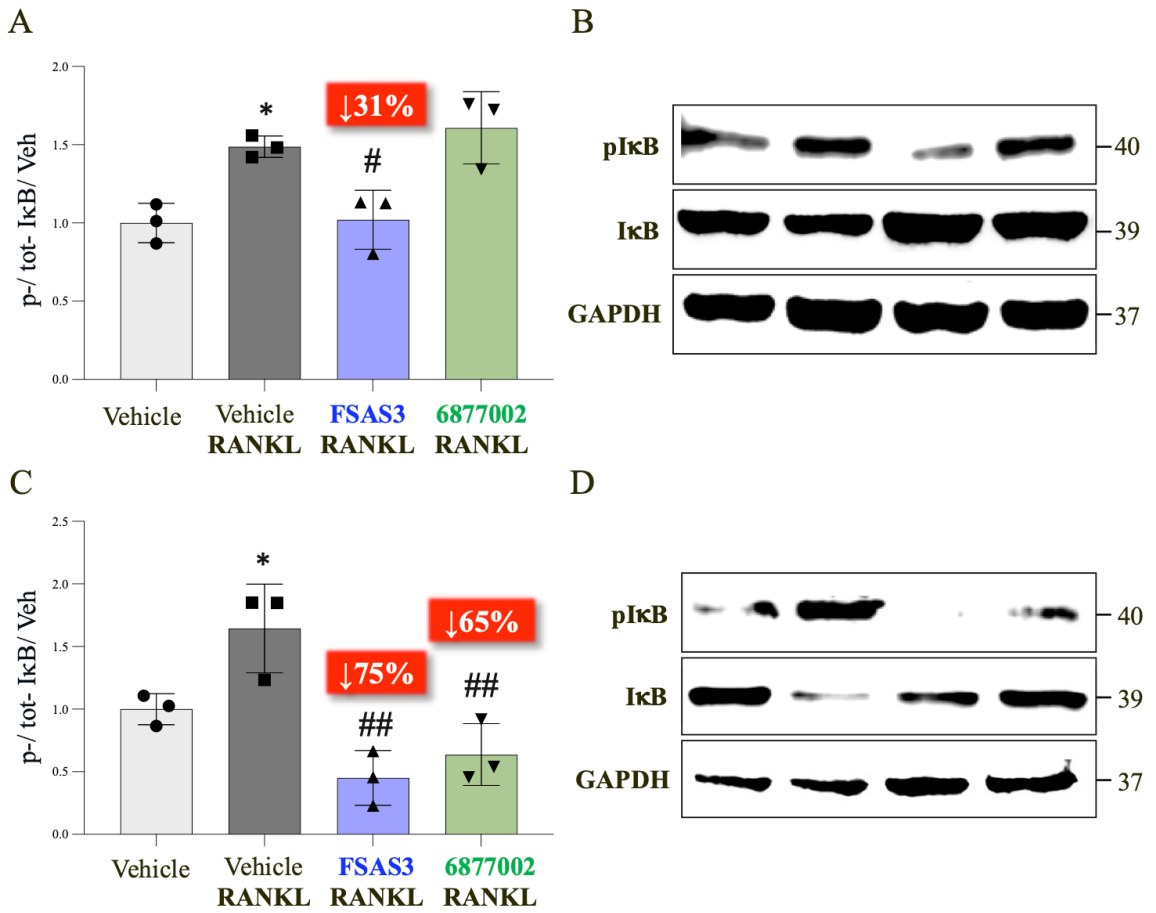

Figure 6.1. The novel FSAS3 reduced the phosphorylation of IκB-α in human MDA-MB-231-luc and murine 4T1-luc induced by RANKL *in vitro*. Relative fold of phosphorylated-IκB-α/IκB-α (% as vehicle) expression of human MDA-MB-231-luc (A) and murine 4T1-luc (C) exposed to vehicle, FSAS3 (50 μM) or 6877002 (50 μM) for 1 hour prior to stimulation with RANKL (100 ng/ml). Representative Western Blot images of expression of p-IκB-α, IκB and GAPDH of MDA-MB-231-luc (B) and 4T1-luc (D) cells exposed to vehicle. Data presented are mean ± standard deviation (n=3). P-values were obtained from ordinary one-way ANOVA followed by Tukey *post hoc* test. **p<0.01 and *p<0.05 compared to vehicle, ##p<0.01, #p<0.05 compared to RANKL treated vehicle cells.

6.4.1.2. The novel FSAS3 reduced RANKL- induced canonical NFκB activation in parental and osteotropic breast cancer via TRAF6 inhibition

To examine the involvement of TRAF6 on the inhibition of RANKL- induced NFκB activation by the novel FSAS3, assessed the relative fold of phosphorylated-IκB-α/IκB-α in mock and TRAF6 knockdown clones after treatment with FSAS3 using western blot (see **section 2.3.2**). As shown in **Figure 6.2 and 6.3**, RANKL (100 ng/ml) increased the phosphorylation of IκB-α by 2 fold ($p<0.05$) in mock MDA-MB-231 cells, and pre-exposure to FSAS3 (50 μM) significantly inhibited this effect by 80% ($p<0.05$) when compared to RANKL treated vehicle (**Figure 6.2A**). This is consistent with the same effect I previously observed in human MDA-MB-231 cells (**Section 6.4.1.1, Figure 6.1A**). I also observed that neither RANKL (100 ng/ml) nor FSAS3 had no effect on the phosphorylation of IκB-α in TRAF6-deficient MDA-MB-231 clones MDA-MB-231 TRAF6$^{\mathbf{KD1}}$ (**Figure 6.2C**) and MDA-MB-231 TRAF6$^{\mathbf{KD3}}$ (**Figure 6.2E**), indicating their TRAF6 dependant effects.

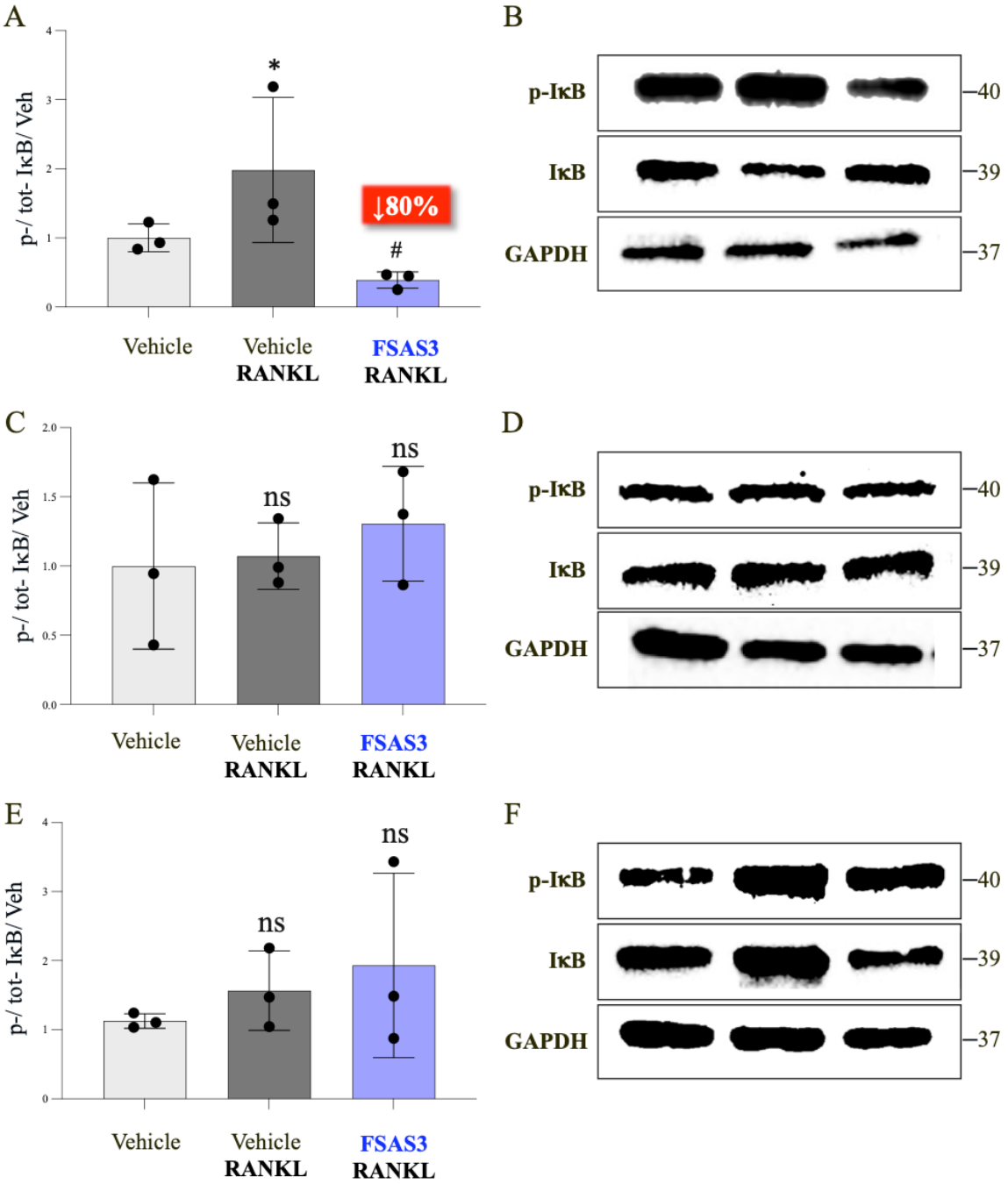

Figure 6.2. The novel FSAS3 reduced the phosphorylation of IκB-α in human MDA-MB-231-Mock rather than MDA-MB-231 TRAF6 deficient cells induced by RANKL *in vitro*. Relative fold of phosphorylated-IκB-α/IκB-α (% as vehicle) expression of human MDA-MB-231-Mock (A), MDA-MB-231-TRAF6KD1 (C) and MDA-MB-231-TRAF6KD3 (E) exposed to vehicle or FSAS3 (50 μM) for 1 hour prior to stimulation with RANKL (100 ng/ml). Representative Western Blot images of expression of p-IκB-α, IκB and GAPDH of MDA-MB-231-Mock (B), MDA-MB-231-TRAF6KD1 (D) and MDA-MB-231-TRAF6KD3 (F) cells exposed to vehicle. Data presented are mean ± standard deviation (n=3). P-values were obtained from ordinary one-way ANOVA followed by Tukey *post hoc* test. *p<0.05 compared to vehicle, #p<0.05 compared to RANKL treated vehicle cells.

Similarly, RANKL (100 ng/ml) increased the phosphorylation of IκB-α by 2 fold ($p<0.05$) in osteotropic mock MDA-231-BT cells by 1.5 fold ($p<0.05$) (**Figure 6.3E**), and pre-exposure to FSAS3 (50 μM) significantly inhibited this effect by 43% ($p<0.05$) when compared to RANKL treated vehicle. (**Figure 6.3A**). This is consistent with the same effect I previously observed in osteotropic human MDA-MB-231 cells (**Section 6.4.1.1, Figure 6.1A**). I also observed that neither RANKL (100 ng/ml) nor FSAS3 had no effect on the phosphorylation of IκB-α in TRAF6-deficient MDA-MB-231 clones MDA231-BT TRAF6$^{\mathbf{KD1}}$ (**Figure 6.3C**) and MDA231-BT TRAF6$^{\mathbf{KD3}}$ (**Figure 6.3E**), indicating their TRAF6 dependant effects.

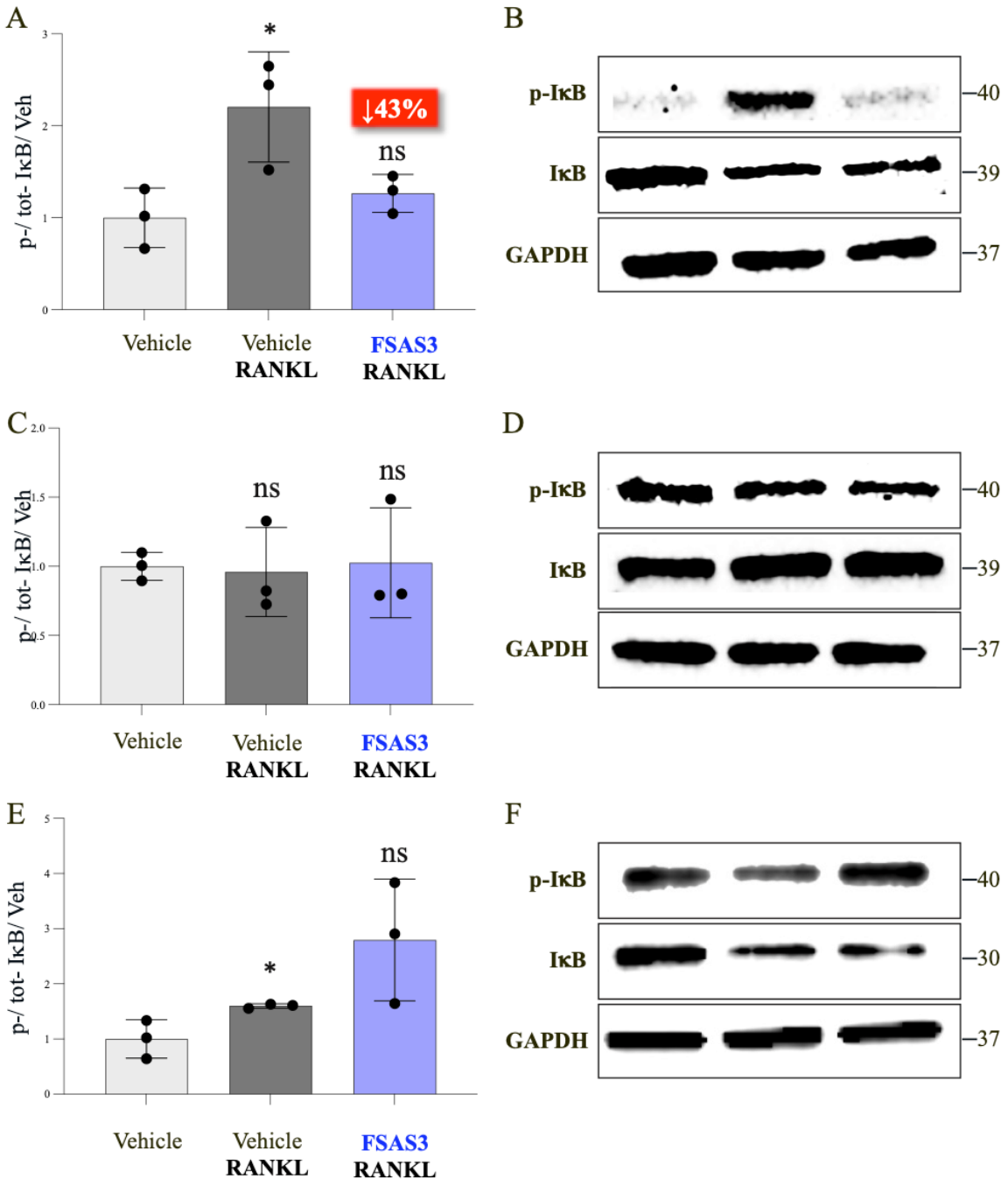

Figure 6.3. The novel FSAS3 reduced the phosphorylation of IκB-α in human MDA-231-BT-Mock rather than MDA-231-BT TRAF6 deficient cells induced by RANKL *in vitro*. Relative fold of phosphorylated-IκB-α/IκB-α (% as vehicle) expression of human MDA-231-BT-Mock (A), MDA-231-BT-TRAF6KD1 (C) and MDA-231-BT-TRAF6KD3 (E) exposed to vehicle or FSAS3 (50 μM) for 1 hour prior to stimulation with RANKL (100 ng/ml). Representative Western Blot images of expression of p-IκB-α, IκB and GAPDH of MDA-231-BT-Mock (B), MDA-231-BT-TRAF6KD1 (D) and MDA-231-BT-TRAF6KD3 (F) cells exposed to vehicle. Data presented are mean ± standard deviation (n=3). P-values were obtained from ordinary one-way ANOVA followed by Tukey *post hoc* test. *p<0.05 compared to vehicle, #p<0.05 compared to RANKL treated vehicle cells.

6.4.2. Effects of FSAS3 on TRAF2-driven NFκB activation *in vitro*

Previous studies have shown that TRAF2 play a role in the activation of canonical NFκB signalling pathway in BCa cells by the pro-inflammatory such as TNFα. In this section, the effects of the novel FSAS3 on TNFα- induced NFκB activation were investigated by assessing the expression of phosphorylated IκB-α and total IκB-α in human MDA-MB-231 and mouse 4T1 BCa cells using western blot (see **section 2.3.2**).

6.4.2.1. The novel FSAS3 inhibited TRAF2-mediated, TNFα-induced canonical NFκB activation in human and mouse triple negative breast cancer cell lines.

Briefly, human MDA-MB-231 and mouse 4T1 BCa cells were treated with FSAS3, 6877002 or vehicle (0.1% DMSO) for 1 hour and then stimulated with TNFα (10 ng/ml) for a previously determined period of time. As shown in **Figure 6.4 A and B**, TNFα (10 ng/ml) enhanced the phosphorylation of IκB-α by 2.7-fold ($p<0.01$) in MDA-MB-231 cells, and pre-treatment with FSAS3 (50 μM) significantly inhibited this effect by 71% ($p<0.01$) when compared to TNFα treated vehicle. In contrast, the verified CD40-TRAF6 inhibitor 6877002 (50 μM) is less potent and it only reduced TNFα (10 ng/ml) induced phosphorylation of IκB-α by 37% ($p<0.05$) when compared to TNFα treated vehicle. TNFα (10 ng/ml) also enhanced the phosphorylation of IκB-α in mouse 4T1 cells by over 40-fold ($p<0.05$), and pre-exposure to FSAS3 (50 μM) significantly reduced this effect by 53% ($p<0.01$) when compared to TNFα treated vehicle (**Figure 6.4 C and D**). In contrast, 6877002 (50 μM) had no effect on TNFα (10 ng/ml) induced phosphorylation of IκB-α in mouse 4T1 cells.

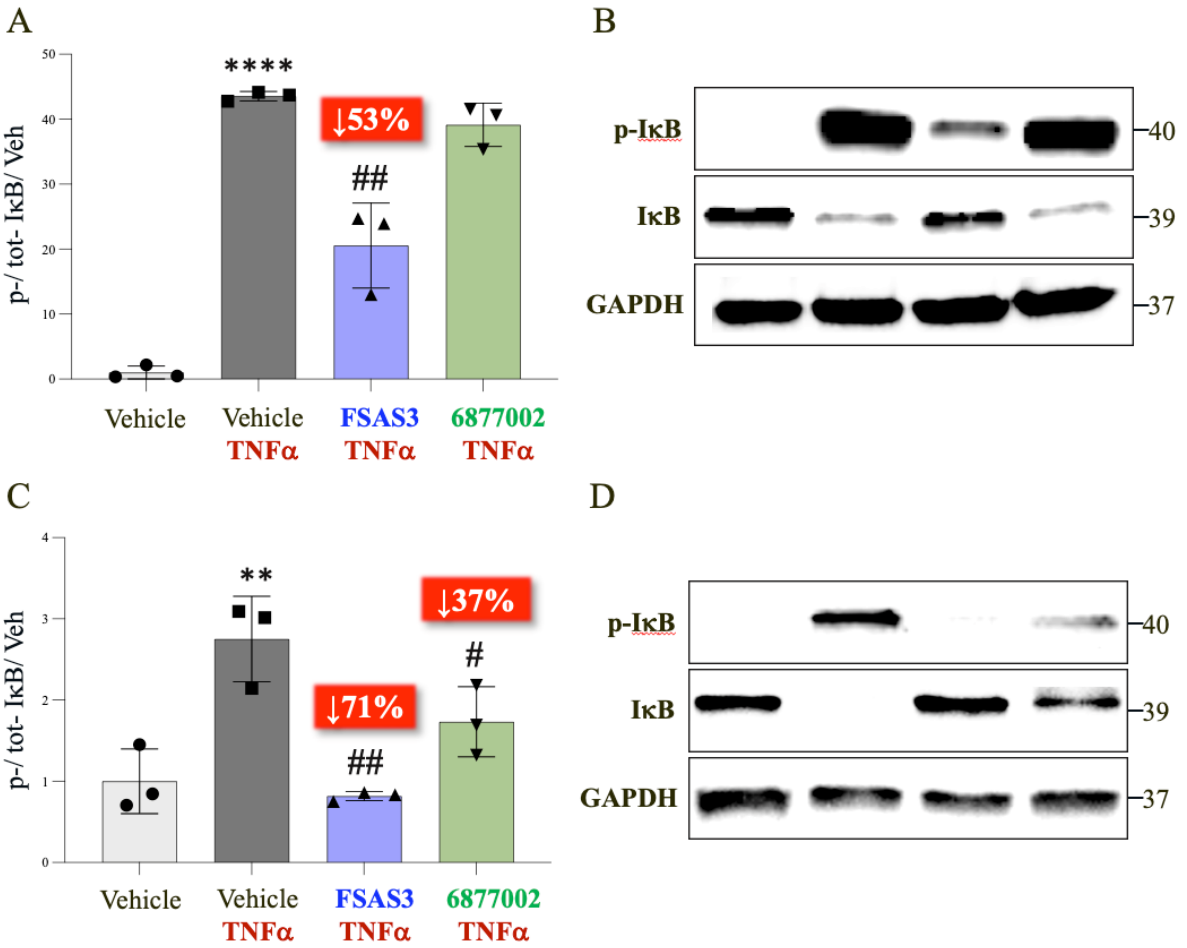

Figure 6.4. The novel FSAS3 reduced the phosphorylation of IκB-α in human MDA-MB-231-luc and murine 4T1-luc induced by TNFα *in vitro*. Relative fold of phosphorylated-IκB-α/IκB-α (% as vehicle) expression of human MDA-MB-231-luc (A) and murine 4T1-luc (C) exposed to vehicle, FSAS3 (50 μM) or 6877002 (50 μM) for 1 hour prior to stimulation with TNFα (10 ng/ml). Representative Western Blot images of expression of p-IκB-α, IκB and GAPDH of MDA-MB-231-luc (B) and 4T1-luc (D) cells exposed to vehicle. Data presented are mean ± standard deviation (n=3). P-values were obtained from ordinary one-way ANOVA followed by Tukey *post hoc* test. **p<0.01 and *p<0.05 compared to vehicle, ##p<0.01, #p<0.05 compared to RANKL treated vehicle cells.

6.4.2.2. The novel FSAS3 reduced TNFα- induced canonical NFκB activation of parental and osteotropic breast cancer via TRAF6 inhibition.

To examine the involvement of TRAF2 on the effects of FSAS3 on TNFα- induced NFκB activation, the relative fold of phosphorylated-IκB-α/IκB-α (% as vehicle) expression in mock and TRAF6 knockdown MDA-MB-231 and MDA231-BT BCa cells was assessed using Western Blot (see **section 2.3.2**), As shown in **Figure 6.5 and 6.6**, TNFα (10 ng/ml) enhanced the phosphorylation of IκB-α by 7 fold ($p<0.01$) in human MDA-MB-231-Mock cells, and pre-exposure to FSAS3 (50 μM) significantly reduced this effect by 63% ($p<0.05$) when compared to TNFα treated vehicle (**Figure 6.5 A**). TNFα (10 ng/ml) increased the phosphorylation of IκB-α in MDA-MB-231 TRAF6$^{\mathbf{KD1}}$ and MDA-MB-231 TRAF6$^{\mathbf{KD3}}$ by 8 fold ($p<0.0001$) and 11 fold ($p<0.05$), respectively, and pre-treatment of these cells with FSAS3 (50 μM) significantly reduced these effects by 43% ($p<0.01$) in MDA-MB-231 TRAF6$^{\mathbf{KD1}}$ (**Figure 6.5 C**) and by 35% (non-significant, $p >0.05$) in MDA-MB-231 TRAF6$^{\mathbf{KD3}}$ when compared to TNFα treated vehicle (**Figure 6.5 E**).

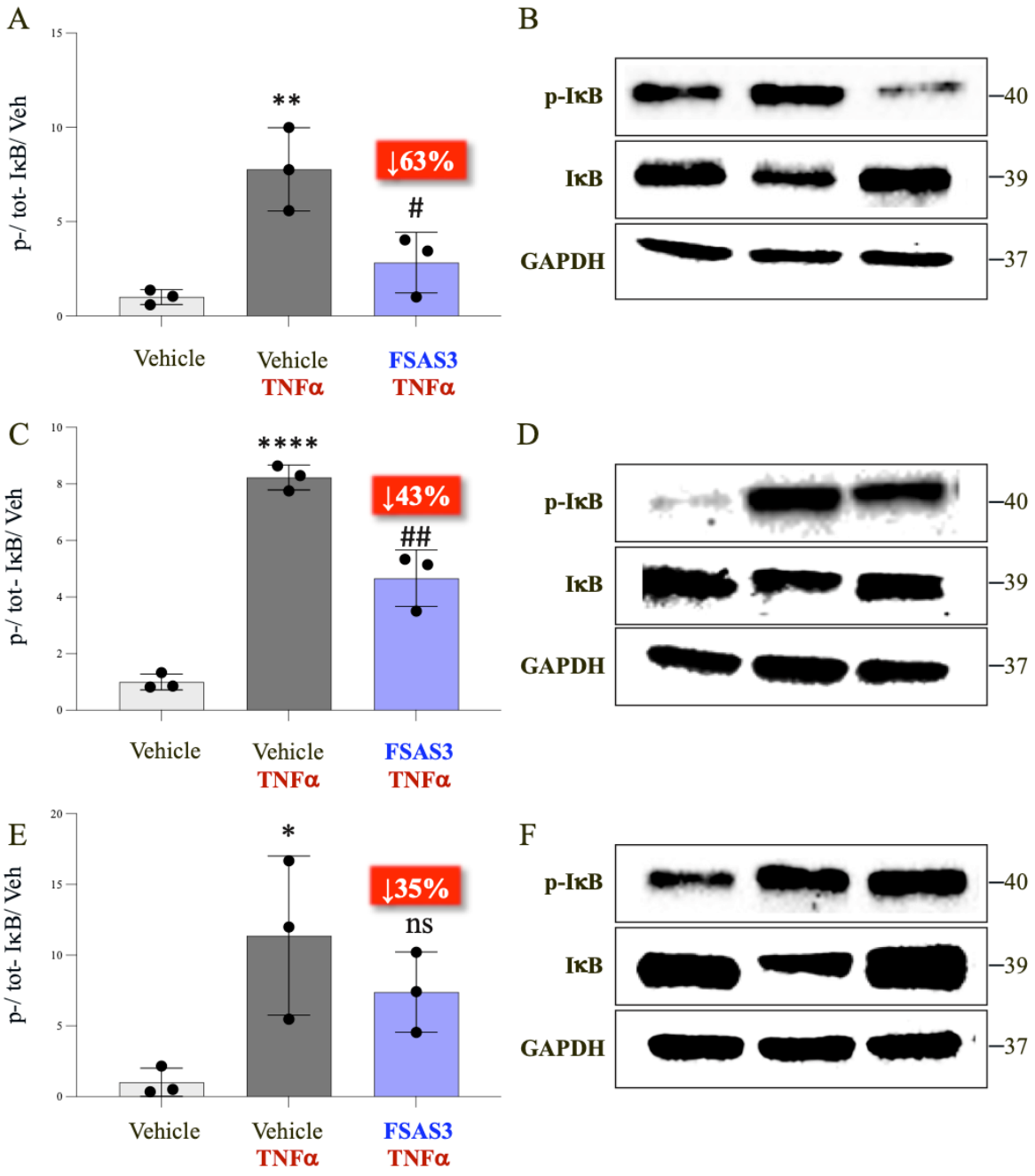

Figure 6.5. The novel FSAS3 reduced the phosphorylation of IκB-α in human MDA-MB-231-Mock rather than MDA-MB-231 TRAF6 deficient cells induced by TNFα *in vitro*. Relative fold of phosphorylated-IκB-α/IκB-α (% as vehicle) expression of human MDA-MB-231-Mock (A), MDA-MB-231-TRAF6KD1 (C) and MDA-MB-231-TRAF6KD3 (E) exposed to vehicle or FSAS3 (50 μM) for 1 hour prior to stimulation with TNFα (10 ng/ml). Representative Western Blot images of expression of p-IκB-α, IκB and GAPDH of MDA-MB-231-Mock (B), MDA-MB-231-TRAF6KD1 (D) and MDA-MB-231-TRAF6KD3 (F) cells exposed to vehicle. Data presented are mean ± standard deviation (n=3). P-values were obtained from ordinary one-way ANOVA followed by Tukey *post hoc* test. *p<0.05 compared to vehicle, #p<0.05 compared to TNFα treated cells.

Similarly, TNFα (10 ng/ml) enhanced the phosphorylation of IκB-α by 37-fold (p<0.05) in MDA231-BT-Mock cells, and pre-exposure to FSAS3 (50 μM) significantly inhibited this effect by 53% (non-

significant, p > 0.05) when compared to TNFα treated vehicle (**Figure 6.6 A**). TNFα (10 ng/ml) also enhanced the phosphorylation of IκB-α by 4 fold (p<0.05) and 11 fold (p<0.05) in MDA231-BT TRAF6^{KD1} and MDA231-BT TRAF6^{KD3}, respectively, and pre-treatment with FSAS3 (50 μM) significantly reduced these effects by 53% (non-significant, P >0.05) in MDA231-BT TRAF6^{KD1} (**Figure 6.6 C**) and by 35% (non-significant, p > 0.05) in MDA231-BT TRAF6^{KD3} when compared to TNFα treated vehicle (**Figure 6.6 E**).

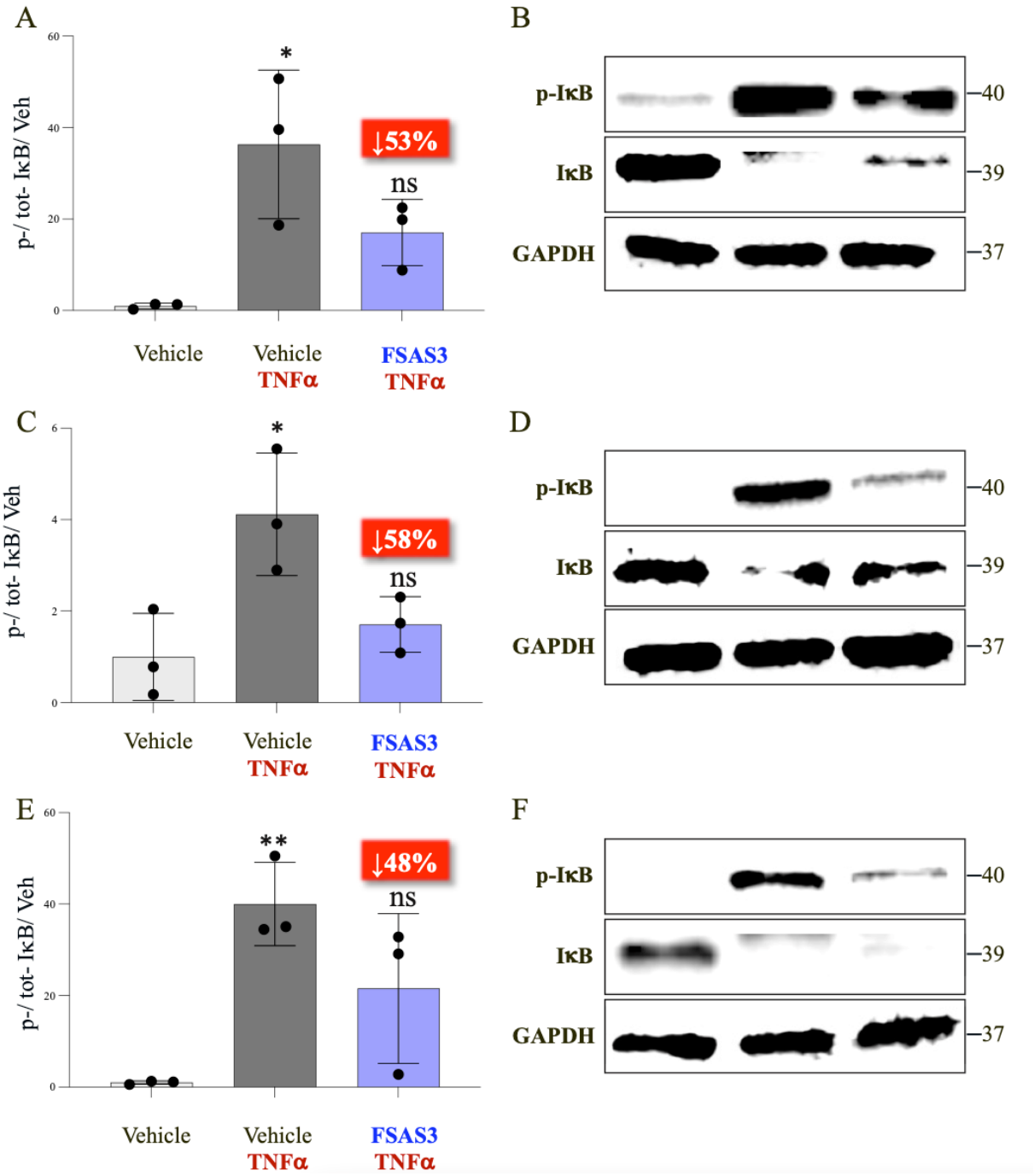

Figure 6.6. The novel FSAS3 reduced the phosphorylation of IκB-α in human MDA-231-BT-Mock rather than MDA-231-BT TRAF6 deficient cells induced by TNFα *in vitro*. Relative fold of phosphorylated-IκB-α/IκB-α (% as vehicle) expression of human MDA-231-BT-Mock (A), MDA-231-BT-TRAF6KD1 (C) and MDA-231-BT-TRAF6KD3 (E) exposed to vehicle or FSAS3 (50 μM) for 1 hour prior to stimulation with TNFα (10 ng/ml). Representative Western Blot images of expression of p-IκB-α, IκB and GAPDH of MDA-231-BT-Mock (B), MDA-231-BT-TRAF6KD1 (D) and MDA-231-BT-TRAF6KD3 (F) cells exposed to vehicle. Data presented are mean ± standard deviation (n=3). P-values were obtained from ordinary one-way ANOVA followed by Tukey *post hoc* test. *p<0.05 compared to vehicle, #p<0.05 compared to TNFα treated cells.

6.4.2.1. Inhibition of NFκB nuclear translocation by the novel FSAS3

Next, I assessed the effects of FSAS3 on the nuclear translocation and DNA binding of canonical NFκB in BCa cells. Briefly, human MDA-MB-231-BT cells were pre-treated with FSAS3 (30μM) for 1 hour and then stimulated with RANKL (150ng/ml) for 45 minutes. Canonical p65 NFκB DNA binding was quantified by using a TransAm kit (Active Motif Europe, Belgium). As shown in **Figure 6.7**, FSAS3 significantly inhibits the canonical TRAF6/IκB/NFκB activation of osteotropic MDA-231-BT cells.

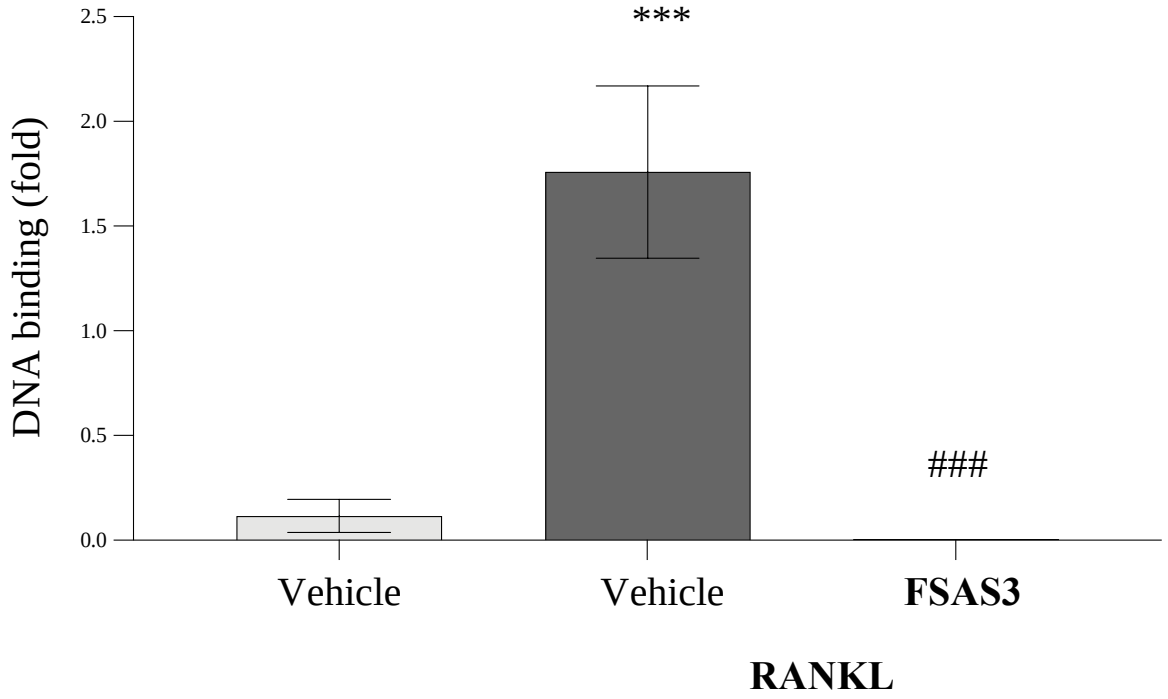

Figure 6.7. Inhibition of breast cancer-specific of canonical TRAF6/IκB/NFκB activation by the novel FSAS3. The human osteotropic MDA-MB-231-BT cells were pre-treated with FSAS3 (30μM), and stimulated with vehicle or RANKL (150ng/ml) for 45 minutes. NFκB binding was quantified by using a TransAm kit (Active Motif Europe, Belgium). Data obtained from 3 independent experiments. ***p<0.001, FSAS3 vs RANKL stimulated group, ###p < 0.001 RANKL treated vehicle vs vehicle. The osteotropic (BT) MDA-MB-231-BT cells are a clone of bone-seeking human MDA-MB-231-BS that was isolated from mouse bone-aspirates and metastasise readily to the skeleton.

6.4.3. Interaction of FSAS3 with TRAF6

6.4.3.1. *In silico* docking studies

To study the interaction between FSAS3 and TRAF6, I first considered the *in silico* docking experiment carried out by our collaborators Dr Ivan Bassanini and his colleagues (University of Milan, Italy). As shown in **Figure 6.8**, Dr Bassanini and colleagues observed that FSAS3 not only binds to the CD40 pocket on TRAF6, but it also binds with a novel pocket (P1) at the C-terminus of both TRAF6 and TRAF2 (Bassanini and Idris et al, unpublished data, personal communication).

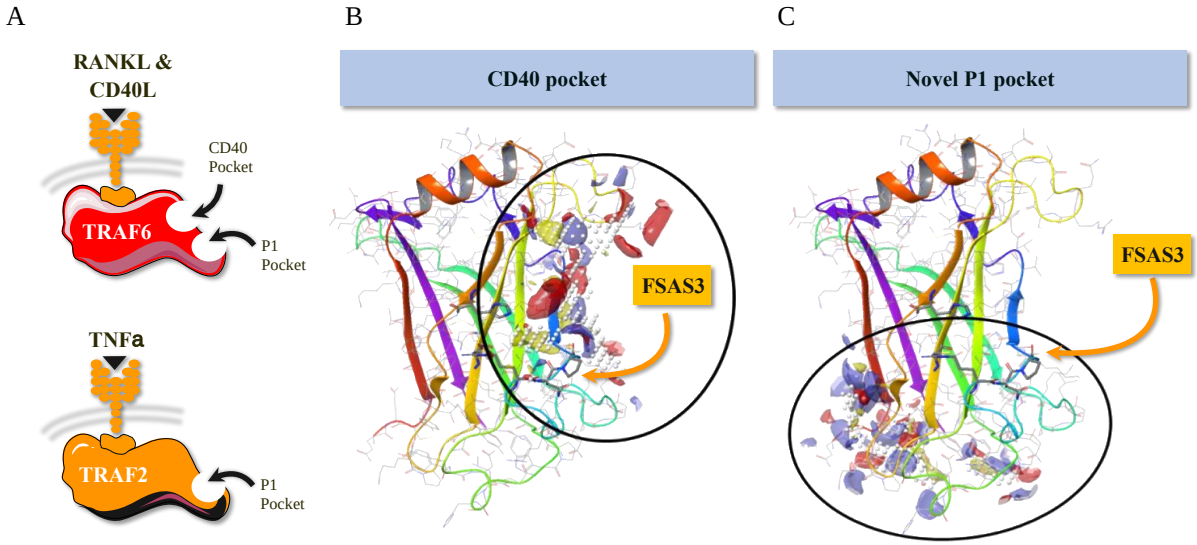

Figure 6.8. Predicted poses of FSAS3 on pockets of TRAF6 and TRAF2. Pharmacophore models that show the predicted pose for FSAS3 on CD40- (B) and the novel P1 (C) pockets (Bassanini and Idris *et al*, unpublished data, personal communication).

6.4.3.2. FSAS3 interacts with TRAF6 and TRAF2

Inspired by these findings, I carried out additional mechanistic experiment that used Drug Affinity Responsive Target Stability (DARTS) assay [201] to assess whether FSAS3 directly interacts, binds to and disrupts TRAF6 or TRAF2 function in BCa cells and macrophages. In this experiment, cell lysate from human BCa cells MDA-MB-231 and mouse RAW264.7 macrophages were incubated with FSAS3 (50μM) for 2 hours at room temperature. The cell lysates were then subjected to limited, controlled proteolytic digestion by adding a cocktail of pronase at a ratio diluted concentration (refer to Materials and Methods for extended description). As shown in **Figure 6.9A**, FSAS3 prompted the stability, enhanced the resistance to and protected TRAF6 from pronase degradation, indicative of direct interaction between FSAS3 and TRAF6. Representative images are shown in panel B.

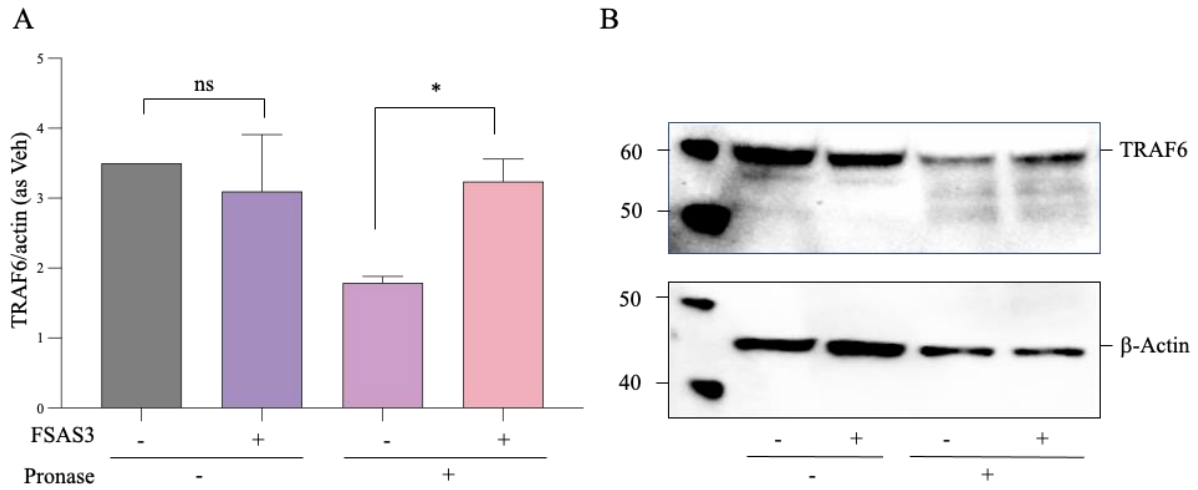

Figure 6.9. Validation of the interaction between FSAS3 and TRAF6 using DARTS assay. (A) RAW264.7 cell lysate were incubated with 2% (v/v) of FSAS3 (50μM) or DMSO and digested with pronase (0.8 μg/ml) at room temperature for 2 hours. (B) Representative images of TRAF6 or b-actin expression of FSAS3 or DMSO treated cell lysates in the presence or absence of pronase detected by western blot. Data obtained from three independent experiments, p-values were determined using unpaired T-test, *p < 0.05, ns denote no significance compared to lysates treated with DMSO.

Similarly, FSAS3 protected TRAF2 from pronase degradation and prompted its stability (**Figure 6.10A)**, indicating their direct interaction in the model described. Representative images are shown in panel B.

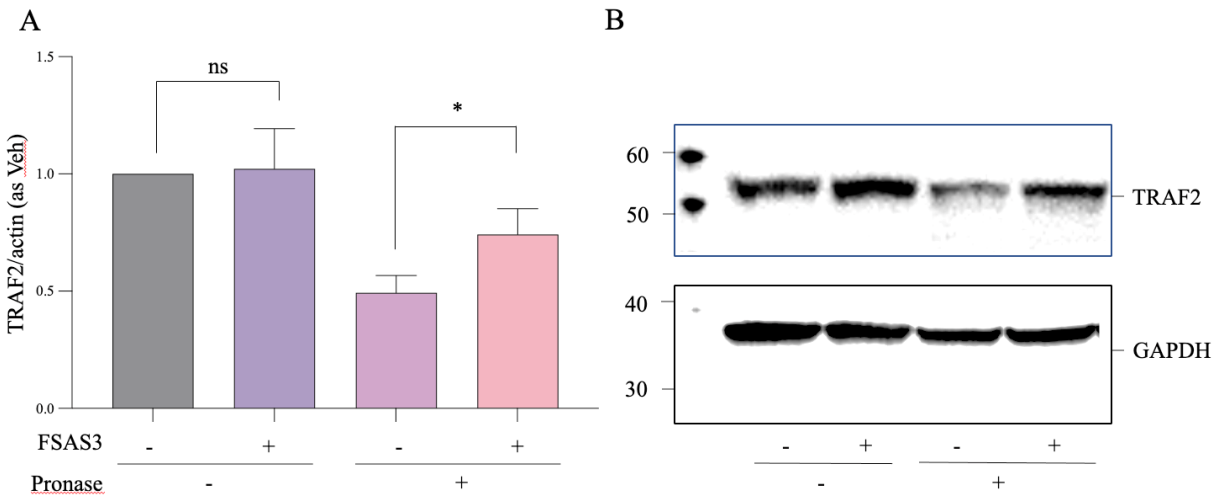

Figure 6.10. Validation of the interaction between FSAS3 and TRAF2 using DARTS assay. (A) MDA-MB-231 cell lysate were incubated with 2% (v/v) of FSAS3 (50μM) or DMSO and digested with pronase (0.8 μg/ml) at room temperature for 2 hours. (B) Representative images of TRAF6 or GAPDH expression of FSAS3 or DMSO treated cell lysates in the presence or absence of pronase detected by western blot. Data obtained from three independent experiments, p-values were determined using unpaired T-test, *p < 0.05, ns denote no significance compared to lysates treated with DMSO.

6.4.3.3. Disruption of TRAF6 interactions with TAK-1/TAB-1 complex by the novel FSAS3

To investigate if and how FSAS3 affect signal transduction pathways at the level of TRAF6/RANK receptor complex, I carried out a series of mechanistic studies that assess the interactions and recruitment of TAK-1 and TAB2 to the TRAF6-RANK receptors in BCa cells using immunoprecipitation followed by Western blot. Briefly, human MDA-MB-231 cells were pre-treated with FSAS3 (50μM) for 1 hour and then stimulated with RANKL (100ng/ml) for 15 minutes. The cell lysates were collected and incubated with anti-TRAF6 antibody and then probed with anti-TAK-1 or anti-TAB-1. IgG at 50kDa is considered as a successful input of antibody. As shown in **Figure 6.11A-B**, treatment with RANKL significantly increased TAK-1 recruitment by TRAF6, and FSAS3 inhibited this effect. Similarly, RANKL increased TAB-1 recruitment by TRAF6, and FSAS3 inhibited this effect (**Figure 6.11C-D**). These results indicate that FSAS3 functions as a small molecular that disrupts the RANKL-stimulated interactions of TRAF6 with TAK-1 and TAB-1.

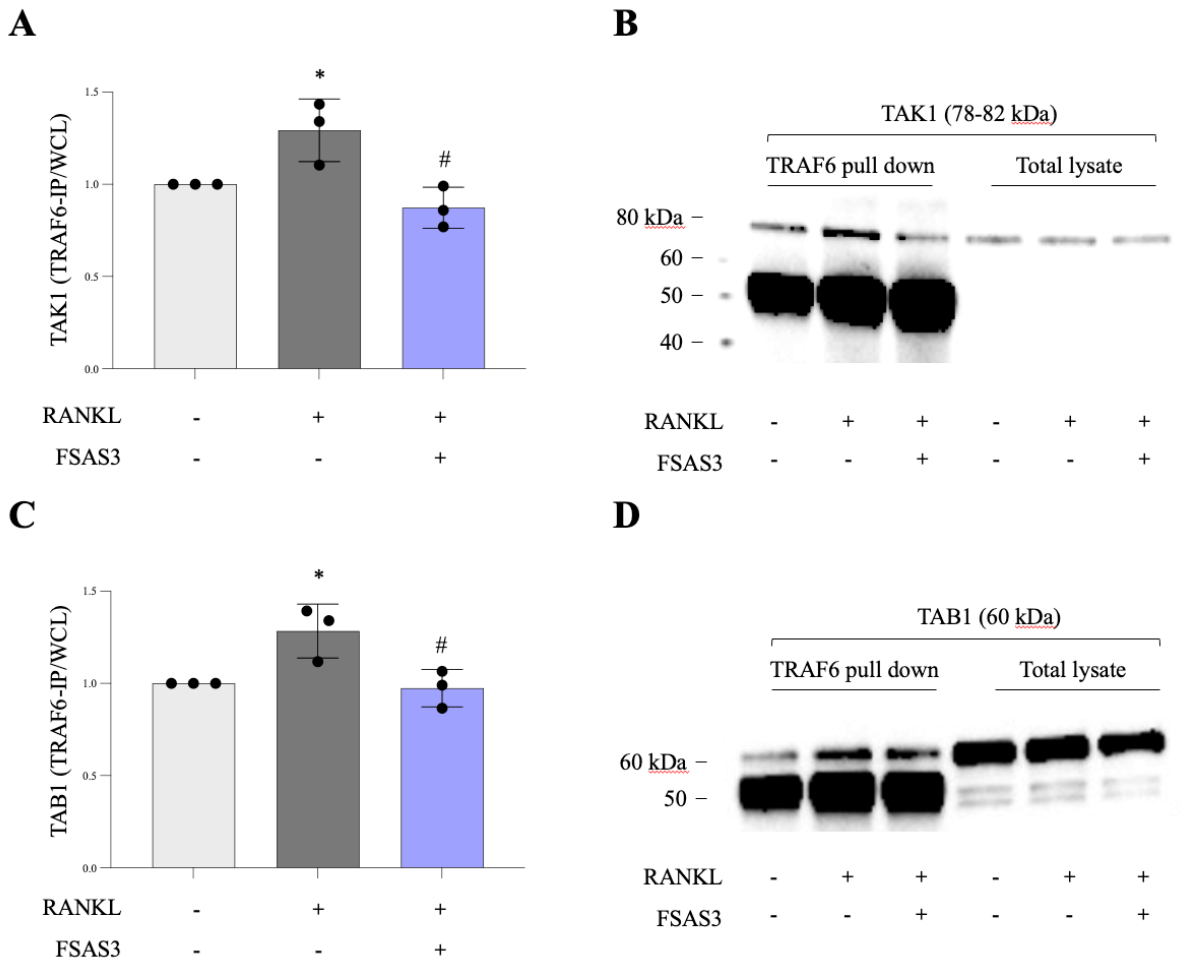

Figure 6.11. Effects of FSAS3 on complex formation of TRAF6 and TAK1, TAB1. MDA-MB-231 cells were starved overnight and then cultured for FSAS3 (50 μM) or DMSO for 1 hour and stimulated with RANKL (100 ng/ml) for 15 minutes with or without FSAS3. Cell lysates were immunoprecipitated (IP) with anti-TRAF6 and immunoblotted with anti-TAK1 (A), or anti-TAB1 (B). The level of co-immunoprecipitated TAK1 or TAB1 was qualified and normalized to total TAK1 or TAB1 in cell lysate, respectively. (C-D) Representative Western Blot images of expression of I TAK1 (C) and TAB1 (D) of MDA-MB-231 cells immunoprecipitated and whole cell lysates. Data presented are mean ± standard deviation (n=3).

6.4.3.1. Disruption TRAF6 interaction with the IKKα/β/γ complex by the novel FSAS3

Next, I examined if FSAS3 affect the formation and interaction of TRAF6 with the IKKα/β/ψ complex in BCa cells using immunoprecipitation followed by Western blot. Briefly, human MDA-MB-231 cells were pre-treated with FSAS3 (50μM) for 1 hour and then stimulated with RANKL (100ng/ml) for 15 minutes. The cell lysates were collected and incubated with anti-TRAF6, and then probed with anti-IKKβ for anti-IKKα pulldown. The immunoblot analysis of TRAF6 pull-down samples using IKKα (as shown in **Figure 6.12A**) and IKKβ (as depicted in **Figure 6.12B**) demonstrates there is no direct binding of TRAF6 with either IKKα or IKKβ.

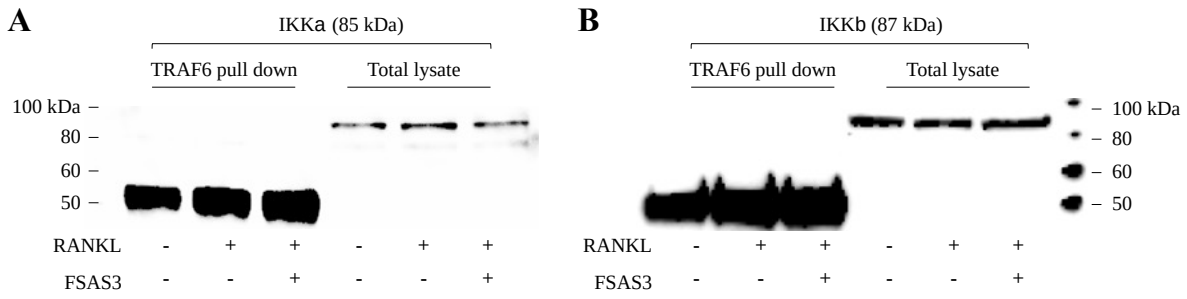

Figure 6.12. Effects of FSAS3 on complex formation of TRAF6 and IKKα, IKKβ. MDA-MB-231 cells were starved overnight and then cultured for FSAS3 (50 μM) or DMSO for 1 hour and stimulated with RANKL (100 ng/ml) for 15 minutes with or without FSAS3. Cell lysates were immunoprecipitated (IP) with anti-TRAF6 and immunoblotted with anti-IKKα (A), or anti-IKKβ (B).

6.4.3.1. Disruption of IKKα/β complex by the novel FSAS3

Next, IKKα was pulled down and the resulting blot was probed with anti-IKKβ in the same treatment panel of MDA-MB-231 cells. As depicted in **Figure 6.13**, RANKL has no effect to activate the binding of IKKα to IKKβ. Furthermore, FSAS3 did not seem to influence the recruitment of IKKβ. Representative images are shown in **Panel B**.

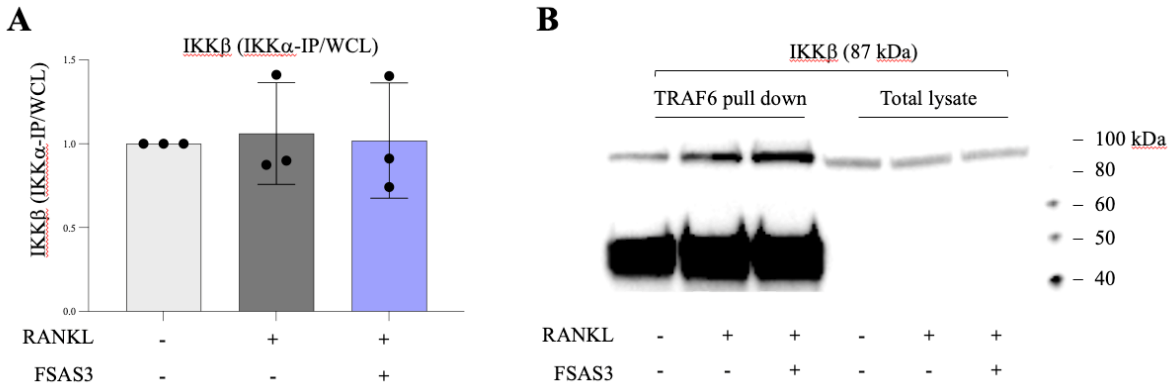

Figure 6.13. Effects of FSAS3 on complex formation of IKKα and IKKβ. MDA-MB-231 cells were starved overnight and then cultured for FSAS3 (50 μM) or DMSO for 1 hour and stimulated with RANKL (100 ng/ml) for 15 minutes with or without FSAS3. Cell lysates were immunoprecipitated (IP) with anti-IKKα and immunoblotted with anti-IKKβ. (A) Relative fold of immunoprecipitated IKK-β (as whole cell lysate) expression of human MDA-MB-231 exposed to vehicle or FSAS3 (50 μM) for 1 hour prior to stimulation with RANKL (100 ng/ml). (B) Representative Western Blot images of expression of IKK-β of MDA-MB-231 cells immunoprecipitated and whole cell lysates. Data presented are mean ± standard deviation (n=3).

Thus, I went to test the effect of FSAS3 on the phosphorylation of IKKα/β. As shown in **Figure 6.14A**, although not significantly, FSAS3 inhibited the phosphorylation of IKKα induced by RANKL. Moreover, FSAS3 significantly inhibited the phosphorylation of IKKβ induced by RANKL (**Figure 6.14B)**, confirming the enrolment of FSAS3 in the activation of NFκB through the canonical pathway.

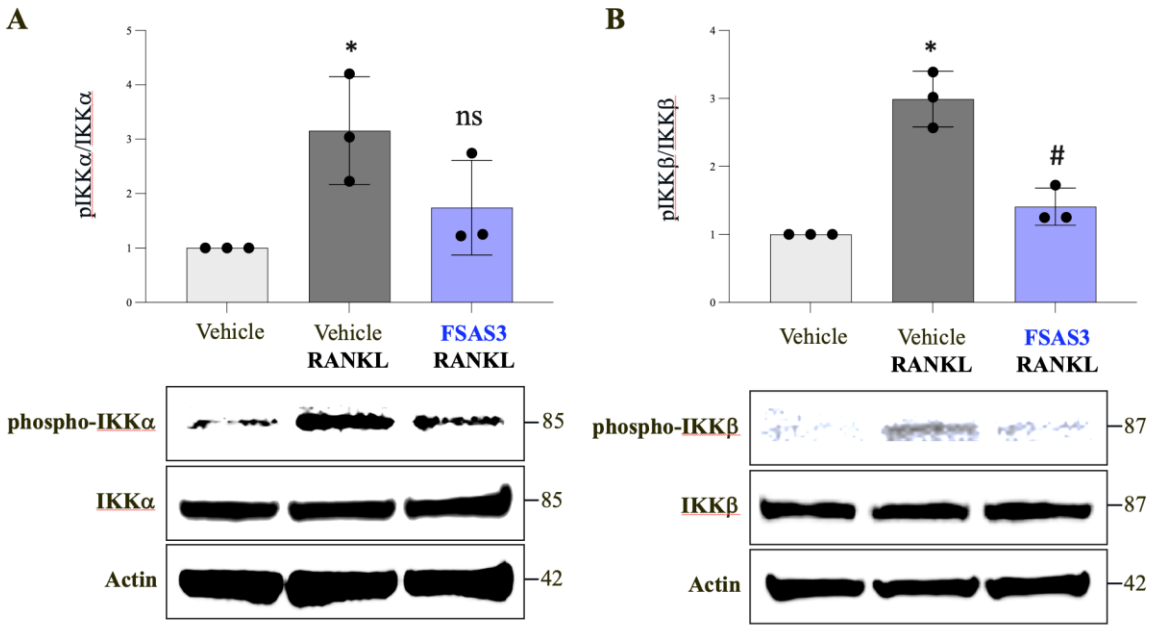

Figure 6.14. The novel FSAS3 reduced the phosphorylation of IKKα and IKKβ in human MDA-MB-231 cells induced by RANKL *in vitro*. Relative fold of phosphorylated-IKK-α (A) and phosphorylated-IKK-β (B) (as vehicle) expression of human MDA-MB-231 exposed to vehicle or FSAS3 (50 μM) for 1 hour prior to stimulation with RANKL (100 ng/ml). Representative Western Blot images of expression of p-IKK-α/b and Actin of MDA-MB-231 cells exposed to vehicle are shown in bottom panel. Data presented are mean ± standard deviation (n=3). P-values were obtained from ordinary one-way ANOVA followed by Tukey *post hoc* test. *p<0.05 compared to vehicle, #p<0.05 compared to RANKL treated cells.

6.5. Discussion

In **Chapter 5**, the anti-tumour, anti-migratory, and anti-invasive effects of the novel NFκB inhibitor FSAS3 and the verified CD40-TRAF6 inhibitor 6877002 were validated in human and mouse BCa cells. In view of the role of the TRAF6/NFκB pathway in BCa and based on the findings in **Chapter 5** that showed that FSAS3 is a potent inhibitor of the *in vitro* behaviour of parental and osteotropic TNBC cells than 6877002, I conducted a head-to head comparison to assess the ability of the two agents to influence canonical TRAF2/6-mediated NFκB activation using a set of mechanistic techniques, namely Western Blot, Immunoprecipitation, Molecular Docking and DARTS.

First, I used Western blot to demonstrate that the novel FSAS3 is a potent inhibitor of both RANKL(TRAF6)- as well as TNFα(TRAF2)-driven canonical NFκB activation in BCa cells than the verified CD40-TRAF6 inhibitor 6877002. The efficacy of 6877002 towards canonical NFκB inhibition in cancer and bone has been previously reported by my colleagues (and I) [154, 156]. Together, these results confirmed that the novel FSAS3 reduces canonical NFκB activation downstream of TRAF6 and TRAF2, which is consistent with the fact that pharmacological inhibition of TRAF2 and TRAF6 are associated with inhibition of p-IKKα/IKKα, p-IκBα/ IκBα and NFκB p65[162, 246], and their genetic inactivation lead to suppression of NFκB p65 [244, 253]. It is important to note that 6877002, which is known to target the CD40 pocket only on TRAF6, is significantly less effective as a TRAF2/6-NFκB inhibitor than FSAS3 in murine 4T1 BCa cells and it had no effect in human MDA-MB-231 BCa cells. I cannot explain this observation, but it can be due to the fact that human MDA-MB-231 cells express higher level of both TRAF6 and TRAF2 than mouse 4T1 BCa, and FSAS3, unlike 6877002, inhibited the effects of both RANKL and TNFα equally - suggesting that its lack of specificity to either TRAF makes it more potent than its verified CD40-TRAF6 congener 6877002.

To investigate the interaction of FSAS3 with TRAF6, I carried out a number of mechanistic and functional studies on wild type and TRAF6 deficient MDA-MB-231 cells and their osteotropic clones MDA231-BT cells. These experiments provided a number of useful insights in the mechanism by which this novel agent disrupts TRAF6 activity. First, it showed that parental MDA-MB-231 cells that express

up to 70% less TRAF6 than their osteotropic clones MDA-231-BT cells (as reported in **Chapter 5**) were significantly insensitive to RANKL(TRAF6)-induced NFκB activation, but sensitive to TNFα(TRAF2)-induced NFκB activation. This provides explanation to why FSAS3 is a potent inhibitor of cell viability and RANKL(TRAF6)-induced NFκB activation in osteotropic MDA-231-BT cells compared to their parental clones. More importantly, inhibition of IκB phosphorylation by FSAS3 is significantly blunted in TRAF6 deficient MDA-MB-231 cells than mock control, further confirming its selectivity for TRAF6. Notwithstanding these findings, it is important to note that FSAS3 is also an inhibitor of TNFα-induced NFκB activation in TRAF6 deficient MDA-MB-231 cells, indicating an off-target effect(s) that is likely to be due to its ability to interact with multiple pockets in TRAF6 and TRAF2. For this, future experiments are needed.

In this chapter, I also confirmed TRAF6 as a target of FSAS3 using DARTS, thereby confirming the previous results from predicted pose from *in silico* docking analysis that suggested that it binds to CD40 and a novel pocket at the c-terminus of TRAF6 (Bassanini and Idris et al, unpublished data, personal communication). The present DARTS analysis confirmed that FSAS3 directly interacts with and disrupts protein – protein interactions. More precisely, it binds to TRAF6 and induce conformational changes to a degree that the process of proteolysis is inhibited. Such changes to TRAF6 protein structure can be a result of FSAS3 directly blocking access to Protease cleavage sites, or by inducing conformational changes that make TRAF6 less susceptible to proteases. Whist further work is needed, the finding of this experiment confirms the direct interaction between FSAS3 and TRAF6 and suggests that FSAS3 disrupts TRAF6 interactions with downstream adaptor protein and receptor recruitments factors from the NFκB signalling transduction pathway.

Encouraged by this finding and the various reports that the C-terminus of TRAF6, as an important domain in the interaction of TRAF6 with upstream signalling molecules, is a promising target for tumour therapy [231, 293, 294], I went on to show that FSAS3 inhibited TRAF6-TAK-1 and TRAF6-TAB1 binding, thereby leading to significant suppression of IκB phosphorylation and p65NFκB nuclear translocation and DNA binding (**Figure 6.15**). This results clearly indicate significant suppression of canonical NFκB signalling from receptor to nuclear. Similar action was also reported by investigator

such as Wei et al who showed that natural extract suppresses the ubiquitination of TRAF6, leading to accumulation of TRAF6-TAK-1 complexes and suppression of osteoclast formation *in vitro* [156].

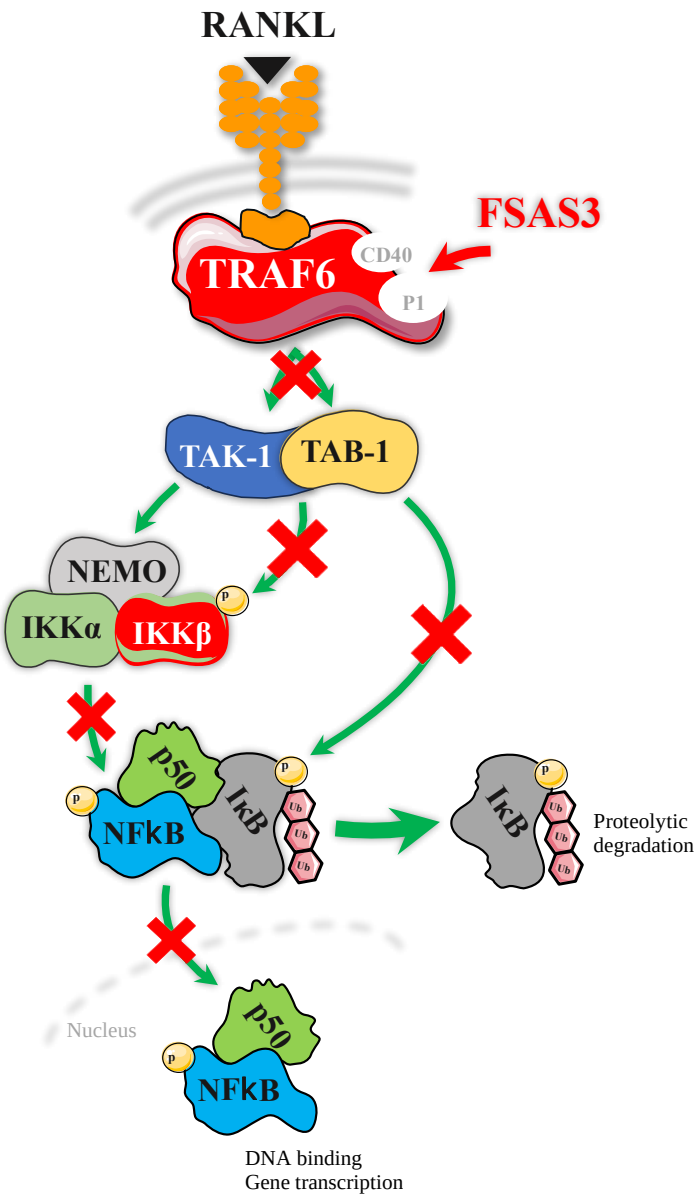

Figure 6.15. Schematic representation of inhibition of RANKL-driven TRAF6/NFκB activation by the novel FSAS3. X denotes inhibition. Refer to text for description and abbreviations.

Collectively, findings from these mechanistic studies suggest that FSAS3 is a selective, but not exclusive, inhibitor of osteolysis (RANKL) and inflammation (TNFα) associated TRAF6 (and TRAF2) NFκB activation in TNBC cells. Thus, this agent can be of value in the treatment of multi-faceted and multi-factorial cancer such as metastatic BCa in bone. Therefore, further *ex vivo* and *in vivo* studies to validate

its anti-osteolytic as well as anti-metastatic effects, alone and in combination with chemotherapy, are needed.

CHAPTER 7. Effects of the novel TRAF6 inhibitor FSAS3 on breast cancer – bone cell crosstalk and osteolysis

7.1. Summary

The TRAF/NFκB axis plays an important role in the regulation of BCa metastasis and bone remodelling, particularly osteoclastic bone loss in health and disease. In **Chapter 3** I confirmed that TRAF6 is associated with bone metastasis in BCa patients, and in **Chapter 4** I observed that TRAF2 expression is associated with osteoclast activity. However, previous published studies by our laboratory have shown that the verified CD40-TRAF6 inhibitor 6877002 supressed BCa bone metastasis in mice bearing mouse 4T1 cells but failed to protect these mice from osteolytic bone loss [185]. 6877002 was effective in inhibiting BCa-induced osteolysis only in combination with Docetaxel[185]. Therefore, I investigated the anti-osteolytic effects of the significantly more potent inhibitor of TRAF/NFκB, FSAS3, on the ability of BCa cells to affect bone cell activity *in vitro* and to cause osteolysis *ex vivo*.

First, I found that FSAS3 inhibits RANKL-induced osteoclast formation in human and murine culture *in vitro*. Additionally, FSAS3 disrupted BCa cell – osteoclast interactions as evidenced by the significant reduction in *in vitro* osteoclast formation in RANKL-stimulated mouse RAW264.7 macrophages co-cultured in the presence of human osteotropic MDA-231-BT BCa cells or their derived factors (conditioned medium. CM). Notably, these effects were observed at concentrations of FSAS3 that failed to affect the viability of mouse macrophages (pre-osteoclasts), thereby excluding cytotoxic effects. Consistently, FSAS3 also reduced the phosphorylation of IκB induced by RANKL in mouse RAW264.7 macrophages.

In osteoblasts, FSAS3 only reduced *in vitro* osteoblast differentiation and bone nodule formation at a concentration that inhibited osteoblast viability. It is important to note that FSAS3 had no effect on osteoblast viability at concentrations that inhibited osteoclastogenesis.

Ex vivo, FSAS3 inhibited BCa-induced osteolysis in human MDA-MB-231-BT - mouse calvarial bone co-culture system, indicating an anti-osteolytic effect *ex vivo*.

Altogether, these results suggest that the novel inhibitor of TRAF6 FSAS3 exhibits anti-osteolytic as well as anti-inflammatory, anti-migratory and anti-tumour effects in the *in vitro* and *ex vivo* models of BCa – bone cell interaction described.

7.2. Introduction

Excessive and unbalanced osteoblast and osteoclast differentiation and activity play an important role in the pathogenesis of BCa bone metastasis and osteolysis [37, 48, 49, 295]. Secondary BCa in the skeleton is a complex, multi-faceted and muti-cellular disease that involves the interplay between osteotropic BCa cells, osteoclasts, and osteoblasts – among other cells in the tumour micro-environment such as osteocytes and immune cells. This process is often described as "vicious cycle". In the early phases, BCa cells acquire the ability to metastasize from the primary site and that to invade the bone marrow, survive in the skeleton (i.e. become osteotropic), express and secrete various pro-tumour, pro-osteolytic and pro-inflammatory factors, such as parathyroid hormone-related protein (PTHrP), that stimulate osteoblasts. This primarily leads to increased expression of RANKL by mature osteoblasts and their precursors. BCa cells also stimulate RANKL production by other cells such as immune cells [296, 297]. By binding to its receptor RANK on osteoclast precursors, RANKL promotes their lineage commitment of early pre-osteclasts into mature, multi-nucleated osteoclasts[183, 298] that capable of resorbing bone matrix. The release of growth factors stored within the bone maxtrix, such as transforming growth factor-beta (TGF-β)stimulate BCa cell proliferation, and further enhance their and other cell ability to drive "vicious cycle" of excessive bone destruction and skeletal tumour growth [299]. Osteoblasts also play another underappreciated role in this process. Some of the factors secreted by BCa cells inhibit the ability of osteoblast to form new bone, leading to significantly reduction in bone formation that further aggravate osteolytic bone loss caused by excessive bone resorption. Previous work by our group has shown that TRAF2 enhances osteotropic BCa growth, migration and their ability to cause osteolysis [239]. Others have also shown that miR-214 that targets TRAF3 in osteoclasts promotes osteolytic bone metastasis of BCa *in vivo* [163].

TRAF6 has been the most studied in this area. As key regulator of RANKL-induced osteoclast formation, survival and bone resorption[300, 301], its deficiency causes osteopetrosis[190] by abolishing osteoclast formation[189]. Previous studies of our group [184, 185] indicated that inhibition of TRAF6 related NFκB activation using 6877002 that selectively binds to the CD40 of the receptor exerts anti-inflammatory, anti-metastatic but not osteoprotective effect in rodent models of BCa. Further work by

my colleagues and I showed that agent exhibits anti-inflmmaotry effects in mice bearing Rheumatoid arthritis but failed these mice from osteolytic bone damage. These findings together highlighted the need for a new class of TRAF6 inhibitors that exhibits anti-inflammatory, anti-metastatic as well as anti-osteolytic effects. Unpublished data by my colleague Giovana suggests that the novel FSAS3 inhibits prostate cancer cell-induced NFκB activation and bone cell activity *in vitro* (Giovana Carrasco, White Rose ethesis, University of Sheffield, UK: https://etheses.whiterose.ac.uk/27832/) – thus suggesting that FSAS3 can be of value in the treatment of osteolysis caused by osteotropic BCa cells.

7.3. Aims

The main aim of this chapter was to test the hypothesis that exposure to FSAS3 disrupts BCa – bone cell crosstalk *in vitro* and inhibits their ability to cause osteolytic bone damage *ex vivo*.

The aims of this chapter were achieved by investigating the effect of FSAS3 on:

- BCa cell-induced osteoclast formation *in vitro*.
- BCa cell-induced osteoblast differentiation and activity *in vitro*.
- BCa cell- and RANKL-induced NFκB activation in bone cells *in vitro*.
- BCa cell-induced osteolytic bone damage *ex vivo*.

7.4. Results

7.4.1. Effects of FSAS3 on RANKL-induced osteoclast formation *in vitro*

First, I established the effects of FSAS3 on osteoclast formation in RANKL stimulated mouse RAW264.7 cells *in vitro*. Cultures of mouse RAW264.7 osteoclast precursors were treated with different concentrations of the novel FSAS3 (0 – 1μM) for 1 hour and then stimulated with RANKL (100 ng/ml) for 72 hours as described in **section 2.3.4.2**. TRAcP staining was used to identify mature, multinucleated (>3 nuclei) osteoclasts (**see section 2.2.6**). Cultures of mouse RAW264.7 osteoclast precursors treated with FSAS3 (0 – 1μM) in the absence of RANKL were used to establish the effects of this agent on the viability of osteoclast precursors. As shown in **Figure 7.1**, FSAS3 significantly reduced the formation of TRAcP-positive multi-nucleated osteoclastsin the presence of RANKL in a concentration-dependent manner (**Figure 7.1A**), without affecting RAW264.7 cells viability (**Figure 7.1C).** Representative images of TRAcP-positive osteoclasts and their precursors are shown in **Figure 7.1B.**

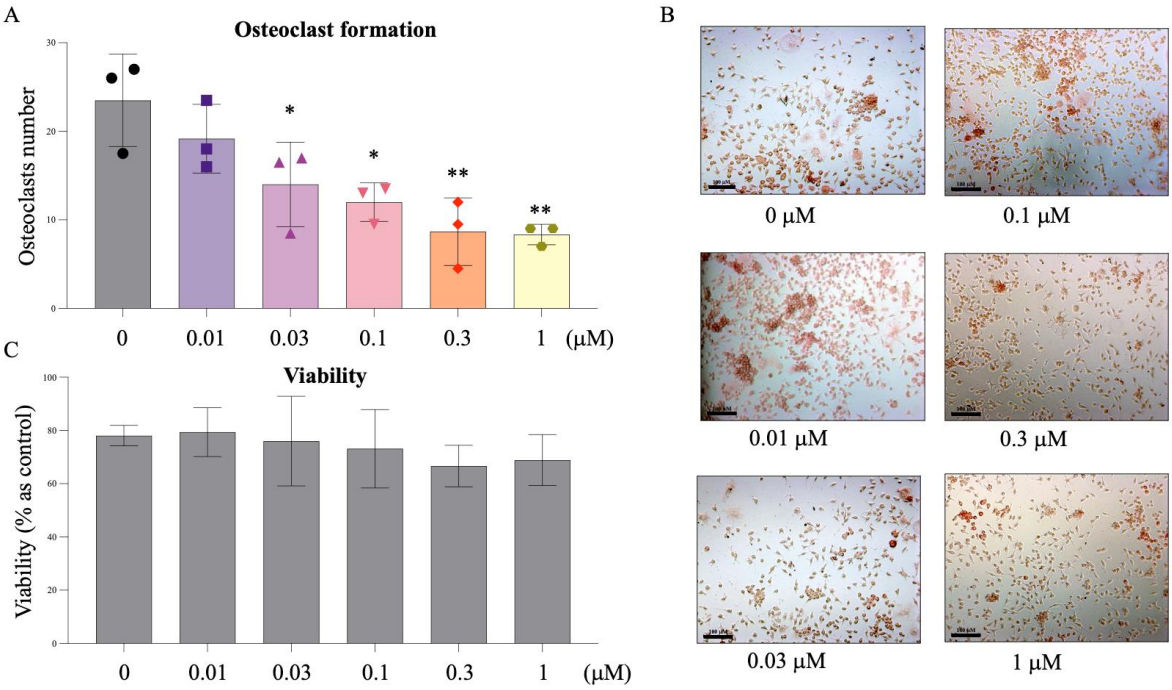

Figure 7.1 The novel FSAS3 decreased RANKL induced osteoclast formation at a dose dependent manner without an effect of viability. (A-B) Osteoclast formation and (C) viability of RAW264.7 cells stimulated with RANKL 100ng/ml and treated with FSAS3 at a range of concentration (0-1 μM) every 48 hours for 72 hours. Cultures were assessed via Alamar Blue™ fixed and TRAcP staining, respectively. Data obtained from three independent experiments. p-values were determined using unpaired T-test. **p<0.01, *p<0.05 compared to cells treated with vehicle. Scale bar=100 μM.

7.4.2. Effects of FSAS3 on RANKL-induced canonical NFκB in osteoclasts and their precursors *in vitro*

Next, I examined the effects of FSAS3 on RANKL induced osteoclast precursors. Briefly, murine macrophage-like RAW264.7 were starved for 16 hours, treated with FSAS3 (50 μM) or vehicle for 1 hour and then stimulated with RANKL (100 ng/ml) for 5 minutes. As shown in **Figure 7.2**, RANKL (100 ng/ml) significantly enhanced the phosphorylation of IκB-α by 2.5-fold ($p<0.05$) in murine RAW264.7 cells, and pre-exposure to FSAS3 (50 μM) completely prevented this effect when compared to vehicle control ($p<0.5$). In some experiments, FSAS3 reduced RANKL induced IκB-α phosphorylation in osteoclast precursors below the control level ($p >0.5$).

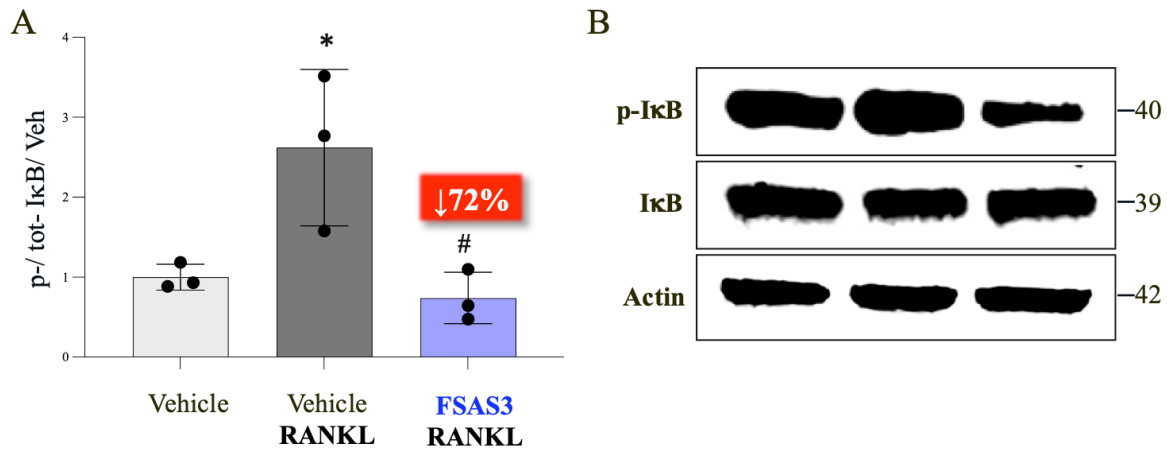

Figure 7.2. The novel FSAS3 reduced the phosphorylation of IκB-α in murine RAW264.7 induced by RANKL *in vitro*. Relative fold of phosphorylated-IκB-α/IκB-α (% as vehicle) expression of murine RAW264.7 (A) exposed to vehicle, FSAS3 (50 μM) for 1 hour prior to stimulation with RANKL (100 ng/ml). (B) Representative Western Blot images of expression of p-IκB-α, IκB and Actin. Data presented are mean ± standard deviation (n=3). P-values were obtained from ordinary one-way ANOVA followed by Tukey *post hoc* test. **p<0.01 and *p<0.05 compared to vehicle, ##p<0.01, #p<0.05 compared to RANKL treated cells.

7.4.3. Effects of FSAS3 on Breast cancer-induced osteoclast formation *in vitro*

In this section, the effects of FSAS3 on the interactions and crosstalk between BCa cells and osteoclasts were studied. First, I performed a number of pilot experiments to define the optimal number of BCa cells, RANKL concentration, and the time point at which to study the effects of FSAS3 on osteoclast formation in the presence of BCa cells or their derived factors (conditioned medium, CM). Briefly, 300

parental MDA-MB-231 and osteotropic MDA-231-BT BCa cells were co-cultured with mouse RAW264.7 osteoclast precursors (2000 cells) and treated with FSAS3 (0.1-0.3 μM) in the presence of RANKL (200 ng/ml) for 120 hours. As shown in **Figure 7.3**, co-culture of MDA-MB-231 and MDA-231-BT caused a modest but not significant increase in osteoclast formation when compared to cultures exposed to RANKL (200ng/ml) alone. Nevertheless, the novel TRAF6 inhibitor FSAS3 significantly inhibited osteoclast formation at all concentrations tested. Representative images of TRAcP-positive osteoclasts and their precursors are shown in **Figure 7.3B.**

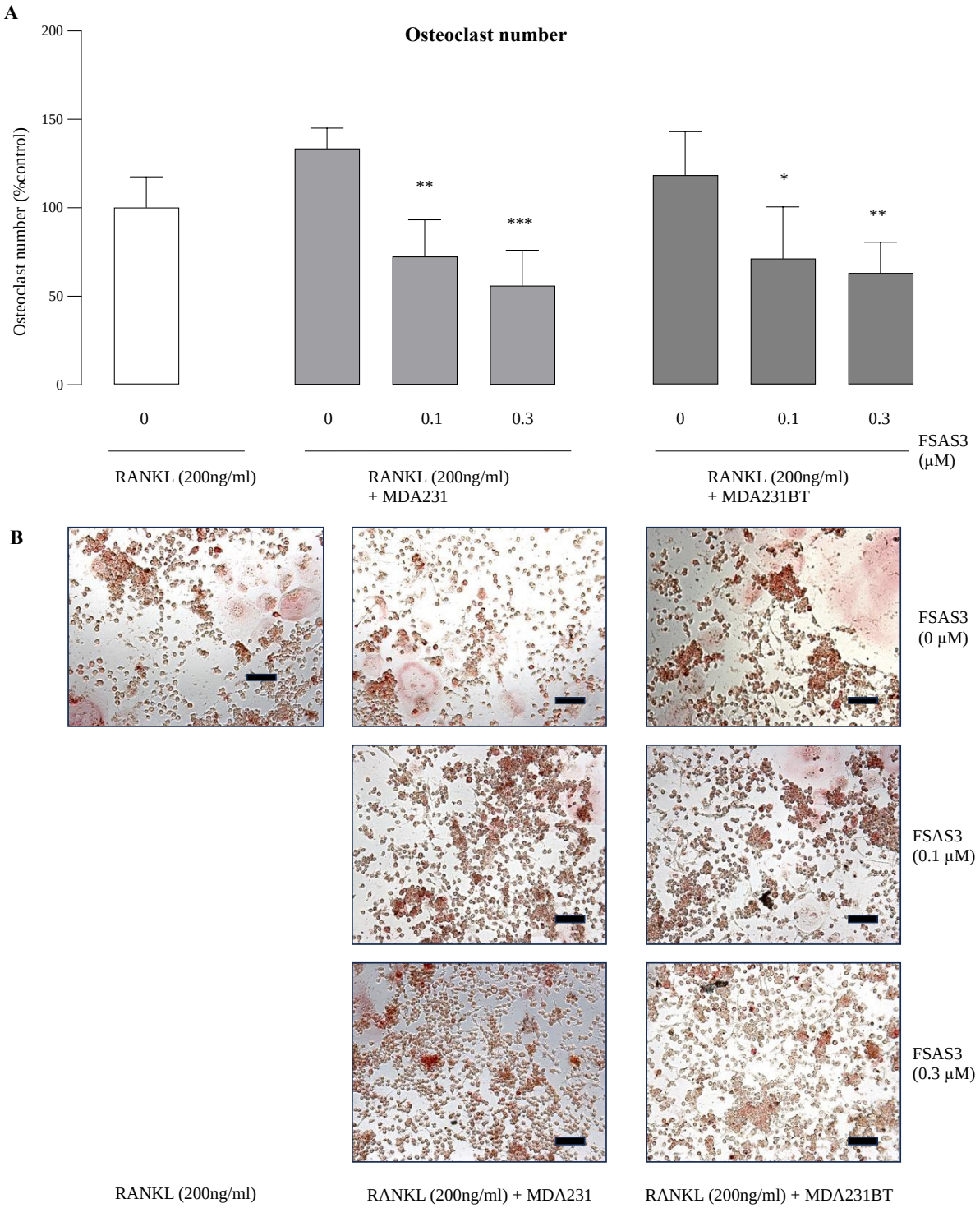

Figure 7.3. FSAS3 reduced osteoclast formation in RAW264.7 cultures co-cultured with MDA-MB-231 and MDA231-BT cells *in vitro*. (A) Percentage of osteoclast formation in RANKL-stimulated RAW264.7 cells in the presence and absence of breast cancer cell MDA-MB-231 (300 cell/well, middle) and MDA231-BT (300 cell/well, right) treated with vehicle or FSAS3 (0.1, 0.3 μM), (B) Representative images of multinucleated TRAcP-positive control cells co-cultured with MDA-MB-231 (middle) and MDA231-BT (right) treated with vehicle or FSAS3. Data obtained from three independent experiments. p values were obtained from two-way ANOVA test. *p<0.05, **p<0.01, ***p<0.001 compared to cells treated with vehicle. Scale bar = 100μM

To test the effect of FSAS3 on osteoclast formation in the presence of cancer cell derived factors, conditioned medium (10% v/v) was collected from parental MDA-MB-231 and osteotropic MDA-231-BT BCa cells added to mouse RAW264.7 osteoclast precursors treated with FSAS3 (0.1- 0.3 μM) in the presence of RANKL (200 ng/ml) for 120 hours. As shown in **Figure 7.4**, the novel TRAF6 inhibitor FSAS3 (0.3 μM) significantly reduced the formation of TRAcP-positive multi-nucleated osteoclasts exposed to conditioned medium from human MDA-MB-231 and its osteotropic clone MDA-MB-BT clone (**Figure 7.4A**). Representative images of TRAcP-positive osteoclasts and their precursors are shown in (**Figure 7.4B).**

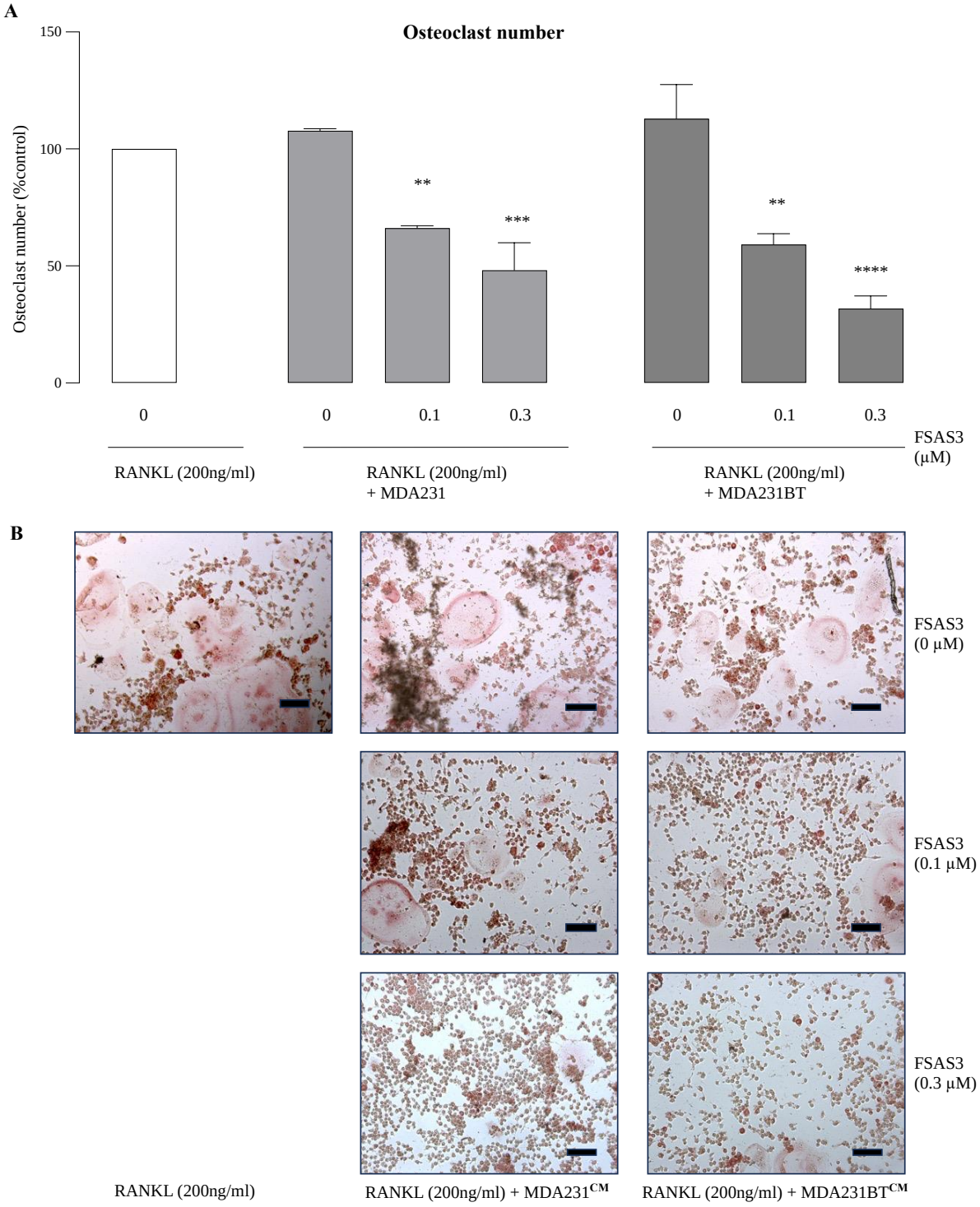

Figure 7.4. FSAS3 reduced osteoclast formation in RAW264.7 cultures exposed to conditioned medium from MDA-MB-231 and MDA231-BT *in vitro*. (A) Percentage of osteoclast formation in RANKL-stimulated RAW264.7 cells in the presence and absence of conditioned medium from breast cancer cell MDA-MB-231 (middle) and MDA231-BT (right) treated with vehicle or FSAS3 (0.1, 0.3 μM), (B) Representative images of multinucleated TRAcP-positive control cells exposed to conditioned medium from MDA-MB-231 (middle) and MDA231-BT (right) treated with vehicle or FSAS3. (C) In vitro cell viability and survival of mouse RAW264.7 macrophage (pre-osteoclast) treated with vehicle or FSAS3 (0-0.3 μM) for 120 hours, as assessed by AlarmaBlue assay. Data obtained from three independent experiments. p values were obtained from two-way ANOVA test. *p<0.05, **p<0.01, ***p<0.001 compared to cells treated with vehicle. Scale bar = 100μM.

7.4.4. Effects of FSAS3 on Breast cancer – osteoclast precursor interaction *in vitro*

Next, I examined the effects of FSAS3 on the viability of osteoclast precursors in the presence and absence of RANKL and BCa cells. The number of osteoclast precursors was assessed in mouse RAW264.7 osteoclast precursors by AlamarBlue assay. As shown in **Figure 7.5**, FSAS3 had no effect on the number of mouse RAW264.7 osteoclast precursors in the presence of RANKL (200ng/ml) or conditioned medium (CM, 10% v/v) from parental MDA-MB-231 and osteotropic MDA-231-BT cultures at concentrations that inhibited osteoclastogenesis.

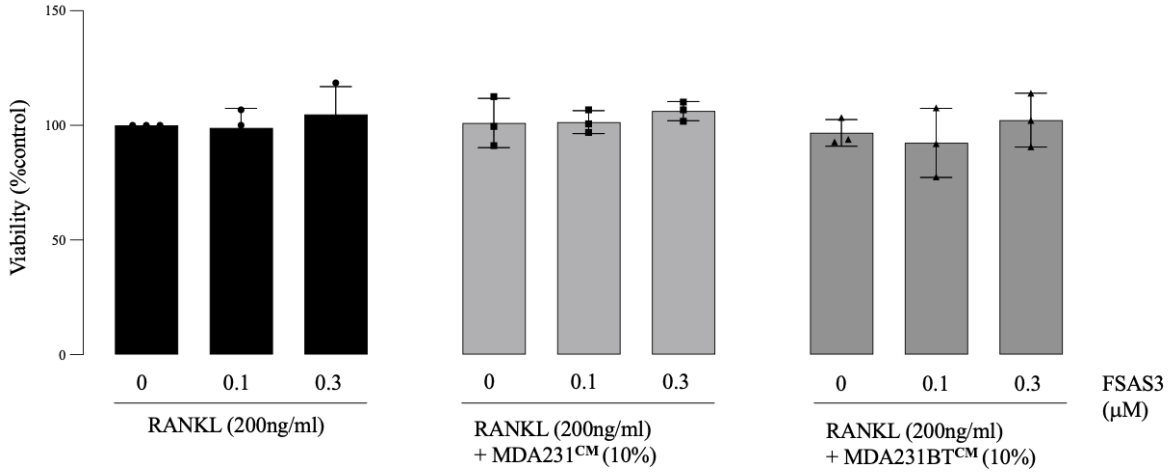

Figure 7.5. FSAS3 has no effect on the cell viability of RANKL and BCa-induced osteoclast formation. In vitro cell viability and survival of mouse RAW264.7 macrophage (pre-osteoclast) treated with vehicle or FSAS3 (0-0.3 μM) in the presence of RANKL (200ng/ml, left panel) or conditioned medium of MDA-MB-231 (10% *v/v*, middle) or MDA-231-BT (10% *v/v*, right) for 120 hours, as assessed by AlarmaBlue assay. Data obtained from three independent experiments. p values were obtained from one-way ANOVA test compared to cells treated with only RANKL (200ng/ml).

7.4.5. Effects of FSAS3 on breast cancer cell – osteoblast interactions *in vitro*

BCa cells in the skeleton are known to influence osteoblast's ability to differentiate, interact with osteoclasts, and produce disorganised woven 'weak' bone. Thus, I decided to use the human osteosarcoma cells, Saos2, as a model for undifferentiated-osteoblast-like precursors to study the effects of the novel TRAF6 inhibitor FSAS3 on all aspects of osteoblastogenesis *in vitro*. To study the ability of osteoblast to mature, grow and make bone nodules, I cultured human Saos2 osteoblast-like cells in the presence of conditioned medium (20% v/v) from human parental MDA-MB-231 and osteotropic MDA-231-BT with or without FSAS3 (0.1-1 μM) for 5, 7 and 10 days and measured osteoblast viability by AlamarBlue assay as described in **section 2.2.5.1**. Additionally, selected samples from these cultures were lysed and assessed for alkaline phosphatase activity (**section 2.2.7.2**) and others were stained for with Alizarin Red, visualized and de-stained to measure mineralisation and bone nodule formation (**section 2.2.5.3)**.

As shown in **Figure 7.6-7.7**, exposure to conditioned medium (20% v/v) from human parental MDA-MB-231 and osteotropic MDA-231-BT TBC cells had no significant effect on osteoblast viability, osteoblast differentiation nor bone nodule formation. More importantly, treatment with FSAS3 for 5 days had no effects on osteoblast viability at 0.1 and 0.3μM but significant inhibition was observed at 1μM. At this time point, FSAS3 has no significant effect on osteoblast differentiation as assessed by ALP activity nor bone nodule formation as assessed by ARS assay, in the presence of conditioned medium (20% v/v) from human osteotropic MDA-231-BT (**Figure 7.6, left panel**). It is important to note that the 5-day time point was chosen on the basis that FSAS3 inhibited BCa cell-induced osteolysis after 5 days of continuous exposure (**Figure 7.8**).

As expected, FSAS3 significantly inhibited both osteoblast differentiation and bone nodule formation at concentrations that reduced osteoblast viability, namely 1 μM at day 7 and 0.3, 0.1 μM at day 10 in the presence of MDA-MB-231-BT conditioned medium (20%, v/v)

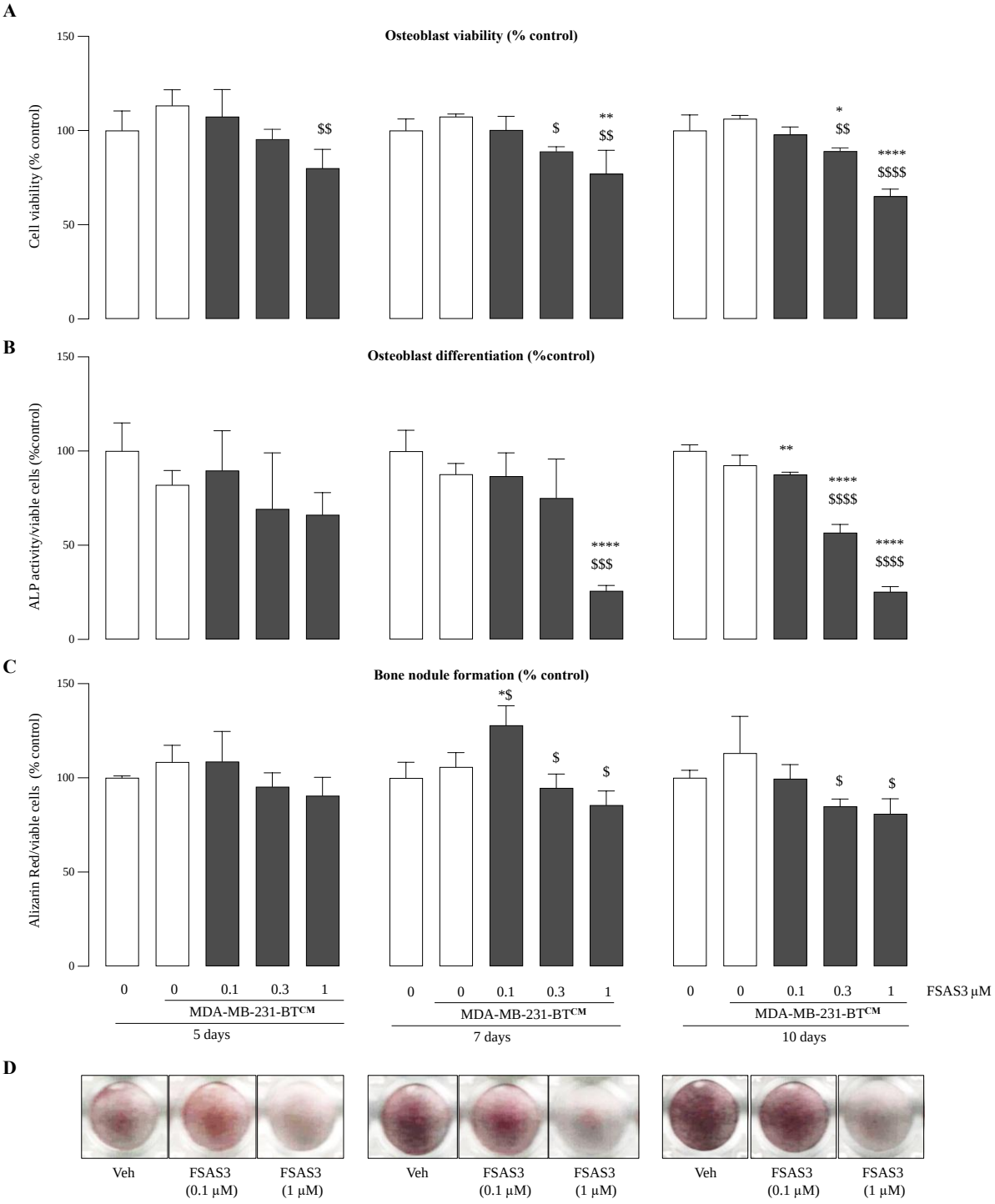

Figure 7.6. FSAS3 reduced osteoblast growth in the presence of osteotropic breast cancer-derived factors. (A) *In vitro* osteoblast viability in human osteoblast-like Saos-2 cultures exposed to standard or conditioned medium from MDA231-MB-231-BT cells (CM, 20% *v/v*) in the presence or absence of FSAS3 (0-1 µM) for 5, 7 and 10 days, as assessed by AlamarBlue assay. (B-C) *In vitro* osteoblast differentiation (b) and bone nodule formation (c) in human osteoblast-like Saos-2 cultures exposed to standard or conditioned medium from MDA-MB-231-BT cells (CM, 20% *v/v*) in the presence or absence of FSAS3 (0.1-1 µM) for 5, 7 and 10 days. Osteoblast viability (a), differentiation (b) and bone nodule formation (c) were assessed by AlamarBlue, Alkaline phosphatase and Alizarin Red assays, respectively. (D) Representative photomicrographs of bone nodule formation from the experiment described in panel c. Values are mean ± SD. **p<0.01 from vehicle without conditioned medium; $$p<0.01 and $$$p<0.001 from vehicle plus MDA231-BT conditioned medium.

Similarly, FSAS3 only reduced osteoblast differentiation and bone nodule formation at concentrations that inhibited cell viability in the presence of MDA-MB-231 conditioned medium (20%, v/v) (**Figure 7.7)**.

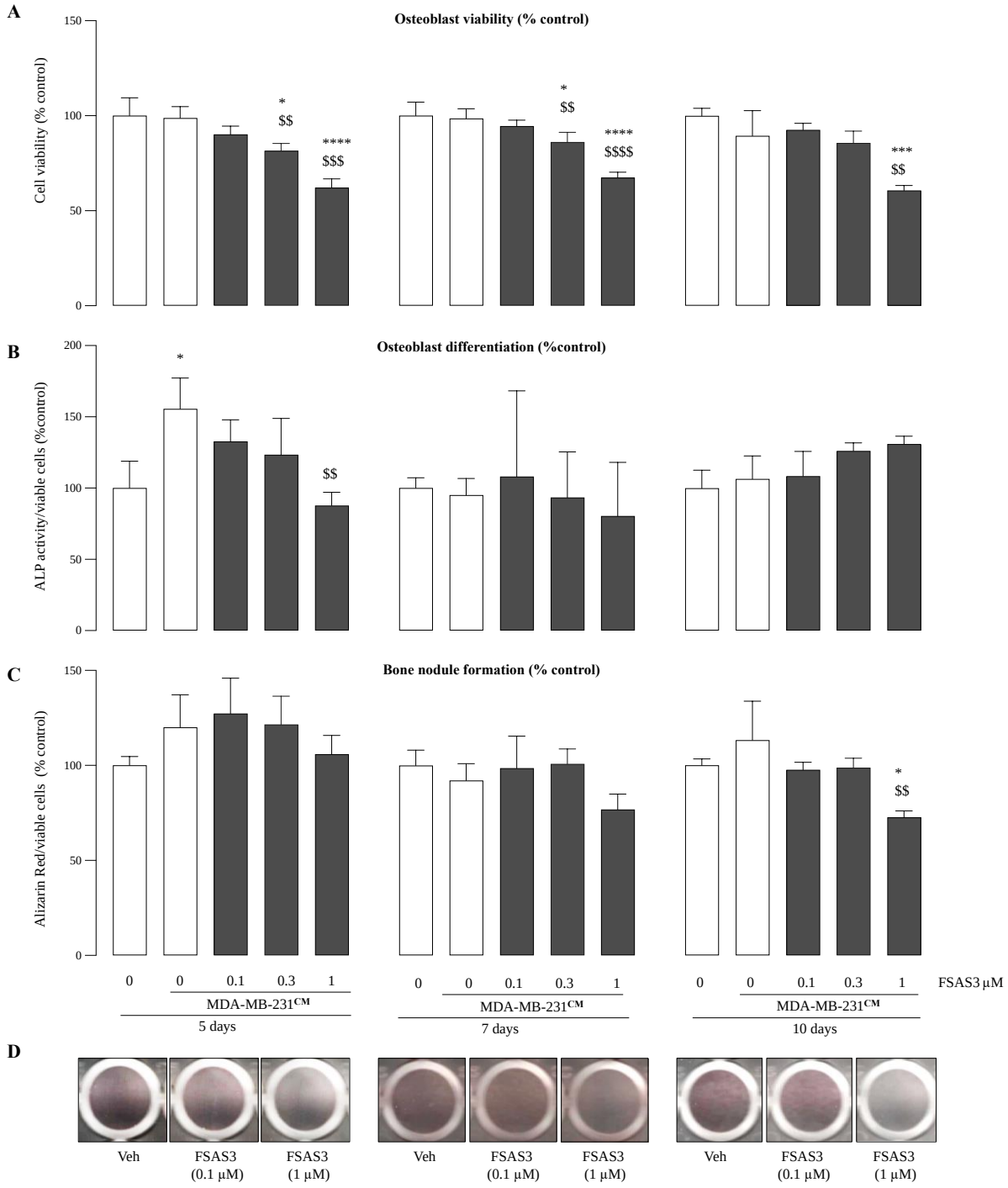

Figure 7.7. FSAS3 reduced osteoblast growth in the presence of breast cancer-derived factors. (A) *In vitro* osteoblast viability in human osteoblast-like Saos-2 cultures exposed to standard or conditioned medium from

MDA-MB-231 cells (CM, 20% *v/v*) in the presence or absence of FSAS3 (0-1 μM) for 5, 7 and 10 days, as assessed by AlamarBlue assay. (B-C) *In vitro* osteoblast differentiation (b) and bone nodule formation (c) in human osteoblast-like Saos-2 cultures exposed to standard or conditioned medium from MDA-MB-231 cells (CM, 20% *v/v*) in the presence or absence of FSAS3 (0.1-1 μM) for 5, 7 and 10 days. Osteoblast viability (a), differentiation (b) and bone nodule formation (c) were assessed by AlamarBlue, Alkaline phosphatase and Alizarin Red assays, respectively. (D) Representative photomicrographs of bone nodule formation from the experiment described in panel c. Values are mean ± SD. ****p<0.0001 from vehicle without conditioned medium; $$$$p<0.0001 from vehicle plus MDA231-MB-231 conditioned medium.

7.4.6. Effects of FSAS3 on breast cancer-induced osteolysis *ex vivo*

Finally, I took advantage of the cancer cell-mouse calvarial organ co-culture system to assess whether FSAS3 preserves bone volume (BV) in the presence of the osteotropic MDA231-BT TNBC cells. Briefly, mouse calvaria was isolated from 2 day-old mice as described in **section 2.4,** and each half was co-cultured with human osteotropic MDA-231-BT cells pre-treated with vehicle or FSAS3 for 1 hour. mouse calvaria - osteotropic MDA231-BT TNBC cells were co-cultured for 5 days and bone volume as tissue volume (BV/TV) was assessed by micro-computed tomography (μCT). As shown in **Figure 7.8,** FSAS3 (1.0 μM) significantly enhanced bone volume (BV/TV, %) after 5 days of continuous treatment, thereby indicating an anti-osteolytic effect (**Figure 7.8**).

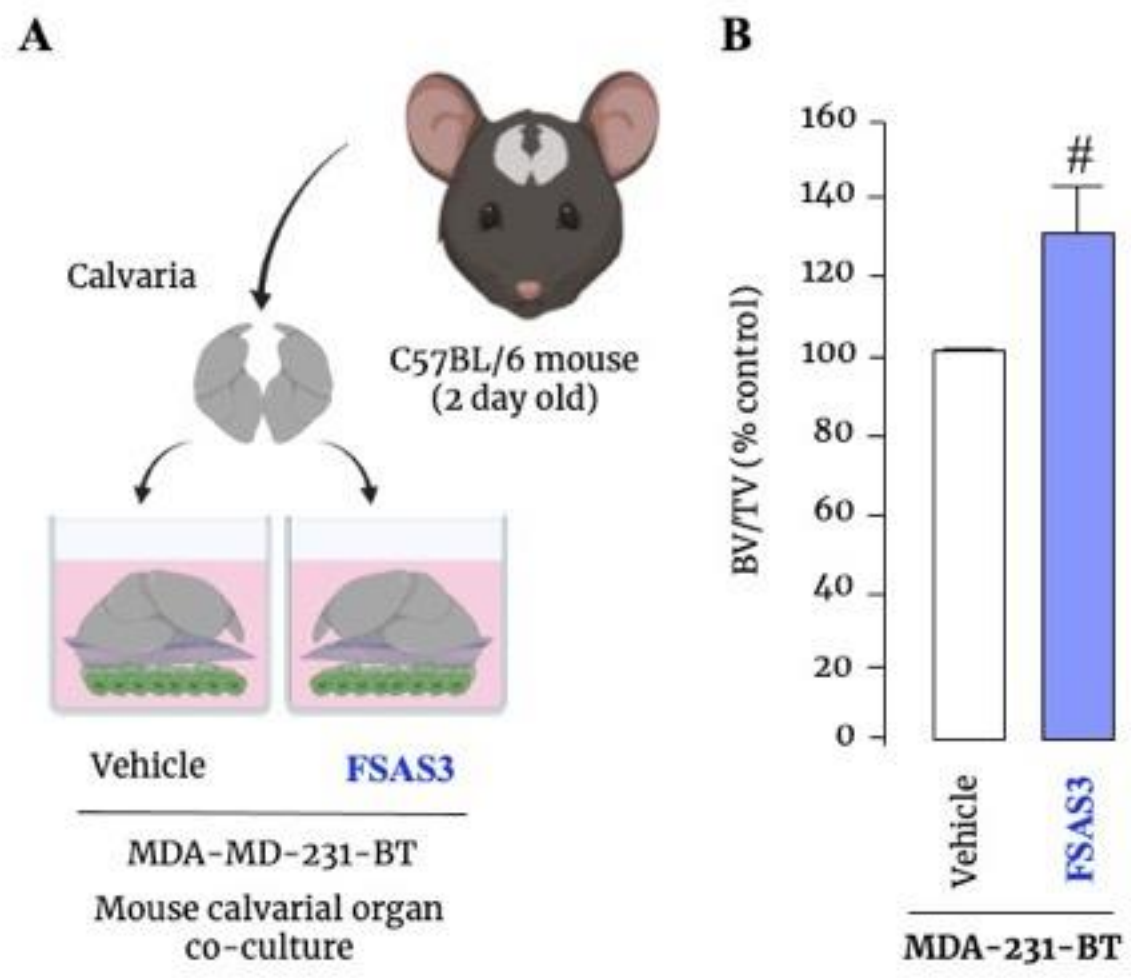

Figure 7.8. FSAS3 reduced human MDA231-BT-induced osteolysis. (A) Graphic representation of *ex vivo* mouse calvarial organ system co-cultured with osteotropic human MDA231-MB-231 (MDA231-BT) cells (300 cells/well) in the presence and absence of vehicle or FSAS3 (1.0 μM) for 7 days. Created with BioRender.com under a paid subscription. (B) *ex vivo* bone volume (BV/TV, %) and osteolysis in the mouse calvarial organ co-culture system described in panel A.

7.5. Discussion

Metastatic BCa patients develop osteolytic bone disease characterized by skeletal tumour burden and excessive osteoclastic bone destruction [37, 48, 49, 295]. The TRAF6/NFκB signalling is implicated in BCa cell growth, migration and invasion as demonstrated in **Chapters 5 to 6**, and plays an important role in osteoclast formation, survival and activity as I showed in **Chapter 4** and report by numerous other investigators [182, 184, 276]. In **chapter 6**, I showed that the novel FSAS3 disrupted the action of the pro-osteolytic and pro-osteoclast factor TANKL at multiple level of NFκB signalling pathways, namely TRAF6, TAK-1 and TAB-1, IκB phosphorylation and NFκB nuclear translocation, thereby indicating strong inhibition of the RANKL/RANK/NFκB axis. In addition, unpublished data of our group indicated that FSAS3 treatment also influence the lineage commitment of monocyte-macrophage lineage by enhancing the polarisation of THP-1 cells into anti-tumorigenic M1 phenotype than pro-tumorigenic M2. (Giovana Carrasco, White Rose ethesis, University of Sheffield, UK: https://etheses.whiterose.ac.uk/27832/)[266]. Carrasco and colleagues also went on to show that FSAS3 inhibits the ability of mouse and human osteotropic prostate cancer cells to influence osteoblasts and osteoclastic activity *in vitro* Altogether, this suggests that the novel FSAS3 has the potential of could be of value in the treatment of cancer-associated bone disease.

With this in mind, I decided to examine the effects of FSAS3 on BCa cell induced osteoclast and osteoblast activity *in vitro* and validate it osteolytic properties *ex vivo*. First, I successfully utilized RANKL to induce the osteoclast differentiation of mouse RAW264.7 cells in the presence and absence of parental and osteotropic TNBC cells [156]. Using this model, I first showed that FSAS3 inhibit osteoclast formation in the presence of RANKL at concentrations that do not exert cytotoxic effects on pre-osteoclasts. Not surprisingly, FSAS3 inhibited RANKL (TRAF6)- induced phosphorylation of IκB in pre-osteoclasts, which is consistent with previous result that showed that TRAF6 inhibitors inhibited osteoclast formation via inhibition of canonical NFκB signalling in macrophage-like RAW264.7 cells in the work by our colleague [184] and others including of Zarzycka and colleagues [155]. This finding is in agreement of the results that prevention of TRAF6-TAK1 complex prone to inhibit osteoclast differentiation [156].

Encouraged by these results, I went on to show that FSAS3 disrupts BCa cell – osteoclast crosstalk. First, I observed that osteotropic BCa cells and their derived factors failed to enhance RANKL-induced osteoclast formation in cultures of mouse RAW264.7 cells, as previously observed by members of my group [184, 302]. One reason for this is that mouse RAW264.7 cells are monocytic cell line that constitutively express high level RANK and thus readily differentiate into mature osteoclasts without the need for other osteolytic mediators such as macrophage colony-stimulating factor (M-SCF) and BCa derived factors - unlike human peripheral blood mononuclear cells (PBMC) and mouse bone macrophage routinely used by our group in previous studies.

Human osteoblasts play an important role in BCa induced bone disease [303]. Thus, I examined the effect of FSAS3 on their viability, differentiation and bone nodule formation in the presence and absence of parental and osteotropic TNBC cells. The osteoblast-like cells Saos-2 was selected because they are human cells, not fully differentiated osteoblasts, express high levels of TRAF6 (**Supplementary Figure 22**), and were previously used by my colleagues to study osteoblast interactions with prostate [304] and BCa [305] cells *in vitro*. My results showed that FSAS3 inhibited osteoblast maturation and activity only at concentrations that reduced the cell viability and it had no effect at concentrations that inhibited osteoclastognesis within the 5 day period. Interestingly, Saos2 cells exhibit a low transcript level of RANK and CD40 than MDA-MB-231 cells (**Supplementary Figure 22**), thus future studies should consider using mouse primary osteoblasts and cell lines such as MG-63, MC3T3-E1 [306].

Finally, I took advantage of the BCa cell-mouse calvarial organ co-culture system, an *ex vivo* model used by our group to examine the complex interaction between cancer cells and the bone microenvironment [307], to validate the ability of FSAS3 to preserve bone volume in the presence of the osteotropic breast MDA231-BT cells. The result confirms that FSAS3 exerts an osteoprotective effect in the *ex vivo* model described. Thus, the novel TRAF6 inhibitor FSAS3 exhibits a promising anti-migratory, anti-inflammatory and anti-osteolytic effects in the *in vitro* and *ex vivo* models of BCa and bone models described.

CHAPTER 8. General Discussion

8.1. General Discussion

The TRAF6/NFκB signalling pathway is known to play a significant role in the development of advanced BCa [36, 292] and inflammation-induced osteoclast bone loss [157, 185, 190, 308, 309]. Numerous preclinical and clinical studies have demonstrated the significant contribution of both constitutive and TRAF2/6-driven canonical NFκB activation in BCa progression [120, 162, 173, 241, 242, 245, 246, 249, 250, 295, 309, 310]. TRAF2 overexpression has been observed in breast tumours, suggesting a role in BCa cell proliferation and survival [120, 162, 182, 239]. Furthermore, TRAF2 has been implicated in the signalling from two receptor of TNFα – TNFR1 and TNFR2, where they activate pathways leading to activation of the NFκB and MAPKs in BCa and healthy cells in the tumour microenvironment [253]. Similarly, TRAF6 has been found to be involved in the oncogenic activity [108, 171, 275, 308] of various types of cancers including BCa [275], it is known to regulate cell survival, proliferation and immune response. In the context of BCa, TRAF6 overexpression has been associated with increased metastatic potential and poorer prognosis [168, 177-179] In addition, TRAF6 has unique binding interaction with receptors CD40 and RANK, two key regulators of bone and immune cell activity and differentiation [288]. Furthermore, TRAF6 is unique among TRAFs because it not only acts as an adapter protein that has key roles in signal transduction, particularly in pathways involved in immune and inflammatory response, but also has E3ubiquitnatin ligase activity [150-152, 171]. Work from our laboratory has found that TRAF2- NFκB activation drives osteolytic behaviour of BCa cells, and pharmacological and cancer-specific inhibition of TRAF2/6 reduces the progression of BCa metastasis to the skeleton [184, 185, 239, 273, 275]. Among the other members of TRAF family, TRAF4 has been found to play a significant role in BCa progression. Overexpression of TRAF4 has been detected in various breast tumours, indicating its involvement in tumour cell migration [162, 165, 166, 260], invasion[165, 166, 260], angiogenesis [235] as well as resistance against apoptosis [311, 312]. Whilst it is clear TRAF activate NFκB signalling and the expression of TRAF2, 4 6 is commonly altered in advanced cancer, particularly TNBC [161, 166-168, 177-179, 231, 255], the TRAF family constitutes of 7 adaptor proteins that exhibit distinct and overlapping functions and thus directly and indirectly influence BCa-induced NFκB activation [108, 227, 238, 240].

In **Chapters 3 and 4**, I present evidence from systematic review, meta-analysis, bioinformatic, *in vitro* and *ex vivo* studies showing that pharmacological inhibition and genetic knockdown of TRAF6 disrupts the ability of BCa cells to grow, migrate, invade and influence the differentiation of macrophages, osteoclast as well as osteoblasts. Selecting which TRAF to study and ultimately target for the treatment of a complex disease such as advanced, metastatic BCa is a difficult challenge. Thus, in **Chapters 3,** I carried out a systematic review and meta-analysis to examine the hypothesis that modulation of the expression and activity of TRAF1 to 7 is associated with BCa progression and metastasis. The meta-analysis yielded 5 key outcomes: **(1)** TRAF2/4/6 inhibition is associated with reduced BCa cell motility *in vitro* and tumour weight/volume *in vivo*; **(2)** TRAF2/4 inhibition is associated with reduced BCa cell adherence *in vitro*; **(3)** TRAF6 inhibition is associated with reduced BCa cell proliferation *in vitro*; **(4)** TRAF4/6 inhibition is associated with reduced BCa cell metastasis *in vivo*; **(5)** TRAF6 expression is associated with BCa survival rate. Based on these findings, I conclude that TRAF6 expression/modulation is associated with BCa cell behaviour *in vitro*, tumour burden and metastasis in mice, and survival rate in BCa patients.

In **Chapters 4,** firstly, functional predictions from GO and KEGG enrichment analysis as well as PPI confirmed the involvement of all members of the TRAF family, except TRAF7, in cancer. This finding is consistent with the fact that TRAF7 is not considered a classical member of TRAF family due to the lack of the highly conserved TRAF domain needed for interactions with the TNFR superfamily members [160]. Next, Bioinformatic analysis using publica databases confirmed that all seven TRAFs were genetically altered, either presenting deletions or amplifications, except TRAF1. Association between TRAF6 amplification and poor survival in BCa patients I found in meta-analysis was confirmed again in a larger cohort of patients. Given the complex role of TRAF6 in facilitating various processes and mechanisms that contribute to the progression of BCa, its interactions and associations with other members of the TRAF family were studied. This analysis revealed significant interactions between TRAF6 and other TRAFs, with the exception of TRAF4 and TRAF7, demonstrating its robust function in influencing other TRAFs and, inconsequence, several biological processes. This is consistent with the evidence from numerous studies [108, 227, 238, 240].

Next, I assessed changes in TRAF protein expression during the early and metastatic phases of BCa. Notably, amplification of all TRAFs was observed in both primary and metastatic BCa cases, with a marked increase in the amplification of TRAF1, TRAF3, TRAF4, and TRAF6 noted among patients with metastatic BCa. This corroborates the findings from research conducted by Sun, Zhao, Bertucci and their teams [161, 265, 313]. Further Bioinformatic analysis using publica databases confirmed that all seven TRAFs were genetically altered, either presenting deletions or amplifications, except TRAF1. This analysis also confirms the association between TRAF6 amplification and poor survival in BCa patients but in a larger cohort of patients than that included in the aforementioned meta-analysis. Notably, TRAF2 and TRAF6 are found to be associated with osteoclast formation, a hallmark of osteolysis. Given that TRAF6 is highly expressed in bone metastases than primary site in combined datasets of BCa patients, it is reasonable to conclude that TRAF2 and 6 inhibition may be of value in the treatment of metastatic BCa in bone.

To explore the role of TRAF2/6 (as well as TRAF4) in primary and metastatic BCa, Western Blot analysis was used to further examine the expression levels of these TRAFs in a panel of human and mouse BCa cell lines with different metastatic abilities. BCa cells expressed higher level of TRAF6 than TRAF2 and 4, and TRAF6 was highest in the metastatic MDA-231-BT human BCa cells that are known to readily metastasise to bone in nude mice. This confirmed the role of TRAF6 in advanced, metastatic, osteotropic BCa, and thus parental and osteotropic BCa cells were selected as models for further mechanistic investigations.

In **Chapter 5**, I firstly stably knocked down TRAF6 in the human parental MDA-MB-231 and their osteotropic MDA-231-BT clone. The successful knockdown of TRAF6 with three different constructs in both cells lines was confirmed by Western Blot in two colonies, with clones that exhibited the lowest TRAF6 expression selected for following experiments. Previous *in vitro* studies showed that knockdown of TRAF2 and TRAF4 reduced the metastatic abilities such as migration and invasion of BCa cells [239] [166, 314], overexpression of TRAF2 has also been shown to increase the invasion of BCa cell *in vitro* [239] [120], and TRAF6 knockdown reduced the tumorigenic potential of BCa cells *in vivo*. In this study, the metastatic behaviour of TRAF6 deficient parental MDA-MB-231 and osteotropic MDA-231-BT

BCa clones was investigated by assessing cell viability and their ability to invade and migrate. As hypothesised, knockdown of TRAF6 significantly reduced the metastatic behaviour of both parental and osteotropic clones but the effect was more prominent in osteotropic MDA-231-BT cells which I have shown that they express higher levels of TRAF6. Furthermore, knockdown of TRAF6 in these cells also significantly reduced their metastatic behaviour, namely cell migration and invasion.

Previous studies by our group and many others have shown inhibition of TRAFs and IKKs reduced breast tumour progression in various models [239]. A recent work by my colleague R. Bishop and others have reported that the selective CD40-TRAF6 inhibitor, 6877002, reduced BCa metastasis and enhanced the anti-tumour and anti-metastatic effects of Docetaxel in mice bearing syngeneic 4T1 BCa cells. However, treatment with 6877002 alone failed to increase bone volume and only did when combined with Docetaxel [184]. This lack of osteoprotective effect was also observed in another publication in which I'm a co-author. My colleagues and I have demonstrated that 6877002 reduced the severity of inflammatory arthritis, but not bone loss, in mice bearing collagen-induced arthritis [185]. Collectively, these results show that inhibition of the CD40 pocket of TRAF6 is associated with anti-inflammatory, anti-metastatic, but not osteoprotective effect.

This finding led us to hypothesise that the novel members of the FSAS family, FSAS1 – FSAS5, that have indicated to bind to multiple pockets on TRAF6 may be of better value for the treatment of BCa osteolytic metastasis than the verified CD40-TRAF6 small-molecule inhibitor 6877002. Among the six small molecules, 6877002 and FSAS3 inhibited the viability of a panel human and mouse BCa cell lines of different hormone status and metastatic capabilities The list includes the human hormone-dependent MCF7, TNBC parental MDA-MB-231 and osteotropic MDA-231-BT and mouse hormone-dependent E0771, triple-negative 4T1 and osteotropic 4T-BT cells. It is worth noting that FSAS3 is the most potent among all the six as assessed by IC50 values. More impotently, FSAS3 is significantly more potent in inhibiting the growth of osteotropic MDA-231-BT BCa cells than their parental clones, which can be explained, at least in part, by the results that osteotropic MDA-231-BT cells express higher levels of TRAF6 than their parental clones. In addition, FSAS3 was also found to be less potent in TRAF6 deficient clones compared to control, again suggesting a TRAF6-dependent manner. The novel FSAS3

is also effective in inhibiting the abilities of parental and osteotropic TNBC cells to migrate and invade at concentrations that had no effect on cell growth, thereby excluding cytotoxic effects.

The treatment of TNBCs often relies on surgery, radiotherapy and/or chemotherapy. NFκB activity has identified as a potential mechanism contributing to resistance against cornerstone chemotherapy treatments in BCa, particularly in TNBC [290]. Previous studies from our group, CD40-TRAF6 inhibitor 6877002 enhanced the anti-metastatic effect of docetaxel[184]. Here, I assessed the effect of FSAS3 in combination with a panel of FDA-approved chemotherapeutic agents, namely docetaxel, paclitaxel, doxorubicin, rapamycin, tamoxifen and 5-fluorouracil and cyclophosphamide. These experiments confirmed that , FSAS3 enhanced the *in vitro* cytotoxic effects of docetaxel, tamoxifen, rapamycin and cyclophosphamide in 4T1 cells, and that of all compounds tested in MDA-MB-231 cells apart from rapamycin and cyclophosphamide. Further combination analysis using Chou-Talalay Method revealed that, in the cultures of murine 4T1 cells, Docetaxel, Paclitaxel, acted synergistically with FSAS3 (10 μM) at all doses tested, and Rapamycin at most doses tested. Interestingly, the combination of Cyclophosphamide, 5-Fluorouracil and FSAS3 (10 μM) was found to be antagonistic since more than half concentrations tested had an CI value greater than 1. Based on previous studies by our group [184] and Xu et al who reported that TRAF6 promotes chemoresistance to paclitaxel in TNBC [315], I the results of this study suggest that future studies should examine the effects of TRAF6 inhibitor FSAS3 in combination with chemotherapy in animal models of BCa osteolytic metastasis.

The TRAF family members demonstrate unique and overlapping roles in cancer via varied mechanisms [108, 227-230, 238, 240]. Among the seven TRAFs, TRAF6 is the most extensively researched. Often associated with E3 ubiquitin ligase activity, TRAF6 is implicated in various processes relevant to hormone-dependent and triple-negative BCa [108, 160, 227, 231, 237]. While TRAF2 also plays a part, TRAF6 predominantly serves as a nexus for multiple BCa-driver signalling pathways, including but not limited to NFκB, PI3K/AKT/mTOR, Toll-like receptor (TLR), mitogen-activated protein kinase (MAPK), Ras/Src Family Kinases, as well as components of the activator protein 1 (AP-1) family [108, 227, 231, 237, 238]. Based on aforementioned studies, in **Chapter 6**, I conducted a head-to-head comparison to study the effects of FSAS3 and 6877002 on canonical TRAF2/6-mediated NFκB

activation using a number of mechanistic techniques, namely Western Blot, Immunoprecipitation, Molecular Docking and DARTS. Firstly, I confirmed the role of TRAF5 on RANKL-induced canonical NFκB activation in BCa cells by demonstrating that RANKL failed to activate the phosphorylation of IκB in TRAF6-deficient parental MDA-MB-231 and osteotropic MDA-231-BT cells. Next, FSAS3 is found to prevent or inhibit the TRAF6- (RANKL-) induced canonical NFκB activation in both human MDA-MB-231 and mouse 4T1 cell culture. In contrast, 6877002 is found to be significantly less effective in mouse 4T1 cells, and completely inactive in human MDA-MB-231 cultures.

However, FSAS3 also inhibited the TRAF2- (TNFα-) induced (but to a less effect than that of TRAF6- (RANKL-) induced canonical NFκB signalling pathway in both human MDA-MB-231 and mouse 4T1 cell culture, suggesting multi-TRAF and/or off-target effects. In contrast, the selective CD40-TRAF6 inhibitor 6877002 was significantly less effective in cultures of mouse 4T1 culture, and completely ineffective in those of human MDA-MB-231 cells, confirming that FSAS3 targets multiple TRAFs. Interestingly, TRAF6 knockdown modestly blunted TNFα induced NFκB activation in both parental MDA-MB-231 and osteotropic MDA-231-BT, confirming the overlapping functions between TRAF2 and other TRAFs, particularly TRAF6. Previous studies showed that TRAF2 and TRAF6 play overlapping roles in CD40-mediated JNK and NFκB activation, [293], suggesting that the novel FSAS3 target to both TRAF2 and TRAF6 will be value of the inhibition of oncogenic inflammatory cellular process. In further support to my hypothesis that FSAS3 exhibits multi-TRAFs action, I showed that FSAS3 inhibited the proteolysis of both TRAF2 and TRAF6 as assessed by DARTS, thereby confirming that both TRAF6 and TRAF2 serve as a potential target. This is consistent of results from predicted pose *in silico* docking analysis that suggested that FSAS3 binds to multiple pockets at the c-terminus of both TRAF6 and TRAF2, namely CD40 and a novel pocket.

Encouraged by these findings, I used a combination of Immunoprecipitation and Western Blot analysis to confirm the effect of FSAS3 on key component of NFκB signalling pathway downstream of TRAF2 and 6. Briefly, I confirmed that FSAS3 inhibits TRAF6-TAK1 and TRAF6-TAB1 binding, two proteins that play an essential role in RANKL-induced osteoclast formation [156, 191]. This gives support to the hypothesis that FSAS3 exhibits anti-osteoclasts and anti-osteolysis effects. As expected, FSAS3 also

inhibited IκB phosphorylation in the cytoplasm and p65NFκB-DNA nuclear translocation as evident of significant inhibition of DNA binding. To gain a better understanding of the mechanisms by which the novel FSAS3 influences the TRAF6/ NFκB axis in metastatic BCa, further mechanistic experiments are needed to examine its effects on ubiquitination, especially Ub-K63 which is known to be activated by TRAF6, as well as other related signalling pathways downstream of TRAF2/6 such as JNKs and p38 MAPKs. Nevertheless, the findings of **Chapter 6** demonstrate that FSAS3, as a multi-TRAF inhibitor, acts at the level of TRAF6 (and to lesser extend TRAF2) to exert an anti-NFκB effect in highly metastatic, and osteotropic human TNBC cells.

Patients with metastatic BCa often exhibit osteolytic metastasis marked by skeletal tumour burden and excessive bone degradation by osteoclasts [37, 48, 49, 295]. As shown in **Chapter 3 to 6** and a number of previous studies[182, 184, 276], the TRAF6/NFκB signalling pathway exerts a significant influence on the metastatic behaviour of TNBC, and the novel FSAS3 exerts significant anti-TRAF2/6, anti-NFκB, anti-growth, anti-migratory and anti-invasive effects in both parental and osteotropic TNBC cells. Thus, further *in vitro*, *ex vivo* and *in vivo* studies were needed to validate FSAS3 anti-osteolytic effects, alone and in combination with chemotherapy. In **Chapter 7**. I tested used standard *in vitro* and *ex vivo* models of bone - BCa cell crosstalk and interactions to study the anti-osteoclast and anti-resorptive effects of FSAS3. These experiments showed that FSAS3 inhibits the RANKL-induced NFκB activation in osteoclast precursors, and significantly reduces RANKL-induced osteoclast formation in the presence and absence of parental and osteotropic BCa cells and their derived factors. These findings are in agreement with previous studies that showed that inhibition of the TRAF6/TAK-1-TAB-1/NFκB axis inhibit osteoclast formation [155, 156, 184]. To further validate the anti-osteoclastic effects of FSAS3, future studies should examine its effect of bone resorption *in vitro* using osteoclasts cultured on dentin slices or artificial bone matrixes such as Corning® Osteo Assay Surface multiple well plates (Corning, USA), and resorbed area quantified by ImageJ. Future studies should also consider measuring (1) synthesis and secretion of adhesion molecules and matrix degrading enzyme such as MMP9, (3) c-src expression, (3) TRAF6 ubiquitination, (4) MAPK makers such as p38 and ERK in osteoclast cultures. Interestingly, BCa cells only modestly increased RANKL induced osteoclast number. Thus, contents of

the conditioned medium from both parental and osteotropic BCa cell lines and other cells need to be identified using ELISA or microarray. Surface markers such as RANK, CXCR4[221, 244, 316], and integrins [317] can also be assessed using flowcytometry in the future.

Beyond the harm inflicted by excessive osteoclastic activity in patients of BCa bone metastases, studies have shown that osteoblastic bone metastases have areas of both osteoblastic and osteolytic lesions patient [37, 318], suggesting a need to examine the effects of anti-cancer agents not only on osteoblast-induced RANKL production and osteoclast formation, but also their maturation and differentiation in the tumour microenvironment . Osteoclast-like cell line Saos-2 was chosen as a model of early osteoblast precursors due to their high level of TRAF6 (**Supplementary Figure 22**) and reports from previous studies in osteoblast interactions with prostate [304] and breast cancers [305]. FSAS3 appears to reduce osteoblast differentiation and maturation only at concentrations that impair cell viability. However, Saos2 cell exhibit low level of RANK and CD40 than MDA-MB-231 cells in the same dataset (**Supplementary Figure 22**), suggesting that Saos2 may not be as sensitive to RANKL-related TRAF6/NFκB activation. Thus, future studies should test the effects of FSAS3 on other osteoblast cell line such as MG-63, MC3T3-E1 and primary osteoblast cells [306].

Finally, I examined the anti-osteolytic properties of FSAS3 by taking advantage of the cancer cell-mouse calvarial organ co-culture system. This is an established *ex vivo* model in our group that used to examine the complex interaction between cancer cells and the bone microenvironment [307]. As hypothesised, FSAS3 treatment enhanced calvarial bone volume, suggesting a osteoprotective effect. It is important to note that FSAS3 exerted a potent anti-osteolytic effect at a concentration of 1.0μM when compared to that of 6877002 at 10μM, as reported as previously reported by my colleagues [184]. To gain additional insights into the anti-TRAF6 action of FSAS3 in BCa cell-osteoblast–osteoclast interactions (**Figure 8.1**), future studies should identify the BCa-derived factors present in the conditioned medium used in the aforementioned *in vitro* and *ex vivo* using commercially-available cytokine micro-array assays.

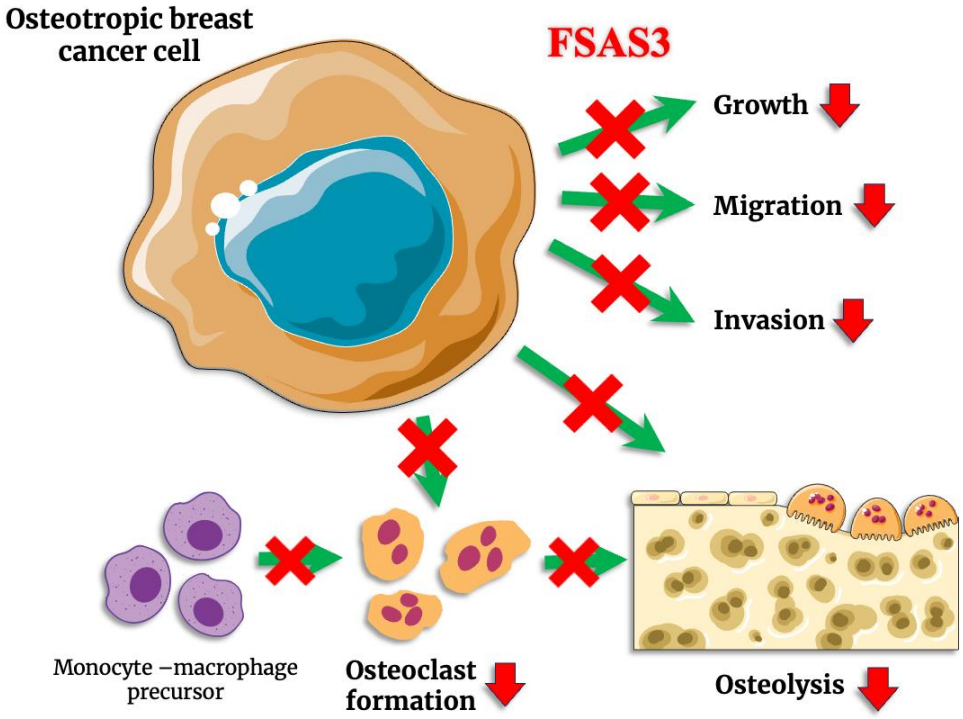

Figure 8.1 Disruption of BCa cell – osteoclast interactions by the novel FSAS3. The novel FSAS3 exhibits anti-tumour, anti-migratory, anti-invasive and anti-osteoclast *in vitro*, anti-osteolytic effect *ex vivo*. Refer to 'Abstract' for more detail and to 'Introduction' for abbreviations.

Collectively, the results of my present investigation (**Chapters 5 – 7)** confirms that the novel TRAF6 inhibitor FSAS3 exhibits a promising anti-cancer, anti-migratory, anti-invasive, anti-inflammatory and anti-osteolytic effects (**Figure 8.1)**. Thus, future studies that examine its *in vivo* anti-metastatic and anti-osteolytic properties in syngeneic mouse models of secondary BCa in bone are needed.

8.2. On-going and Future studies

8.2.1. Effect of FSAS3 on additional TRAF6 related signalling pathways

TRAF6 act as a E3 ligase a process that plays a key part in not only NFκB activation, but also in MAPK and PI3K/AKT/mTOR signalling [319]. In light of the present results that shows that FSAS3 inhibited the formation of the TRAF6/TAK1/TAB1 complex, the question that remains is whether FSAS3 also impacts TRAF6-associated MAPK and PI3K/AKT/mTOR signalling too. The ERK1/2, JNK and p38 MAPK pathways together with AKT are implicated in BCa and regulate osteoclast formation [154, 156-158], and thus it of great interest to assess if are affected in response to FSAS3 on these axes.

The effects of FSAS3 on TRAF6 related ubiquitination can also be investigated by using similar molecular technology techniques used to study the aforementioned pathways, namely Western blot and immunoprecipitation. It's worth noting that this experiment can vary depending on the ubiquitin involved. TRAF6 related K63-linked ubiquitination mostly led to activation of proteins and signal transduction mechanisms such as the activation of TAK-1, which I have shown to be inhibited by FSAS3 (**Chapter 6**). In other cases, it may lead to the degradation of target proteins. For example, TRAF6 mediated K48 polyubiquitylation of DOK3 [151] and proteasomal degradation of TAGLIN in prostate cancer[150]. Furthermore, TRAF6 itself can be degraded via K48-liked polyubiquitination [320].

8.2.2. Effects of FSAS3 on bone metastasis and osteolysis in immune-competent mice

In this study, I demonstrated that pharmacological inhibition and knockdown of TRAF6 using FSAS3 reduces the ability of osteotropic tumour cell to grow, migrate, invade, enhance osteoclastogenesis *in vitro and* cause osteolysis *ex vivo*. Thus, further investigation is needed to establish the anti-metastatic and anti-osteolytic effects of FSAS3 in wild type and TRAF6-knockout (KO) mice bearing mock and TRAF6 knockdown syngeneic BCa cells. However, TRAF6-KO mice die between embryonic day 14 and birth due to disruption of normal bone formation (osteoclast defects) and immune defect [152, 153]. Syngeneic mouse model bearing bone metastasis would suffice. First, maximum tolerated dose (MTD)

determined via assessing weight loss and clinical score in a pilot experiment should be carried out first [321]. Then, the effects of this dose will be tested on BALB/c mice inoculated intracardially with an osteotropic clone of the syngeneic TNBC BCa cells 4T1-BT expressing luciferase. Skeletal tumour burden and bone metastasis will be measured by IVIS (*In vivo* imaging system), and osteolytic bone damage will be assessed by μCT and histochemistry *ex vivo*. The effects of FSAS3 on inflammatory biomarkers in serum will be measured by Flow Cytometry.

8.2.3. Effect of combined administration of chemotherapies and FSAS3 on growth of solid tumours in humanized mice

TRAF6 is a potential druggable target for the treatment of metastatic TNBC in the 9.3% of metastatic BCa patient harbouring somatic copy number amplification of TRAF6. These patients have a significantly shorter overall survival, and these data suggests that targeting TRAF6 may provide a life prolonging benefit. My results have demonstrated that FSAS3 enhanced the efficacy of a panel of chemotherapeutic agents in both human TNBC cell lines by acting synergistically with several drugs, including Docetaxel, Paclitaxel, and Rapamycin. Thus, I propose to assess the anti-metastatic effect of FSAS3 in combination with Docetaxel in nude mice injected orthotopically with luciferase expressing human MDA-MB-231 cells into the mammary fat pads. D-luciferin will be used to monitor primary tumour development. Tumours will be surgically excised, and the development of secondary metastases in bone and other organs such as the lungs will be monitored and assessed as described in **section 8.2.2**.

8.2.4. Effects of combined administration of chemotherapies and FSAS3 on tumour burden and osteolysis in mice bearing Multiple Myeloma

Multiple myeloma (MM) is a haematological malignancy that arises from plasma cells, which are a specialized type of B lymphocyte that primarily reside in the bone marrow. The growth and expansion of MM cells within the bone microenvironment disrupt the balance between bone-forming osteoblasts and bone-resorbing osteoblasts, leading to the formation of pathological bone lesions - the hallmarks of

this disease [322]. MM is the nineteenth most prevalent cancer in the UK, making up 2% of all new cancer cases, and it stands as the second most common form of blood cancer [323]. Several studies have shown that TRAF6 is a potential therapeutic target in MM treatment [308]. Chen et al reported that downregulation of TRAF6 via siRNA targeting the c-domain significantly inhibited MM cell proliferation and enhanced their apoptosis [294], Hostager et al showed that TRAF2 and TRAF6 play overlapping roles in CD40-mediated JNK and NFκB activation in mouse B lymphocyte [293]. Coupled with the anti-growth, anti-migratory and anti-invasion effect of the novel TRAF2/6 inhibitor FSAS3 in cancer and bone model, I am interested in studying the effects of FSAS3, alone and in combination with an existing MM treatment, in mice bearing MM in mice. Current studies are being performed in collaboration with Dr Shelly Lawson (University of Sheffield, UK). Briefly, C57Bl'6 mice will receive tail-vein injection of the mouse myeloma cells 5TGM1 expressing GFP or luciferase. On day 2, intraperitoneal administration of vehicle or FSAS3 (20mg/kg/3-week) will be performed based on the treatment regime used to study the CD40-TRAF6 inhibitor 6877002 in previously *in vivo* studies [309, 322, 324]. Skeletal tumour burden will be measured by IVIS (*In vivo* imaging system) and flowcytometry of bone marrow, and osteolytic bone damage will be assessed by μCT and histochemistry ex vivo. The effects of FSAS3 on inflammatory biomarkers in serum and bone marrow will be measured by q-PCR, western blot and/or proteomic microarray.

Supplementary Figures

Supplementary Figure 1. Risk of bias (RoB) assessment for in vivo studies using the SYRCLE RoB tool. (a) Representative summary Table for the risk of bias assessment. Green cells with '+' designate low risk of bias, yellow cells with '?' designate unclear risk of bias, and red cells with '-' designate high risk of bias. (b) Representative summary of risk of bias analysis across studies.

a

	Sequence generation (Item 1)	Baseline characteristics (Item 2)	Allocation concealment (Item 3)	Random housing (Item 4)	Blinding (Item 5)	Random outcome assessment (Item 6)	Blinding (Item 7)	Incomplete outcome data (Item 8)	Selective outcome reporting (Item 9)	Other sources of bias (Item 10)
Bishop et al,. 2020	?	+	-	+	-	?	-	?	+	+
Jiang et al,. 2016	?	+	-	+	-	?	-	+	+	+
Lin et al,. 2014	?	+	-	+	-	?	-	?	+	+
Liu et al,. 2015	-	+	-	+	-	?	-	?	+	+
Liu et al,. 2020	?	+	-	+	-	?	-	?	+	+
Peramuhendige et al,. 2018	-	+	-	+	-	?	-	?	+	+
Rezaeian et al,. 2017	-	+	-	+	-	?	-	+	+	+
Shi et al,. 2019	?	+	-	+	-	?	-	+	+	+
Yao et al,. 2017	?	+	-	+	-	?	-	?	+	+
Zhang et al,. 2013	-	+	-	+	-	?	+	+	+	+
Zhu et al,. 2018	?	+	-	+	-	?	+	+	+	+

b

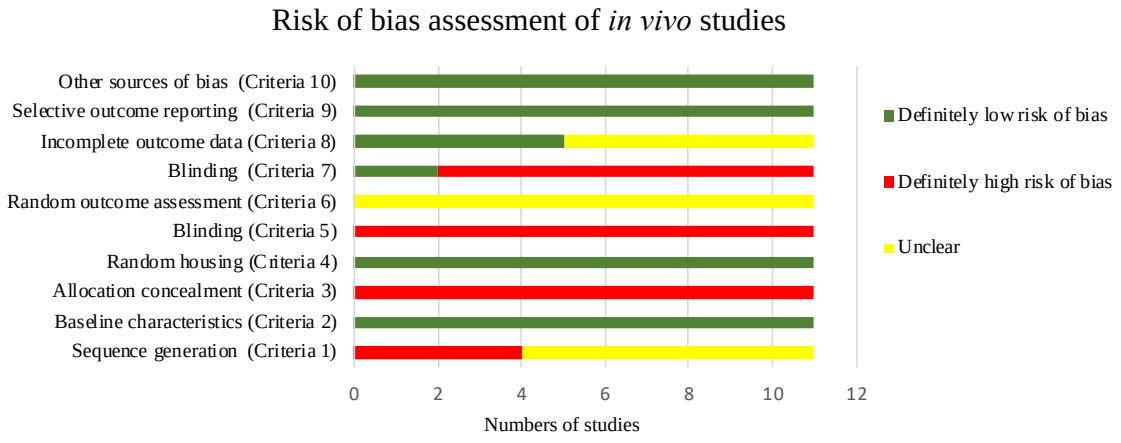

Supplementary Figure 2. Risk of bias (RoB) assessment for in vitro studies using the OHAT RoB tool. (a) Representative summary Table for the risk of bias assessment. Dark green cells with '++' designate definitely low risk of bias, light green cells with '+' designate low risk of bias, light pink cells with '-'designate probably high risk of bias, and yellow cells with '?' designate unclear risk of bias. (b) Representative summary of risk of bias analysis across studies. In bold and italics are the articles that consist of in vivo and in vitro experiments and their quality was assessed with both tools (for *in vivo* and *in vitro* studies).

a

	Randomization (criterion 1)	Allocation concealment (criterion 2)	Identical experimental conditions (criterion 3)	Blingding of reseachers during study (criterion 4)	Missing outcome data (criterion 5)	Exposure characterization (criterion 6)	Outcome assessment (criterion 7)	Outcome reporting (criterion 8)	Other potential threats (criterion 9)
Bishop et al,. 2020	++	++	++	-	+	+	+	++	++
Jiang et al,. 2016	++	++	++	-	+	+	+	++	++
Choi et al,. 2013	++	++	++	-	+	++	+	++	++
Jang et al,. 2011	++	++	++	-	+	++	+	++	++
Li et al,. 2012	++	++	++	-	+	+	+	++	++
Liu et al,. 2015	++	++	++	-	+	+	+	++	++
Liu et al,. 2020	++	++	++	-	+	+	+	++	++
Peramuhendige et al,. 2018	++	++	++	-	+	++	+	++	++
Shi et al,. 2019	++	++	++	-	+	++	+	++	++
Wang et al,. 2013	++	++	++	-	+	++	+	++	++
Wang et al,. 2021	++	++	++	-	+	+	+	++	++
Yao et al,. 2017	++	++	++	-	+	+	+	++	++
Zhang et al,. 2013	++	++	++	-	+	++	+	++	++
Zheng et al,. 2015	++	++	++	-	+	+	+	++	++

b

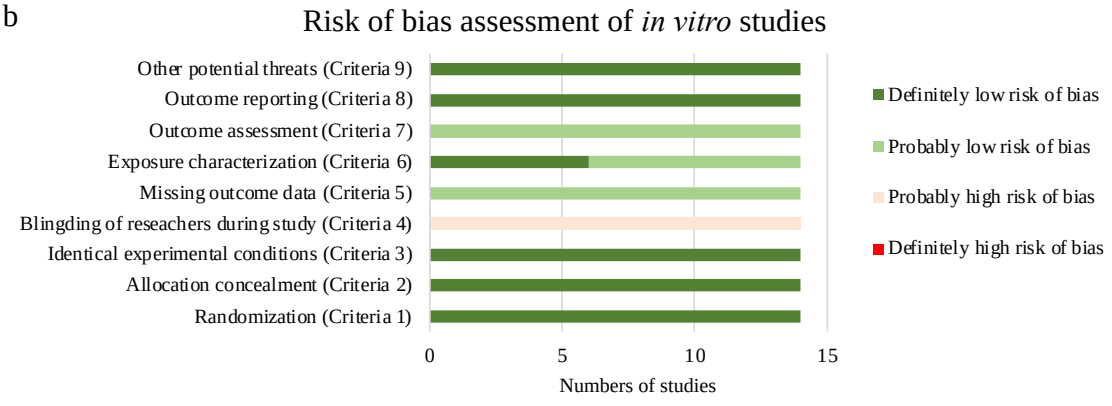

Supplementary Figure 3. Overall survival of breast cancer patients with TRAFs copy number variants (CNVs). Patients with TRAF3, TRAF4, TRAF5 homozygous or hemizygous deletion exhibit significantly poor overall survival compared to patients with neutral or no change**.** Data were obtained from METABRIC via cBioPortal (n=1826).

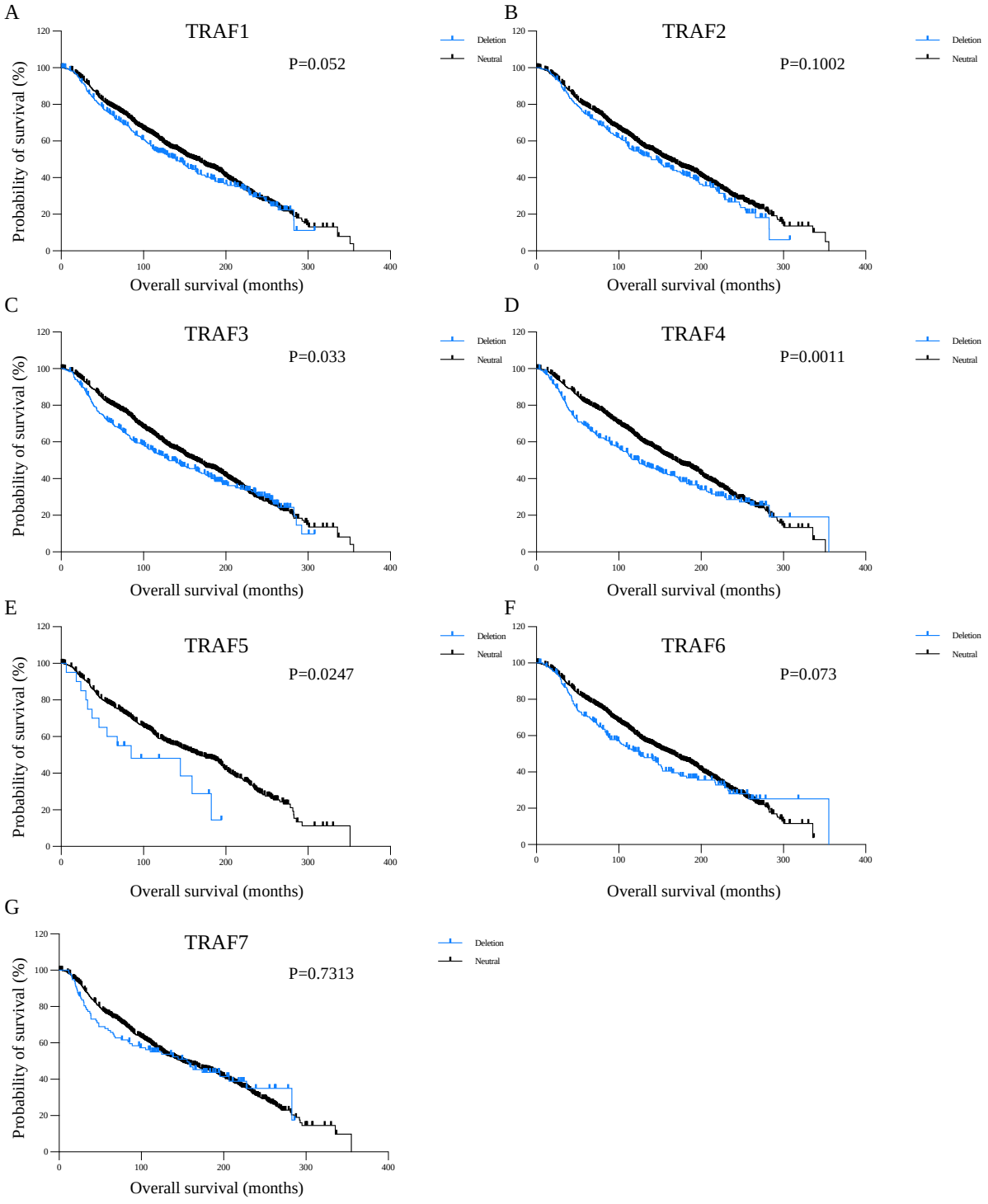

Supplementary Figure 4. Overall survival of triple negative breast cancer patients with TRAFs copy number variants (CNVs). Patients with TRAF2 gain or high-level amplification exhibit significantly poor overall survival compared to patients with neutral or no change. Data were obtained from METABRIC via cBioPortal (n=427).

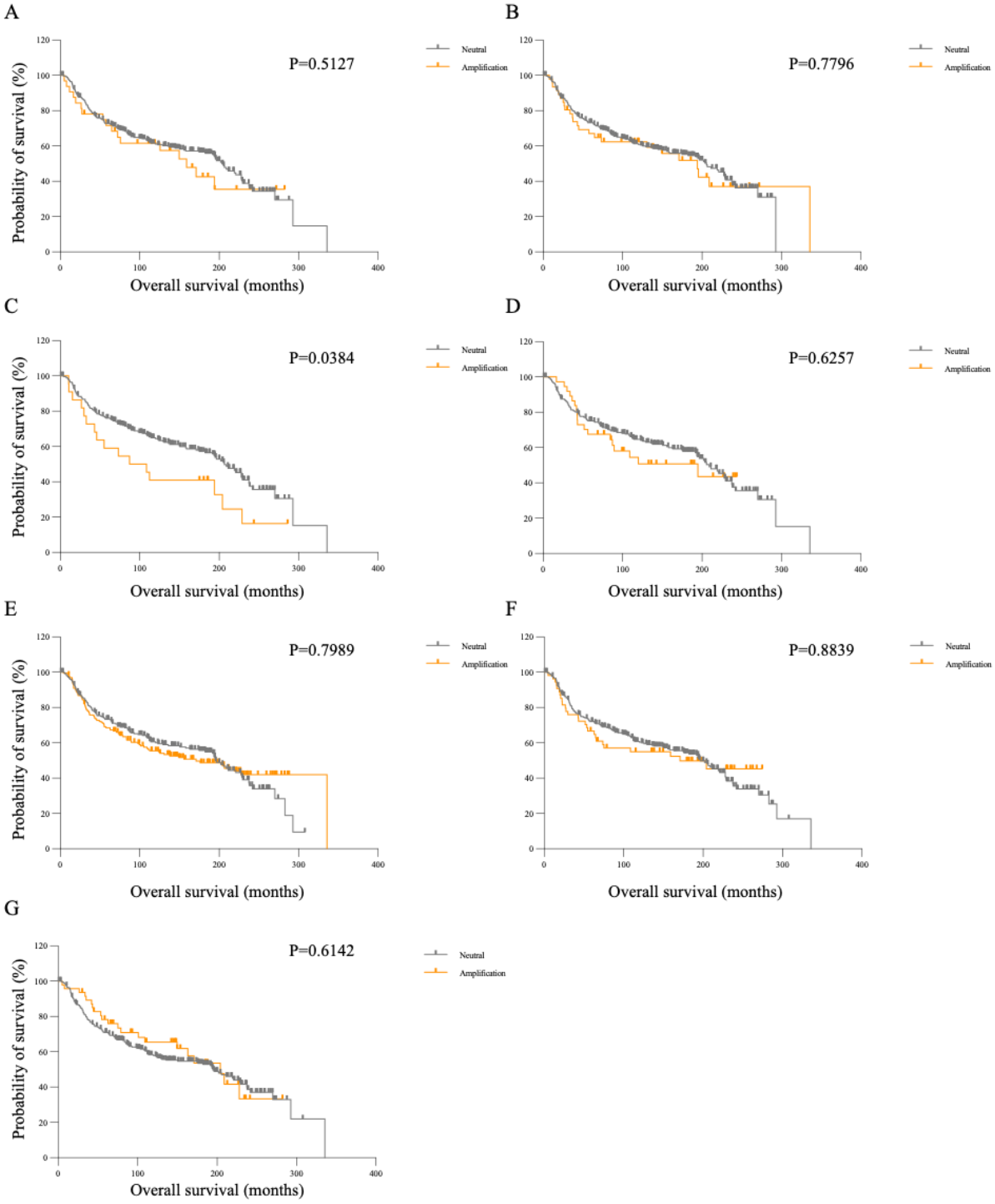

Supplementary Figure 5. Overall survival of triple negative breast cancer patients with TRAFs copy number variants (CNVs). Data were obtained from METABRIC via cBioPortal (n=427).

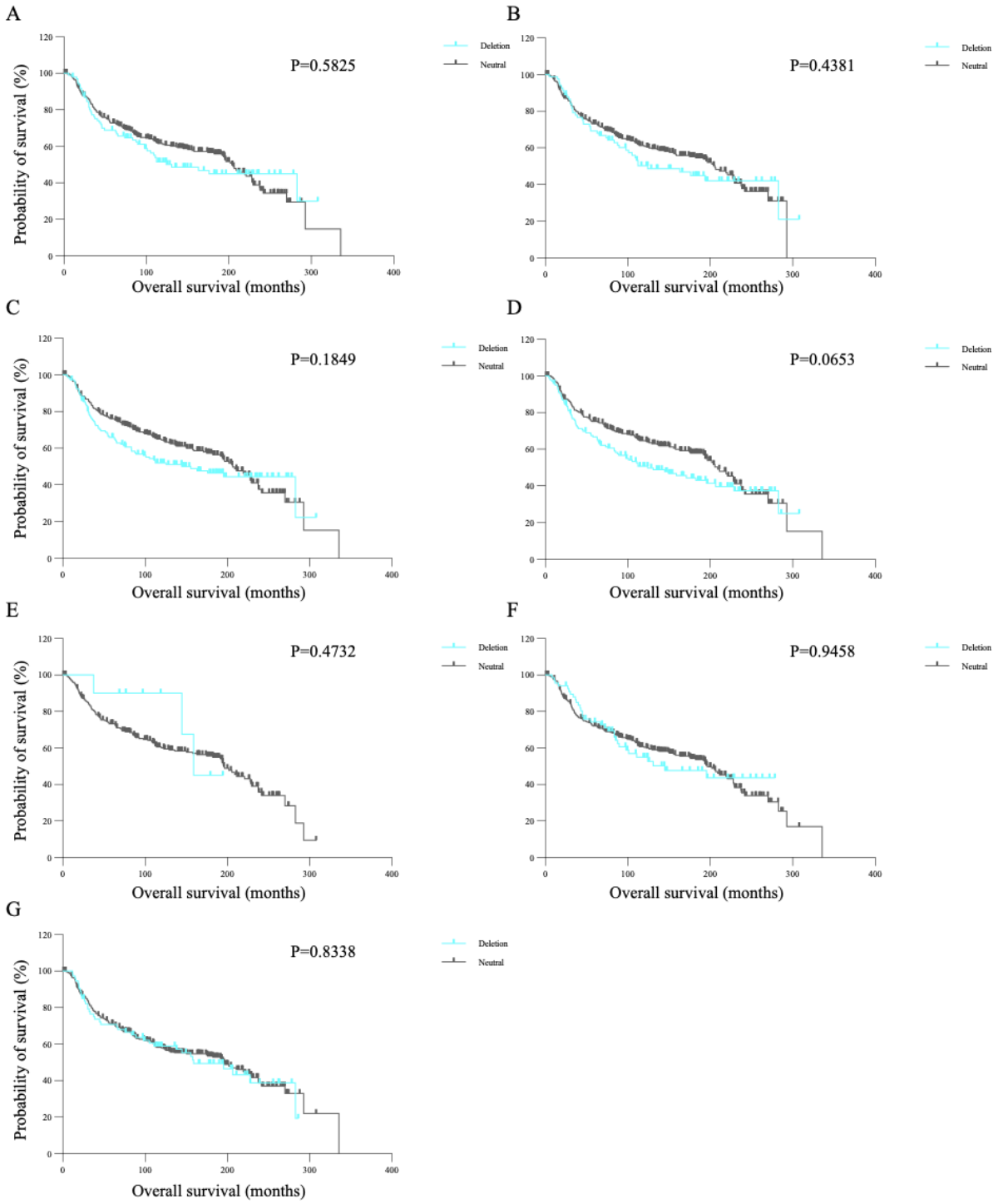

Supplementary Figure 6. Overall survival of triple negative breast cancer patients with TRAFs copy number variants (CNVs). Patients with TRAF1 high-level amplification exhibit significantly poor overall survival compared to patients with hemizygous deletion. And patients with TRAF6 high-level amplification exhibit non-significant poor overall survival compared to patients with hemizygous deletion Data were obtained from METABRIC via cBioPortal (n=427).

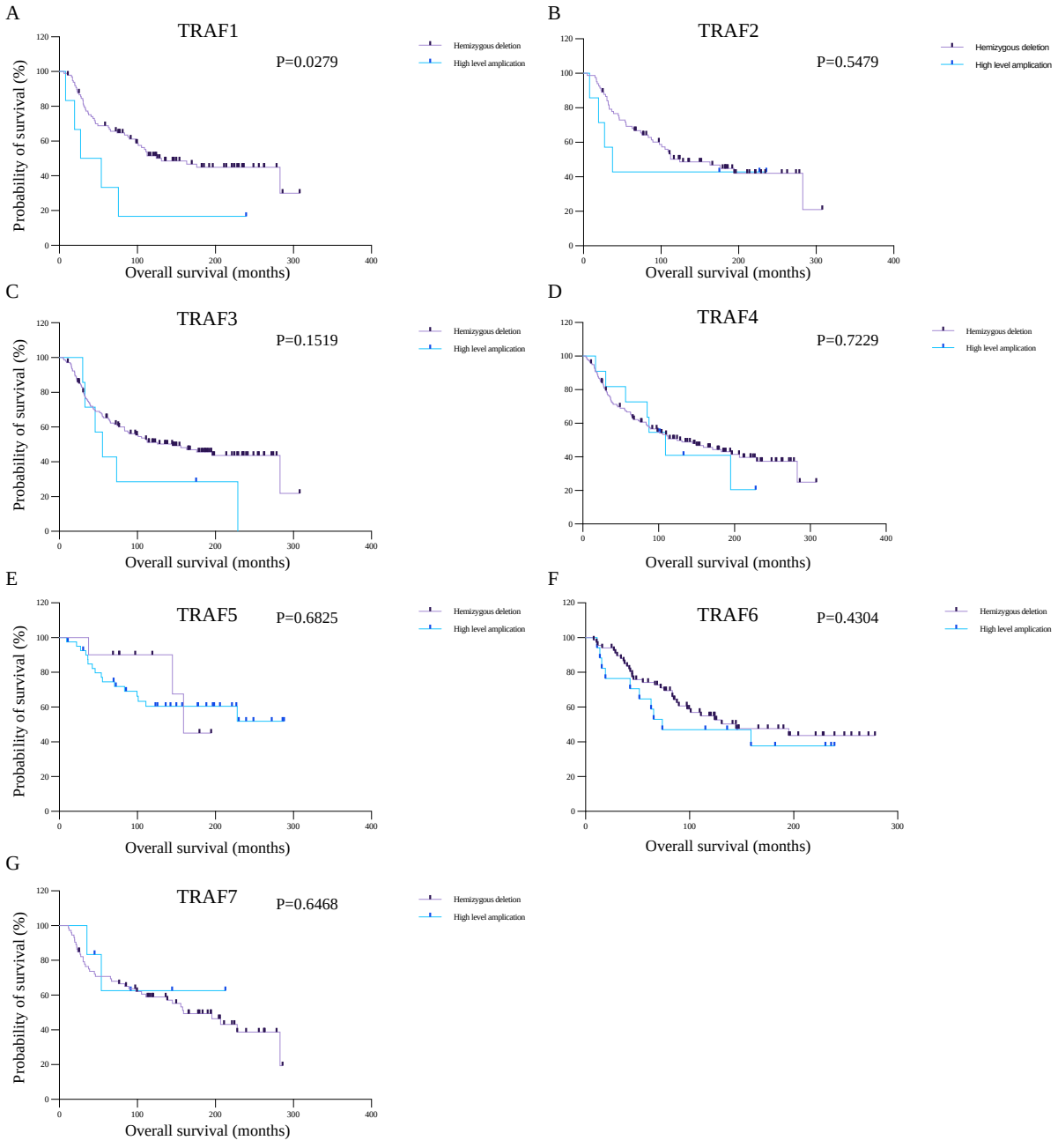

Supplementary Figure 7. TRAF2, 4 and TRAF6 expression in a panel of human and murine breast cancer cell lines. Relative fold of (A, E) TRAF6/GAPHD, (B, D) TRAF2/GAPDH and (C, F) TRAF4/GAPDH expression human breast cancer cell MDA-MB-231, MCF7 (A-D) and mouse breast cancer cell 4T1 and E0771 (E-H). Representative Western blot images of TRAF2/4/6 (D, H) expression in breast cancer cell lines. The data are mean ± standard deviation (n=3). p-values were determined using unpaired t test. *p<0.5, **p<0.01 compared to hormone dependent breast cancer cell. ns represents no significance.

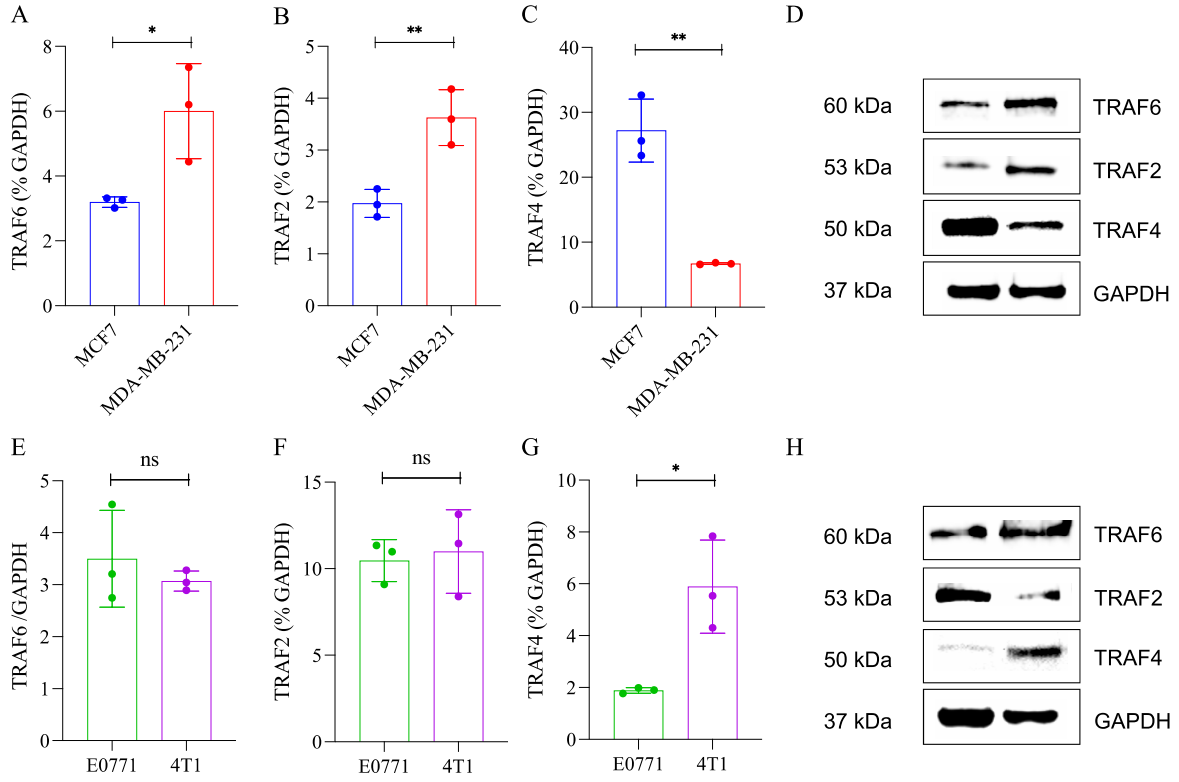

Supplementary Figure 8. Effects on cell viability of a panel of human breast cancer cells treated with verified CD40-TRAF6 inhibitor 6877002 and the most potent novel TRAF6 inhibitor FSAS3 *in vitro*. Dose-response curves of the verified 6877002 and novel FSAS3 on the viability of hormone-dependent MCF7 (A), triple-negative MDA-MB-231 (D) and osteotropic triple-negative MDA-231-BT (E) breast cancer cells after 48 hours, as assessed via Alamar Blue™ assay. Representative images of cells invasion after 48 hours from MCF7 (B), MDA-MB-231 (D) and MDA-231-BT (E) cells. Values are expressed as mean ± SD and were obtained from three independent experiments. p-values were obtained from two-way ANOVA test followed by Tukey post hoc test. ****p < 0.0001, ***p < 0.0005, **p < 0.005 and *p < 0.05 compared to vehicle, ####p < 0.0001, ###p < 0.0005, ##p < 0.005 compare FSAS3 to 6877002. Scale bar = 100 μM.

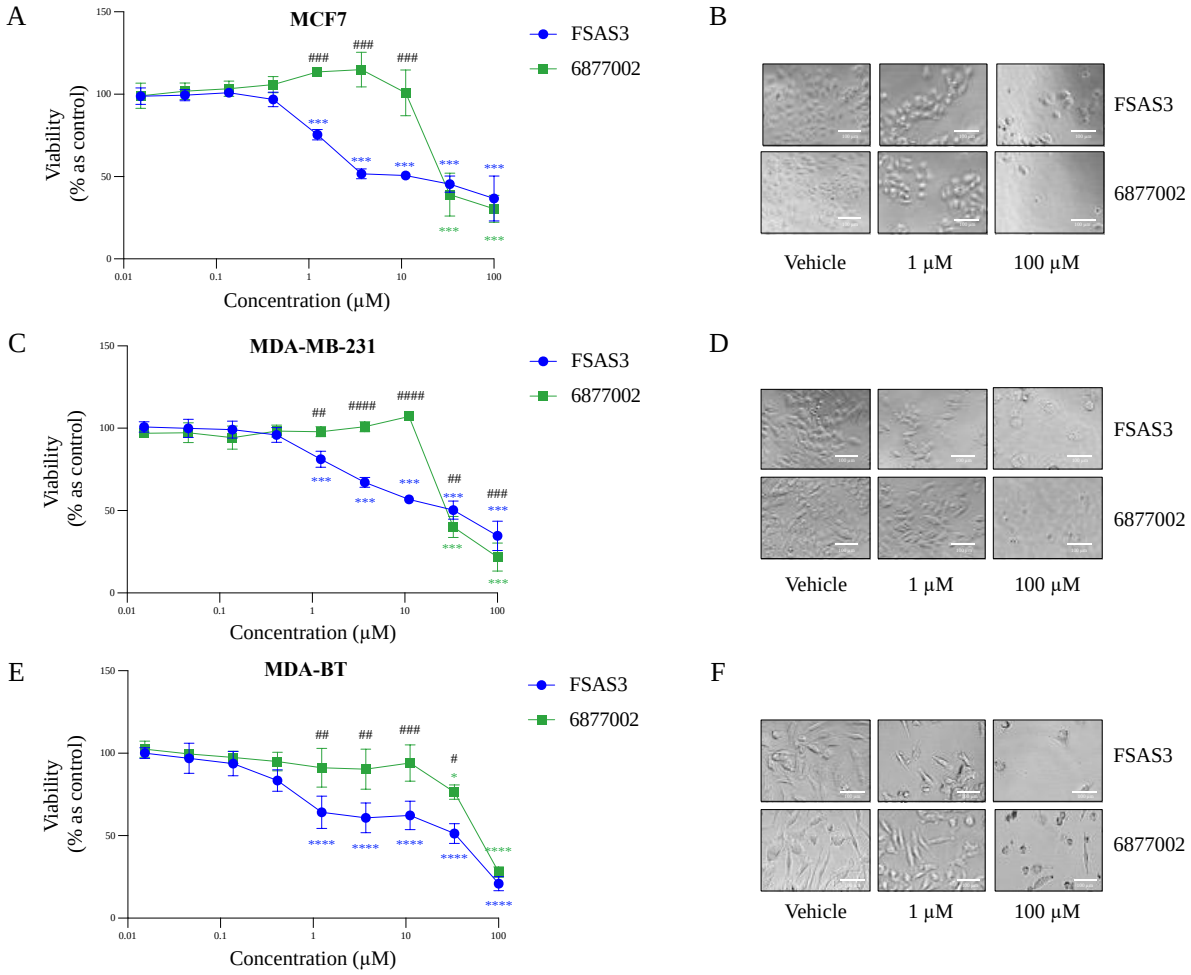

Supplementary Figure 9. Effects on cell viability of a panel of murine breast cancer cells treated with verified CD40-TRAF6 inhibitor 6877002 and the most potent novel TRAF6 inhibitor FSAS3 *in vitro*. Dose-response curves of the verified 6877002 and novel FSAS3 on the viability of hormone-dependent E0771 (A), triple-negative 4T1 (D) and osteotropic triple-negative 4T1-BT (E) breast cancer cells after 48 hours, as assessed via Alamar Blue™ assay. Representative images of cells invasion after 48 hours from E0771 (B), 4T1 (D) and 4T1-BT (E) cells. Values are expressed as mean ± SD and were obtained from three independent experiments. p-values were obtained from two-way ANOVA test followed by Tukey post hoc test. ****p < 0.0001, ***p < 0.0005, **p < 0.005 and *p < 0.05 compared to vehicle, ####p < 0.0001, ###p < 0.0005, ##p < 0.005 compare FSAS3 to 6877002. Scale bar = 100 μM.

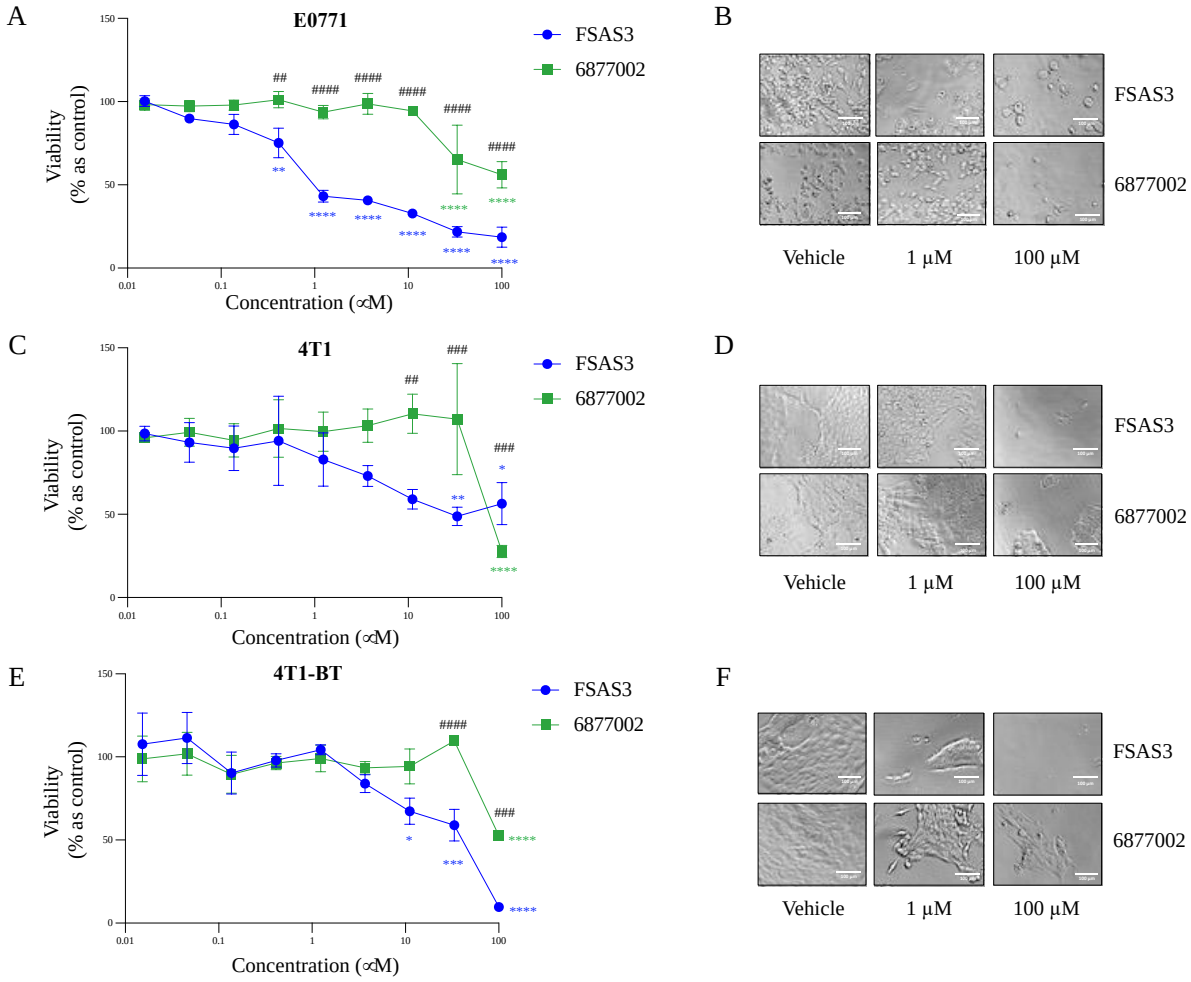

Supplementary Figure 10. FSAS3 reduced cell viability of MDA-MB-231 and MDA-231-BT TRAF6 knockdown cells and their mock control *in vitro*, and FSAS3 was most potent in mock control. Dose-response curves of the novel FSAS3 on the viability of MDA-MB-231 TRAF6 knockdown clones and mock control (A), MDA-231-BT TRAF6 knockdown clones and its mock control (B) after 72 hours, as assessed via Alamar Blue™ assay. Values are expressed as mean ± SD and were obtained from three independent experiments.

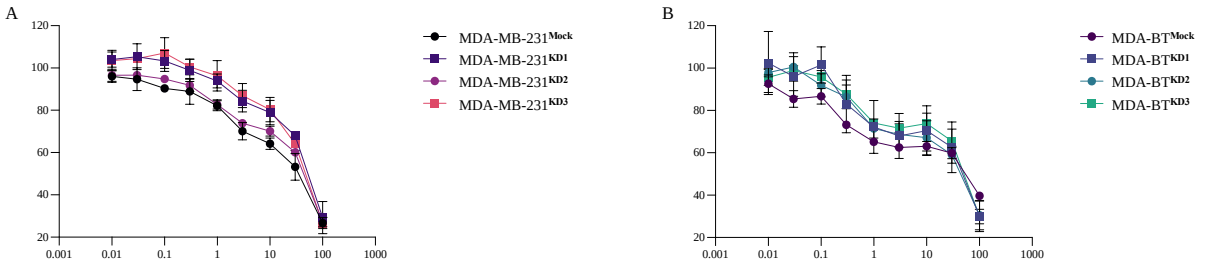

Supplementary Figure 11. Effects on cell viability of hormone-dependent human breast cancer MCF7 cells treated with FSAS1, FSAS2, FSAS4 and FSAS5 *in vitro*. Dose-response curves and representative of FSAS1 (A and E), FSAS2 (B and F), FSAS4 (C and G), FSAS5 (D and H) on the viability of hormone-dependent human MCF7 breast cancer cells after 48 (A-D) and 72 (E-H) hours, as assessed via Alamar Blue™ assay. Values are expressed as mean ± SD and were obtained from three independent experiments. p-values were obtained from two-way ANOVA test followed by Tukey post hoc test. ****p < 0.0001, ***p < 0.0005, **p < 0.005 and *p < 0.05 compared to vehicle. Scale bar = 100 μM

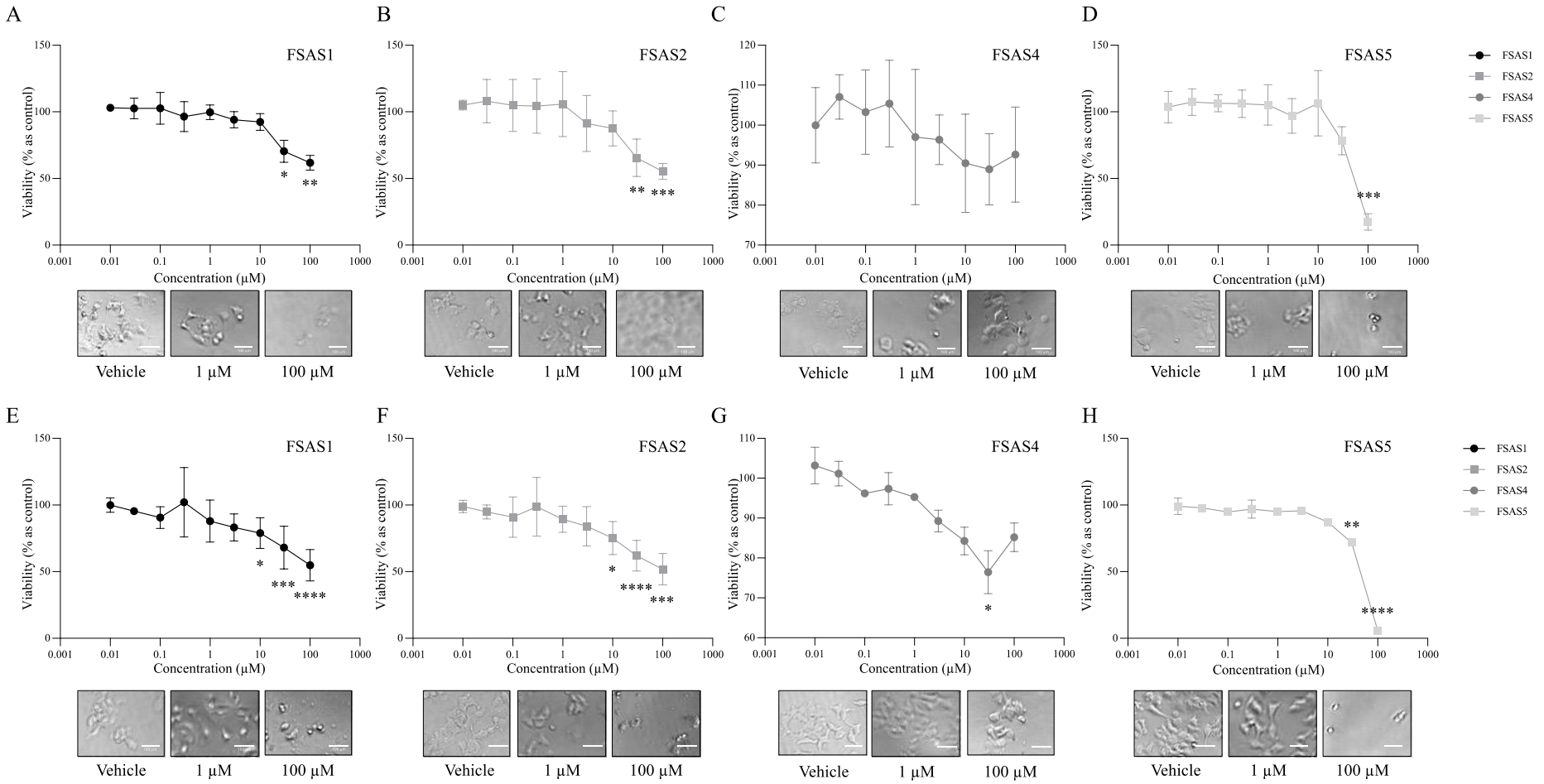

Supplementary Figure 12. Effects on cell viability of triple negative human breast cancer MDA-MB-231 cells treated with FSAS1, FSAS2, FSAS4 and FSAS5 *in vitro*. Dose-response curves and representative of FSAS1 (A and E), FSAS2 (B and F), FSAS4 (C and G), FSAS5 (D and H) on the viability of triple negative human MDA-MB-231 breast cancer after 48 (A-D) and 72 (E-H) hours, as assessed via Alamar Blue™ assay. Values are expressed as mean ± SD and were obtained from three independent experiments. p-values were obtained from two-way ANOVA test followed by Tukey post hoc test. ****p < 0.0001, ***p < 0.0005, **p < 0.005 and *p < 0.05 compared to vehicle. Scale bar = 100 μM

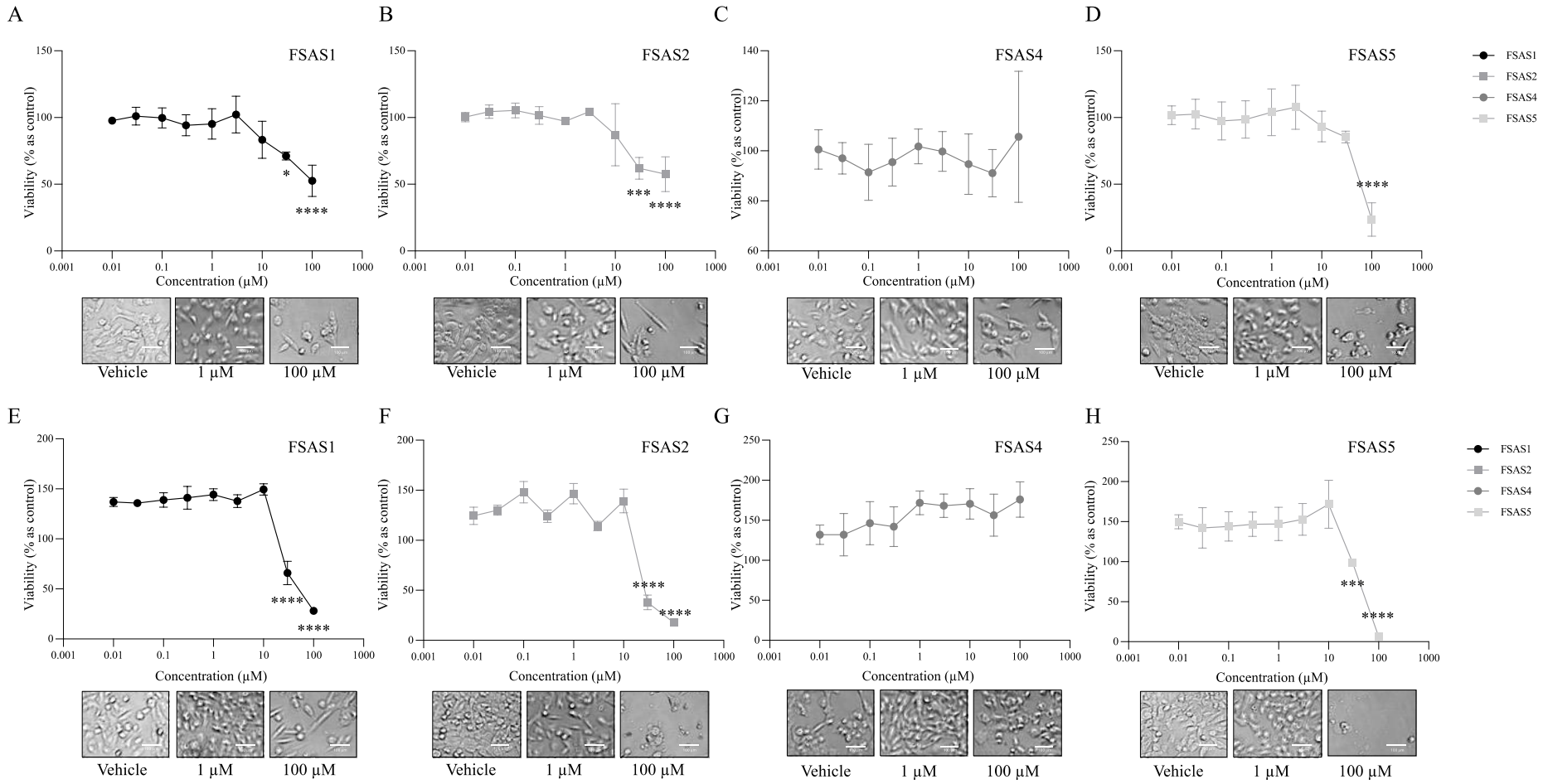

Supplementary Figure 13. Effects on cell viability of osteotropic triple negative human breast cancer MDA231-BT cells treated with FSAS1, FSAS2, FSAS4 and FSAS5 *in vitro*. Dose-response curves and representative of FSAS1 (A and E), FSAS2 (B and F), FSAS4 (C and G), FSAS5 (D and H) on the viability of osteotropic triple negative human MDA231-BT breast cancer after 48 (A-D) and 72 (E-H) hours, as assessed via Alamar Blue™ assay. Values are expressed as mean ± SD and were obtained from three independent experiments. p-values were obtained from two-way ANOVA test followed by Tukey post hoc test. ****p < 0.0001, ***p < 0.0005, **p < 0.005 and *p < 0.05 compared to vehicle. Scale bar = 100 μM

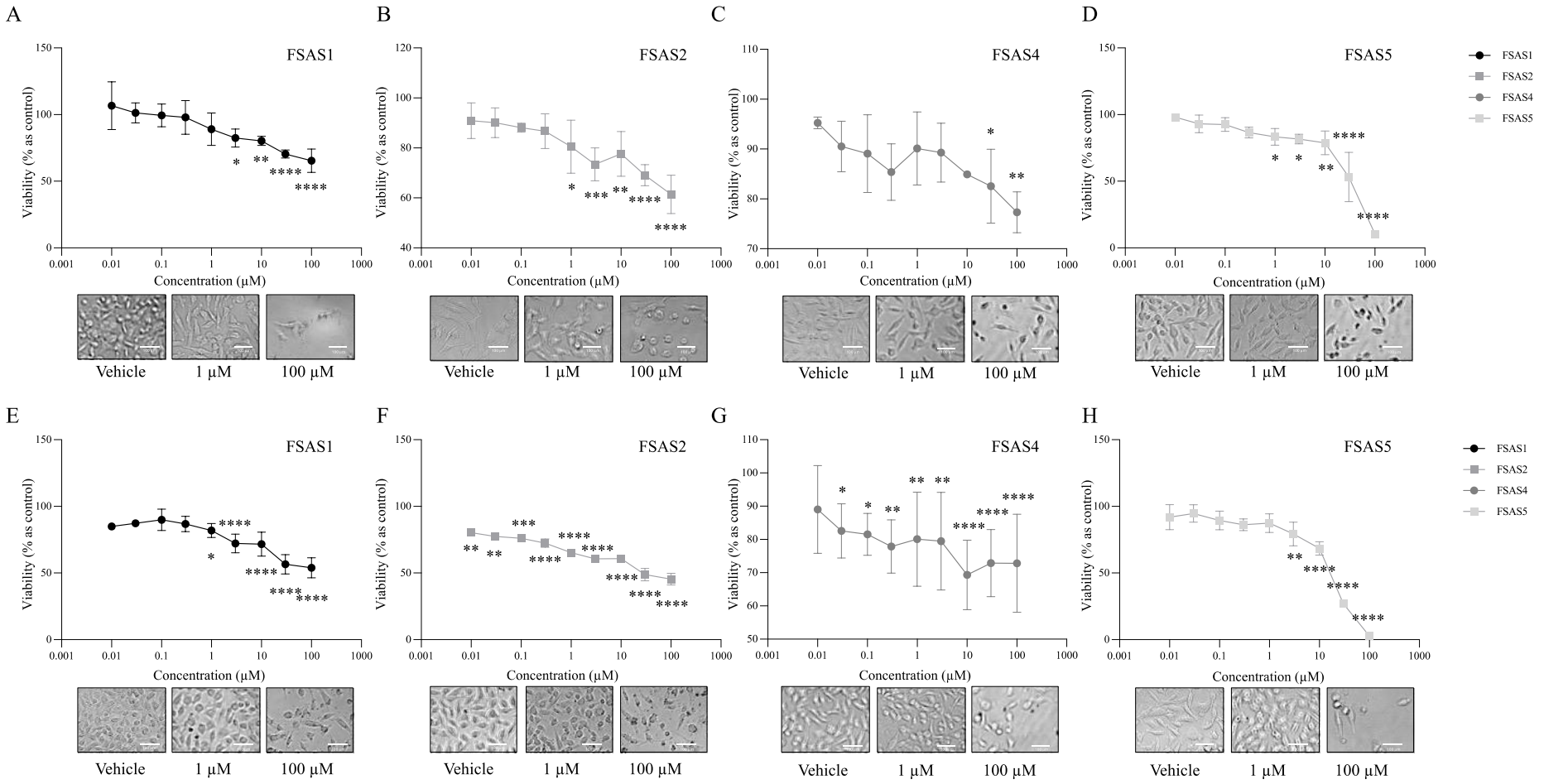

Supplementary Figure 14. Effects on cell viability of hormone-dependent murine breast cancer E0771 cells treated with FSAS1, FSAS2, FSAS4 and FSAS5 *in vitro*. Dose-response curves and representative of FSAS1 (A and E), FSAS2 (B and F), FSAS4 (C and G), FSAS5 (D and H) on the viability of hormone-dependent murine E0771 breast cancer cells after 48 (A-D) and 72 (E-H) hours, as assessed via Alamar Blue™ assay. Values are expressed as mean ± SD and were obtained from three independent experiments. p-values were obtained from two-way ANOVA test followed by Tukey post hoc test. ****p < 0.0001, ***p < 0.0005, **p < 0.005 and *p < 0.05 compared to vehicle. Scale bar = 100 μM

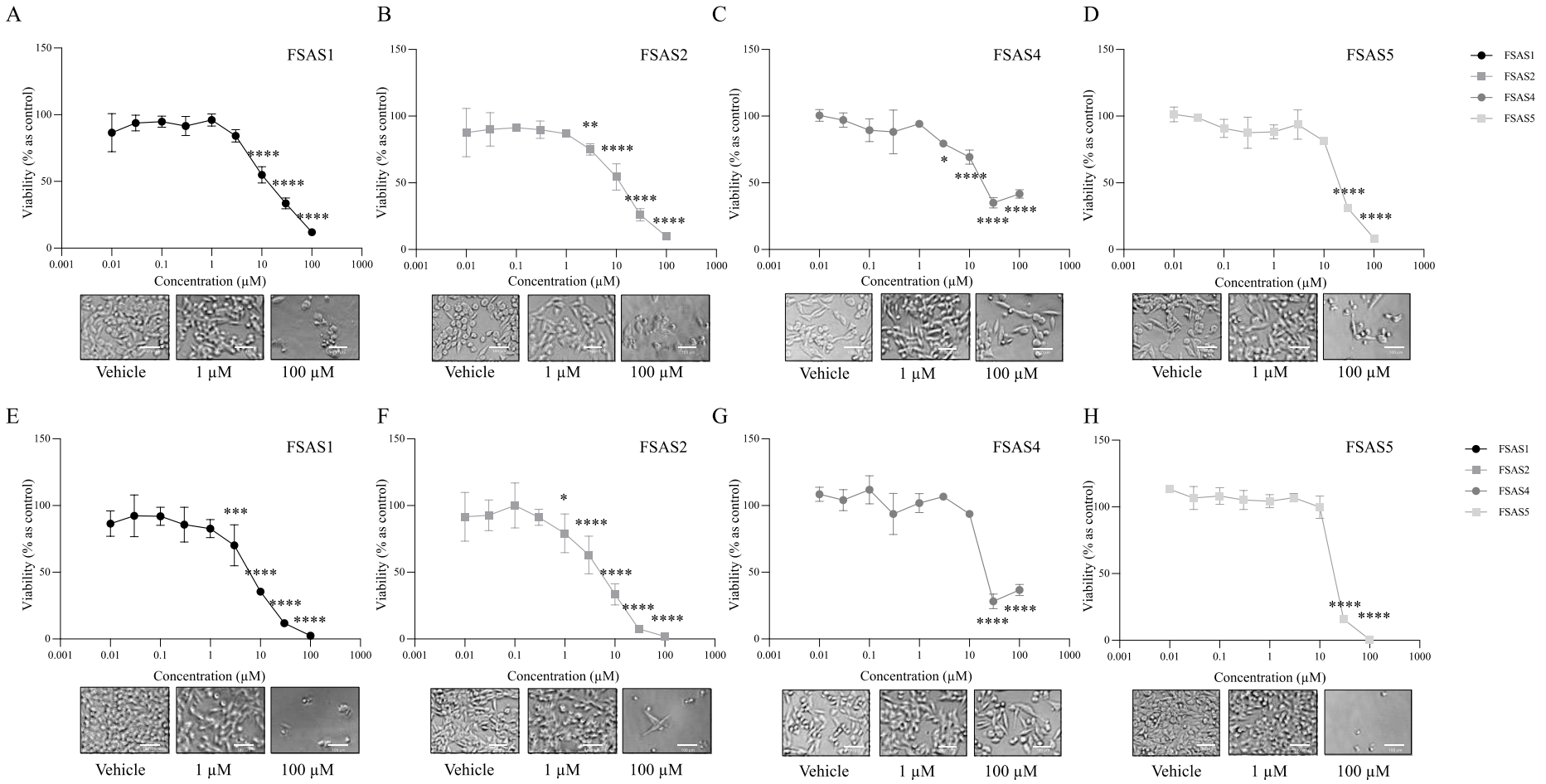

Supplementary Figure 15. Effects on cell viability of triple negative murine breast cancer 4T1 cells treated with FSAS1, FSAS2, FSAS4 and FSAS5 *in vitro*. Dose-response curves and representative of FSAS1 (A and E), FSAS2 (B and F), FSAS4 (C and G), FSAS5 (D and H) on the viability of triple negative murine 4T1 breast cancer after 48 (A-D) and 72 (E-H) hours, as assessed via Alamar Blue™ assay. Values are expressed as mean ± SD and were obtained from three independent experiments. p-values were obtained from two-way ANOVA test followed by Tukey post hoc test. ****p < 0.0001, ***p < 0.0005, **p < 0.005 and *p < 0.05 compared to vehicle. Scale bar = 100 μM

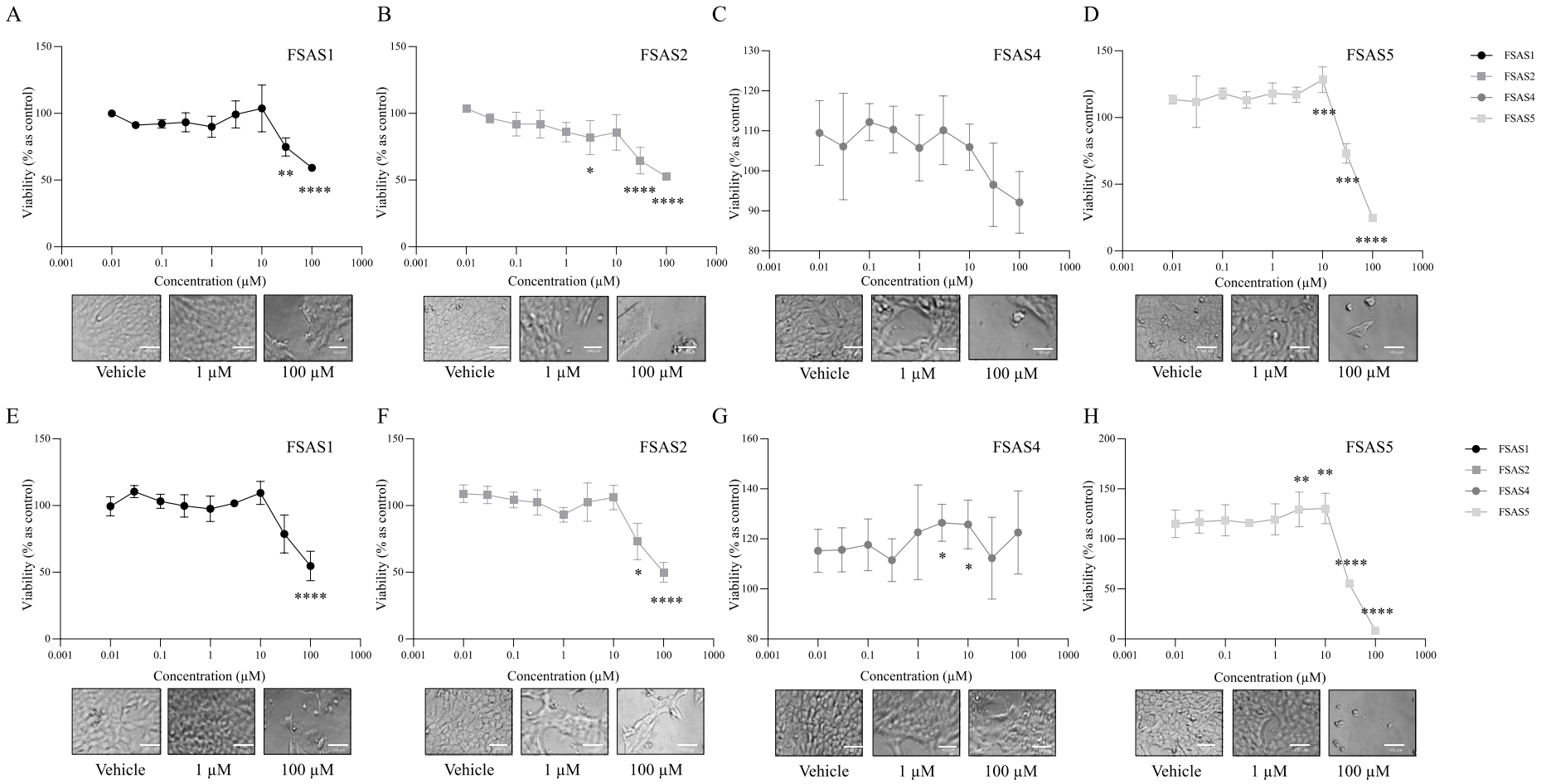

Supplementary Figure 16. Effects on cell viability of osteotropic triple negative murine breast cancer 4T1-BT cells treated with FSAS1, FSAS2, FSAS4 and FSAS5 *in vitro*. Dose-response curves and representative of FSAS1 (A and E), FSAS2 (B and F), FSAS4 (C and G), FSAS5 (D and H) on the viability of osteotropic triple negative murine 4T1-BT breast cancer after 48 (A-D) and 72 (E-H) hours, as assessed via Alamar Blue™ assay. Values are expressed as mean ± SD and were obtained from three independent experiments. p-values were obtained from two-way ANOVA test followed by Tukey post hoc test. ****p < 0.0001, ***p < 0.0005, **p < 0.005 and *p < 0.05 compared to vehicle. Scale bar = 100 μM

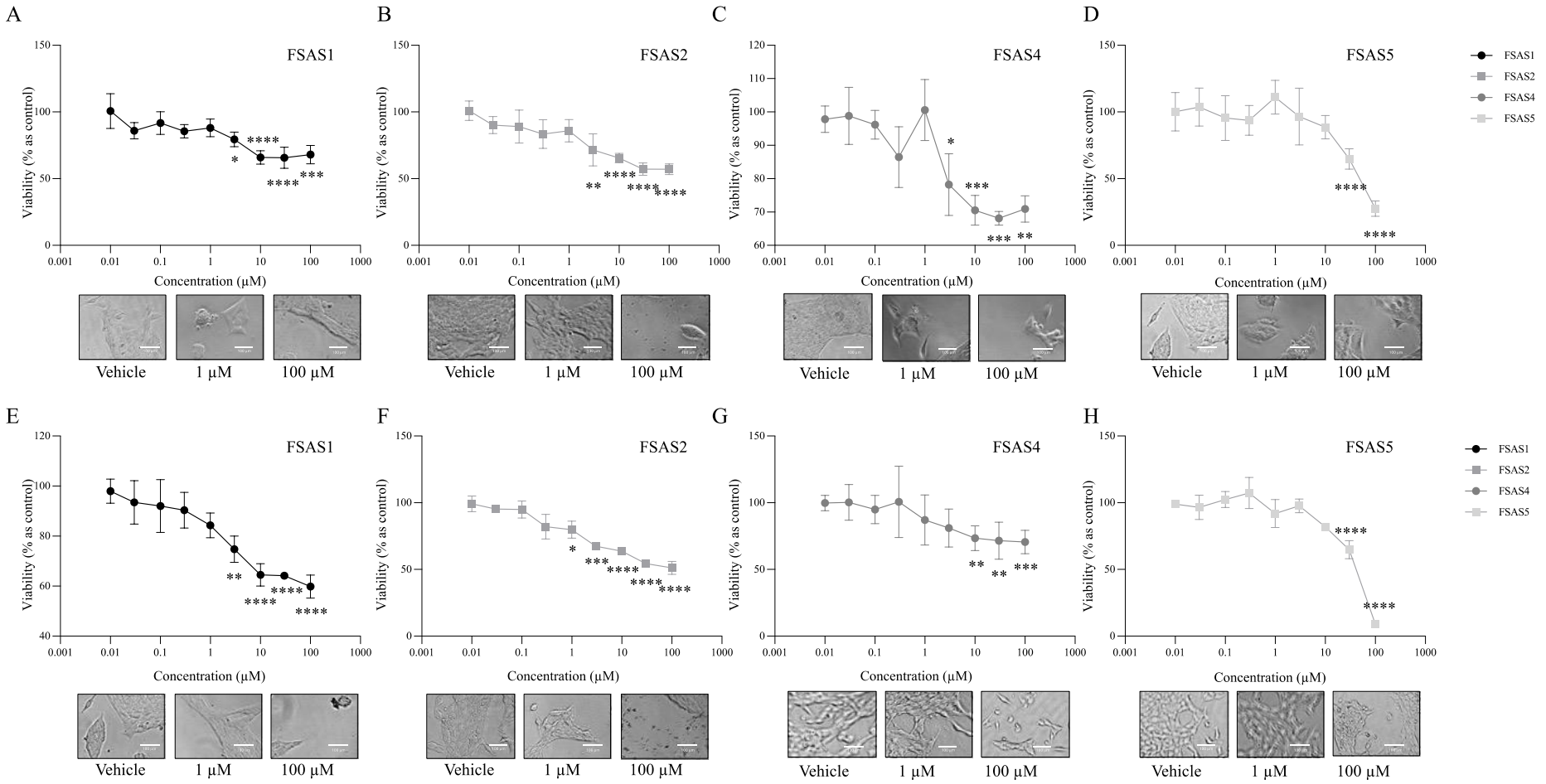

Supplementary Figure 17. Viability of RAW264.7 cells treated with FSAS3 (0-1 μM) and RANKL (100ng/ml) after 72 hours.

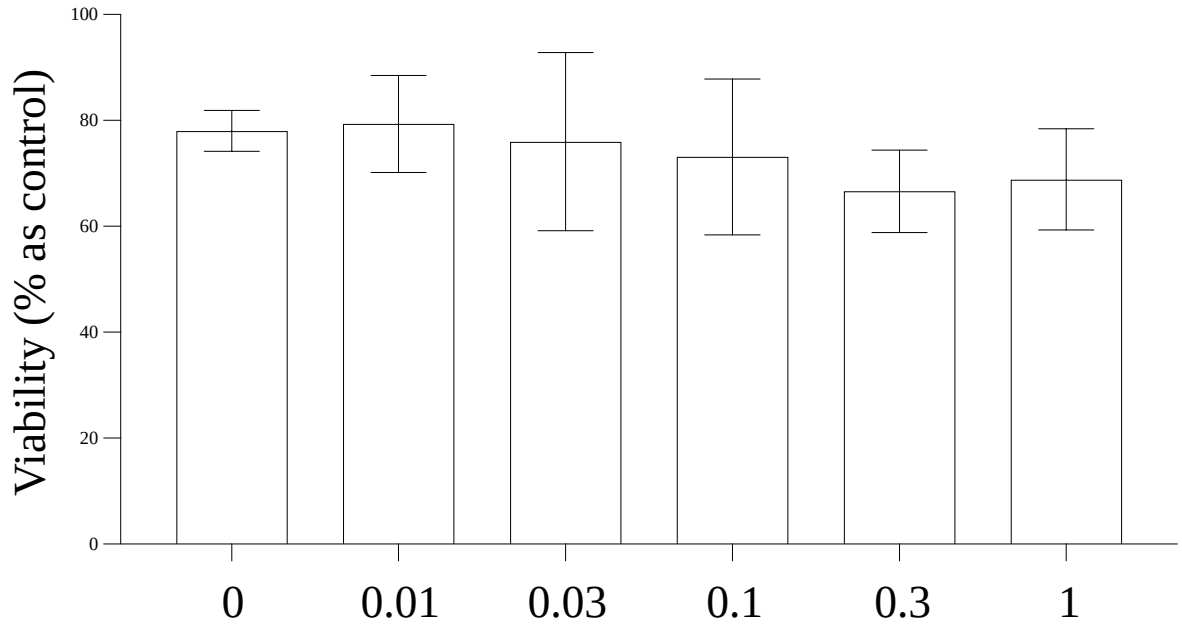

Supplementary Figure 18. Pro-inflammation cytokines regulate the activation of NFκB of MDA-231 cell in a time-dependent manner. (A) Upper panel - Relative expression of phospho-IkB/GAPDH of MDA-MB-231 cell stimulated with RANKL (100 ng/ml) for different time periods (0 min, 5 min, 10 min, 15 min, 30 min and 1 hour). Bottom panel – representative western blot images of RANKL induced protein expression. (B) Upper panel - Relative expression of phospho-IkB/GAPDH of MDA-MB-231 cell stimulated with TNFa (10 ng/ml) for different time periods (0 min, 5 min, 10 min, 15 min, 30 min and 1 hour). Bottom panel – representative western blot images of RANKL induced protein expression. (C) Upper panel - Relative expression of phospho-IkB/GAPDH of MDA-MB-231 cell stimulated with CD40L (100 ng/ml) for different time periods (0 min, 5 min, 10 min, 15 min, 30 min and 1 hour). Bottom panel – representative western blot images of RANKL induced protein expression. (D) Upper panel - Relative expression of phospho-IkB/GAPDH of MDA-MB-231 cell stimulated with RANKL (100 ng/ml) for different time periods (0 min, 5 min, 10 min, 15 min, 30 min and 1 hour). Bottom panel – representative western blot images of IL1b induced protein expression.

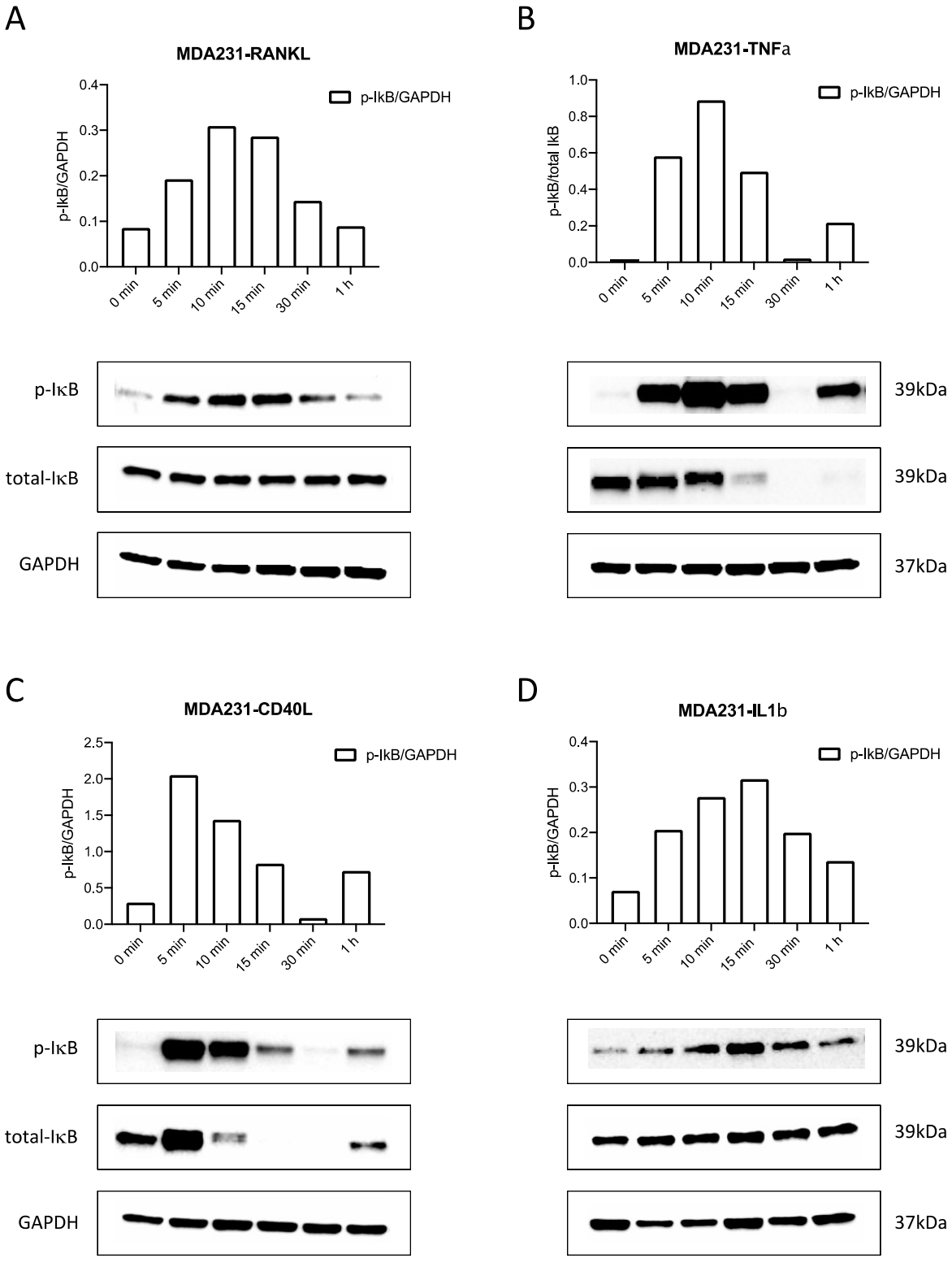

Supplementary Figure 19. Pro-inflammation cytokines regulate the activation of NFκB of 4T1 cell in a time-dependent manner. (A) Upper panel - Relative expression of phospho-IkB/GAPDH of 4T1 cell stimulated with RANKL (100 ng/ml) for different time periods (0 min, 5 min, 10 min, 15 min, 30 min and 1 hour). Bottom panel – representative western blot images of RANKL induced protein expression. (B) Upper panel - Relative expression of phospho-IkB/GAPDH of 4T1 cell stimulated with TNFa (10 ng/ml) for different time periods (0 min, 5 min, 10 min, 15 min, 30 min and 1 hour). Bottom panel – representative western blot images of RANKL induced protein expression. (C) Upper panel - Relative expression of phospho-IkB/GAPDH of 4T1 cell stimulated with CD40L (100 ng/ml) for different time periods (0 min, 5 min, 10 min, 15 min, 30 min and 1 hour). Bottom panel – representative western blot images of RANKL induced protein expression. (D) Upper panel - Relative expression of phospho-IkB/GAPDH of 4T1 cell stimulated with RANKL (100 ng/ml) for different time periods (0 min, 5 min, 10 min, 15 min, 30 min and 1 hour). Bottom panel – representative western blot images of IL1b induced protein expression.

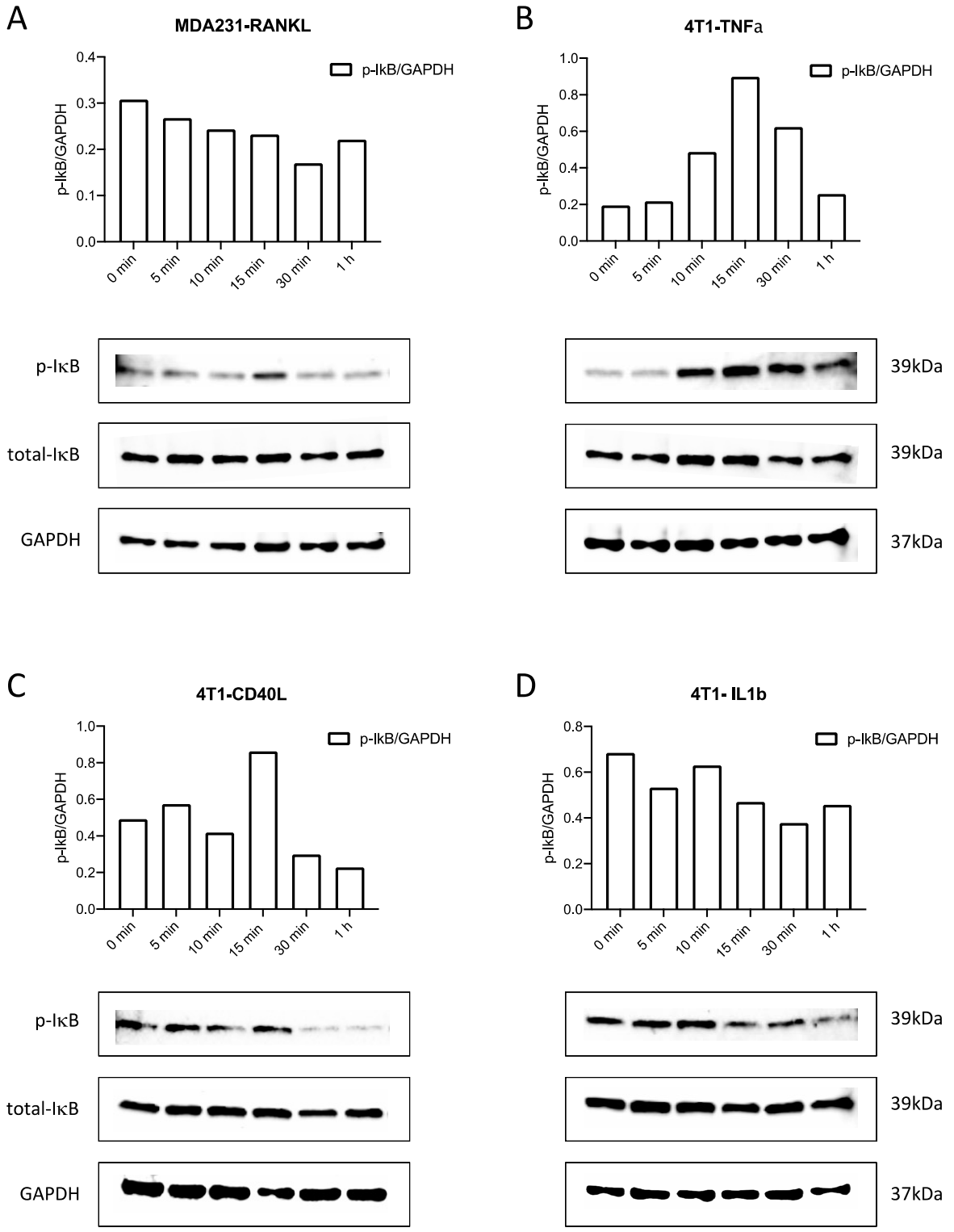

Supplementary Figure 20. Effect of RANKL and BCa cell conditioned medium on phosphorylated IκB-α after a short period of time (5 minutes and 10 minutes). (A) Relative fold of phosphorylated IκB-α/total IκB-α of murine macrophage-like RAW264.7 cells exposed to RANKL (100 ng/ml) or MDA-MB-231, MDA231-BT, 4T1-, 4T1-BT conditioned medium (10% v/v), for the specified timepoints. (B) Representative Western Blot images of expression of p-IκB-α, total IκB-α and actin of RAW264.7 exposed to RANKL or BCa conditioned medium.

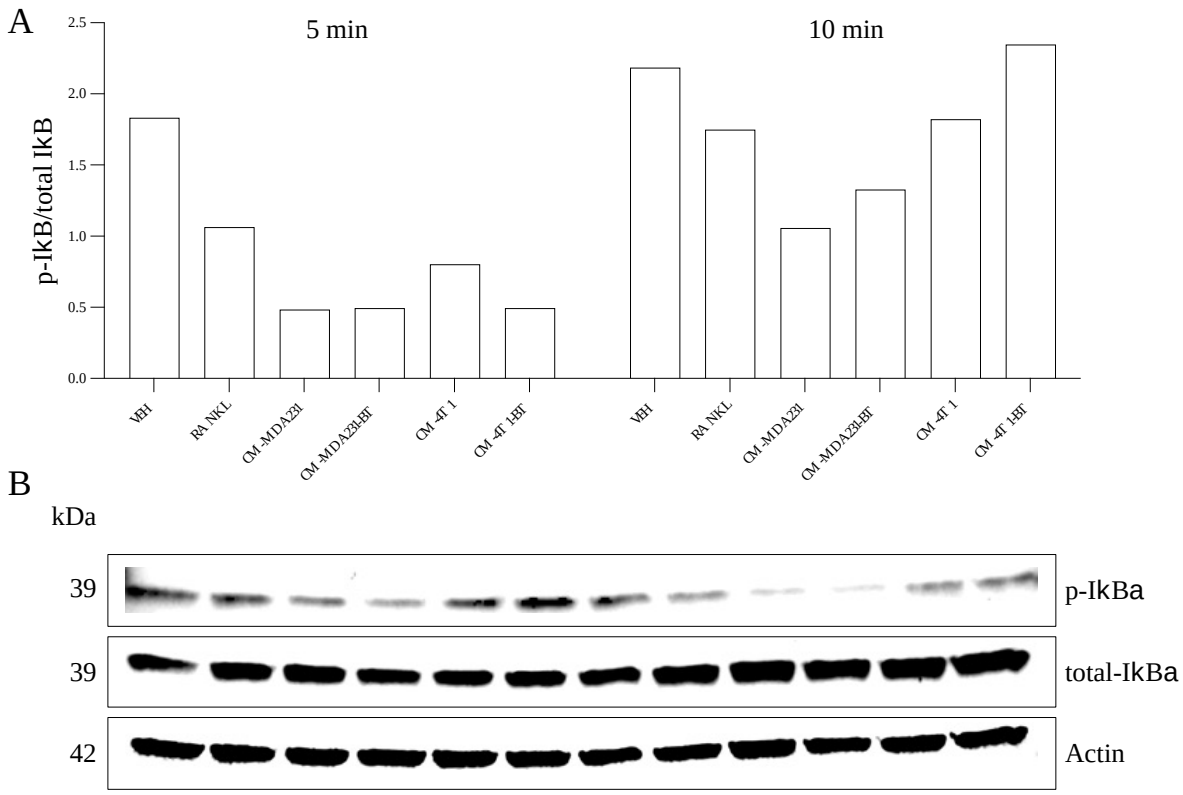

Supplementary Figure 21. Expression of TRAF2/6 and cytokine receptors (RANK, CD40, TNFR1, TNFR2, IL1R1) in human osteoblast-like cell lines Saos-2, macrophage THP1 and breast cancer MDA-MB-231 cells from RNA-seq of 1019 human cancer cell lines from the Cancer Cell Line Encyclopaedia, Expression Atlas website [325, 326].

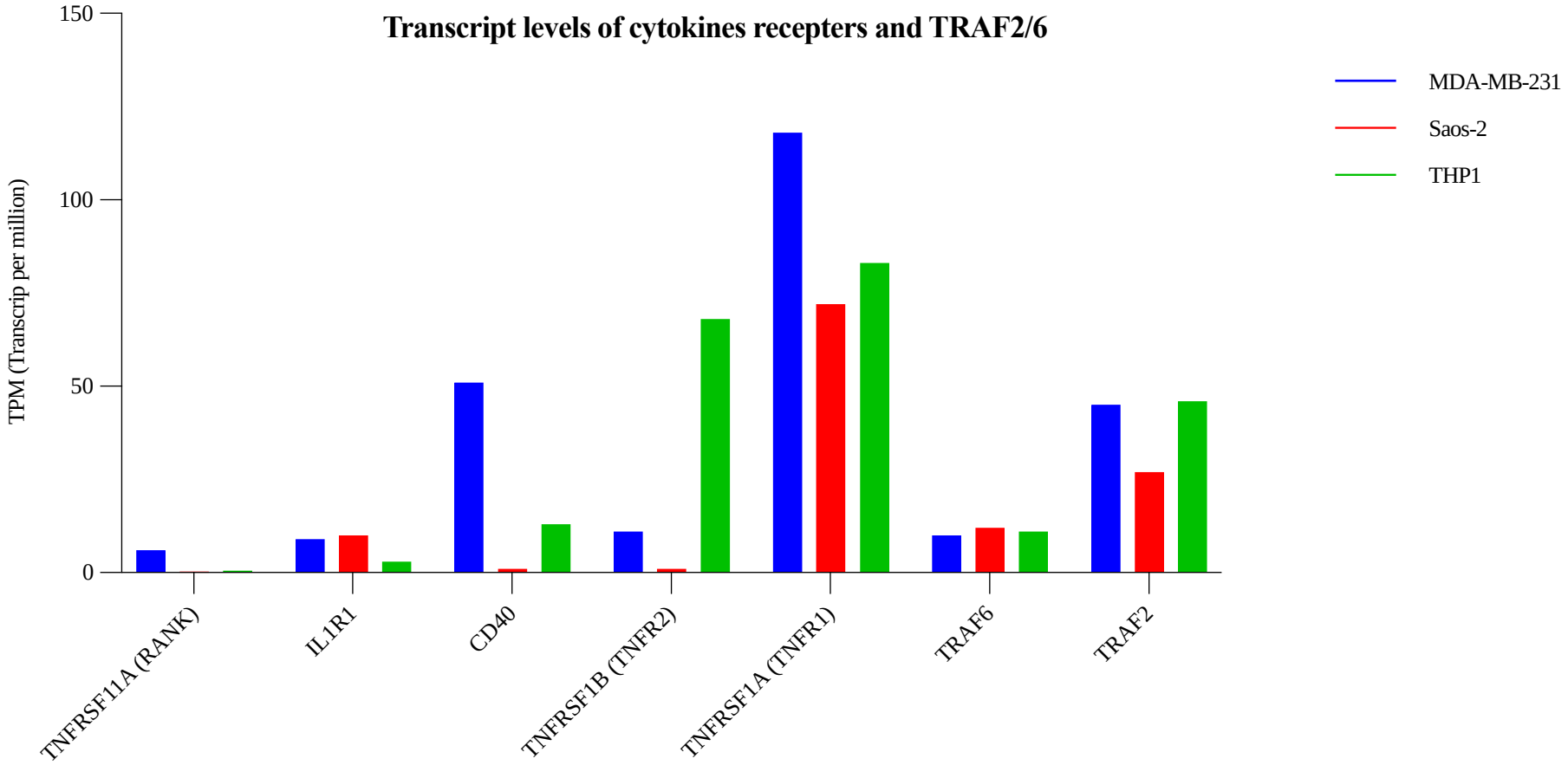

Supplementary Tables

Supplementary Table 1. Search strings for Medline, Web of Science and Scopus.

PubMed (Medline)	Web of Science	Scopus
1. ('cancer' or '*carcinoma' or 'neoplasm$' or 'tumo?r).tw. 2. "tumor necrosis factor receptor-associated peptides and proteins"/ 3. 'TRAF*'.tw. 4. ('TRAF* adj3 protein$').tw. 5. ('TNF* receptor$ associated factor$ family' or 'TRAF* family').tw. 6. ('TNF* receptor$ associated factor$' or 'TNF* receptor$-associated factor$').tw. 7. ('Tumo?r necrosis factor$ receptor$ associated factor$' or 'Tumo?r necrosis factor$ receptor$-associated factor$').tw. 8. 'TRAF$ interacti* protein$'.tw. 9. 'Adaptor protein*'.mp. 10. 'E3 ligase$'.mp. 11. ('Breast Neoplasm$' or 'Neoplasm$, Breast').tw. 12. ('Breast tumo?r' or 'tumo?r, breast').tw. 13. ('breast cancer$' or 'cancer$, breast').tw. 14. ('Mammary Cancer$' or 'Cancer$, Mammary').tw. 15. ('Breast Malignant Neoplasm$' or 'Malignant Neoplasm$ of Breast').tw. 16. ('*Mammary Carcinoma$' or 'Carcinoma$, * Mammary').tw. 17. ('*Mammary Neoplasm$' or 'Neoplasm$, * Mammary').tw. 18. ('*Breast Carcinoma$' or 'Carcinoma$, * Breast').tw. 19. ('Breast metastas*s' or 'metastas*s, Breast').tw. 20. ('Breast adj2 metastas*s').tw. 21. ('Mammary adj2 metastas*s').tw. 22. review.pt. 23. 10 or 9 or 8 or 7 or 6 or 5 or 4 or 3 or 2 24. 18 or 17 or 16 or 15 or 14 or 13 or 12 or 11 25. 21 or 20 or 19 26. 1 and 23 and 24 and 25 27. 26 not 22	1. TS=('cancer' or '*carcinoma or neoplasm$' or 'tumo?r') 2. TS=('TRAF*') 3. TS=('TRAF*' protein$') 4. TS=('TNF* receptor$ associated factor$ family' or 'TRAF* family') 5. TS=('TNF* receptor$ associated factor$' or 'TNF* receptor$-associated factor$') 6. TS=('Tumo?r necrosis factor$ receptor$ associated factor$' or 'Tumo?r necrosis factor$ receptor$-associated factor$') 7. TS=('TRAF$ interacti* protein$') 8. TS=('Adaptor protein*') 9. TS=('E3 ligase$') 10. TS=('Breast Neoplasm$' OR 'Neoplasm$, Breast') 11. TS=('Breast tumo?r' OR 'tumo?r, breast') 12. TS=('breast cancer$' OR 'cancer$, breast') 13. TS=('Mammary Cancer$' OR 'Cancer$, Mammary') 14. TS=('Breast Malignant Neoplasm$' OR 'Malignant Neoplasm$ of Breast') 15. TS=('*Mammary Carcinoma$' OR 'Carcinoma$, *Mammary') 16. TS=('*Mammary Neoplasm$' or 'Neoplasm$, *Mammary') 17. TS=('*Breast Carcinoma$' OR 'Carcinoma$, *Breast') 18. TS=('Breast metastas*s' OR 'metastas*s , Breast') 19. #17 OR #16 OR #15 OR #14 OR #13 OR #12 OR #11 OR #10 20. #9 OR #8 OR #7 OR #6 OR #5 OR #4 OR #3 OR #2 21. #20 AND #18 AND #19 AND #1 22. (#21) AND DOCUMENT TYPES: (Review) 23. #21 NOT #22	1. TITLE-ABS-KEY (cancer OR *carcinoma OR neoplasm$ OR tumo?r) 2. TITLE-ABS-KEY ("tumor necrosis factor receptor-associated peptides and proteins") 3. TITLE-ABS-KEY (traf*) 4. TITLE-ABS-KEY ("TRAF* protein$") 5. TITLE-ABS-KEY ("TNF* receptor$ associated factor$ family" OR "TRAF* family") 6. TITLE-ABS-KEY ("TNF* receptor$ associated factor$" OR "TNF* receptor$-associated factor$") 7. TITLE-ABS-KEY ("Tumo?r necrosis factor$ receptor$ associated factor$" OR "Tumo?r necrosis factor$ receptor$-associated factor$") 8. TITLE-ABS-KEY ("TRAF$ interacti* protein$") 9. TITLE-ABS-KEY ("Adaptor protein*") 10. TITLE-ABS-KEY ("E3 ligase$") 11. TITLE-ABS-KEY ("Breast Neoplasm$" OR "Breast tumo?r" OR "breast cancer$" OR "Mammary Cancer$" OR "Breast Malignant Neoplasm$" OR "*Mammary Carcinoma$" OR "*Mammary Neoplasm$" OR "*Breast Carcinoma$") 12. TITLE-ABS-KEY ("metastas*s") 13. #10 or #9 or #8 or #7 or #6 or #5 or #4 or #3 or #2 14. #13 and #12 and #1

Supplementary Table 2. List of excluded studies.

Studies	Reason for exclusion
Brincas *et al*., 2019 [327]	No relevant data.
Billir *et al*., 2015 [328]	No relevant data.
Chan *et al*., 2012 [329]	No relevant data.
He *et al*., 2020 [330]	No relevant data.
Helbig *et al*., 2003 [316]	No relevant data.
Li *et al*., 2010 [331]	Review.
Li *et al*., 2020 [332]	No relevant data.
Moelans *et al*., 2014 [333]	No relevant data.
Niu *et al*., 2021 [334]	No relevant data.
Patel *et al*., 2000 [335]	No relevant data.
Qi *et al*., 2021 [336]	No relevant data.
Sato *et al*., 2020 [337]	No relevant data.
Song *et al*., 2015 [310]	Book chapter.
Sun *et al*., 2019 [338]	No relevant data.
Tomasetto *et al*., 1998 [339]	Review.
Van *et al*., 2020 [340]	No relevant data.

Supplementary Table 3. Characteristics and outcomes of *in vitro* studies.

Study	*Species*	*Intervention (pharmacological or genetic manipulation)*	*Target*	*Method of analysing study outcomes*	*Funding source*
Bishop *et al*. 2020 **[184]**	Human	6877002	Inhibit TRAF6	Migration and invasion of MDA-231-BT cells.	Cancer Research UK Development Fund (University of Edinburgh) and funding from Breast Cancer Now (University of Sheffield).
Choi *et al*. 2013 **[253]**	Mouse	Ei24 shRNA and overexpression	Upregulate and inhibit TRAF2	Migration of B16F10 cells.	National Research Foundation of Korea (NRF) funded by the MEST (2009-0081177 and 2010-0020878), National R&D Program for Cancer Control, MoHWFA (1020220), and Bio-industry Technology Development Program, MAFRA (311054-03-2-HD110), Republic of Korea.
Jang *et al*. 2011 **[120]**	Human	TRAF2-siRNA	Inhibit TRAF2	Migration of MDA-MB-231 cells.	Basic Science Research Program through the National Research Foundation of Korea (NRF) funded by the Ministry of Education, Science and Technology (grant no. 2009-0075206 & grant no. 2011-0003981). This study was also supported by a faculty research grant of Yonsei University College of Medicine for 2010 (8-2010-0023).
Jiang *et al*. 2016 **[241]**	Human	miRZip-892b	Upregulate TRAF2	Invasion and colony formation of MDA-MB-231 and ZR-75-30 cells.	Ministry of Science and Technology of China grant (973 Program, no. 2014CB910604); the Distinguished Young Scholar of Guangdong Province, China (no. 2015A030306033);GDUPS (2012); Natural Science Foundation of China (81325013, 81530082, 81201548, 81201546, and 91529301); the Science and Technology of Guangdong Province (No. 2013B021800096, 2015A030313468, 2014A030313008, and 2014A030313220); the Guangdong special Support program (2014TX01R076); the Guangzhou scholars research projects of Guangzhou municipal colleges and universities (no. 12A009D); Pearl River projects (Young Talents of Science and Technology) in Guangzhou (no.

					2013J2200028); and Foundation of Key Laboratory of Gene Engineering of the Ministry of Education.
Li *et al*. 2012 **[194]**	Human	Plumbagin	Inhibit TRAF6	Migration, invasion and viability of MDA-MB-231 and BT549 cells.	973 Program (2012CB910400, 2010CB529704), National Natural Science Foundation of China (30800653, 30930055 and 81071437) and the Fundamental Research Funds for the Central Universities.
Liu *et al*. 2015 **[242]**	Human	miRNA-146a/b inhibitor	Upregulate TRAF6	Migration of MCF7 cells.	NIH/National Cancer Institute (CA164688, CA179282, and CA118948; L. Wang), the Department of Defense (PC130594; L. Wang and W.-H. Yang), the UAB Faculty Development Grant (R. Liu), the Larsen Endowment Fellowship Program Grant (W.-H. Yang), and the Mercer University Seed Grant (W.-H. Yang).
Liu *et al*. 2020**[246]**	Human	TJ-M2010-2	Inhibit TRAF6	Migration, invasion, proliferation and cell apoptosis of MCF7 and MDA-MB-231 cells.	National Natural Science Foundation of China (Grant No. 81802895), the Health and Family Planning Commission of Wuhan Municipality (Grant No. WX17Q16), the Fundamental Research Funds for the Central Universities (Grant No. 2042019kf0229).
Peramuhendige *et al*. 2018 **[239]**	Human	TRAF2 overexpression and knockdown	Upregulate and inhibit TRAF2	Migration (% wound closure) and invasion (% distance) of MDA-MB-231 cells.	Breast Cancer Now, Darwin Endowment Fund and Cancer Research UK.
Shi *et al*. 2019 **[341]**	Mouse	TLR5 overexpression	Upregulate TRAF6	Proliferation of 4T1 cell.	National Natural Science Foundation of China (81371601, to G.H.) and the Natural Science Foundation of Shandong Province (ZR2019MH019, to G.H.)

Wang *et al*. 2013 **[342]**	Human	TRAF4-siRNA, TRAF4-overexpression	Inhibit TRAF4, Upregulate TRAF4	Migration of MCF7 cells, proliferation of MCF7 cells.	Not stated.
Wang *et al*. 2021 **[243]**	Human	miRNA-7	Inhibit TRAF6	Migration of MCF7 cell.	Youth High End Talent Cultivation Project of Peihua University.
Yao *et al*. 2017 **[162]**	Human	Wogonoside	Inhibit TRAF2/4	Migration, invasion, adhesion of MDA-MB-231, MDA-MB-435, BT-474 cells.	National Science & Technology Major Project (No. 2017ZX09301014, 2017ZX09101003-005-023, 2017ZX09101003-003-007), Program for Changjiang Scholars and Innovative Research Team in University (IRT1193), the Project Program of State Key Laboratory of Natural Medicines, China Pharmaceutical University (SKLNMZZCX201606), the National Natural Science Foundation of China (No. 81603135, 81673461, 81373449, 81373448), the Fundamental Research Funds for the Central Universities (2016ZPY005).
Zhang *et al*. 2013[166]	Human	TRAF4-shRNA	Inhibit TRAF4	Migration (trans-well cell numbers), invasion of MDA-MB-231 cells.	A Netherlands Organization of Scientific Research grant (MW-NWO 918.66.606), Cancer Genomics Centre Netherlands, and the Centre for Biomedical Genetics. This work was supported in part by Key Construction Program of the National ‘‘985’’ Project and Zhejiang University Special Fund for Fundamental Research, as well as the Fundamental Research Funds for the Central Universities.

Zheng *et al*. 2015 **[244]**	Human	miRNA-146a mimics/inhibitor	Inhibit/upregulate TRAF6	Migration, invasion, proliferation and adhesion of MCF7 cells.	National Natural Science Foundation of China [Grants 81372331] (to Tao Xi), Major Drug Discovery of Science and Technology Major Projects [Grants 2009ZX09103-652] and the project funded by the Priority Academic Program Development (PAPD) of Jiangsu Higher Education Institutions.

Supplementary Table 4. Characteristics and outcomes of *in vivo* studies.

Study	*Species*	*Intervention (pharmacological or genetic manipulation)*	*Target*	*Method of analysing study outcomes*	*Funding source*
Bishop *et al*. 2020 **[184]**	Mouse	6877002	Inhibit TRAF6	Bone metastasis (log_2 photons/sec) of 4T1 intracardiac injection BALB/c mice (female, 8 weeks of age).	Cancer Research UK Development Fund (University of Edinburgh) and funding from Breast Cancer Now (University of Sheffield).
Jiang *et al*. 2016 **[241]**	Mouse	miR-892b	Inhibit TRAF2	Lung metastasis (surface metastasis nodules) of MDA-MB-231 cell xenograft BALB/c nude mice (female, 4-5 weeks of age, 18-20g).	Ministry of Science and Technology of China grant (973 Program, no. 2014CB910604); the Distinguished Young Scholar of Guangdong Province, China (no. 2015A030306033); GDUPS (2012); Natural Science Foundation of China (81325013, 81530082, 81201548, 81201546, and 91529301); the Science and Technology of Guangdong Province (No. 2013B021800096, 2015A030313468, 2014A030313008, and 2014A030313220); the Guangdong special Support program (2014TX01R076); the Guangzhou scholars research projects of Guangzhou municipal colleges and universities (no. 12A009D); Pearl River projects (Young Talents of Science and Technology) in Guangzhou (no. 2013J2200028); and Foundation of Key Laboratory of Gene Engineering of the Ministry of Education.
Lin *et al*. 2014**[179] [178]**	Mouse	TRAF6-shRNA	Inhibit TRAF6	Lung metastasis (numbers of lung metastases nodules) of MDA-MB-231 cell intracardiac injection nude mice (female, 6 weeks of age).	the National Basic Research Program (2011CB510106), the National Natural Science Foundation of China (30971137, 31171308, and 81172208), the National High Technology Research and Development Program of China (2013AA032201), and the Science and Technology Commission of Shanghai Municipality (10140901600 and 11DZ1910200).

Liu *et al.* 2015 **[242] [242]**	Mouse	miRNA146a/b-inhibitors	Upregulate TRAF6	Lung metastasis tumour burden (% tissue area) of MDA-MB-231 cell intravenously injected into 8-week-old female NSG mice.	NIH/National Cancer Institute (CA164688, CA179282, and CA118948; L. Wang), the Department of Defense (PC130594; L. Wang and W.-H. Yang), the UAB Faculty Development Grant (R. Liu), the Larsen Endowment Fellowship Program Grant (W.-H. Yang), and the Mercer University Seed Grant (W.-H. Yang).
Liu *et al*. 2020**[246]**	Mouse	TJ-M2010-2	Inhibit TRAF6	Tumour volume (mm^3) of MDA-MD-231 and MCF7 cell xenograft BALB/c nude mice (female, 5 weeks of age).	National Natural Science Foundation of China (Grant No. 81802895), the Health and Family Planning Commission of Wuhan Municipality (Grant No. WX17Q16), the Fundamental Research Funds for the Central Universities (Grant No. 2042019kf0229).
Peramuhendige *et al.* 2018 **[239]**	Mouse	TRAF2-overexpression	Upregulate TRAF2	Tumour growth (% tissue area) of MDA-MB-231 cell orthotropic injection into mammary fat pads of adult mice.	Breast Cancer Now, Darwin Endowment Fund and Cancer Research UK.
Rezaeian *et al.* 2017**[168]**	Mouse	TRAF6-overexpression	Upregulate TRAF6	Tumour volume (×100 mm3) of MDA-MB-231 cell 6 weeks after subcutaneously injection into the right flank of 6-week-old nude mice.	NIH R01 grants (R01CA182424- 01A1, R01CA193813-01), the MD Anderson Cancer Center SPORE development grant, the R. Clark Fellowship award, MD Anderson Cancer Center Prostate Moonshot Program funds, and Start-up funds from Wake Forest University School of Medicine to H.K.L. and MOST104-2314-B-384-009-MY3 and MOHW104-TDU-M-212-133004 grants from Taiwan to C.F,L.
Shi *et al.* 2019 **[341]**	Mouse	TLR5 knockdown	Upregulate TRAF6	Tumour volume (mm3) of 4T1 cell model mice 6 days after injection into the lower left and right flanks of male nude mice.	National Natural Science Foundation of China (81371601, to G.H.) and the Natural Science Foundation of Shandong Province (ZR2019MH019, to G.H.)
Yao *et al*. 2017 **[162]**	Mouse	Wogonoside	Inhibit TRAF2/4	Tumour volume (mm^3) of MDA-MB-231 cell orthotopic BALB/c	National Science & Technology Major Project (No. 2017ZX09301014, 2017ZX09101003-005-023,

				nude mice (female, 4 weeks of age).	2017ZX09101003-003-007), Program for Changjiang Scholars and Innovative Research Team in University (IRT1193), the Project Program of State Key Laboratory of Natural Medicines, China Pharmaceutical University (SKLNMZZCX201606), the National Natural Science Foundation of China (No. 81603135, 81673461, 81373449, 81373448), the Fundamental Research Funds for the Central Universities (2016ZPY005).
Zhang *et al*. 2013[166]	Mouse	TRAF4-shRNA	Inhibit TRAF4	Bone metastasis (numbers of bone metastasis, bone metastasis BLI signals) of MDA-MB-231 cell intracardiac injection TRAF4$^{-/-}$ mice.	A Netherlands Organization of Scientific Research grant (MW-NWO 918.66.606), Cancer Genomics Centre Netherlands, and the Centre for Biomedical Genetics. This work was supported in part by Key Construction Program of the National ‘‘985’’ Project and Zhejiang University Special Fund for Fundamental Research, as well as the Fundamental Research Funds for the Central Universities.
Zhu *et al*. 2018 **[165]**	Mouse	TRAF4-shRNA	Inhibit TRAF4	Tumour volume (mm^3) of MDA-MB-231 cell orthotopic BALB/c nude mice (female, 4-6 weeks of age, 16-20g).	National Natural Science Foundation of China (no. 81260394).

Supplementary Table 5. Characteristics and outcomes of breast cancer patient studies

Study	*Study center or data source*	*Study population*	*Outcome (Type of survival)*	*Target*	*Sample size (High expression/ Low expression)*	*P Value*	*HR (95%CI)*	*Ln (HR), SE*	*Funding Source*
Lin et al,. 2014 **[179]**	Shanghai Ruijin Hospital, Shanghai Jiao Tong University, School of Medicine	Breast cancer patients	Overall survival	TRAF6	134 (33/101)	<0.01	2.26 (1.23-3.30)	0.8154, 0.3104	National Basic Research Program (2011CB510106), the National Natural Science Foundation of China (30971137, 31171308, and 81172208), the National High Technology Research and Development Program of China (2013AA032201), and the Science and Technology Commission of Shanghai Municipality (10140901600 and 11DZ1910200).
Rezaeian et al,. 2017 **[168]**	Chi-Mei Foundational Medical Center	Taiwanese cohort of human breast carcinomas	Disease specific survival	TRAF6	212[#] (NA/NA)	0.017	1.008 (1.001-1.015)	0.008, 0.0036	NIH R01 grants (R01CA182424- 01A1, R01CA193813-01), the MD Anderson Cancer Center SPORE development grant, the R. Clark Fellowship award, MD Anderson Cancer Center Prostate Moonshot Program funds, and Start-up funds from Wake Forest University School of Medicine to H.K.L. and MOST104-2314-B-384-009-MY3 and MOHW104-TDU-M-212-133004 grants from Taiwan to C.F,L.
Rezaeian et al,. 2017 **[168]**	Chi-Mei Foundational Medical Center	Taiwanese cohort of human breast carcinomas	Metastasis-free survival	TRAF6	212[#] (NA/NA)	<0.001	1.009 (1.005-1.013)	0.009, 0.002	
Zhang et al,. 2013[166]	NA	Breast cancer patients	Relapse free period for 20 years	TRAF4	327 (129/198)	0.049	1.36 (1.001-1.845)	0.307, 0.024	Netherlands Organization of Scientific Research grant (MW-NWO918.66.606), Key Construction Program of the National ‘‘985’’ Project and Zhejiang University Special Fund for

									Fundamental Research and Fundamental Research Funds for the Central Universities.
Zhao et al,. 2015 **[161]**	Department of Pathology of the First Affiliated Hospital of China Medical University	Chinese BCa patients	Overall survival	Expression of TRAF2 in the Cytoplasm of Malignant Plural Effusion Cells of BCa	46[$] (34/12)	NA	2.03 (0.96-4.29) [*]	0.71, 0.38	Natural Scientific Foundation of China (81572615)
Zhao et al,. 2015 **[161]**	Department of Pathology of the First Affiliated Hospital of China Medical University	Chinese BCa patients	Overall survival	TRAF4 in cytoplasm	46[$] (40/6)	NA	4.45 (1.10-18.06) [*]	1.49, 0.76	Natural Scientific Foundation of China (81572615)
Zhao et al,. 2015 **[161]**	Department of Pathology of the First Affiliated Hospital of China Medical University	Chinese BCa patients	Overall survival	TRAF4 in nuclei	46[$] (20/26)	NA	0.12 (0.03-0.33) [*]	-2.16, 0.54	

[*]refers to HR (95%CI) are estimated as previously described in Tierney et al. 2007. [$] refers to studies using the same cohort of patients' samples but patients were stratified by different signatures. [#] refers to studies using the same cohort of patients' sample but evaluate different outcomes via univariate or multivariate survival analyses.

Supplementary Table 6. Summary of meta-analysis showing non-significant association of cell behaviours changes in in vitro breast cancer cell lines with pharmacological and genetic modulation of TRAF 2/4/6.

Outcome		Intervention	Type of cell cultures (no. studies)	Overall (std.) mean difference (95% CI)	Statistical method	Test for heterogeneity	Test for overall effect
TRAF4	**Proliferation**	Genetic inhibition	MCF7 (3)	-0.01 [-0.03, 0.02]	Mean Difference (IV, Fixed, 95% CI)	$Chi^2 = 0.47$, df = 2 (P = 0.79); I^2 = 0%	Z = 0.65 (P = 0.52)
TRAF6	**Migration**	Pharmacological inhibition	BT459 (3)	-5.60 [-11.76, 0.56]	Std. Mean Difference (IV, Random, 95% CI)	$Tau^2 = 17.19$; $Chi^2 = 4.68$, df = 2 (P = 0.10); I^2 = 57%	Z = 1.78 (P = 0.07)
			MCF7 (1)	-9.20 [-18.23, -0.17]	Std. Mean Difference (IV, Fixed, 95% CI)	*NA*	Z = 2.00 (P = 0.05)
	Invasion	Pharmacological inhibition	BT459 (3)	-5.78 [-12.04, 0.47]	Mean Difference (IV, Random, 95% CI)	$Tau^2 = 17.51$; $Chi^2 = 4.57$, df = 2 (P = 0.10); I^2 = 56%	Z = 1.81 (P = 0.07)
			MCF7 (1)	-9.50 [-18.82, -0.19]	Mean Difference (IV, Random, 95% CI)	NA	Z = 2.00 (P = 0.05)

Supplementary Table 7. Summary of meta-analysis showing non-significant association of tumour weight/ volume and overt metastasis in in vivo mice model with pharmacological and genetic modulation of TRAF 2/4/6

Outcome		Intervention	Type of cell cultures (no. studies)	Subgroup (std.) mean difference (95% CI)	Overall (std.) mean difference (95% CI)	Statistical method	Test for heterogeneity	Test for overall effect
TRAF6	**Metastasis**	Genetic upregulation	Lung metastasis (2) Liver metastasis (1)	5.21 [-4.66, 15.08] 1.20 [0.23, 2.17]	1.41 [-0.14, 2.96]	Std. Mean Difference (IV, Random, 95% CI)	$Tau^2 = 1.06$; $Chi^2 = 6.64$, df = 2 (P = 0.04); $I^2 = 70\%$	Z = 1.79 (P = 0.07)

Supplementary Table 8. Summary of meta-analysis showing non-significant association between TRAF4 expression and poor survival in breast cancer patients.

Intervention	Outcome	Type of survival (no. studies)	Subgroup hazard ratio (95% CI)	Overall hazard ratio (95% CI)	Statistical method	Test for heterogeneity	Test for overall effect
TRAF4 expression	HR (95%CI)	Kaplan-Meier survival analysis (3)	NA	0.69 [0.02, 24.58]	Hazard Ratio (IV, Random, 95% CI)	$Tau^2 = 6.23$; $Chi^2 = 15.33$, df = 1 ($P < 0.0001$); $I^2 = 93\%$	$Z = 0.21$ ($P = 0.84$)

Supplementary Table 9. Quality assessment for human studies

Study ID	Diagnosis		Numbers of patients		Consecutive patients		TRAF judgment		Data source		Total (out of 10)
	Clear (☆☆)	Unclear (☆)	>100 (☆☆)	<100 (☆)	Yes (☆☆)	Unclear (☆)	Detailed criteria (☆☆)	No description (☆)	HR and 95%CI (☆☆)	Survival curve (☆)	
Lin et al,. 2014	☆☆		☆☆		☆		☆☆		☆☆		☆☆☆☆☆☆ ☆☆☆ (9)
Rezaeian et al,. 2017	☆☆		☆☆		☆		☆☆		☆☆		☆☆☆☆☆☆ ☆☆☆ (9)
Zhang et al,. 2013	☆☆		☆☆		☆		☆☆		☆☆		☆☆☆☆☆☆ ☆☆ (8)
Zhao et al,. 2015	☆☆		☆		☆		☆☆		☆		☆☆☆☆☆☆ ☆ (7)

≤5 stars indicate low quality; 6–7 stars indicate medium quality; 8–10 stars indicate high quality.

Supplementary Table 10. PRISMA checklist for article.

Section and Topic	Item #	Checklist item	Location where item is reported (page #)
TITLE			1
Title	1	Identify the report as a systematic review.	
ABSTRACT			
Abstract	2	See the PRISMA 2020 for Abstracts checklist.	2
INTRODUCTION			
Rationale	3	Describe the rationale for the review in the context of existing knowledge.	3
Objectives	4	Provide an explicit statement of the objective(s) or question(s) the review addresses.	4
METHODS			
Eligibility criteria	5	Specify the inclusion and exclusion criteria for the review and how studies were grouped for the syntheses.	4-5
Information sources	6	Specify all databases, registers, websites, organisations, reference lists and other sources searched or consulted to identify studies. Specify the date when each source was last searched or consulted.	4
Search strategy	7	Present the full search strategies for all databases, registers and websites, including any filters and limits used.	Supplementary Table S1
Selection process	8	Specify the methods used to decide whether a study met the inclusion criteria of the review, including how many reviewers screened each record and each report retrieved, whether they worked independently, and if applicable, details of automation tools used in the process.	6
Data collection process	9	Specify the methods used to collect data from reports, including how many reviewers collected data from each report, whether they worked independently, any processes for obtaining or confirming data from study investigators, and if applicable, details of automation tools used in the process.	6-7
Data items	10a	List and define all outcomes for which data were sought. Specify whether all results that were compatible with each outcome domain in each study were sought (e.g. for all measures, time points, analyses), and if not, the methods used to decide which results to collect.	6-7, Supplementary Tables S3-S5
	10b	List and define all other variables for which data were sought (e.g. participant and intervention characteristics, funding sources). Describe any assumptions made about any missing or unclear information.	Supplementary Tables S3-S5
Study risk of bias assessment	11	Specify the methods used to assess risk of bias in the included studies, including details of the tool(s) used, how many reviewers assessed each study and whether they worked independently, and if applicable, details of automation tools used in the process.	7-8
Effect measures	12	Specify for each outcome the effect measure(s) (e.g. risk ratio, mean difference) used in the synthesis or presentation of results.	7

Section and Topic	Item #	Checklist item	Location where item is reported (page #)
Synthesis methods	13a	Describe the processes used to decide which studies were eligible for each synthesis (e.g. tabulating the study intervention characteristics and comparing against the planned groups for each synthesis (item #5)).	7
	13b	Describe any methods required to prepare the data for presentation or synthesis, such as handling of missing summary statistics, or data conversions.	6-7
	13c	Describe any methods used to tabulate or visually display results of individual studies and syntheses.	7
	13d	Describe any methods used to synthesize results and provide a rationale for the choice(s). If meta-analysis was performed, describe the model(s), method(s) to identify the presence and extent of statistical heterogeneity, and software package(s) used.	7
	13e	Describe any methods used to explore possible causes of heterogeneity among study results (e.g. subgroup analysis, meta-regression).	7
	13f	Describe any sensitivity analyses conducted to assess robustness of the synthesized results.	NA
Reporting bias assessment	14	Describe any methods used to assess risk of bias due to missing results in a synthesis (arising from reporting biases).	7-8
Certainty assessment	15	Describe any methods used to assess certainty (or confidence) in the body of evidence for an outcome.	7-8
RESULTS			
Study selection	16a	Describe the results of the search and selection process, from the number of records identified in the search to the number of studies included in the review, ideally using a flow diagram.	8-9, Figure 1
	16b	Cite studies that might appear to meet the inclusion criteria, but which were excluded, and explain why they were excluded.	Supplementary Table S2
Study characteristics	17	Cite each included study and present its characteristics.	Supplementary Tables S3-S5
Risk of bias in studies	18	Present assessments of risk of bias for each included study.	10-12, Supplementary Tables S9, Supplementary Figures S1-S2
Results of individual studies	19	For all outcomes, present, for each study: (a) summary statistics for each group (where appropriate) and (b) an effect estimate and its precision (e.g. confidence/credible interval), ideally using structured tables or plots.	Tables 2-4, Supplementary tables S6-S8
	20a	For each synthesis, briefly summarise the characteristics and risk of bias among contributing studies.	10-12

Section and Topic	Item #	Checklist item	Location where item is reported (page #)
Results of syntheses	20b	Present results of all statistical syntheses conducted. If meta-analysis was done, present for each the summary estimate and its precision (e.g. confidence/credible interval) and measures of statistical heterogeneity. If comparing groups, describe the direction of the effect.	12-18
	20c	Present results of all investigations of possible causes of heterogeneity among study results.	NA
	20d	Present results of all sensitivity analyses conducted to assess the robustness of the synthesized results.	NA
Reporting biases	21	Present assessments of risk of bias due to missing results (arising from reporting biases) for each synthesis assessed.	NA
Certainty of evidence	22	Present assessments of certainty (or confidence) in the body of evidence for each outcome assessed.	11-12
DISCUSSION			
Discussion	23a	Provide a general interpretation of the results in the context of other evidence.	19
	23b	Discuss any limitations of the evidence included in the review.	20-21
	23c	Discuss any limitations of the review processes used.	20-21
	23d	Discuss implications of the results for practice, policy, and future research.	18-20
OTHER INFORMATION			
Registration and protocol	24a	Provide registration information for the review, including register name and registration number, or state that the review was not registered.	23
	24b	Indicate where the review protocol can be accessed, or state that a protocol was not prepared.	23
	24c	Describe and explain any amendments to information provided at registration or in the protocol.	NA
Support	25	Describe sources of financial or non-financial support for the review, and the role of the funders or sponsors in the review.	22
Competing interests	26	Declare any competing interests of review authors.	23
Availability of data, code and other materials	27	Report which of the following are publicly available and where they can be found: template data collection forms; data extracted from included studies; data used for all analyses; analytic code; any other materials used in the review.	22-23

Supplementary Table 11.PRISMA checklist for abstract.

Section and Topic	Item #	Checklist item	Reported (Yes/No)
TITLE			
Title	1	Identify the report as a systematic review.	Yes
BACKGROUND			
Objectives	2	Provide an explicit statement of the main objective(s) or question(s) the review addresses.	NO
METHODS			
Eligibility criteria	3	Specify the inclusion and exclusion criteria for the review.	NO
Information sources	4	Specify the information sources (e.g. databases, registers) used to identify studies and the date when each was last searched.	YES
Risk of bias	5	Specify the methods used to assess risk of bias in the included studies.	NO
Synthesis of results	6	Specify the methods used to present and synthesise results.	YES
RESULTS			
Included studies	7	Give the total number of included studies and participants and summarise relevant characteristics of studies.	YES
Synthesis of results	8	Present results for main outcomes, preferably indicating the number of included studies and participants for each. If meta-analysis was done, report the summary estimate and confidence/credible interval. If comparing groups, indicate the direction of the effect (i.e. which group is favoured).	YES
DISCUSSION			
Limitations of evidence	9	Provide a brief summary of the limitations of the evidence included in the review (e.g. study risk of bias, inconsistency and imprecision).	YES
Interpretation	10	Provide a general interpretation of the results and important implications.	YES
OTHER			
Funding	11	Specify the primary source of funding for the review.	NO
Registration	12	Provide the register name and registration number.	NA

Supplementary Table 12. Table of KEGG enrichment.

Term ID	Term Description	Observed proteins
hsa05222	Small cell lung cancer	TRAF2,TRAF5,TRAF4,TRAF1,TRAF6,TRAF3
hsa04657	IL-17 signaling pathway	TRAF2,TRAF5,TRAF4,TRAF6,TRAF3
hsa04064	NF-kappa B signaling pathway	TRAF2,TRAF5,TRAF1,TRAF6,TRAF3
hsa05200	Pathways in cancer	TRAF2,TRAF5,TRAF4,TRAF1,TRAF6,TRAF3
hsa04668	TNF signaling pathway	TRAF2,TRAF5,TRAF1,TRAF3
hsa04621	NOD-like receptor signaling pathway	TRAF2,TRAF5,TRAF6,TRAF3
hsa05203	Viral carcinogenesis	TRAF2,TRAF5,TRAF1,TRAF3
hsa05169	Epstein-Barr virus infection	TRAF2,TRAF5,TRAF6,TRAF3
hsa04622	RIG-I-like receptor signaling pathway	TRAF2,TRAF6,TRAF3
hsa05168	Herpes simplex virus 1 infection	TRAF2,TRAF5,TRAF6,TRAF3
hsa05160	Hepatitis C	TRAF2,TRAF6,TRAF3
hsa05170	Human immunodeficiency virus 1 infection	TRAF2,TRAF5,TRAF6
hsa05131	Shigellosis	TRAF2,TRAF5,TRAF6
hsa04620	Toll-like receptor signaling pathway	TRAF6,TRAF3
hsa04380	Osteoclast differentiation	TRAF2,TRAF6
hsa05135	Yersinia infection	TRAF2,TRAF6
hsa04210	Apoptosis	TRAF2,TRAF1
hsa05162	Measles	TRAF6,TRAF3
hsa04217	Necroptosis	TRAF2,TRAF5
hsa05161	Hepatitis B	TRAF6,TRAF3
hsa05130	Pathogenic Escherichia coli infection	TRAF2,TRAF6
hsa05167	Kaposi sarcoma-associated herpesvirus infection	TRAF2,TRAF3
hsa05132	Salmonella infection	TRAF2,TRAF6
hsa05163	Human cytomegalovirus infection	TRAF2,TRAF5

Supplementary Table 13. Table of GO enrichment.

Term ID	Term Description	Observed proteins
GO:0035631	CD40 receptor complex	TRAF2,TRAF5,TRAF6,TRAF3
GO:0009898	Cytoplasmic side of plasma membrane	TRAF2,TRAF5,TRAF1,TRAF6,TRAF3
GO:0005886	Plasma membrane	TRAF2,TRAF5,TRAF4,TRAF7,TRAF1,TRAF6,TRAF3
GO:0031996	Thioesterase binding	TRAF2,TRAF5,TRAF4,TRAF1,TRAF6,TRAF3
GO:0005164	Tumor necrosis factor receptor binding	TRAF2,TRAF5,TRAF4,TRAF1,TRAF6,TRAF3
GO:0031625	Ubiquitin protein ligase binding	TRAF2,TRAF5,TRAF4,TRAF1,TRAF6,TRAF3
GO:0008270	Zinc ion binding	TRAF2,TRAF5,TRAF4,TRAF7,TRAF1,TRAF6,TRAF3
GO:0004842	Ubiquitin-protein transferase activity	TRAF2,TRAF5,TRAF7,TRAF6,TRAF3
GO:0031435	Mitogen-activated protein kinase kinase kinase binding	TRAF2,TRAF6
GO:0019901	Protein kinase binding	TRAF2,TRAF4,TRAF6,TRAF3
GO:0042802	Identical protein binding	TRAF2,TRAF5,TRAF4,TRAF1,TRAF6
GO:0070534	Protein k63-linked ubiquitination	TRAF2,TRAF5,TRAF4,TRAF1,TRAF6,TRAF3
GO:0033209	Tumor necrosis factor-mediated signaling pathway	TRAF2,TRAF5,TRAF4,TRAF1,TRAF6,TRAF3
GO:0046330	Positive regulation of jnk cascade	TRAF2,TRAF5,TRAF4,TRAF1,TRAF6,TRAF3
GO:0043410	Positive regulation of mapk cascade	TRAF2,TRAF5,TRAF4,TRAF7,TRAF1,TRAF6,TRAF3
GO:0043122	Regulation of i-kappab kinase/nf-kappab signaling	TRAF2,TRAF5,TRAF4,TRAF1,TRAF6,TRAF3
GO:0016567	Protein ubiquitination	TRAF2,TRAF5,TRAF4,TRAF7,TRAF1,TRAF6,TRAF3
GO:0042981	Regulation of apoptotic process	TRAF2,TRAF5,TRAF4,TRAF7,TRAF1,TRAF6,TRAF3
GO:0007250	Activation of nf-kappab-inducing kinase activity	TRAF2,TRAF4,TRAF6
GO:0006915	Apoptotic process	TRAF2,TRAF5,TRAF4,TRAF7,TRAF1,TRAF3
GO:0051090	Regulation of dna-binding transcription factor activity	TRAF2,TRAF5,TRAF1,TRAF6,TRAF3
GO:0051092	Positive regulation of nf-kappab transcription factor activity	TRAF2,TRAF5,TRAF1,TRAF6
GO:0044093	Positive regulation of molecular function	TRAF2,TRAF5,TRAF4,TRAF7,TRAF1,TRAF6
GO:0032147	Activation of protein kinase activity	TRAF2,TRAF4,TRAF7,TRAF6
GO:0051023	Regulation of immunoglobulin secretion	TRAF2,TRAF6
GO:0002726	Positive regulation of t cell cytokine production	TRAF2,TRAF6
GO:0043123	Positive regulation of i-kappab kinase/nf-kappab signaling	TRAF2,TRAF5,TRAF6
GO:0032743	Positive regulation of interleukin-2 production	TRAF2,TRAF6
GO:0065009	Regulation of molecular function	TRAF2,TRAF5,TRAF4,TRAF7,TRAF1,TRAF6,TRAF3
GO:0043406	Positive regulation of map kinase activity	TRAF2,TRAF7,TRAF6
GO:0016579	Protein deubiquitination	TRAF2,TRAF6,TRAF3

GO:0010803	Regulation of tumor necrosis factor-mediated signaling pathway	TRAF2,TRAF1
GO:0051865	Protein autoubiquitination	TRAF2,TRAF6
GO:0007249	I-kappaB kinase/NF-kappaB signaling	TRAF2,TRAF6
GO:0043507	Positive regulation of jun kinase activity	TRAF2,TRAF6
GO:2001233	Regulation of apoptotic signaling pathway	TRAF2,TRAF7,TRAF1
GO:0002697	Regulation of immune effector process	TRAF2,TRAF6,TRAF3

Supplementary Table 14. Effect of TRAF6 knockdown on the growth of parental MDA-MB-231 and osteotropic MDA-231-BT breast cancer cells.

Percentage of decreased viability (%)	MDA-MB-231			MDA-231-BT		
Time (hours)	**Mock**	**KD1**	**KD3**	**Mock**	**KD1**	**KD3**
24	100	86.47	21.75	100	40.71	50.21
48	100	45.12	23.04	100	40.62	55.48
72	100	59.40	37.68	100	25.96	48.78
96	100	46.50	20.95	100	25.71	49.88
Knockdown efficacy	-	93%	69%	-	74%	85%

Supplementary Table 15. Molecule subtype and hormone receptor status of a panel of human and murine breast cancer cell line.

	MDA-MB-231	**MCF7**	**4T1**	**EO771**
Species	Human	Human	Mouse	Mouse
Subtype	TNBC	Luminal A	TNBC	Luminal B
ER	-	+	-	ER-α – ER-β +
PR	-	-	-	+
HER2	-	-	-	+

Supplementary Table 16. Effects of the verified TRAF6 inhibitor 6877002 and five congeners on the viability of a panel of murine and human breast cancer cells with different metastatic abilities *in vitro*. Cell viability was measured after 48 hours of continuous exposure to the six profiled TRAF inhibitors. Calculation of half maximal inhibitory concentration (IC_{50}) was performed as previous described. Values are expressed as mean ± SD and were obtained from three independent experiments.

			Half maximal inhibitory concentration (IC50) in µM after 48 hours					
	Cell type	**Classification**	**FSAS1**	**FSAS2**	**FSAS3**	**FSAS4**	**FSAS5**	**6877002**
Murine cell lines	E0771	Hormone dependent	13.96±2.78	10.26±3.05	14.47±3.16	29.13±3.22	20.22±1.55	>100
	4T1	Triple negative	>100	>100	38.86±2.60	>100	56.32±5.13	82.76±16.08
	4T1-BT	Triple negative Bone tropic	>100	>100	22.90±1.18	>100	47.44±13.07	100.67±0.32
Human cell lines	MCF7	Hormone dependent	>100	>100	25.64±6.60	>100	51.72±3.38	37.37±17.39
	MDA-MB-231	Triple negative	87.21±19.20	75.74±31.48	23.1±3.94	>100	66.01±9.69	33.12±4.64
	MDA-MB-231-BT	Triple negative Bone tropic	>100	>100	14.33±7.80	>100	25.48±10.96	60.9±1.04

Scientific Appendix

Buffers	
ALP lysis buffer	Add 2 ml 1M Trizma base (pH 8.0-8.3, Sigma-Aldrich, No. T6066), 0.5 m 0.2M $MgCl_2$ (Sigma-Aldrich, No.M1028) in 100 ml H_2O Add 0.2ml (0.2g) Triton X-100 (Final conc 0.2%).
ARS solution	Dissolve 0.547 g of ARS (Sigma-Aldrich, No. A5533) in 40 ml de-ionised water. Adjust pH between 4.1-4.3 with ammonium hydroxide (10% v/v).
Loading buffer	5.2 ml Trizma HCl (Sigma-Aldrich, No. T3253;1 M) pH 6.8 (use Trizma Base (Sigma-Aldrich, No. T6066) 1M to adjust pH) 1g DL-Dithiothreitol (DTT; Sigma-Aldrich, No. 43819) 1.3 g SDS (Melford, No. B2008) in 37ºC to dissolve. 6.5 ml glycerol (Sigma-Aldrich, No. G9012) 130 µl 10% Bromophenol Blue (Sigma-Aldrich, No. B6896) **Stir for 30 min.** **Store in -20 ºC.**
pNPP + PicoGreen solution	10 ml dH2O 10 mg 4-nitrophenyl phosphate disodium salt hexahydrate (pNPP, Sigma-Aldrich, No. N4645) 0.2 ml 1M Trizma base (Sigma-Aldrich, No. T6066), pH 8.0-8.3, 0.05 ml 0.2M $MgCl_2$ (0.05 ml Pico Green reagent (Once added, wrap the tube with aluminium foil)
RIPA lysis buffer	1 ml 1% Triton X-100 0.5 g 0.5% (w/v) sodium deoxycholate (Sigma-Aldrich, No. D6750) 0.1 g 0.1% (w/v) SDS Trizma HCl (50 mM using 0.788g in 100 ml) pH 7.4 0.877 g NaCl (Thermo Fisher Scientific, No. S/3100/65;150mM)

Stripping buffer	1 mM DTT, 2% (w/v) SDS and 62.5 mM Tris-HCl (pH 6.7). Stored at room temperature.
TRAcP Staining solution	For 4 full plates: • Naphtol-AS-BI-phosphate solution: 15 mg Naphtol-AS-BI-phosphate (Sigma-Aldrich, No. N2250) in 1.5 ml Dimethylformamide (Sigma-Aldrich, No. D4551) • Solution A: -1.5 ml Naphtol-AS-BI-phosphate solution -7.5 ml Veronal buffer (1.17 g sodium acetate anhydrous (Sigma-Aldrich, No. S2889) and 2.94 g sodium 5,5-diethylbarbiturate (Sigma-Aldrich, No. B0500) in 100 ml distilled water) -9 ml Acetate buffer (0.82 g sodium acetate anhydrous in 100 ml distilled water and 0.6 ml acetic acid glacial in 10 ml distilled water) -9 ml Acetate buffer with 100 mM sodium tartrate (0.82 g sodium acetate anhydrous in 100 ml distilled water, 2.3 g sodium tartrate (Sigma-Aldrich, No. S4797) and 0.6 ml acetic acid glacial in 100 ml distilled water) • Solution B: -1.2 ml Pararosaniline solution (1 g Pararosaniline hydrochloride (Sigma-Aldrich, No. P1528) in 20 ml distilled water and 5 ml concentrated HCl (Honeywell, No. 30721)) -1.2 ml Sodium nitrite (4%) **Pour solution A into B and filter with Acrodisc® Syringe pore size of 0.45 µM.**
Tris buffer saline solution (TBS)	For 1 L: 60.57 g Trizma Base (500 mM) 78.8 g Trizma HCl (500 mM) 175.32 g NaCl (3 M)
TNC (Tris, NaCl, $CaCl_2$) Buffer, 10×	7.88 g Trizma HCl (500 mM) 2.922 g NaCl (500 mM) 1.1098 g $CaCl_2$ (100 mM) 1× TNC buffer were diluted with dH_2O.

Pronase stock solution	Weight out a desired amount of Pronase (ROCHE, cat. no.10165921001) and dissolve it in dH_2O to a final concentration of 10 mg/ml. Prepare a desired number of 20- to 50-ml aliquots and store up to 1 year at -20°C. Use a new aliquot for each DARTS experiments.

Reference

1. Siegel, R.L., et al., *Cancer Statistics, 2021.* CA Cancer J Clin, 2021. **71**(1): p. 7-33.
2. Singletary, S.E., et al., *Revision of the American Joint Committee on Cancer Staging System for Breast Cancer.* Journal of Clinical Oncology, 2002. **20**(17): p. 3628-3636.
3. Giuliano, A.E., S.B. Edge, and G.N. Hortobagyi, *Eighth Edition of the AJCC Cancer Staging Manual: Breast Cancer.* Annals of Surgical Oncology, 2018. **25**(7): p. 1783-1785.
4. Polyak, K., *Heterogeneity in breast cancer.* The Journal of Clinical Investigation, 2011. **121**(10): p. 3786-3788.
5. Allison, K.H., *Molecular Pathology of Breast Cancer: What a Pathologist Needs to Know.* American Journal of Clinical Pathology, 2012. **138**(6): p. 770-780.
6. Pike, M.C., et al., *Estrogens, Progestogens, Normal Breast Cell Proliferation, and Breast Cancer Risk.* Epidemiologic Reviews, 1993. **15**(1): p. 17-30.
7. Fuqua, S.A.W., et al., *Estrogen receptor beta protein in human breast cancer: correlation with clinical tumor parameters.* Cancer research, 2003. **63**(10): p. 2434-2439.
8. Moasser, M.M., *The oncogene HER2: its signaling and transforming functions and its role in human cancer pathogenesis.* Oncogene, 2007. **26**(45): p. 6469-6487.
9. Bevers, T.B., et al., *Breast Cancer Screening and Diagnosis, Version 3.2018, NCCN Clinical Practice Guidelines in Oncology.* J Natl Compr Canc Netw, 2018. **16**(11): p. 1362-1389.
10. Kamińska, M., et al., *Breast cancer risk factors.* Przeglad menopauzalny = Menopause review, 2015. **14**(3): p. 196-202.
11. Tamimi, R.M., et al., *Traditional breast cancer risk factors in relation to molecular subtypes of breast cancer.* Breast Cancer Research and Treatment, 2012. **131**(1): p. 159-167.
12. Ciriello, G., et al., *Emerging landscape of oncogenic signatures across human cancers.* Nat Genet, 2013. **45**(10): p. 1127-33.
13. Kerlikowske, K., et al., *Risk Factors That Increase Risk of Estrogen Receptor–Positive and –Negative Breast Cancer.* JNCI: Journal of the National Cancer Institute, 2017. **109**(5).
14. Pfeiffer, R.M., et al., *Proportion of U.S. Trends in Breast Cancer Incidence Attributable to Long-term Changes in Risk Factor Distributions.* Cancer Epidemiology Biomarkers & Prevention, 2018. **27**(10): p. 1214.
15. Harbeck, N., et al., *Breast cancer.* Nat Rev Dis Primers, 2019. **5**(1): p. 66.
16. Nielsen, T.O., et al., *Assessment of Ki67 in Breast Cancer: Updated Recommendations From the International Ki67 in Breast Cancer Working Group.* J Natl Cancer Inst, 2021. **113**(7): p. 808-819.
17. Perou, C.M., et al., *Molecular portraits of human breast tumours.* Nature, 2000. **406**(6797): p. 747-752.
18. Kwan, M.L., et al., *Breastfeeding, PAM50 Tumor Subtype, and Breast Cancer Prognosis and Survival.* JNCI: Journal of the National Cancer Institute, 2015. **107**(7).
19. Pellacani, D., et al., *Transcriptional regulation of normal human mammary cell heterogeneity and its perturbation in breast cancer.* The EMBO Journal, 2019. **38**(14): p. e100330.
20. Goldhirsch, A., et al., *Strategies for subtypes—dealing with the diversity of breast cancer: highlights of the St Gallen International Expert Consensus on the Primary Therapy of Early Breast Cancer 2011.* Annals of Oncology, 2011. **22**(8): p. 1736-1747.
21. Cardoso, F., et al., *5th ESO-ESMO international consensus guidelines for advanced breast cancer (ABC 5).* Ann Oncol, 2020. **31**(12): p. 1623-1649.
22. Prat, A., et al., *Clinical implications of the intrinsic molecular subtypes of breast cancer.* Breast, 2015. **24 Suppl 2**: p. S26-35.
23. Prat, A., et al., *Phenotypic and molecular characterization of the claudin-low intrinsic subtype of breast cancer.* Breast Cancer Res, 2010. **12**(5): p. R68.
24. Hance, K.W., et al., *Trends in inflammatory breast carcinoma incidence and survival: the surveillance, epidemiology, and end results program at the National Cancer Institute.* J Natl Cancer Inst, 2005. **97**(13): p. 966-75.

25. Vranic, S., et al., *Potential Novel Therapy Targets in Neuroendocrine Carcinomas of the Breast.* Clin Breast Cancer, 2019. **19**(2): p. 131-136.
26. Irelli, A., et al., *Neuroendocrine Cancer of the Breast: A Rare Entity.* J Clin Med, 2020. **9**(5).
27. Tray, N., J. Taff, and S. Adams, *Therapeutic landscape of metaplastic breast cancer.* Cancer Treat Rev, 2019. **79**: p. 101888.
28. Tan, B.Y., et al., *Phyllodes tumours of the breast: a consensus review.* Histopathology, 2016. **68**(1): p. 5-21.
29. Riggio, A.I., K.E. Varley, and A.L. Welm, *The lingering mysteries of metastatic recurrence in breast cancer.* British journal of cancer, 2021. **124**(1): p. 13-26.
30. Chaffer, C.L. and R.A.J.S. Weinberg, *A perspective on cancer cell metastasis.* 2011. **331**(6024): p. 1559-1564.
31. Gupta, G.P. and J. Massagué, *Cancer Metastasis: Building a Framework.* Cell, 2006. **127**(4): p. 679-695.
32. Weigelt, B., J.L. Peterse, and L.J. van't Veer, *Breast cancer metastasis: markers and models.* Nature Reviews Cancer, 2005. **5**(8): p. 591-602.
33. Berry, D.A., et al., *Effect of Screening and Adjuvant Therapy on Mortality from Breast Cancer.* New England Journal of Medicine, 2005. **353**(17): p. 1784-1792.
34. Plevritis, S.K., et al., *Association of Screening and Treatment With Breast Cancer Mortality by Molecular Subtype in US Women, 2000-2012.* JAMA, 2018. **319**(2): p. 154-164.
35. Caswell-Jin, J.L., et al., *Change in Survival in Metastatic Breast Cancer with Treatment Advances: Meta-Analysis and Systematic Review.* JNCI Cancer Spectrum, 2018. **2**(4).
36. Scully, O.J., et al., *Breast Cancer Metastasis.* Cancer Genomics - Proteomics, 2012. **9**(5): p. 311.
37. Roodman, G.D., *Mechanisms of Bone Metastasis.* New England Journal of Medicine, 2004. **350**(16): p. 1655-1664.
38. Paget, S., *The distribution of secondary growths in cancer of the breast. 1889.* Cancer Metastasis Rev, 1989. **8**(2): p. 98-101.
39. Coleman, R.E., P. Smith, and R.D. Rubens, *Clinical course and prognostic factors following bone recurrence from breast cancer.* Br J Cancer, 1998. **77**(2): p. 336-40.
40. Xiao, W., et al., *Breast cancer subtypes and the risk of distant metastasis at initial diagnosis: a population-based study.* Cancer Manag Res, 2018. **10**: p. 5329-5338.
41. Peyre, L., et al., *TRAIL receptor-induced features of epithelial-to-mesenchymal transition increase tumour phenotypic heterogeneity: potential cell survival mechanisms.* British Journal of Cancer, 2021. **124**(1): p. 91-101.
42. Gould Rothberg, B.E. and M.B. Bracken, *E-cadherin Immunohistochemical Expression as a Prognostic Factor in Infiltrating Ductal Carcinoma of the Breast: a Systematic Review and Meta-Analysis.* Breast Cancer Research and Treatment, 2006. **100**(2): p. 139-148.
43. Hugo, H.J., et al., *Epithelial requirement for in vitro proliferation and xenograft growth and metastasis of MDA-MB-468 human breast cancer cells: oncogenic rather than tumor-suppressive role of E-cadherin.* Breast cancer research : BCR, 2017. **19**(1): p. 86-86.
44. Na, T.-Y., et al., *The functional activity of E-cadherin controls tumor cell metastasis at multiple steps.* Proceedings of the National Academy of Sciences of the United States of America, 2020. **117**(11): p. 5931-5937.
45. Berx, G., et al., *E-cadherin is a tumour/invasion suppressor gene mutated in human lobular breast cancers.* The EMBO journal, 1995. **14**(24): p. 6107-6115.
46. Fischer, K.R., et al., *Epithelial-to-mesenchymal transition is not required for lung metastasis but contributes to chemoresistance.* Nature, 2015. **527**(7579): p. 472-476.
47. Neelakantan, D., et al., *EMT cells increase breast cancer metastasis via paracrine GLI activation in neighbouring tumour cells.* Nature Communications, 2017. **8**(1): p. 15773.
48. Yin, J.J., C.B. Pollock, and K. Kelly, *Mechanisms of cancer metastasis to the bone.* Cell Res, 2005. **15**(1): p. 57-62.
49. Mundy, G.R., *Metastasis to bone: causes, consequences and therapeutic opportunities.* Nat Rev Cancer, 2002. **2**(8): p. 584-93.
50. Halsted, W.S., *I. A Clinical and Histological Study of certain Adenocarcinomata of the Breast: and a Brief Consideration of the Supraclavicular Operation and of the Results of Operations*

for Cancer of the Breast from 1889 to 1898 at the Johns Hopkins Hospital. Annals of surgery, 1898. **28**(5): p. 557-576.
51. Veronesi, U., et al., *Twenty-Year Follow-up of a Randomized Study Comparing Breast-Conserving Surgery with Radical Mastectomy for Early Breast Cancer.* New England Journal of Medicine, 2002. **347**(16): p. 1227-1232.
52. Wang, X., et al., *Effect of evidence-based nursing intervention on upper limb function in postoperative radiotherapy patients with breast cancer.* Medicine, 2020. **99**(11): p. e19183-e19183.
53. Homsy, A., et al., *Breast Reconstruction: A Century of Controversies and Progress.* Annals of Plastic Surgery, 2018. **80**(4).
54. Cady, B., *The need to reexamine axillary lymph node dissection in invasive breast cancer.* Cancer, 1994. **73**(3): p. 505-508.
55. Volders, J.H., et al., *Breast-conserving surgery following neoadjuvant therapy-a systematic review on surgical outcomes.* Breast cancer research and treatment, 2018. **168**(1): p. 1-12.
56. Hortobagyi, G.N., *Treatment of Breast Cancer.* New England Journal of Medicine, 1998. **339**(14): p. 974-984.
57. Drãgãnescu, M. and C.J.C. Carmocan, *Hormone therapy in breast cancer.* 2017. **112**(4): p. 413-417.
58. Patel, H.K. and T. Bihani, *Selective estrogen receptor modulators (SERMs) and selective estrogen receptor degraders (SERDs) in cancer treatment.* Pharmacology & Therapeutics, 2018. **186**: p. 1-24.
59. Cameron, D., et al., *11 years' follow-up of trastuzumab after adjuvant chemotherapy in HER2-positive early breast cancer: final analysis of the HERceptin Adjuvant (HERA) trial.* Lancet, 2017. **389**(10075): p. 1195-1205.
60. von Minckwitz, G., et al., *Adjuvant Pertuzumab and Trastuzumab in Early HER2-Positive Breast Cancer.* N Engl J Med, 2017. **377**(2): p. 122-131.
61. Cortes, J., et al., *Trastuzumab Deruxtecan versus Trastuzumab Emtansine for Breast Cancer.* N Engl J Med, 2022. **386**(12): p. 1143-1154.
62. Narayan, P., et al., *FDA Approval Summary: Fam-Trastuzumab Deruxtecan-Nxki for the Treatment of Unresectable or Metastatic HER2-Positive Breast Cancer.* Clin Cancer Res, 2021. **27**(16): p. 4478-4485.
63. Gu, G., D. Dustin, and S.A.W. Fuqua, *Targeted therapy for breast cancer and molecular mechanisms of resistance to treatment.* Current Opinion in Pharmacology, 2016. **31**: p. 97-103.
64. Murthy, R.K., et al., *Tucatinib, Trastuzumab, and Capecitabine for HER2-Positive Metastatic Breast Cancer.* N Engl J Med, 2020. **382**(7): p. 597-609.
65. Lin, N.U., et al., *Intracranial Efficacy and Survival With Tucatinib Plus Trastuzumab and Capecitabine for Previously Treated HER2-Positive Breast Cancer With Brain Metastases in the HER2CLIMB Trial.* J Clin Oncol, 2020. **38**(23): p. 2610-2619.
66. Saura, C., et al., *Neratinib Plus Capecitabine Versus Lapatinib Plus Capecitabine in HER2-Positive Metastatic Breast Cancer Previously Treated With >/= 2 HER2-Directed Regimens: Phase III NALA Trial.* J Clin Oncol, 2020. **38**(27): p. 3138-3149.
67. Seligmann, J.F., et al., *Lapatinib plus Capecitabine versus Trastuzumab plus Capecitabine in the Treatment of Human Epidermal Growth Factor Receptor 2-positive Metastatic Breast Cancer with Central Nervous System Metastases for Patients Currently or Previously Treated with Trastuzumab (LANTERN): a Phase II Randomised Trial.* Clin Oncol (R Coll Radiol), 2020. **32**(10): p. 656-664.
68. Slamon, D.J., et al., *Phase III Randomized Study of Ribociclib and Fulvestrant in Hormone Receptor-Positive, Human Epidermal Growth Factor Receptor 2-Negative Advanced Breast Cancer: MONALEESA-3.* J Clin Oncol, 2018. **36**(24): p. 2465-2472.
69. Sledge, G.W., Jr., et al., *The Effect of Abemaciclib Plus Fulvestrant on Overall Survival in Hormone Receptor-Positive, ERBB2-Negative Breast Cancer That Progressed on Endocrine Therapy-MONARCH 2: A Randomized Clinical Trial.* JAMA Oncol, 2020. **6**(1): p. 116-124.
70. Tripathy, D., et al., *Ribociclib plus endocrine therapy for premenopausal women with hormone-receptor-positive, advanced breast cancer (MONALEESA-7): a randomised phase 3 trial.* Lancet Oncol, 2018. **19**(7): p. 904-915.

71. Sledge, G.W., Jr., et al., *MONARCH 2: Abemaciclib in Combination With Fulvestrant in Women With HR+/HER2- Advanced Breast Cancer Who Had Progressed While Receiving Endocrine Therapy.* J Clin Oncol, 2017. **35**(25): p. 2875-2884.
72. Graziani, G. and C. Szabó, *Clinical perspectives of PARP inhibitors.* Pharmacological Research, 2005. **52**(1): p. 109-118.
73. Tung, N.M., et al., *TBCRC 048: Phase II Study of Olaparib for Metastatic Breast Cancer and Mutations in Homologous Recombination-Related Genes.* J Clin Oncol, 2020. **38**(36): p. 4274-4282.
74. Robson, M.E., et al., *OlympiAD final overall survival and tolerability results: Olaparib versus chemotherapy treatment of physician's choice in patients with a germline BRCA mutation and HER2-negative metastatic breast cancer.* Ann Oncol, 2019. **30**(4): p. 558-566.
75. Dieras, V., et al., *Veliparib with carboplatin and paclitaxel in BRCA-mutated advanced breast cancer (BROCADE3): a randomised, double-blind, placebo-controlled, phase 3 trial.* Lancet Oncol, 2020. **21**(10): p. 1269-1282.
76. Ju, J., A.-J. Zhu, and P. Yuan, *Progress in targeted therapy for breast cancer.* Chronic Diseases and Translational Medicine, 2018. **4**(3): p. 164-175.
77. Baselga, J., et al., *Everolimus in postmenopausal hormone-receptor-positive advanced breast cancer.* N Engl J Med, 2012. **366**(6): p. 520-9.
78. Andre, F., et al., *Alpelisib for PIK3CA-Mutated, Hormone Receptor-Positive Advanced Breast Cancer.* N Engl J Med, 2019. **380**(20): p. 1929-1940.
79. Howell, S.J., et al., *Fulvestrant plus capivasertib versus placebo after relapse or progression on an aromatase inhibitor in metastatic, oestrogen receptor-positive, HER2-negative breast cancer (FAKTION): overall survival, updated progression-free survival, and expanded biomarker analysis from a randomised, phase 2 trial.* Lancet Oncol, 2022. **23**(7): p. 851-864.
80. Turner, N., et al., *Ipatasertib plus paclitaxel for PIK3CA/AKT1/PTEN-altered hormone receptor-positive HER2-negative advanced breast cancer: primary results from cohort B of the IPATunity130 randomized phase 3 trial.* Breast Cancer Res Treat, 2022. **191**(3): p. 565-576.
81. Shepherd, J.H., et al., *CALGB 40603 (Alliance): Long-Term Outcomes and Genomic Correlates of Response and Survival After Neoadjuvant Chemotherapy With or Without Carboplatin and Bevacizumab in Triple-Negative Breast Cancer.* J Clin Oncol, 2022. **40**(12): p. 1323-1334.
82. Mackey, J.R., et al., *Primary results of ROSE/TRIO-12, a randomized placebo-controlled phase III trial evaluating the addition of ramucirumab to first-line docetaxel chemotherapy in metastatic breast cancer.* J Clin Oncol, 2015. **33**(2): p. 141-8.
83. Coleman, R., et al., *Bone health in cancer: ESMO Clinical Practice Guidelines.* Ann Oncol, 2020. **31**(12): p. 1650-1663.
84. Coleman, R., et al., *Adjuvant denosumab in early breast cancer (D-CARE): an international, multicentre, randomised, controlled, phase 3 trial.* Lancet Oncol, 2020. **21**(1): p. 60-72.
85. Coleman, R., et al., *Adjuvant zoledronic acid in patients with early breast cancer: final efficacy analysis of the AZURE (BIG 01/04) randomised open-label phase 3 trial.* Lancet Oncol, 2014. **15**(9): p. 997-1006.
86. Schmid, P., et al., *Atezolizumab and Nab-Paclitaxel in Advanced Triple-Negative Breast Cancer.* New England Journal of Medicine, 2018. **379**(22): p. 2108-2121.
87. Adams, S., et al., *Phase 2 study of pembrolizumab (pembro) monotherapy for previously treated metastatic triple-negative breast cancer (mTNBC): KEYNOTE-086 cohort A.* Journal of Clinical Oncology, 2017. **35**(15_suppl): p. 1008-1008.
88. Adams, S., et al., *Phase 2 study of pembrolizumab as first-line therapy for PD-L1–positive metastatic triple-negative breast cancer (mTNBC): Preliminary data from KEYNOTE-086 cohort B.* Journal of Clinical Oncology, 2017. **35**(15_suppl): p. 1088-1088.
89. Vinayak, S., et al., *TOPACIO/Keynote-162: Niraparib + pembrolizumab in patients (pts) with metastatic triple-negative breast cancer (TNBC), a phase 2 trial.* Journal of Clinical Oncology, 2018. **36**(15_suppl): p. 1011-1011.
90. Schneble, E.J., et al., *The HER2 peptide nelipepimut-S (E75) vaccine (NeuVax) in breast cancer patients at risk for recurrence: correlation of immunologic data with clinical response.* Immunotherapy, 2014. **6**(5): p. 519-31.

91. O'Shea, A.E., et al., *Phase II Trial of Nelipepimut-S Peptide Vaccine in Women with Ductal Carcinoma In Situ.* Cancer Prev Res (Phila), 2023. **16**(6): p. 333-341.
92. Adusumilli, P.S., et al., *A Phase I Trial of Regional Mesothelin-Targeted CAR T-cell Therapy in Patients with Malignant Pleural Disease, in Combination with the Anti-PD-1 Agent Pembrolizumab.* Cancer Discov, 2021. **11**(11): p. 2748-2763.
93. Pascual, T., et al., *SOLTI-1503 PROMETEO TRIAL: combination of talimogene laherparepvec with atezolizumab in early breast cancer.* Future Oncol, 2020. **16**(24): p. 1801-1813.
94. Soliman, H., et al., *Oncolytic T-VEC virotherapy plus neoadjuvant chemotherapy in nonmetastatic triple-negative breast cancer: a phase 2 trial.* Nat Med, 2023. **29**(2): p. 450-457.
95. Bardia, A., et al., *Sacituzumab Govitecan-hziy in Refractory Metastatic Triple-Negative Breast Cancer.* New England Journal of Medicine, 2019. **380**(8): p. 741-751.
96. Edwards, S.C., W.H.M. Hoevenaar, and S.B. Coffelt, *Emerging immunotherapies for metastasis.* British Journal of Cancer, 2021. **124**(1): p. 37-48.
97. Anderson, K.S., *Tumor Vaccines for Breast Cancer.* Cancer Investigation, 2009. **27**(4): p. 361-368.
98. Kavanagh, K.L., et al., *The molecular mechanism of nitrogen-containing bisphosphonates as antiosteoporosis drugs.* Proc Natl Acad Sci U S A, 2006. **103**(20): p. 7829-34.
99. Body, J.J., et al., *Effects of Denosumab in Patients with Bone Metastases, with and without Previous Bisphosphonate Exposure.* J Bone Miner.Res., 2009.
100. Mitchell, S., J. Vargas, and A. Hoffmann, *Signaling via the NFκB system.* Wiley Interdiscip Rev Syst Biol Med, 2016. **8**(3): p. 227-41.
101. Gilmore, T.D., *Introduction to NF-κB: players, pathways, perspectives.* Oncogene, 2006. **25**(51): p. 6680-6684.
102. Hayden, M.S. and S. Ghosh, *Regulation of NF-κB by TNF family cytokines.* Seminars in immunology, 2014. **26**(3): p. 253-266.
103. Dhillon, B., et al., *The Evolving Role of TRAFs in Mediating Inflammatory Responses.* Frontiers in immunology, 2019. **10**: p. 104-104.
104. Bouwmeester, T., et al., *A physical and functional map of the human TNF-alpha/NF-kappa B signal transduction pathway.* Nat Cell Biol, 2004. **6**(2): p. 97-105.
105. Lai, J.L., et al., *Indirubin Inhibits LPS-Induced Inflammation via TLR4 Abrogation Mediated by the NF-kB and MAPK Signaling Pathways.* Inflammation, 2017. **40**(1): p. 1-12.
106. Sun, S.C., *Non-canonical NF-kappaB signaling pathway.* Cell Res, 2011. **21**(1): p. 71-85.
107. Napetschnig, J. and H. Wu, *Molecular basis of NF-kappaB signaling.* Annu Rev Biophys, 2013. **42**: p. 443-68.
108. Bradley, J.R. and J.S. Pober, *Tumor necrosis factor receptor-associated factors (TRAFs).* Oncogene, 2001. **20**(44): p. 6482-6491.
109. Bonizzi, G. and M. Karin, *The two NF-κB activation pathways and their role in innate and adaptive immunity.* Trends in Immunology, 2004. **25**(6): p. 280-288.
110. Zhu, T., et al., *BatchServer: A Web Server for Batch Effect Evaluation, Visualization, and Correction.* J Proteome Res, 2021. **20**(1): p. 1079-1086.
111. Razani, B., A.D. Reichardt, and G. Cheng, *Non-canonical NF-κB signaling activation and regulation: principles and perspectives.* Immunol Rev, 2011. **244**(1): p. 44-54.
112. Lalani, A.I., et al., *TRAF molecules in inflammation and inflammatory diseases.* Curr Pharmacol Rep, 2018. **4**(1): p. 64-90.
113. Xie, P., *TRAF molecules in cell signaling and in human diseases.* J Mol Signal, 2013. **8**(1): p. 7.
114. Nagashima, H., et al., *The adaptor TRAF5 limits the differentiation of inflammatory CD4(+) T cells by antagonizing signaling via the receptor for IL-6.* Nat Immunol, 2014. **15**(5): p. 449-56.
115. Wang, X., et al., *TRAF5-mediated Lys-63-linked Polyubiquitination Plays an Essential Role in Positive Regulation of RORgammat in Promoting IL-17A Expression.* J Biol Chem, 2015. **290**(48): p. 29086-94.
116. Borghi, A., L. Verstrepen, and R. Beyaert, *TRAF2 multitasking in TNF receptor-induced signaling to NF-kappaB, MAP kinases and cell death.* Biochem Pharmacol, 2016. **116**: p. 1-10.
117. Villanueva, J.E., et al., *TRAF2 regulates peripheral CD8(+) T-cell and NKT-cell homeostasis by modulating sensitivity to IL-15.* Eur J Immunol, 2015. **45**(6): p. 1820-31.

118. Petersen, S.L., et al., *TRAF2 is a biologically important necroptosis suppressor.* Cell Death Differ, 2015. **22**(11): p. 1846-57.
119. Siegmund, D., J. Wagner, and H. Wajant, *TNF Receptor Associated Factor 2 (TRAF2) Signaling in Cancer.* Cancers (Basel), 2022. **14**(16).
120. Jang, K.W., et al., *Ubiquitin Ligase CHIP Induces TRAF2 Proteasomal Degradation and NF-kappa B Inactivation to Regulate Breast Cancer Cell Invasion.* Journal of Cellular Biochemistry, 2011. **112**(12): p. 3612-3620.
121. Tobin, D., M. van Hogerlinden, and R. Toftgård, *UVB-induced association of tumor necrosis factor (TNF) receptor 1/TNF receptor-associated factor-2 mediates activation of Rel proteins.* Proc Natl Acad Sci U S A, 1998. **95**(2): p. 565-9.
122. Lalani, A.I., et al., *Myeloid cell TRAF3 regulates immune responses and inhibits inflammation and tumor development in mice.* J Immunol, 2015. **194**(1): p. 334-48.
123. Samak, M., et al., *Cardiac Hypertrophy: An Introduction to Molecular and Cellular Basis.* Med Sci Monit Basic Res, 2016. **22**: p. 75-9.
124. Zirlik, A., et al., *TRAF-1, -2, -3, -5, and -6 are induced in atherosclerotic plaques and differentially mediate proinflammatory functions of CD40L in endothelial cells.* Arterioscler Thromb Vasc Biol, 2007. **27**(5): p. 1101-7.
125. Qiao, Y.Q., et al., *Gene expression of tumor necrosis factor receptor associated-factor (TRAF)-1 and TRAF-2 in inflammatory bowel disease.* J Dig Dis, 2013. **14**(5): p. 244-50.
126. Kedinger, V. and M.C. Rio, *TRAF4, the unique family member.* Adv Exp Med Biol, 2007. **597**: p. 60-71.
127. Shiels, H., et al., *TRAF4 deficiency leads to tracheal malformation with resulting alterations in air flow to the lungs.* Am J Pathol, 2000. **157**(2): p. 679-88.
128. Shen, J., et al., *Different activation of TRAF4 and TRAF6 in inflammatory bowel disease.* Mediators Inflamm, 2013. **2013**: p. 647936.
129. Plenge, R.M., et al., *TRAF1-C5 as a risk locus for rheumatoid arthritis--a genomewide study.* N Engl J Med, 2007. **357**(12): p. 1199-209.
130. Heßler, N., et al., *Linkage and Association Analysis Identifies TRAF1 Influencing Common Carotid Intima-Media Thickness.* Stroke, 2016. **47**(12): p. 2904-2909.
131. Pryhuber, G.S., et al., *Acute tumor necrosis factor-alpha-induced liver injury in the absence of tumor necrosis factor receptor-associated factor 1 gene expression.* Am J Pathol, 2005. **166**(6): p. 1637-45.
132. Xiang, M., et al., *Targeting hepatic TRAF1-ASK1 signaling to improve inflammation, insulin resistance, and hepatic steatosis.* J Hepatol, 2016. **64**(6): p. 1365-77.
133. Lu, Y.Y., et al., *TRAF1 is a critical regulator of cerebral ischaemia-reperfusion injury and neuronal death.* Nat Commun, 2013. **4**: p. 2852.
134. Alvarez, S.E., et al., *Sphingosine-1-phosphate is a missing cofactor for the E3 ubiquitin ligase TRAF2.* Nature, 2010. **465**(7301): p. 1084-1088.
135. Kayagaki, N., et al., *A Deubiquitinase That Regulates Type I Interferon Production.* Science, 2007. **318**(5856): p. 1628.
136. Lu, C.H., et al., *USP17 mediates macrophage-promoted inflammation and stemness in lung cancer cells by regulating TRAF2/TRAF3 complex formation.* Oncogene, 2018. **37**(49): p. 6327-6340.
137. Miao, Y., J. Wu, and S.N. Abraham, *Ubiquitination of Innate Immune Regulator TRAF3 Orchestrates Expulsion of Intracellular Bacteria by Exocyst Complex.* Immunity, 2016. **45**(1): p. 94-105.
138. Zhou, Y., et al., *The kinase CK1ε controls the antiviral immune response by phosphorylating the signaling adaptor TRAF3.* Nature Immunology, 2016. **17**(4): p. 397-405.
139. Ye, H., et al., *Distinct molecular mechanism for initiating TRAF6 signalling.* Nature, 2002. **418**(6896): p. 443-447.
140. Chatzigeorgiou, A., et al., *Blocking CD40-TRAF6 signaling is a therapeutic target in obesity-associated insulin resistance.* Proc Natl Acad Sci U S A, 2014. **111**(7): p. 2686-91.
141. Lee, S.Y. and Y. Choi, *TRAF1 and its biological functions.* Adv Exp Med Biol, 2007. **597**: p. 25-31.

142. Su, X., et al., *TNF receptor-associated factor-1 (TRAF1) negatively regulates Toll/IL-1 receptor domain-containing adaptor inducing IFN-beta (TRIF)-mediated signaling.* Eur J Immunol, 2006. **36**(1): p. 199-206.
143. Missiou, A., et al., *Tumor necrosis factor receptor-associated factor 1 (TRAF1) deficiency attenuates atherosclerosis in mice by impairing monocyte recruitment to the vessel wall.* Circulation, 2010. **121**(18): p. 2033-44.
144. Zhang, X.F., et al., *TRAF1 is a key mediator for hepatic ischemia/reperfusion injury.* Cell Death Dis, 2014. **5**(10): p. e1467.
145. So, T., H. Nagashima, and N. Ishii, *TNF Receptor-Associated Factor (TRAF) Signaling Network in CD4(+) T-Lymphocytes.* Tohoku J Exp Med, 2015. **236**(2): p. 139-54.
146. Yang, X.D. and S.C. Sun, *Targeting signaling factors for degradation, an emerging mechanism for TRAF functions.* Immunol Rev, 2015. **266**(1): p. 56-71.
147. Nagashima, H., et al., *TNFR-Associated Factors 2 and 5 Differentially Regulate the Instructive IL-6 Receptor Signaling Required for Th17 Development.* J Immunol, 2016. **196**(10): p. 4082-9.
148. Shen, J., et al., *Intestinal protein expression profile identifies inflammatory bowel disease and predicts relapse.* Int J Clin Exp Pathol, 2013. **6**(5): p. 917-25.
149. Lalani, A.I., et al., *TRAF3: a novel tumor suppressor gene in macrophages.* Macrophage (Houst), 2015. **2**: p. e1009.
150. Wen, F., et al., *TAGLN Is Downregulated by TRAF6-Mediated Proteasomal Degradation in Prostate Cancer Cells.* Mol Cancer Res, 2021. **19**(7): p. 1113-1122.
151. Liu, N., et al., *TRAF6-mediated degradation of DOK3 is required for production of IL-6 and TNFalpha in TLR9 signaling.* Mol Immunol, 2015. **68**(2 Pt C): p. 699-705.
152. Petrova, T., et al., *Why are the phenotypes of TRAF6 knock-in and TRAF6 knock-out mice so different?* PLoS One, 2022. **17**(2): p. e0263151.
153. Naito, A., et al., *TRAF6-deficient mice display hypohidrotic ectodermal dysplasia.* Proc Natl Acad Sci U S A, 2002. **99**(13): p. 8766-71.
154. Lee, K., et al., *Selective Regulation of MAPK Signaling Mediates RANKL-dependent Osteoclast Differentiation.* Int J Biol Sci, 2016. **12**(2): p. 235-45.
155. Zarzycka, B., et al., *Discovery of small molecule CD40-TRAF6 inhibitors.* J Chem Inf Model, 2015. **55**(2): p. 294-307.
156. Wei, Z.F., et al., *Norisoboldine suppresses osteoclast differentiation through preventing the accumulation of TRAF6-TAK1 complexes and activation of MAPKs/NF-kappaB/c-Fos/NFATc1 Pathways.* PLoS One, 2013. **8**(3): p. e59171.
157. Chen, K., et al., *Shikonin mitigates ovariectomy-induced bone loss and RANKL-induced osteoclastogenesis via TRAF6-mediated signaling pathways.* Biomed Pharmacother, 2020. **126**: p. 110067.
158. Xiao, L., et al., *Puerarin alleviates osteoporosis in the ovariectomy-induced mice by suppressing osteoclastogenesis via inhibition of TRAF6/ROS-dependent MAPK/NF-kappaB signaling pathways.* Aging (Albany NY), 2020. **12**(21): p. 21706-21729.
159. Zhang, Q., X. Zhang, and W. Dong, *TRAF7 contributes to tumor progression by promoting ubiquitin-proteasome mediated degradation of P53 in hepatocellular carcinoma.* Cell Death Discov, 2021. **7**(1): p. 352.
160. Zhu, S., et al., *Genetic Alterations of TRAF Proteins in Human Cancers.* Front Immunol, 2018. **9**: p. 2111.
161. Zhao, Z.J., et al., *Expression, correlation, and prognostic value of TRAF2 and TRAF4 expression in malignant plural effusion cells in human breast cancer.* Diagn Cytopathol, 2015. **43**(11): p. 897-903.
162. Yao, Y., et al., *Wogonoside inhibits invasion and migration through suppressing TRAF2/4 expression in breast cancer.* Journal of experimental & clinical cancer research : CR, 2017. **36**(1): p. 103.
163. Liu, J., et al., *Osteoclastic miR-214 targets TRAF3 to contribute to osteolytic bone metastasis of breast cancer.* Scientific reports, 2017. **7**: p. 40487.
164. Zhang, B., et al., *miR-29b-3p promotes progression of MDA-MB-231 triple-negative breast cancer cells through downregulating TRAF3.* Biological Research, 2019. **52**(1): p. 38.

165. Zhu, L., et al., *Down-regulation of TRAF4 targeting RSK4 inhibits proliferation, invasion and metastasis in breast cancer xenografts.* Biochemical and biophysical research communications, 2018. **500**(3): p. 810-816.
166. Zhang, L., et al., *TRAF4 Promotes TGF-beta Receptor Signaling and Drives Breast Cancer Metastasis.* Molecular Cell, 2013. **51**(5): p. 559-572.
167. Zhao, Z.J., et al., *Expression, Correlation, and Prognostic Value of TRAF2 and TRAF4 Expression in Malignant Plural Effusion Cells in Human Breast Cancer.* Diagnostic Cytopathology, 2015. **43**(11): p. 897-903.
168. Rezaeian, A.H., et al., *A hypoxia-responsive TRAF6-ATM-H2AX signalling axis promotes HIF1alpha activation, tumorigenesis and metastasis.* Nat Cell Biol, 2017. **19**(1): p. 38-51.
169. Sakurai, H., et al., *Phosphorylation-dependent activation of TAK1 mitogen-activated protein kinase kinase kinase by TAB1.* FEBS Lett., 2000. **474**(2-3): p. 141-145.
170. Mizukami, J., et al., *Receptor activator of NF-kappaB ligand (RANKL) activates TAK1 mitogen-activated protein kinase kinase kinase through a signaling complex containing RANK, TAB2, and TRAF6.* Mol.Cell Biol., 2002. **22**(4): p. 992-1000.
171. Yang, W.L., et al., *The E3 ligase TRAF6 regulates Akt ubiquitination and activation.* Science, 2009. **325**(5944): p. 1134-8.
172. Cao, Y. and M. Karin, *NF-kappaB in mammary gland development and breast cancer.* J Mammary Gland Biol Neoplasia, 2003. **8**(2): p. 215-23.
173. Tan, W., et al., *Tumour-infiltrating regulatory T cells stimulate mammary cancer metastasis through RANKL-RANK signalling.* Nature, 2011. **470**(7335): p. 548-553.
174. Starczynowski, D.T., et al., *TRAF6 is an amplified oncogene bridging the RAS and NF-kappaB pathways in human lung cancer.* J Clin Invest, 2011. **121**(10): p. 4095-105.
175. Kim, H., et al., *Direct Interaction of CD40 on Tumor Cells with CD40L on T Cells Increases the Proliferation of Tumor Cells by Enhancing TGF-beta Production and Th17 Differentiation.* PLoS One, 2015. **10**(5): p. e0125742.
176. Coffelt, S.B., et al., *IL-17-producing gammadelta T cells and neutrophils conspire to promote breast cancer metastasis.* Nature, 2015. **522**(7556): p. 345-8.
177. Rezaeian, A.H., et al., *A hypoxia-responsive TRAF6-ATM-H2AX signalling axis promotes HIF1 alpha activation, tumorigenesis and metastasis.* Nature Cell Biology, 2017. **19**(1): p. 38-51.
178. Lin, Y., et al., *Functional role of asparaginyl endopeptidase ubiquitination by TRAF6 in tumor invasion and metastasis.* Journal of the National Cancer Institute, 2014. **106**(4).
179. Lin, Y., et al., *Functional role of asparaginyl endopeptidase ubiquitination by TRAF6 in tumor invasion and metastasis.* J Natl Cancer Inst, 2014. **106**(4): p. dju012.
180. Gori, F., et al., *The expression of osteoprotegerin and RANK ligand and the support of osteoclast formation by stromal-osteoblast lineage cells is developmentally regulated.* Endocrinology, 2000. **141**(12): p. 4768-76.
181. Oryan, A., et al., *Bone morphogenetic proteins: a powerful osteoinductive compound with non-negligible side effects and limitations.* Biofactors, 2014. **40**(5): p. 459-81.
182. Poblenz, A.T., et al., *Inhibition of RANKL-mediated osteoclast differentiation by selective TRAF6 decoy peptides.* Biochem Biophys Res Commun, 2007. **359**(3): p. 510-5.
183. Yasuda, H., et al., *Osteoclast differentiation factor is a ligand for osteoprotegerin/osteoclastogenesis-inhibitory factor and is identical to TRANCE/RANKL.* Proc Natl Acad Sci U S A, 1998. **95**(7): p. 3597-602.
184. Bishop, R.T., et al., *Combined administration of a small-molecule inhibitor of TRAF6 and Docetaxel reduces breast cancer skeletal metastasis and osteolysis.* Cancer Lett, 2020. **488**: p. 27-39.
185. Marino, S., et al., *Anti-inflammatory, but not osteoprotective, effect of the TRAF6/CD40 inhibitor 6877002 in rodent models of local and systemic osteolysis.* Biochem Pharmacol, 2022. **195**: p. 114869.
186. Wei, Z., et al., *Norisoboldine inhibits the production of interleukin-6 in fibroblast-like synoviocytes from adjuvant arthritis rats through PKC/MAPK/NF-kappaB-p65/CREB pathways.* J Cell Biochem, 2012. **113**(8): p. 2785-95.
187. Luo, Y., et al., *Therapeutic effect of norisoboldine, an alkaloid isolated from Radix Linderae, on collagen-induced arthritis in mice.* Phytomedicine, 2010. **17**(10): p. 726-31.

188. Kearns, A.E., S. Khosla, and P.J. Kostenuik, *Receptor activator of nuclear factor kappaB ligand and osteoprotegerin regulation of bone remodeling in health and disease.* Endocr Rev, 2008. **29**(2): p. 155-92.
189. Naito, A., et al., *Severe osteopetrosis, defective interleukin-1 signalling and lymph node organogenesis in TRAF6-deficient mice.* Genes Cells, 1999. **4**(6): p. 353-62.
190. Lomaga, M.A., et al., *TRAF6 deficiency results in osteopetrosis and defective interleukin-1, CD40, and LPS signaling.* Genes Dev, 1999. **13**(8): p. 1015-24.
191. Yasui, T., et al., *Regulation of RANKL-induced osteoclastogenesis by TGF-beta through molecular interaction between Smad3 and Traf6.* J Bone Miner Res, 2011. **26**(7): p. 1447-56.
192. Magilnick, N., et al., *miR-146a-Traf6 regulatory axis controls autoimmunity and myelopoiesis, but is dispensable for hematopoietic stem cell homeostasis and tumor suppression.* Proc Natl Acad Sci U S A, 2017. **114**(34): p. E7140-E7149.
193. Mourskaia, A.A., et al., *ABCC5 supports osteoclast formation and promotes breast cancer metastasis to bone.* Breast Cancer Res, 2012. **14**(6): p. R149.
194. Li, Z., et al., *Plumbagin inhibits breast tumor bone metastasis and osteolysis by modulating the tumor-bone microenvironment.* Current Molecular Medicine, 2012. **12**(8): p. 967-981.
195. Rampersad, S.N., *Multiple applications of Alamar Blue as an indicator of metabolic function and cellular health in cell viability bioassays.* Sensors (Basel), 2012. **12**(9): p. 12347-60.
196. Csepregi, R., et al., *Complex Formation of Resorufin and Resazurin with B-Cyclodextrins: Can Cyclodextrins Interfere with a Resazurin Cell Viability Assay?* Molecules, 2018. **23**(2).
197. Riss, T.L., et al., *Cell Viability Assays*, in *Assay Guidance Manual*, S. Markossian, et al., Editors. 2004, Eli Lilly & Company and the National Center for Advancing Translational Sciences: Bethesda (MD).
198. Borra, R.C., et al., *A simple method to measure cell viability in proliferation and cytotoxicity assays.* Braz Oral Res, 2009. **23**(3): p. 255-62.
199. Chou, T.C., *Drug combination studies and their synergy quantification using the Chou-Talalay method.* Cancer Res, 2010. **70**(2): p. 440-6.
200. Geback, T., et al., *TScratch: a novel and simple software tool for automated analysis of monolayer wound healing assays.* Biotechniques, 2009. **46**(4): p. 265-74.
201. Lomenick, B., et al., *Target identification using drug affinity responsive target stability (DARTS).* Proc Natl Acad Sci U S A, 2009. **106**(51): p. 21984-9.
202. Marino, S. and A.I. Idris, *Analysis of Signaling Pathways by Western Blotting and Immunoprecipitation.* Methods Mol Biol, 2019. **1914**: p. 131-143.
203. Campbell, G.M. and A. Sophocleous, *Quantitative analysis of bone and soft tissue by micro-computed tomography: applications to ex vivo and in vivo studies.* Bonekey Rep, 2014. **3**: p. 564.
204. Moher, D., et al., *Preferred reporting items for systematic reviews and meta-analyses: the PRISMA statement.* Ann Intern Med, 2009. **151**(4): p. 264-9, W64.
205. Parmar, M.K., V. Torri, and L. Stewart, *Extracting summary statistics to perform meta-analyses of the published literature for survival endpoints.* Stat Med, 1998. **17**(24): p. 2815-34.
206. Tierney, J.F., et al., *Practical methods for incorporating summary time-to-event data into meta-analysis.* Trials, 2007. **8**(1): p. 16.
207. Hooijmans, C.R., et al., *SYRCLE's risk of bias tool for animal studies.* BMC Med Res Methodol, 2014. **14**: p. 43.
208. *OHAT Risk of Bias Rating Tool for Human and Animal Studies.* 2015.
209. *Handbook for Conducting Systematic Reviews for Health Effects Evaluations.* 2015.
210. Dai, J., et al., *Prognostic Value of FOXM1 in Patients with Malignant Solid Tumor: A Meta-Analysis and System Review.* Dis Markers, 2015. **2015**: p. 352478.
211. Ryan, R.H., S. , *How to GRADE the quality of the evidence. Cochrane Consumers and Communication Group.* 2016.
212. Hooijmans, C.R., et al., *Facilitating healthcare decisions by assessing the certainty in the evidence from preclinical animal studies.* PLoS One, 2018. **13**(1): p. e0187271.
213. Cumpston, M., et al., *Updated guidance for trusted systematic reviews: a new edition of the Cochrane Handbook for Systematic Reviews of Interventions.* Cochrane Database Syst Rev, 2019. **10**: p. ED000142.

214. Cerami, E., et al., *The cBio cancer genomics portal: an open platform for exploring multidimensional cancer genomics data.* (2159-8290 (Electronic)).
215. Gao, J., et al., *Integrative analysis of complex cancer genomics and clinical profiles using the cBioPortal.* (1937-9145 (Electronic)).
216. Goldman, M.A.-O., et al., *Visualizing and interpreting cancer genomics data via the Xena platform.* (1546-1696 (Electronic)).
217. Szklarczyk, D., et al., *STRING v11: protein-protein association networks with increased coverage, supporting functional discovery in genome-wide experimental datasets.* Nucleic Acids Res, 2019. **47**(D1): p. D607-D613.
218. Ucaryilmaz Metin, C. and G. Ozcan, *Comprehensive bioinformatic analysis reveals a cancer-associated fibroblast gene signature as a poor prognostic factor and potential therapeutic target in gastric cancer.* BMC Cancer, 2022. **22**(1): p. 692.
219. Curtis, C., et al., *The genomic and transcriptomic architecture of 2,000 breast tumours reveals novel subgroups.* (1476-4687 (Electronic)).
220. Pereira, B., et al., *The somatic mutation profiles of 2,433 breast cancers refines their genomic and transcriptomic landscapes.* (2041-1723 (Electronic)).
221. Zhang, X.H., et al., *Latent bone metastasis in breast cancer tied to Src-dependent survival signals.* Cancer Cell, 2009. **16**(1): p. 67-78.
222. Xu, J., et al., *14-3-3zeta turns TGF-beta's function from tumor suppressor to metastasis promoter in breast cancer by contextual changes of Smad partners from p53 to Gli2.* Cancer Cell, 2015. **27**(2): p. 177-92.
223. Foukakis, T., et al., *Immune gene expression and response to chemotherapy in advanced breast cancer.* Br J Cancer, 2018. **118**(4): p. 480-488.
224. Tobin, N.P., et al., *PAM50 Provides Prognostic Information When Applied to the Lymph Node Metastases of Advanced Breast Cancer Patients.* Clin Cancer Res, 2017. **23**(23): p. 7225-7231.
225. Kjallquist, U., et al., *Exome sequencing of primary breast cancers with paired metastatic lesions reveals metastasis-enriched mutations in the A-kinase anchoring protein family (AKAPs).* BMC Cancer, 2018. **18**(1): p. 174.
226. Tobin, N.P., et al., *Molecular subtype and tumor characteristics of breast cancer metastases as assessed by gene expression significantly influence patient post-relapse survival.* Ann Oncol, 2015. **26**(1): p. 81-88.
227. Chung, J.Y., et al., *All TRAFs are not created equal: common and distinct molecular mechanisms of TRAF-mediated signal transduction.* J.Cell Sci., 2002. **115**(Pt 4): p. 679-688.
228. Arkee, T. and G.A. Bishop, *TRAF family molecules in T cells: Multiple receptors and functions.* J Leukoc Biol, 2020. **107**(6): p. 907-915.
229. So, T., *The immunological significance of tumor necrosis factor receptor-associated factors (TRAFs).* Int Immunol, 2022. **34**(1): p. 7-20.
230. Bishop, G.A., *The many faces of TRAF molecules in immune regulation.* J Immunol, 2013. **191**(7): p. 3483-5.
231. Li, J., et al., *The relationship between TRAF6 and tumors.* Cancer Cell International, 2020. **20**(1): p. 429.
232. Kim, C.M., et al., *Crystal structure of TRAF1 TRAF domain and its implications in the TRAF1-mediated intracellular signaling pathway.* Scientific Reports, 2016. **6**(1): p. 25526.
233. Wajant, H., F. Henkler, and P. Scheurich, *The TNF-receptor-associated factor family: scaffold molecules for cytokine receptors, kinases and their regulators.* Cell Signal, 2001. **13**(6): p. 389-400.
234. Edilova, M.I., A.A. Abdul-Sater, and T.H. Watts, *TRAF1 Signaling in Human Health and Disease.* Front Immunol, 2018. **9**: p. 2969.
235. Kim, E., et al., *TRAF4 promotes lung cancer aggressiveness by modulating tumor microenvironment in normal fibroblasts.* Sci Rep, 2017. **7**(1): p. 8923.
236. Arch, R.H., R.W. Gedrich, and C.B. Thompson, *Tumor necrosis factor receptor-associated factors (TRAFs)--a family of adapter proteins that regulates life and death.* Genes Dev, 1998. **12**(18): p. 2821-30.

237. Walsh, M.C., J. Lee, and Y. Choi, *Tumor necrosis factor receptor- associated factor 6 (TRAF6) regulation of development, function, and homeostasis of the immune system.* Immunol Rev, 2015. **266**(1): p. 72-92.
238. Wang, Y., et al., *TRAF-mediated regulation of immune and inflammatory responses.* Sci China Life Sci, 2010. **53**(2): p. 159-68.
239. Peramuhendige, P., et al., *TRAF2 in osteotropic breast cancer cells enhances skeletal tumour growth and promotes osteolysis.* Sci Rep, 2018. **8**(1): p. 39.
240. Darnay, B.G., et al., *TRAFs in RANK signaling.* Adv Exp Med Biol, 2007. **597**: p. 152-9.
241. Jiang, L., et al., *MiR-892b silencing activates NF-kB and promotes aggressiveness in breast cancer.* Cancer Research, 2016. **76**(5): p. 1101-1111.
242. Liu, R.H., et al., *FOXP3 Controls an miR-146/NF-kappa B Negative Feedback Loop That Inhibits Apoptosis in Breast Cancer Cells.* Cancer Research, 2015. **75**(8): p. 1703-1713.
243. Wang, S., et al., *Dysregulation of tumour microenvironment driven by circ-TPGS2/miR-7/TRAF6/NF-κB axis facilitates breast cancer cell motility.* Autoimmunity, 2021. **54**(5): p. 284-293.
244. Zheng, T., et al., *CXCR4 3'UTR functions as a ceRNA in promoting metastasis, proliferation and survival of MCF-7 cells by regulating miR-146a activity.* European Journal of Cell Biology, 2015. **94**(10): p. 458-469.
245. Liu, J.-H., et al., *The MyD88 inhibitor TJ-M2010-2 suppresses proliferation, migration and invasion of breast cancer cells by regulating MyD88/GSK-3beta and MyD88/NF-kappaB signalling pathways.* Experimental cell research, 2020. **394**(2): p. 112157.
246. Liu, J.H., et al., *The MyD88 inhibitor TJ-M2010-2 suppresses proliferation, migration and invasion of breast cancer cells by regulating MyD88/GSK-3 beta and MyD88/NF-kappa B signalling pathways.* Experimental Cell Research, 2020. **394**(2).
247. Kim, M.J., et al., *AMPK alpha 1 Regulates Lung and Breast Cancer Progression by Regulating TLR4-Mediated TRAF6-BECN1 Signaling Axis.* Cancers, 2020. **12**(11).
248. Mestre-Farrera, A., et al., *Glutamine-Directed Migration of Cancer-Activated Fibroblasts Facilitates Epithelial Tumor Invasion.* Cancer Research, 2021. **81**(2): p. 438-451.
249. Sirinian, C., et al., *RANK-c attenuates aggressive properties of ER-negative breast cancer by inhibiting NF-kappa B activation and EGFR signaling.* Oncogene, 2018. **37**(37): p. 5101-5114.
250. Liu, R., et al., *FOXP3 Controls an miR-146/NF-kappaB Negative Feedback Loop That Inhibits Apoptosis in Breast Cancer Cells.* Cancer research, 2015. **75**(8): p. 1703-13.
251. Wang, Z., et al., *Differential effect of anti-apoptotic genes Bcl-xL and c-FLIP on sensitivity of MCF-7 breast cancer cells to paclitaxel and docetaxel.* Anticancer Res, 2005. **25**(3c): p. 2367-79.
252. Regnier, C.H., et al., *Presence of a new conserved domain in CART1, a novel member of the tumor necrosis factor receptor-associated protein family, which is expressed in breast carcinoma.* Journal of Biological Chemistry, 1995. **270**(43): p. 25715-25721.
253. Choi, J.M., et al., *EI24 regulates epithelial-to-mesenchymal transition and tumor progression by suppressing TRAF2-mediated NF-κB activity.* Oncotarget, 2013. **4**(12): p. 2383-2396.
254. Wang, A., et al., *Expression of tumor necrosis factor receptor-assicated factor 4 correlates with expression of Girdin and promotes nuclear translocation of Girdin in breast cancer.* Molecular Medicine Reports, 2015. **11**(5): p. 3635-3641.
255. Camilleri-Broet, S., et al., *TRAF4 overexpression is a common characteristic of human carcinomas.* Oncogene, 2007. **26**(1): p. 142-147.
256. Zhou, F.F., et al., *TRAF4 mediates activation of TGF-β signaling and is a biomarker for oncogenesis in breast cancer.* Science China Life Sciences, 2014. **57**(12): p. 1172-1176.
257. Talevi, A., *Multi-target pharmacology: possibilities and limitations of the "skeleton key approach" from a medicinal chemist perspective.* Frontiers in Pharmacology, 2015. **6**.
258. Katt, M.E., et al., *In Vitro Tumor Models: Advantages, Disadvantages, Variables, and Selecting the Right Platform.* Front Bioeng Biotechnol, 2016. **4**: p. 12.
259. Holliday, D.L. and V. Speirs, *Choosing the right cell line for breast cancer research.* Breast Cancer Res, 2011. **13**(4): p. 215.

260. Zhu, L.Y., et al., *Down-regulation of TRAF4 targeting RSK4 inhibits proliferation, invasion and metastasis in breast cancer xenografts.* Biochemical and Biophysical Research Communications, 2018. **500**(3): p. 810-816.
261. Zhang, L., et al., *TRAF4 promotes TGF-beta receptor signaling and drives breast cancer metastasis.* Molecular cell, 2013. **51**(5): p. 559-72.
262. Tulotta, C. and P. Ottewell, *The role of IL-1B in breast cancer bone metastasis.* Endocr Relat Cancer, 2018. **25**(7): p. R421-R434.
263. Liang, Y., et al., *Metastatic heterogeneity of breast cancer: Molecular mechanism and potential therapeutic targets.* Semin Cancer Biol, 2020. **60**: p. 14-27.
264. Kanazawa, K. and A. Kudo, *TRAF2 is essential for TNF-alpha-induced osteoclastogenesis.* J Bone Miner Res, 2005. **20**(5): p. 840-7.
265. Sun, J., et al., *TRAF6 correlated to invasion and poor prognosis of glioblastoma via elevating MMP9 expression.* NeuroReport, 2019. **30**(2).
266. Carrasco, G., *Effects of pharmacological inhibition and knockdown of TRAF6 on prostate cancer-induced bone cell activity and osteolysis. Available at: https://etheses.whiterose.ac.uk/27832/.* White Rose eTheses Online, 2020.
267. Sun, H., et al., *TRAF6 is upregulated in colon cancer and promotes proliferation of colon cancer cells.* Int J Biochem Cell Biol, 2014. **53**: p. 195-201.
268. Zu, Y., et al., *MiR-146a suppresses hepatocellular carcinoma by downregulating TRAF6.* Am J Cancer Res, 2016. **6**(11): p. 2502-2513.
269. Huang, H., et al., *Wogonoside inhibits TNF receptor-associated factor 6 (TRAF6) mediated-tumor microenvironment and prognosis of pancreatic cancer.* Ann Transl Med, 2021. **9**(18): p. 1460.
270. Meng, G., et al., *Inhibition of miR146b-5p suppresses CT-guided renal cell carcinoma by targeting TRAF6.* J Cell Biochem, 2019. **120**(2): p. 2382-2390.
271. Liu, L., et al., *MiR-146a regulates PM(1) -induced inflammation via NF-kappaB signaling pathway in BEAS-2B cells.* Environ Toxicol, 2018. **33**(7): p. 743-751.
272. Liu, X., et al., *miR-146a-5p Plays an Oncogenic Role in NSCLC via Suppression of TRAF6.* Front Cell Dev Biol, 2020. **8**: p. 847.
273. Marino, S., et al., *Regulation of breast cancer induced bone disease by cancer-specific IKKbeta.* Oncotarget, 2018. **9**(22): p. 16134-16148.
274. Wu, H. and J.R. Arron, *TRAF6, a molecular bridge spanning adaptive immunity, innate immunity and osteoimmunology.* Bioessays, 2003. **25**(11): p. 1096-1105.
275. Zeng, F., et al., *TRAF6 as a potential target in advanced breast cancer: a systematic review, meta-analysis, and bioinformatics validation.* Scientific Reports, 2023. **13**(1): p. 4646.
276. Marino, S., et al., *Anti-inflammatory, but not osteoprotective, effect of the TRAF6/CD40 inhibitor 6877002 in rodent models of local and systemic osteolysis.* Biochemical Pharmacology, 2021: p. 114869.
277. Feng, X., *RANKing intracellular signaling in osteoclasts.* IUBMB.Life, 2005. **57**(6): p. 389-395.
278. Tak, P.P. and G.S. Firestein, *NF-kappaB: a key role in inflammatory diseases.* J Clin Invest, 2001. **107**(1): p. 7-11.
279. Han, Z., et al., *AP-1 and NF-kappaB regulation in rheumatoid arthritis and murine collagen-induced arthritis.* Autoimmunity, 1998. **28**(4): p. 197-208.
280. Tsao, P.W., et al., *The effect of dexamethasone on the expression of activated NF-kappa B in adjuvant arthritis.* Clin Immunol Immunopathol, 1997. **83**(2): p. 173-8.
281. Deng, T., et al., *TRAF6 autophagic degradation by avibirnavirus VP3 inhibits antiviral innate immunity via blocking NFKB/NF-kappaB activation.* Autophagy, 2022. **18**(12): p. 2781-2798.
282. Dolcet, X., et al., *NF-kB in development and progression of human cancer.* Virchows Arch, 2005. **446**(5): p. 475-82.
283. Bakshi, H.A., et al., *Crocin Inhibits Angiogenesis and Metastasis in Colon Cancer via TNF-alpha/NF-kB/VEGF Pathways.* Cells, 2022. **11**(9).
284. Liu, J., et al., *Increased alveolar epithelial TRAF6 via autophagy-dependent TRIM37 degradation mediates particulate matter-induced lung metastasis.* Autophagy, 2022. **18**(5): p. 971-989.

285. Mu, Y., et al., *TRAF6 ubiquitinates TGFbeta type I receptor to promote its cleavage and nuclear translocation in cancer.* Nat.Commun., 2011. **2**: p. 330.
286. Aarts, S., et al., *Inhibition of CD40-TRAF6 interactions by the small molecule inhibitor 6877002 reduces neuroinflammation.* J Neuroinflammation, 2017. **14**(1): p. 105.
287. Seijkens, T.T.P., et al., *Targeting CD40-Induced TRAF6 Signaling in Macrophages Reduces Atherosclerosis.* J Am Coll Cardiol, 2018. **71**(5): p. 527-542.
288. van den Berg, S.M., et al., *Blocking CD40-TRAF6 interactions by small-molecule inhibitor 6860766 ameliorates the complications of diet-induced obesity in mice.* Int J Obes (Lond), 2015. **39**(5): p. 782-90.
289. Cardoso, F., et al., *Early breast cancer: ESMO Clinical Practice Guidelines for diagnosis, treatment and follow-updagger.* Ann Oncol, 2019. **30**(8): p. 1194-1220.
290. Chuang, S.E., et al., *Basal levels and patterns of anticancer drug-induced activation of nuclear factor-kappaB (NF-kappaB), and its attenuation by tamoxifen, dexamethasone, and curcumin in carcinoma cells.* Biochem Pharmacol, 2002. **63**(9): p. 1709-16.
291. Wang, B., et al., *A randomized phase 3 trial of Gemcitabine or Nab-paclitaxel combined with cisPlatin as first-line treatment in patients with metastatic triple-negative breast cancer.* Nat Commun, 2022. **13**(1): p. 4025.
292. Nakshatri, H., et al., *Constitutive activation of NF-kappaB during progression of breast cancer to hormone-independent growth.* Mol Cell Biol, 1997. **17**(7): p. 3629-39.
293. Hostager, B.S., et al., *Tumor necrosis factor receptor-associated factor 2 (TRAF2)-deficient B lymphocytes reveal novel roles for TRAF2 in CD40 signaling.* J Biol Chem, 2003. **278**(46): p. 45382-90.
294. Chen, H., et al., *Interference with nuclear factor kappa B and c-Jun NH2-terminal kinase signaling by TRAF6C small interfering RNA inhibits myeloma cell proliferation and enhances apoptosis.* Oncogene, 2006. **25**(49): p. 6520-7.
295. Vicic, I. and B. Belev, *The pathogenesis of bone metastasis in solid tumors: a review.* Croat Med J, 2021. **62**(3): p. 270-282.
296. Ono, T., et al., *RANKL biology: bone metabolism, the immune system, and beyond.* Inflamm Regen, 2020. **40**: p. 2.
297. Anderson, D.M., et al., *A homologue of the TNF receptor and its ligand enhance T-cell growth and dendritic-cell function.* Nature, 1997. **390**(6656): p. 175-9.
298. Lacey, D.L., et al., *Osteoprotegerin ligand is a cytokine that regulates osteoclast differentiation and activation.* Cell, 1998. **93**(2): p. 165-76.
299. Hauge, E.M., et al., *Cancellous bone remodeling occurs in specialized compartments lined by cells expressing osteoblastic markers.* J Bone Miner Res, 2001. **16**(9): p. 1575-82.
300. Yen, M.L., et al., *TRAF-6 dependent signaling pathway is essential for TNF-related apoptosis-inducing ligand (TRAIL) induces osteoclast differentiation.* PLoS One, 2012. **7**(6): p. e38048.
301. Armstrong, A.P., et al., *A RANK/TRAF6-dependent signal transduction pathway is essential for osteoclast cytoskeletal organization and resorptive function.* J Biol Chem, 2002. **277**(46): p. 44347-56.
302. Bishop, R., *The Role of IKKε in the Initiation and Progression of Breast Cancer Bone Metastasis. Available at: https://etheses.whiterose.ac.uk/21247/.* White Rose eTheses Online, 2018.
303. Kingsley, L.A., et al., *Molecular biology of bone metastasis.* Mol Cancer Ther, 2007. **6**(10): p. 2609-17.
304. Yuen, H.F., et al., *Prostate cancer cells modulate osteoblast mineralisation and osteoclast differentiation through Id-1.* Br J Cancer, 2010. **102**(2): p. 332-41.
305. Miki, Y., et al., *Effects of aromatase inhibitors on human osteoblast and osteoblast-like cells: a possible androgenic bone protective effects induced by exemestane.* Bone, 2007. **40**(4): p. 876-87.
306. Czekanska, E.M., et al., *In search of an osteoblast cell model for in vitro research.* Eur Cell Mater, 2012. **24**: p. 1-17.
307. Bellido, T. and J. Delgado-Calle, *Ex Vivo Organ Cultures as Models to Study Bone Biology.* JBMR Plus, 2020. **4**(3).

308. Liu, H., et al., *TRAF6 activation in multiple myeloma: a potential therapeutic target.* Clin Lymphoma Myeloma Leuk, 2012. **12**(3): p. 155-63.
309. Idris, A.I., et al., *Pharmacologic inhibitors of IkappaB kinase suppress growth and migration of mammary carcinosarcoma cells in vitro and prevent osteolytic bone metastasis in vivo.* Mol Cancer Ther, 2009. **8**(8): p. 2339-47.
310. Song, L., et al., *Sinomenine inhibits breast cancer cell invasion and migration by suppressing NF-kappaB activation mediated by IL-4/miR-324-5p/CUEDC2 axis.* Biochemical and biophysical research communications, 2015. **464**(3): p. 705-10.
311. Gu, Y., et al., *TRAF4 Silencing Induces Cell Apoptosis and Improves Retinoic Acid Sensitivity in Human Neuroblastoma.* Neurochem Res, 2023. **48**(7): p. 2116-2128.
312. Hao, M., et al., *TRAF4 Inhibits the Apoptosis and Promotes the Proliferation of Breast Cancer Cells by Inhibiting the Ubiquitination of Spindle Assembly-Associated Protein Eg5*. Front Oncol, 2022. **12**: p. 855139.
313. Bertucci, F., et al., *Gene expression profiling shows medullary breast cancer is a subgroup of basal breast cancers.* Cancer Res, 2006. **66**(9): p. 4636-44.
314. Zheng, T., et al., *CXCR4 3'UTR functions as a ceRNA in promoting metastasis, proliferation and survival of MCF-7 cells by regulating miR-146a activity.* European journal of cell biology, 2015. **94**(10): p. 458-69.
315. Han Xu, L.L., Bing Dong *TRAF6 promotes chemoresistance to paclitaxel of triple negative breast cancer via regulating PKM2-mediated glycolysis,*. PREPRINT (Version 1) available at Research Square [https://doi.org/10.21203/rs.3.rs-2393717/v1], 2023.
316. Helbig, G., et al., *NF-kappa B promotes breast cancer cell migration and metastasis by inducing the expression of the chemokine receptor CXCR4.* Journal of Biological Chemistry, 2003. **278**(24): p. 21631-21638.
317. Zhang, L., et al., *EZH2 engages TGFbeta signaling to promote breast cancer bone metastasis via integrin beta1-FAK activation.* Nat Commun, 2022. **13**(1): p. 2543.
318. Dai, J., et al., *Vascular endothelial growth factor contributes to the prostate cancer-induced osteoblast differentiation mediated by bone morphogenetic protein.* Cancer Res, 2004. **64**(3): p. 994-9.
319. Li, J., et al., *The relationship between TRAF6 and tumors.* Cancer Cell Int, 2020. **20**: p. 429.
320. Zhao, W., et al., *E3 ubiquitin ligase tripartite motif 38 negatively regulates TLR-mediated immune responses by proteasomal degradation of TNF receptor-associated factor 6 in macrophages.* J Immunol, 2012. **188**(6): p. 2567-74.
321. Aston, W.J., et al., *A systematic investigation of the maximum tolerated dose of cytotoxic chemotherapy with and without supportive care in mice.* BMC Cancer, 2017. **17**(1): p. 684.
322. Marino, S., et al., *JZL184, A Monoacylglycerol Lipase Inhibitor, Induces Bone Loss in a Multiple Myeloma Model of Immunocompetent Mice.* Calcif Tissue Int, 2020. **107**(1): p. 72-85.
323. UK, C.R., *Myeloma incidence statistics (2016-2018). Available from: https://www.cancerresearchuk.org/health-professional/cancer-statistics/statistics-by-cancer-type/myeloma#heading-Zero.* cited 2023 July 18.
324. Marino, S. and A.I. Idris, *Emerging therapeutic targets in cancer induced bone disease: A focus on the peripheral type 2 cannabinoid receptor.* Pharmacol Res, 2017. **119**: p. 391-403.
325. Barretina, J., et al., *The Cancer Cell Line Encyclopedia enables predictive modelling of anticancer drug sensitivity.* Nature, 2012. **483**(7391): p. 603-7.
326. Ghandi, M., et al., *Next-generation characterization of the Cancer Cell Line Encyclopedia.* Nature, 2019. **569**(7757): p. 503-508.
327. Brincas, H.M., et al., *A genetic variant in microrna-146a is associated with sporadic breast cancer in a southern brazilian population.* Genetics and Molecular Biology, 2019. **42**(4).
328. Bilir, C., et al., *The prognostic role of inflammation and hormones in patients with metastatic cancer with cachexia.* Medical Oncology, 2015. **32**(3).
329. Chan, C.-H., et al., *The Skp2-SCF E3 ligase regulates Akt ubiquitination, glycolysis, herceptin sensitivity, and tumorigenesis.* Cell, 2012. **149**(5): p. 1098-111.
330. He, J., et al., *Integrative analysis of genomic amplification-dependent expression and loss-of-function screen identifies ASAP1 as a driver gene in triple-negative breast cancer progression.* Oncogene, 2020. **39**(20): p. 4118-4131.

331. Li, L., X.P. Chen, and Y.J. Li, *MicroRNA-146a and human disease.* Scandinavian Journal of Immunology, 2010. **71**(4): p. 227-231.
332. Li, Z., et al., *Methylation of EZH2 by PRMT1 regulates its stability and promotes breast cancer metastasis.* Cell death and differentiation, 2020. **27**(12): p. 3226-3242.
333. Moelans, C.B., et al., *Genomic evolution from primary breast carcinoma to distant metastasis: Few copy number changes of breast cancer related genes.* Cancer letters, 2014. **344**(1): p. 138-146.
334. Niu, M.M., et al., *Noncanonical TGF-beta signaling leads to FBXO3-mediated degradation of Delta Np63 alpha promoting breast cancer metastasis and poor clinical prognosis.* Plos Biology, 2021. **19**(2).
335. Patel, N.M., et al., *Paclitaxel sensitivity of breast cancer cells with constitutively active NF-kappa B is enhanced by I kappa B alpha super-repressor and parthenolide.* Oncogene, 2000. **19**(36): p. 4159-4169.
336. Qi, J.L., et al., *SQSTM1/p62 regulate breast cancer progression and metastasis by inducing cell cycle arrest and regulating immune cell infiltration.* Genes and Diseases, 2021.
337. Sato, Y., et al., *Possible Roles of Proinflammatory Signaling in Keratinocytes Through Aryl Hydrocarbon Receptor Ligands for the Development of Squamous Cell Carcinoma.* Frontiers in Immunology, 2020. **11**.
338. Sun, Y., et al., *Jatrorrhizine inhibits mammary carcinoma cells by targeting TNIK mediated Wnt/beta-catenin signalling and epithelial-mesenchymal transition (EMT).* Phytomedicine : international journal of phytotherapy and phytopharmacology, 2019. **63**: p. 153015.
339. Tomasetto, C., et al., *TRAF-4 expression in breast carcinomas [1] (multiple letters).* American Journal of Pathology, 1998. **153**(6): p. 2007-2008.
340. van Dam, P.A., Y. Verhoeven, and X.B. Trinh, *The Non-Bone-Related Role of RANK/RANKL Signaling in Cancer*, in *Tumor Microenvironment: Molecular Players, Pt B*, A. Birbrair, Editor. 2020. p. 53-62.
341. Shi, D., et al., *TLR5: A prognostic and monitoring indicator for triple-negative breast cancer.* Cell Death and Disease, 2019. **10**(12).
342. Wang, X., et al., *Ubiquitination of tumor necrosis factor receptor-associated factor 4 (TRAF4) by smad ubiquitination regulatory factor 1 (Smurf1) regulates motility of breast epithelial and cancer cells.* Journal of Biological Chemistry, 2013. **288**(30): p. 21784-21792.

Copyright

The following figures were created in part using Servier Medical Art (SMART Creative commons license) and may have been edited in some aspects:

- Figure 1.3. Patterns of breast cancer metastatic dissemination.
- Figure 1.5. The canonical NFκB signalling transduction pathways.
- Figure 1.6. The non-canonical NFκB signalling pathway.
- Figure 1.7. The bone metastatic process.
- Figure 2.1. Alamar Blue™ reaction equation.
- Figure 2.2. Cell viability assessed by Alamar Blue™ assay.
- Figure 2.5. Western Blot technique.
- Figure 2.6. Workflow of DARTS assay.
- Figure 2.7. Experimental scheme of DARTS using RAW264.7 cell lysates.
- Figure 6.8. Predicted poses of FSAS3 on pockets of TRAF6 and TRAF2.
- Figure 6.15. Schematic representation of inhibition of RANKL-driven TRAF6/NFκB activation by the novel FSAS3.
- Figure 8.1. Disruption of BCa cell – osteoclast interactions by the novel FSAS3.